# Natural Gradient Tracer Tests to Investigate the Fate and Migration of Oil Sands Process-Affected Water in the Wood Creek Sand Channel

by

Trevor G. Tompkins

A thesis
presented to the University of Waterloo
in fulfillment of the
thesis requirement for the degree of
Master of Science
in
Earth Sciences

Waterloo, Ontario, Canada, 2009

AUTHOR’S DECLARATION

I hereby declare that I am the sole author of this thesis. This is a true copy of the thesis, including any required final revisions, as accepted by my examiners.

I understand that my thesis may be made electronically available to the public.

# ABSTRACT

The In Situ Aquifer Test Facility (ISATF) has been established on Suncor Energy Inc's (Suncor) oil sands mining lease north of Fort McMurray, Alberta to investigate the fate and transport of oil sands process-affected (PA) water in the Wood Creek Sand Channel (WCSC) aquifer. In 2008, the ISATF was used for preliminary injection experiments in which 3,000 and 4,000 L plumes of PA water were created in the WCSC. Following injection, the evolution of the plumes was monitored to determine if naphthenic acids (NAs) naturally attenuated in the WCSC and if trace metals were mobilized from the aquifer solids due to changes in redox conditions. Post-injection monitoring found groundwater velocities through the aquifer were slow (~3-10 cm/day) despite hydraulic conductivities on the order of $10^{-3}$ m/s. While microbes in the WCSC were capable of metabolizing acetate under the manganogenic/ferrogenic redox conditions, field evidence suggests naphthenic acids behaved conservatively. Following the injections, there was an apparent enrichment in the dissolved concentrations of iron, manganese, barium, cobalt, strontium and zinc not attributable to elevated levels in the PA injectate. Given the manganogenic/ferrogenic conditions in the aquifer, Mn(II) and Fe(II) were likely released through reductive dissolution of manganese and iron oxide and oxyhydroxide mineral coatings on the aquifer solids. Because naphthenic acids make up the bulk of dissolved organic carbon (DOC) in the injectate and are apparently recalcitrant to oxidation in the WCSC, some question remains as to what functioned as the electron donor in this process.

# ACKNOWLEDGEMENTS

The fieldwork completed for this project would not have been possible without the considerable time, equipment and personnel provided by Suncor. Specifically, I must thank Sam Saforo, Leanne Lane, Jamel Sgaoula, Mike Bowron, Norm Eenkooren and Heather Sutherland for their assistance in arranging camp accommodations, drill rigs, health and safety training, vacuum trucks, field supplies, work space and many other things. Shawn Stringer and Coreen Luchka provided crucial insight and assistance on the implementation of my work plans and Charity Zayonc collected groundwater samples at the ISATF when I was unable to be onsite (notably, when the temperatures started to decline), an effort I am extremely grateful for.

This project is part of a collaborative effort with researchers from University of Alberta and University of British Columbia. Special thanks to Sasha Holden for coordinating this effort and to the other researchers, Ania Ulrich, Uli Mayer, Jon Martin, Leo Perez, Carl Mendoza and Dave Sego, for your input and technical support. A special thanks to Shama Haque from the University of British Columbia for her concerted effort in completing the metals extractions and providing me with the data in time for inclusion in this document.

I also must thank Marianne VanderGriendt, Shirley Chatten and Wayne Noble for analyzing my groundwater and soil samples and helping with the arrangement of field equipment and bottles prior to departing for Fort McMurray. I'll be forever grateful for the help I received from Paul Johnson who had the pleasure of accompanying me on my first visit to Fort McMurray in November 2007 and who built the pump/packer/probe system that I deployed in the injection wells at my site. Marcelo Sousa spent several afternoons in the first floor EIT computer lab helping with the development of my numeric models. If not for his guidance, I would in all likelihood still be sitting at a computer in that lab. Thanks for all the help and the great conversations Marcelo. Matt Alexander taught me to use the University of Waterloo's falling head permeameter and provided several pointers to produce successful tests. Along with assisting on fieldwork, Vahid Sohrabi added a unique perspective to the interpretation of my data. Good luck with the next stages of the project Vahid.

A big thanks to my committee members, Dave Rudolph and Andre Unger for finding the time to meet with me over the last two years to provide feedback and direction. I was extremely lucky

to have Jim Barker as my advisor. He gave me the freedom to implement this project as I saw fit, but was always available to provide guidance and a few calming words when needed. I also must thank the other professors I have worked with at the University of Waterloo, each of whom fielded questions related to my project at some point. Similarly, several grad students in the department were willing to demonstrate the use of equipment or provide advice based on their experiences. I won't provide a list for fear of forgetting someone, but was fortunate to have this input from my peers.

Finally, I want to thank Joanna for her love and patience over the last two years. It takes a special person to listen attentively as I scribble away on a post-it note at the breakfast table and explain how branching on the alkyl substituent effects the biodegradability of a naphthenic acid. Thanks for the support; I couldn't have done this without you.

# DEDICATION

I am dedicating this thesis to my parents for their love, encouragement and guidance over the last twenty-seven years.

# TABLE OF CONTENTS

APPENDICES

# List of Tables

# List of Figures

# 1 Introduction

The presence of oil sands in Northeast Alberta was first documented in the 1780s (Holowenko, 2000). Recent estimates project these deposits hold 1.7 to 2.5 trillion barrels of bitumen, the world's largest known oil reserve (Government of Alberta, 2008). At 174 billion barrels, the volume of bitumen that can be extracted using available technology, is significantly less, (Allen, 2008), putting the volume of Canada's marketable oil reserves second to Saudi Arabia's. As of 2006, the oil sands accounted for 47 percent of crude oil production in Canada (Government of Alberta: Energy, 2009).

The oil sands are distributed across the Athabasca, Cold Lake and Peace River areas of Northern Alberta as shown in Figure 1-1. Of these regions, the Athabasca oil sands cover the largest area (50,000 $km^2$) and contain the majority of shallow deposits that can be extracted via surface mining techniques. As such, the majority of extraction operations have been concentrated within the Athabasca region. Presently, 1.3 million barrels of oil are produced per day from the oil sands with production expected to increase to 3 million barrels per day by 2020 (Government of Alberta, 2008).

## 1.1 Environmental Impact of Oil Sands Mining Operations

Oil sand ores contain an average of 9-12% bitumen (Clemente and Fedorak, 2005), which is separated from the mineral solids using the Clark caustic hot water extraction method, a process that generates large volumes of process-affected (PA) water and tailings. Processing one tonne of oil sands ore generates 0.65 $m^3$ of wastewater (Lai et al., 1996). In other terms, extraction of the bitumen from 1 $m^3$ of oil sands ore requires 3 $m^3$ of water and generates 4 $m^3$ of slurry waste (Holowenko et al., 2000). The waste slurry contains the ore's solid fraction, unrecovered bitumen, chemicals introduced during the extraction process, dissolved compounds from the oil sands connate water and dissolved constituents from the Athabasca River water used for extraction. Under their "zero discharge policies" the oil sands mining companies including, Suncor Energy Inc. (Suncor), Albian Sands Energy Inc. (Albian) and Syncrude Canada Ltd. (Syncrude), have agreed not to release contaminants into the surrounding environment and have sequestered all PA water in large man-made tailings ponds. By 2020, the volume of tailings ponds at Syncrude and Suncor alone are projected to exceed one billion cubic meters (National

Energy Board, 2004). MacKinnon and Retallack (1981) identified the three primary hazards associated with the oil sands tailings ponds as: (1) physical (e.g. floating bitumen mats that are dangerous to waterfowl); (2) chemical (mainly the tailings ponds' poor water quality relative to natural surface water bodies) and; (3) the potential for tailings ponds to recharge to groundwater. Preventing introduction of naphthenic acids (NAs), a group of non-volatile, chemically stable, organic compounds that are the primary source of toxicity in PA water, to surface and groundwater is of special concern to the oil sands mining companies (Clemente and Fedorak, 2005; Headley and McMartin, 2004; MacKinnon and Boerger, 1986; Holowenko et al., 2002).

## 1.2 Location of Study Site

Suncor Energy Inc., (Suncor), was the first commercially viable oil sands mining facility, starting production in 1967. Suncor's main mining, extraction and processing operation is located approximately 30 km north of Fort McMurray, Alberta, with facilities straddling the Athabasca River (Figure 1-2).

From 2005 to 2006, the combined surface area of Suncor's tailings ponds increased substantially from 2,319 ha to 3,013 ha (Suncor Energy Inc, 2007). This increase is largely the result of the completion of a new tailings impoundment, the South Tailings Pond (STP) which began receiving waste tailings discharge on June 29, 2006. As shown in Figure 1-3, the STP is located at the Southeast corner of Suncor's lease. Once full, the STP is expected to cover an area of 2300 ha and have a 366 $Mm^3$ storage capacity. Figure 1-4 shows the STP from ground level as of June 24, 2009.

While the majority of tailings ponds constructed to date were built over low permeability glacial till and/or shale bedrock, nearly 50% of the STP's footprint overlies the Wood Creek Sand Channel (WCSC), a high permeability glaciofluvial channel. Approximately 8 km of the STP's South and West dikes were purposely aligned above the WCSC to improve dike stability and maximize the storage capacity of the impoundment (Klohn Crippen Consultants Ltd., 2004). Generally, beneath the dikes, the WCSC is capped by 8 to 15 m of glacial till, but in some areas the till thickness decreases to less than 5 meters. The WCSC also daylights in some areas beneath the footprint of the STP. Klohn Crippen Consultants Ltd. (2004) expects these areas with limited or no till to provide recharge pathways for PA water to infiltrate to the WCSC. The

WCSC could then provide a preferential pathway for PA water migration away from the Site. Of special concern is McLean Creek, which flows through the Suncor site and into the Athabasca River. The WCSC discharges to the creek where they intersect northwest of the STP. To prevent PA water from discharging to McLean Creek, Suncor installed a line of pumping wells across the WCSC at the northwest corner of the STP to intercept impacted water in the aquifer and return it to the tailings pond. A bentonite cut-off wall was also installed across a branch of the WCSC that extends southwest from beneath the STP's west dike. Contingent plans are also in place for installation of a cut-off wall or pumping wells across the southeastern end of the WCSC if the discharge of tailings to the STP begins to drive southeasterly flow through that portion of the aquifer.

Suncor's construction of the STP above the WCSC provides a unique opportunity to examine the interaction of PA waters with a sandy aquifer. Because Suncor has established hydraulic controls (i.e. cutoff walls and pumping wells) for the WCSC, researchers from the University of Waterloo and the University of Alberta have collaborated to establish the In Situ Aquifer Test Facility (ISATF) to facilitate a series of injection experiments examining the fate and migration of PA water within the WCSC aquifer. The location of the ISATF is highlighted on Figure 1-5.

As part of their lease agreements with the Provincial Government of Alberta, the oil sands mining companies must reclaim their mining sites, including tailings ponds. This will require returning the land to a condition equivalent to the pre-mining environment (Kasperski, 1992). More specifically, Nix (1992) states that, "with respect to eventual mine abandonment, Suncor is required to reclaim tailings ponds to a viable land surface or water body that will be free of long-term maintenance requirements." Extensive research has been completed focusing on the detoxification of surface water in tailings ponds via ageing/microbial degradation and chemical treatment (e.g. addition of gypsum) and have identified processes by which the toxic character of PA water can be eliminated or significantly reduced (MacKinnon and Retallack, 1981; Nix, 1992; Herman, et al., 1994; Lai, et al., 1996; Holowenko, et al., 2002). Additionally, a "wet-landscape" approach has been developed to deal with the sludge/mature fine tailings (MFT) in the ponds where the MFT are transferred to a mined out pit and capped with a layer of clean water creating end-pit-lakes (EPLs). With this approach, the concentration of NAs in the cap layer is expected to drop below levels toxic to aquatic life within 1-2 years. Researchers

anticipate that with the establishment of an aquatic ecosystem within the cap water, the death of the organisms in their natural life cycles will form a detrital layer separating the MFT from the overlying water cap (Quagraine, et al., 2005). Suncor intends to use a wet-landscape approach for the STP and transfer the MFT from the STP into the abandoned Millennium Mine pit once mining activities have been completed.

Because of the STP's construction, removal/remediation of contaminated water and treatment of MFT via the wet landscape approach may not be sufficient to restore this area. These treatments will address the physical and chemical hazards associated with the STP impoundment itself, but not the impacts that could occur to the underlying groundwater. By the time reclamation activities are initiated, PA water will likely have infiltrated into the WCSC aquifer if not directly from the pond itself, through dewatering of the dikes. Because the majority of older tailings ponds were constructed over lower permeability glacial till such that infiltration to groundwater was minimized, research on the interaction of PA waters in groundwater systems has been limited. Therefore, understanding the interaction of PA water in the WCSC will be crucial in developing methods to restore the aquifer during reclamation of the STP.

## 1.3 Purpose of Study

The goal of this study is to identify and characterize the subsurface heterogeneities that control groundwater and contaminant movement to and through the WCSC; determine the capacity of the WCSC aquifer and its microbes to naturally attenuate naphthenic acids; and evaluate if trace metals are mobilized from the aquifer solids through the introduction of PA water. A series of injection experiments were initiated at the ISATF to meet these research objectives. Preliminary injections were completed to study flow conditions and quantify the capacity of the aquifer's microbes to utilize a simple organic substrate. After these experiments, simulated releases of PA water were completed and monitored to study the interaction between the injectate and aquifer.

With a total of 9 oil sands mines potentially in operation by 2011, the continued expansion of Athabasca oil sands mining will necessitate construction of more tailings ponds and dikes proximate to high permeability units like the WCSC. Andriashek and Atkinson (2007) have identified several buried fluvial features similar to the WCSC throughout the Athabasca oil sands area north of Fort McMurray (Figure 1-6). In their interpretation, the WCSC, which extends for

several kilometers beneath the STP, is only the northwest branch of the Clark Channel. These buried channels are significant because they can function as water-supply aquifers but also because they can serve as pathways by which oil sands PA water can migrate to streams and rivers that intersect the channels or, if cut deep enough, as windows for PA water migration into deeper bedrock aquifers (Andriashek and Atkinson, 2007).

Andriashek and Atkinson (2007) lumped the surficial deposits in the Fort McMurray region into two groups; coarse-grained deposits with high intrinsic permeability and fine-grained deposits with low intrinsic permeability and mapped the extent of each group (Figure 1-7). While existing facilities just north of Fort McMurray are generally situated over the lower permeability materials, much of the area is underlain by coarser-grained sediments. As new facilities come on-line in these areas, construction of tailings ponds that effectively contain PA water will be more difficult. Andriashek and Atkinson (2007) point out that the high permeability surficial deposits will likely enhance recharge of PA water to the buried fluvial aquifer systems. The buried channels will then function as migratory pathways distributing the PA water to streams, rivers and deeper groundwater. Understanding the fate and transport of PA water in these high permeability units will be needed to limit migration of PA water to sensitive environmental receptors. As such, the results of this research will have significance that extends beyond the Suncor site to the entire oil sands mining region.

Recent investigations have found that given the low proportion of clays and organic carbon and the anaerobic conditions in the WCSC, NAs are unlikely to naturally biodegrade (Oiffer, 2006). In methanogenic laboratory microcosm studies Holowenko, et al. (2001) found that microbes were unable to readily metabolize NAs as the primary organic substrate, and in the short-term, NAs inhibited methanogenesis of less complex organic compounds. Similarly, Gervais (2004) did not observe a noticeable change in NA concentrations in sulfate-reducing and methanogenic microcosm studies.

The potential for longer duration studies and the larger monitored area available to test through injections at the ISATF may produce different results from those previously observed. Additionally, injections at the ISATF will provide the opportunity to examine the biodegradability of NAs under the WCSC's manganogenic/ferrogenic conditions. Finally, the use of a positive control to evaluate potential factors limiting contaminant attenuation in the

WCSC will provide valuable data for future experiments evaluating remediation techniques such as in-situ chemical oxidation to treat NAs.

# 2 Background

## 2.1 Geology and Hydrogeology

The following review will focus on the geologic units of significance to this study and study area, specifically providing information on those units that influenced the construction of the South Tailings Pond and those units that may function as migratory pathways for PA water to escape the STP impoundment. Three overburden deposits and 2 bedrock formations will be discussed.

### Bedrock Geology

***McMurray Formation*** - The oil sand formation targeted by mining operations in Northern Alberta is the Early Cretaceous McMurray Formation, part of the Manville Group. It is a very fine grained to fine grained unconsolidated sandstone with 30-35% porosity and little mineral cements (Schramm, 2000). The McMurray unconformably overlies Devonian limestone. The oil in the Manville Group was generated west of the current mining operations in a deeper part of the sedimentary basin and migrated in an easterly direction, up-dip (Greiner and Chi, 1995) as illustrated in Figure 2-1, before it was trapped in a shallow anticline. Because the McMurray Formation was near surface at this Northeast edge of the basin, it was water saturated when the oil migrated into the sandstone. This had two important consequences. First, interaction with the water and microbes within the water led to degradation of the oil, creating heavy, viscous bitumen (Greiner and Chi, 1995; Schramm, 2000). Second, because the sand grains were water-wet, the bitumen did not attach directly to the grains. Instead, a thin film of water separates the bitumen from the mineral grain (Schramm, 2000). This makes processing the McMurray oil sands significantly easier. In boreholes completed by Klohn Crippen Consultants Ltd. (2004) during their field investigation to support the design of the STP, the McMurray Formation was encountered between 32 and 98 m below ground surface (bgs) near the STP.

***Clearwater Formation*** - The McMurray Formation is conformably overlain by the Cretaceous Clearwater Formation. The Clearwater consists of marine deposits of clay shale with thin interbedded carbonate cemented siltstone. In the vicinity of the STP, the upper, younger sub-units have been eroded and the Clearwater is overlain by 10-50 m of overburden. At the ISATF, the overburden is up to 50 m thick (Klohn Crippen Consultants Ltd., 2004).

Of significance to the design of the STP are shear zones identified in the clay shale of the Clearwater Formation evidenced by smooth slickensides and striated surfaces observed by Klohn Crippen Consultants Ltd. (2004). Similar shear zones have caused significant movement of dike foundations at Syncrude's Mildred Lake Settling Basin. As such, additional design considerations, such as toe berms must be made for dike structures built over the Clearwater.

**Surficial Geology**

***Wood Creek Sand Channel*** **-** The Wood Creek Sand Channel (WCSC) is a high permeability Pleistocene glaciofluvial channel present beneath much of the footprint of the STP (Figure 2-2). In most areas, the WCSC unconformably overlies the Clearwater Formation, although in some locales the channel cuts through the Clearwater and into the McMurray. The WCSC is composed predominantly of fine to medium sand with silt/clay interbeds mainly in the upper portion of the unit. Coarse sand and fine gravel become more predominant at its base. In most areas, the WCSC is overlain by 8-15 m of lower permeability glacial till, but it does daylight at the southeast corner of the STP as shown in Figure 2-3. As previously mentioned Klohn Crippen Consultants Ltd. (2004) expects these areas with limited or no till to provide recharge pathways for PA water to infiltrate to the WCSC.

As part of their investigation in designing the STP, Klohn Crippen Consultants Ltd. (2004) identified 4 different zones of the WCSC (Figure 2-2). The main channel is considered Zone 1, striking Southeast to Northwest beneath the southern and western dikes of the STP. The channel is 1.0 to 1.5 km wide and is generally 20-30 m thick. A secondary channel, Zone 2, strikes from Southwest to Northeast, connecting with the main channel beneath the STP's West Dike. This channel is 800 to 1000 m in width with a sand/gravel thickness of approximately 25 m. Suncor constructed a bentonite cut-off wall across this channel to prevent migration of PA-impacted water away from the site. Zone 3, extends to the Northeast from the main channel and is significantly thinner than Zones 1 and 2, with a thickness of 10 to 15m. This is not considered a "channel-style" feature and may be an over-bank deposit. Zone 4, located north of Zone 2, is a steepwalled feature covering a limited area spatially. This feature may have formed as part of a separate depositional event or may be a channel feature that eventually disconnected from the main channel, such as an ox-bow.

***Glacial Till –*** The WCSC is overlain by Pleistocene glacial till, composed primarily of silt and clay with varying amounts of sand and gravel. In the vicinity of the STP, the till averages a thickness of approximately 11 m and reaches a maximum thickness of 35 m (Klohn Crippen Consultants Ltd., 2004). At the ISATF, the glacial till is roughly 13 m thick. In some areas, the till is overlain by 1-2 m of glaciolacustrine sand, silt and/or clay.

***Muskeg –*** The upper 1 – 2 m of soil in the area of the STP is Holocene muskeg composed of clay, silt, peat, roots and wood fragments with a dark brown to black color.

**Wood Creek Sand Channel Hydrogeology**

The WCSC aquifer is unconfined at the ISATF, with the water table first encountered between 14 and 15 m below ground surface (bgs) at an elevation of approximately 355 m above mean sea level (amsl). Groundwater elevations are provided in Table 2-1. Slug and pump test analysis of the WCSC by Klohn Crippen Berger (KCB) found the mean hydraulic conductivity to be $4.98 \times 10^{-4}$ m/s. Klohn Crippen Consultants Ltd. (2004) also completed pumping tests within the WCSC, and based on these tests, calculated an average storativity of $2.0 \times 10^{-2}$ for the unconfined portions of the aquifer and $4.3 \times 10^{-4}$ for the confined portions of the aquifer. Hydraulic parameters were further investigated as part of this project and are discussed in further detail in the Results and Discussion.

**Wood Creek Sand Channel Redox Conditions**

Dissolved oxygen (DO) levels in the aquifer were less than 1.0 mg/L suggesting the aquifer is at least mildly anaerobic. Lyngkilde and Christensen (1992) provide useful guidance for assigning redox zones in groundwater using indicator parameters. Table 2-2 provides a summary of background concentrations of redox parameters reported at injection wells STP-07-158-SS and STP-07-159-SS. Compared to their criteria, the dissolved oxygen and nitrate concentrations in the WCSC are too low for aerobic or nitrate-reducing reactions to be of significance. In the absence of dissolved oxygen and nitrate, manganese and iron reduction are the thermodynamically and metabolically favoured terminal electron accepting processes in groundwater systems where sufficient Mn(IV) and/or Fe(III) are available from aquifer solids (Chapelle and Lovley, 1992). In most aquifer systems, Fe(III) oxides will be the most abundant oxidants when conditions shift from aerobic to anaerobic (Stumm and Sulzberger, 1992). The

dissolved concentrations of oxygen, nitrate, nitrite, and sulfate in the WCSC compare favourably to those typical of the Mn(IV) and Fe(III) reducing zones observed by Lyngkilde and Christensen (1992) in a landfill leachate plume (Table 2-2). While the dissolved Mn(II) and Fe(II) concentrations in the WCSC are below levels specified as typical of manganogenic or ferrogenic conditions, this does not preclude the possibility of Mn(IV) or Fe(III) reduction. Mn(IV) and Fe(III) are relatively insoluble at near neutral pH and will be available for reaction from the aquifer solids. Therefore, the presence of the more soluble reduced species is generally the best way to demonstrate manganogenic or ferrogenic conditions from groundwater geochemistry. This characterization is not straightforward, however, because Mn(II) and Fe(II) will associate with aquifer solids through adsorption or precipitation as carbonate, sulfide, or oxide mineral coatings depending on pH, redox conditions, and aqueous and solid phase geochemistry (Baedecker et al., 1993; Heron and Christensen, 1995; Heron et al., 1994; Hunter et al., 1998). The dissolved concentrations of Mn(II) and Fe(II) are therefore in many cases less than predicted from balanced stoichiometric equations of the oxidation of organic carbon with Fe(III) or Mn(IV) functioning as the terminal electron acceptors.

## 2.2 Oils Sands Mining and Extraction Process

Currently, the majority of bitumen in the oil sands is extracted using surface mining techniques dependent on hydraulic shovels and heavy haulers to excavate and transport oil sand ore to upgrading facilities. Estimates project that 65 billion barrels of oil can be produced using these methods (Government of Alberta, 2008). In situ technologies, such as steam assisted gravity drainage (SAGD), are beginning to come online in areas where the oil sands are buried too deeply to be extracted using surface mining techniques.

Where surface mining is used, the McMurray Formation is overlain by 30 m of overburden on average such that the production of 1 U.S. (0.16 $m^3$) barrel of oil will require the excavation of one-half tonne of overburden and 2 tonnes of oil sand ore containing 10% bitumen (Schramm, et al., 2000). The heavy haulers used to move the ore have loading capacities between 100 and 400 tonnes while the hydraulic shovels are capable of digging 80 to 90 tonnes per scoop (Government of Alberta, 2008). Once loaded, the haulers dump each load into crushers where the oil sands ore is broken into smaller chunks. Suncor uses hydrotransport pipelines to move the ore from the mines to the extraction facilities by mixing the oil sand with hot water to create

a slurry. During hydrotransport, conditioning of the ore is initiated. In addition to hot water, the ore was originally mixed with sodium hydroxide (NaOH). The sodium ions bond with naphthenic acids, which occur naturally in the bitumen, to form naphthenates. By increasing pH, the addition of the NaOH also increased the concentration of naphthenates that could dissolve into the slurry. Most significantly, because the naphthenates have hydrophilic and hydrophobic components, they behave as surfactants, reducing the surface tension on the film of water between the mineral grain and the bitumen, allowing the bitumen to break free from the solid (Schramm, 2000; Quagraine et al., 2005). At present, because Suncor recycles the majority of its extraction water from the tailings ponds, they have no need to add process chemicals because of the high concentration of ions already dissolved in the tailings water.

Hydrotransport pipelines move the oil sand slurry to separation vessels where three layers form. The bitumen attaches to air bubbles and floats to the top of the vessel. Sand sinks to the bottom and is removed for tailings pond beach and dike construction. The layer between the sand and the bitumen froth, the "middlings" - composed of water, unextracted bitumen, and fine minerals - is reprocessed to remove the maximum amount of bitumen. After secondary extraction, the middlings are discharged to tailings ponds. The bitumen froth then undergoes a series of upgrading processes including coking or catalytic conversion, distillation, and hydrotreating to produce lighter crude oil to be shipped to refineries for final processing.

## 2.3 Tailings Ponds

The final waste by-product of the extraction process is a slurry of water, solids and unextracted bitumen in an approximate proportion of 50:50:1 by weight, respectively (MacKinnon, 1981). The waste slurry is transported via pipeline to the tailings ponds, where upon discharging, more than 95% of the coarse solids in the slurry (particles larger than 22 μm) settle out for use in dike and beach construction. Approximately 50% of the fines (particles less than 22 μm) also settle out or are trapped by the coarse solids as they settle to form the beaches. The "thin slurry" that ultimately discharges to the pond is composed of 7 to 10% solids by weight (MacKinnon, 1989).

Following the caustic hot water extraction process, the mineral grains in the tailings slurry remain "water wet." As a result, it can take decades for the solids discharged to the tailings ponds to settle out of suspension (MacKinnon, 1989). Tailings ponds therefore become highly

stratified. Particulate matter settles out of the upper ten meters rapidly, creating a relatively sediment free zone with less than 0.5% solid particulate matter (SPM) that is recycled for use in the extraction process. From approximately 10-11 m, a pynocline develops where the density of the water changes to an immature sludge. The immature sludge zone extends from 11-17 m and is composed of 10-30% SPM. Primarily, these are particulates that settle out in 2-3 years. Mature fine tailings composed of 25-50% SPM are found below 17 meters (MacKinnon, 1989).

Tailings pond water has a pH of 8.0-8.4 with a moderate hardness (15-25 mg/L $Ca^{2+}$ and 5-10 mg/L $Mg^{2+}$) and an alkalinity of 800-1,000 mg/L as $HCO_3^-$. Total dissolved solids (TDS) concentrations are increasing at ~75 mg/L per year in tailings ponds at Syncrude and Suncor, with levels already considered slightly brackish at concentrations of 2,000 to 2,500 mg/L. The primary dissolved solids include sodium (500-700 mg/L), bicarbonate (75-550 mg/L), chloride (75-550 mg/L) and sulphate (200-300 mg/L). Bitumen not recovered during the extraction process and naphthenic acids are the primary organic compounds in tailings water, but benzene, toluene, phenols and polycyclic aromatic hydrocarbons (PAHs) are also frequently detected, generally at low concentrations (Allen, 2008). STP tailings water major ion geochemistry as reported from the PA water injectate samples are presented in Table 2-3. Concentrations are similar to those listed above.

## 2.4 Water Usage

In 2006, Suncor withdrew 50.9 million $m^3$ of freshwater from the Athabasca River (0.3% of the River's total annual flow) and another 0.3 million $m^3$ from groundwater wells, a water withdrawal intensity of 3.3 $m^3$ of freshwater withdrawn per 1 $m^3$ of bitumen produced (Suncor, 2007). Water recycled from the tailings ponds provided the balance of water needed in extraction and operations on-site.

## 2.5 Naphthenic Acids

The primary source of toxicity in the water of the tailings ponds are a group of non-volatile, chemically stable, organic compounds called naphthenic acids (Clemente and Fedorak, 2005; Headley and McMartin, 2004; MacKinnon and Boerger, 1986; Holowenko et al., 2002). Naphthenic acids are created through the biodegradation of mature oil. On average, the mass of naphthenic acids in Athabasca oil sand ore is 200 mg/kg (Clemente and Fedorak, 2005).

Clemente et al. (2003) reported a sample of Suncor ore contained 370 mg/kg of naphthenic acids. Because NAs are highly corrosive, they damage oil transport pipelines, so their removal from the bitumen during extraction is important (Quagraine et al., 2005).

### 2.5.1 Naphthenic Acid Chemistry

Naphthenic acids are a group of alkyl-substituted acyclic and cycloaliphatic carboxylic acids with the general formula: $C_nH_{2n+z}O_2$ where n represents the number of carbon atoms in the molecule and z is 0 or a negative, even integer that accounts for hydrogen deficiency in the molecule as the result of ring formation. The absolute value of z divided by two will be the number of rings in the NA structure, with Z=0 corresponding to saturated linear or branched hydrocarbon chains, Z=-2 for monocyclic NAs, Z=-4 for bicyclic NAs, etc. (Headley and McMartin, 2004). The ring structures are normally composed of 5 or 6 carbon atoms (Holowenko et al., 2001). In most instances, the carboxyl group will bond to a side chain rather than directly to the cycloalkane (Brient et al, 1995). The molecular weight of NAs can range from 200 to 700 with the peak distribution between 300 and 400 (Brient et al., 1995). Generally, there are between 5 and 33 carbon atoms in a NA molecule from oil sands PA water (Holowenko et al., 2002). Figure 2-4 shows the structure of NAs with Z = 0, -2, -4, or -6 and 5 or 6 carbons in the ring structure.

Pure phase naphthenic acids are a viscous liquid with a yellow to dark amber colour with a wide range of boiling points (250-350°C) (Brient et al, 1995). NAs are non-volatile and chemically stable (Clemente and Fedorak, 2005), with non-volatility and polarity of the molecule increasing with molecular weight (Headley and McMartin, 2004).

### 2.5.2 Occurrence and Toxicity of Naphthenic Acids

Naphthenic acids are normally insoluble in water, with a maximum solubility less than 50 mg/L at neutral pH (Brient et al., 1995). However, the addition of NaOH to the process stream during bitumen extraction significantly increases their solubility. The sodium ions combine with the NAs to form sodium naphthenates that are more readily solubilised in the elevated pH conditions of the process water (Schramm et al., 2000; Headley and McMartin, 2004; Clemente and Fedorak, 2005).

Naphthenic acid concentrations in the rivers around Fort McMurray are generally less than 1 mg/L (Headley and McMartin, 2004). Tailings pond waters have 20 to 120 mg/L and concentrations of 0.4 to 51 mg/L have been reported for groundwater samples collected near the tailings ponds (Clemente and Fedorak, 2005). While tricyclic acids (Z=-6) dominate the naphthenic acid fraction of unrefined bitumen (>90% of the total carboxylic fraction), no single Z-group between Z=0 and Z=-6 is predominant in the tailings water. NAs with Z=-8 to -12 comprise a large portion of the NA fraction in PA water as well (Headley and McMartin, 2004).

An early study by MacKinnon and Retallack (1981) found PA water to be highly toxic to rainbow trout and fathead minnows with 96-hour $LC_{50}$ values of less than 10% for both. They found it to be only slightly less toxic to the crustacean *Daphnia magna* with a 96-hour $LC_{50}$ value of 20%. Based on their ability to detoxify the water with acid chemical treatments and their inability to significantly reduce the toxicity with base chemical treatments despite removing similar amounts of dissolved organic carbon (DOC), they hypothesized that the main source of toxicity must be the organic acids.

### 2.5.3 Naphthenic Acid Degradation

MacKinnon and Boerger (1986) found the toxicity of tailings water declined with aging. Herman et al. (1994) determined that aerobic microbial populations from oil sands tailings water could degrade NAs with the biodegradation apparently contributing to the reduction in toxicity of the NA mixtures studied. To further understand the decrease in toxicity, Holowenko et al. (2002) examined shifts in the relative proportion of naphthenic acid isomer groups in PA water with aging. They found that with age, the relative proportion of NAs with 22 or more carbon atoms increased while the percentage of NAs with lower carbon numbers decreased. They concluded that the lower molecular weight NAs were more biodegradable and likely contribute more to the toxicity of PA water. Using improved analytical techniques, Bataineh et al. (2006) and Han et al. (2008) have since determined that carbon number has minimal or no influence on the biodegradability of naphthenic acids. Instead, they found that cyclization (Z-number), alkyl-branching, alkanoate-branching, and stereoisomerism are the primary structural features controlling biodegradability (Bataineh et al, 2006; Han et al., 2008; Smith et al., 2008). Han et al. (2008) hypothesized β-oxidation is the most likely pathway by which microorganisms will

metabolize naphthenic acids, with α-oxidation and aromatization contributing to the degradation of certain NA isomers.

To test the influence of alkyl-branching on the biodegradability of naphthenic acids, Smith et al. (2008) created four surrogate NAs of butylcyclohexylbutanoic acid (BCHBA), with identical cycloalkane and alkanoate structures, but different branched and unbranched alkyl (butyl) substituents. The surrogates created were *n*-BCHBA, *sec*-BCHBA, *iso*-BCHBA and *tert*-BCHBA where *n*-, *iso*-, *sec*- and *tert*- describe the arrangement of the alkyl substituent as depicted in Figure 2-5. Additionally, they created a fifth surrogate, isobutylcyclohexylpentanoic acid (*iso*-BCHPA), with branching on both the alkyl and alkanoate (carboxyl) substituents. The difference in the arrangement of the alkanoate substituents of BCHBA and BCHPA is illustrated in Figure 2-6. Biodegradability of the surrogate NAs was tested in aerobic microcosms inoculated with bacteria isolated from boatyard sediments where periodic hydrocarbons spills occurred.

The results reported by Smith et al. (2008) were consistent with those observed by Bataineh et al. (2006) and Han et al. (2008). The most highly branched NA (*tert*-BCHBA) was most resistant to biodegradation by the consortium of microbes. The least branched surrogate, *n*-BCHBA, underwent the greatest amount of biodegradation (97% in 9 days) followed by *iso*-BCHBA (77% in 30 days), *sec*-BCHBA (47% in 30 days) and finally *tert*-BCHBA (2.5% in 30 days). Additionally, they found the position of the butyl and alkanoate functional groups on the cyclohexane ring structure influenced biodegradability. Two GC/MS peaks were present for each surrogate NA, one for *cis* and one for *trans* isomers. While the researchers were unable to assign the peaks to the *cis* or *trans* stereoisomers, they determined the stereoisomer that eluted second in the GC/MS scan was more susceptible to biodegradation.

Biotransformation of the *iso*-BCHPA was not observed after 42 days of incubation in the bacterial consortium. This proved that branching on the alkanoate side chain is a greater inhibitor to naphthenic acid biodegradation than alkyl-branching (although alkyl-branching is still significant). Further, Smith et al. (2008) identified the metabolites of the BCHBA biotransformations to be butylcyclohexylethanoic acids. These compounds are the most likely by-products generated in the β-oxidation of cyclohexylalkyl acids demonstrating β-oxidation was a dominant degradation pathway of the surrogate NAs.

# 3 Methods and Materials

The In Situ Aquifer Test Facility (ISATF) was built at the Southeast corner of the STP to meet the research goals of this study and establish a functional test facility that could be used and expanded by future researchers. Currently, the ISATF consists of two injection/monitoring wells, two multi-level well nests, and an injection system.

## 3.1 Injection Well Construction

Two standard 2-inch PVC wells were installed at the ISATF to facilitate the injection of PA water into the WCSC. The wells are screened at different depths to permit study of potentially different redox environments within the aquifer. Field geologists for Klohn Crippen Berger noted the uncontaminated WCSC sediments changed colour from yellowish red to gray with depth, indicating a possible shift from oxidizing to reducing conditions. Oiffer (2006) concluded that a similar color change in a sand aquifer adjacent to a Syncrude tailings pond was a transition between variously weathered soils developed shortly after the sand's deposition and had no bearing on the current terminal electron accepting process in the aquifer. Nonetheless, the color change in the WCSC is indicative of unique chemistries on the outer surfaces of the mineral grains so it is plausible that injectate plumes could interact differently.

Installation of the injection wells was completed from April 9-10, 2007 using dual rotary drilling techniques with oversight from Klohn Crippen Berger (KCB) field personnel. The wells are constructed of 2-Inch Schedule 80 PVC and screened with 1.5 meters of 0.040-Inch Slot PVC screen. Each well has two ID numbers; a KCB ID and a Suncor ID. The shallow well (KCB ID: MW07-035; Suncor ID: STP-07-158-SS) is screened within yellowish-red sand from approximately 15.5 to 17.0 m below ground surface (bgs). The deeper well (KCB ID: MW07-034; Suncor ID: STP-07-159-SS) extends into gray sand first encountered at approximately 26 m bgs and is screened from roughly 27.5 to 29 m bgs (KCB well logs list the screened interval as 27 to 28.5 m bgs, but field measurements taken on November 6, 2007 indicate the bottom of this well is actually 29 m bgs). The KCB well construction diagrams are provided in Appendix A. Because KCB produced these diagrams, the wells are labelled with KCB IDs. For all other aspects of this project, the Suncor well IDs will be used.

The injection wells also functioned as monitoring points. Following release of the plumes, groundwater flow pushed the up-gradient side of the injectate back through the injection wells. As a result, the evolution of the up-gradient half of the plume could be studied through monitoring and sampling at the injection point. This required special instrumentation that will be described in Section 3.1.2.

### 3.1.1 Monitoring Well Installation and Construction

Monitoring the evolution of the plumes at the injection points was straightforward and did not require an understanding of groundwater velocity or flow direction. However, the plumes were only able to interact with a small volume of aquifer before moving through/past the injection points, limiting the time period and volume of aquifer material in which geochemical or metabolic reactions could occur. To permit study of plumes after longer residence times and exposure to larger volumes of aquifer, monitoring points were installed in the presumed down-gradient direction of each injection well. The layout of the ISATF and position of the injection and monitoring wells is shown in Figures 3-1 and 3-2.

Monitoring and modelling of water levels within the WCSC by KCB identified southeast to northwest regional flow through the channel. In contrast, groundwater elevations measured between May 26 and June 3, 2008 from the injection wells and a nearby monitoring well (STP-04-40-SS) suggested local flow at the ISATF was to the south-southwest at a bearing between 195° and 204°. Because local deviations from regional flow direction are likely, the groundwater elevation data was considered representative of the site's flow regime. The monitoring well nests were therefore positioned to the south-southwest of the injection wells at a bearing of approximately 200°. Due to the uncertainty of groundwater flow direction, the monitoring well nests were positioned close to the injection wells to maximize the likelihood of intercepting the injectate.

Installation of the monitoring well nests was completed from June 20-22, 2008 using rotosonic drilling techniques. Continuous soil cores were collected at each boring location using a 4-Inch outside diameter (OD) core barrel. Sample cores were logged for lithology, photographed, and sampled for hydraulic conductivity testing and extractable metals analysis. To prevent borehole collapse during withdrawal of the core barrel, a 5 ½-Inch OD outer casing was advanced behind the core barrel.

Monitoring well nest STP-08-158A was installed 3.7 meters south-southwest of injection well STP-07-158-SS. The borehole for the well nest was drilled to a final depth of 19.8 m bgs. A cobble blocked the rotosonic cutting shoe from 0 to 6 m bgs, limiting recovery across that interval to 0.3 meters. A large boulder at 12.5 m bgs damaged the drill bit and rods and prevented recovery of soil core from ~12.5 to 15.25 m bgs. Aside from these intervals, continuous cores were collected to 19.8 m bgs. Soil core photographs are provided in Appendix B and a description of the core material is included in the STP-08-158A well log (Appendix D). Depth intervals in the photographs in Appendices B and C are labelled in feet rather than meters because the drill rods and core barrels were 5 or 10 feet. Rather than convert to metric units, the use of consistent units in the field expedited logging and photographing. Generally, the core barrel was advanced 10 feet in each run and then withdrawn to transfer the core material to plastic liners. In a few instances, the length of the core in the plastic liners was only 8-9 feet. This does not mean the bottom 1-2 feet of sediments were lost from the soil core. Instead, compaction during drilling and/or the process used to transfer the sediments from the core barrel to the plastic liner made it appear as though there was not a full 10 feet of recovery.

After reaching the target depth, three, 1-inch diameter schedule 40 PVC wells were installed in the borehole with each 1.5 meter screen positioned at different depths. Machine slotted 1-inch screens were not available, so screens were hand slotted with a hacksaw. To prevent sand from entering the wells, the screens were wrapped with filter fabric as shown in Figure 3-3 and 3-4. The original plan was to place the deepest well of the cluster at the base of the borehole and slowly withdraw the drill rods to allow the sandy formation to collapse into the annular space around the well and form a natural filter pack. After pulling the drill stem up 2 meters, the second, intermediate well would be installed, with the base of the well resting upon the soil that collapsed into the borehole. The ultimate goal was to have the base of the second/intermediate well 0.5 meters above the top of the first/deep well screen and to have the base of the third/shallow well 0.5 meters above the top of the second/intermediate well screen with natural filter pack around all wells.

In keeping with this plan, the first well (STP-08-158A3) was placed in the borehole with the base of the screen situated approximately 19.4 m bgs. Unfortunately, the syringe-like action of withdrawing the drill stem caused running sands to flow inside the rods. Sand filled the rods and

borehole to approximately 15.5 m bgs so that it was not possible to install the intermediate well to its target depth. The drillers attempted to re-drill the hole from 15.5 to 17.0 m bgs, but had a difficult time forcing the sand out of the rods. Because the deep well was locked in place by the running sands, the attempt to re-drill the hole damaged it. It appears that the torque from the drill stem broke the well screen away from the PVC riser. Because of this damage, the well provides elevation data, but is nearly impossible to sample (sampling pulls sand in through the base of the well).

After re-drilling to 17.0 m bgs, an alternative installation methodology was employed for the intermediate (STP-08-158A2) and shallow (STP-08-158A1) wells. The wells were placed in the borehole simultaneously with the shallow well (STP-08-158A1) modified to position the screen at the correct depth. A 2 meter length of 1-inch schedule 40 PVC was added to the base of the well as a riser to elevate the bottom of the screen to 15.25 m bgs. A PVC cap was installed between the base of the screen and the riser so there was not a sump/reservoir of water below the screen. This installation positioned the STP-08-158A1 well screen from 13.75 to 15.25 m bgs and the STP-08-158A2 well screen from 15.5 to 17.0 m bgs. A small amount of sandpack was installed around the wells to lock them in position while the drill rods were withdrawn from the hole. The entire length of drill rods were then withdrawn to allow the formation to collapse into the annular space. This filled the borehole to 1.25 m bgs. The annular space from 0 to 1.25 m bgs was backfilled with hydrated granular bentonite to prevent preferential infiltration and recharge down the borehole. Well construction details are provided in Appendix D.

Monitoring well nest STP-08-159A was installed 8.6 meters south-southwest of injection well STP-07-159-SS with the borehole drilled to a final depth of 31.5 m bgs. The core material from 0.0 to 13.41 m bgs, 15.25-16.75 m bgs, 23.75-24.4 m bgs and 31.0 to 31.5 m bgs was immediately placed in 4-inch split PVC, capped, duct taped, and placed in freezers at the end of the day to provide material for geochemical analysis. To limit atmospheric exposure, the bags that held the core material were not cut open, and as such, the soil from 0.0 to 13.41 m bgs was not photographed or described. A drill rod broke between 26 and 29 m bgs, preventing recovery of soil core from that interval. Photographs are provided in Appendix C and a description of the core material is included in the STP-08-159A well log (Appendix D).

The installation methodology used for STP-08-158A1 and STP-08-158A2 was repeated for the entire STP-08-159A cluster. Schedule 40 PVC riser was attached below the screened intervals of each well to position the screens at their target depths. The borehole remained opened to approximately 31.5 m bgs, requiring the use of 0.25 m of riser on the deep well (STP-08-159A3) to position the screen from 29.75 to 31.25 m bgs; 2.25 m of riser on the intermediate well (STP-08-159A2) to position the screen from 27.75 to 29.25 m bgs; and 4.25 m of riser on the shallow well (STP-08-159A1) to position the screen from 25.75 to 27.25 m bgs. As above, a PVC cap was installed between the base of the screens and the risers so that there was not a sump/reservoir of water below the screen. A filterpack of Target® Filter Sand was installed from 24.5 m bgs to 31.5 m bgs and capped with a seal of hydrated bentonite pellets from 19.8 to 24.5 m bgs. The formation was allowed to collapse into the annular space from the top of the bentonite seal. The upper 0.9 m was backfilled with hydrated bentonite pellets. Well construction details are provided in Appendix D.

Monitoring well STP-08-158A1, STP-08-158A2, STP-08-159A1, STP-08-159A2 and STP-08-159A3 were developed with a Waterra foot-valve connected to dedicated 1/2" x 5/8" polyethylene tubing. Approximately 95 litres was pumped from each well. Attempts to develop STP-08-158A3 were unsuccessful and pulled sand into the well.

### 3.1.2 Well Instrumentation

Mixing and diffusion between water in the screened interval and the overlying stagnant water column of the injection wells had to be limited if they were to serve a dual function as injection and monitoring points. Isolation of the screened interval had to be accomplished in a manner that permitted passive monitoring with dataloggers and collection of groundwater samples. To meet these objectives, each well was fitted with a RST Instruments N-Packer, a Schlumberger CTD-diver (monitors groundwater conductivity, temperature and groundwater elevation), and a Grundfos Redi-flo 2 submersible pump connected to 3/8" x 1/2" polyethylene tubing. The packers were modified at the University of Waterloo to allow the wires and tubing of the probe and sample pump to pass through the packer and up the well casing to ground surface, making it possible to sample the well without removing the packer. The bases of the packers were positioned just above the top of the well screens so that the probes and pumps were suspended

within the screened intervals. Photographs of the packer/probe/pump system are provided in Figures 3-5 through 3-8.

CTD-Divers were also placed in each of the wells in the monitoring well nests. Additionally, a Solinst Barologger was deployed to record shifts in barometric pressure which were used to correct the pressure readings recorded by the Divers. The barologger was placed approximately 4 m bgs in monitoring well STP-08-159A3 so that it remained within a relatively constant temperature setting above the water table.

## 3.2 Injection Process and System Design

The injection system was designed for the controlled, rapid release of a known volume of water (PA or "natural") via gravity drainage. It consists of a 275-gallon (~1000 litre) polyethylene tank fitted with a valve, 2-inch PVC pipes, and a standard garden hose. The tank sits on an earthen mound constructed approximately 3 meters west of STP-07-159-SS. The purpose of the mound is to elevate the tank's base above the top of the injection wells' PVC risers (Figure 3-2). The mound, which is topped by a platform of 4" x 4" boards, is approximately 7 meters by 7 meters in length and width and 0.75 meters in height. The tank's stand elevates its lower outlet an additional 0.5 meters. When set up, the base of the elbow exiting the injection tank is approximately 1.25 meters above ground level. This set up ensures that all water drains from the tank and associated piping during injection. To accommodate the injections, the wells' risers were fitted with PVC "$T^{S}$" to allow insertion of the garden hose into the wells without removing the packer/pump/probe systems. For injections, the garden hose was placed approximately 5 meters into the well, creating a hydraulic gradient to drive the injections. The valve at the base of the tank was then opened, initiating the injection. With the water table roughly 15 meters bgs, this injection set up allowed the water to cascade across a length of approximately 10 meters from the outlet of the garden hose to the top of the water column in the well. The injection system is shown in Figures 3-9 and 3-10.

Water used for the preliminary injections was drawn directly from the WCSC to minimize the geochemical differences between the injectate and porewater. Approximately 1,000 litres were pumped from the well where the injection was to be completed. The water was pumped into the injection/holding tank where 42 g of sodium acetate ($NaCH_3COO$) and 322 g of sodium bromide

(NaBr) were added and mixed for 1 hour to bring the dissolved concentrations of acetate and bromide to approximately 30 and 250 mg/L, respectively. Groundwater parameters measured during pumping are provided in Tables 3-1 and 3-2.

The preliminary injection at STP-07-158-SS was completed on June 4, 2008. Nine hundred forty litres of injectate marked with sodium bromide and sodium acetate were released into STP-07-158-SS in 5 hours and 11 minutes (an average injection rate of 3.02 litres per minute (lpm)). This injection rate was significantly slower than all other injections at the ISATF. Instead of inserting the garden hose into the injection well, the outlet was placed near the top of the well, limiting the head gradient from the tank to the hose outlet and reducing the gravitational driving force for the injection. As the injection proceeded, the gradient became smaller and consequently, the injection rate dropped off. For all injections that followed, the garden hose was inserted approximately 5 meters into the well, increasing the head gradients and injection rates. As an example, the preliminary injection at STP-07-159-SS was completed on June 5, 2008 in 1 hour and 5 minutes because the hose was inserted into the well. A total of 1,020 Ls was injected at STP-07-159-SS for an average injection rate of 15.7 lpm. Immediately after completing the injections, the RST packer in the injection well was inflated to approximately 100 P.S.I. to isolate the well screen.

Approximately 3,000 litres of STP-derived PA water was injected at STP-07-158-SS on July 17, 2008. On August 7, 2008, approximately 4,000 litres of PA water was injected at STP-07-159-SS. The PA water was withdrawn from the STP with a vacuum truck (Figure 3-11) and transported to the ISATF. Because of the limited capacity of the ISATF's holding tank, successive 1,000 L injections were completed to reach 3,000 and 4,000 L. The PA water was transferred from the vacuum truck to the holding tank (Figure 3-12) where it was marked with chloride, bromide or boron conservative tracers which were pre-dissolved in 18.9 litre carboys. Details on the duration of the injections, concentration of tracers added, volumes injected, pH, and DO concentrations of the PA water are provided in Table 3-3. The PA water had high concentrations of chloride (500 to >600 mg/L in STP water) such that ultimately, chloride concentrations were most useful as the conservative tracer. This was fortunate because the sampling frequency (once a week) was too low to discern concentration trends from the individual tracers. For future injections, the use of multiple tracers could provide insight into the

hydraulics of the flow system, but will require more frequent sample collection. Immediately after completing the PA water injections, the RST packer in the injection well was inflated to approximately 100 P.S.I. to isolate the well screen.

### 3.3 Groundwater Sample Collection and Analysis

The goal of groundwater sampling was to collect representative samples while minimizing purge volumes to avoid impacting the natural migration of the plumes. This was complicated at the ISATF because of the site's flat hydraulic gradient, and in turn slow groundwater velocity. Any length of pumping would set up gradients drawing the body of the plume towards the pumping site. Therefore, standard purging procedures (e.g. purging until temperature, pH, DO, turbidity, and conductivity stabilize or pumping 3 well volumes) could not be used.

Submersible pumps were used to collect samples from the injection wells. Pump controls were programmed to the lowest setting that conveyed water to ground surface. At this setting, the pumps yielded approximately 1.6 litres per minute (Lpm). STP-07-158-SS was purged approximately 30 seconds prior to sample collection and STP-07-159-SS was purged approximately 1 minute. The screened interval for each of the injection wells was isolated post injection by the inflation of the packers so it was assumed that water within the screened interval was representative of water from the formation. The goal of the small purges was to remove stagnant water from the pump tubing. The 1-inch monitoring wells were sampled with a Waterra foot-valve connected to 1/2" x 5/8" polyethylene tubing. The screened intervals of these wells were not isolated by packers so mixing and diffusion likely occurred with the overlying water column. Large volume purges from these wells still were not desirable. As such, the foot-valve was lowered within the screened interval and approximately 1-litre was purged prior to sample collection. All pumps and sample tubing were dedicated, eliminating the need for decontamination of sample equipment from well to well.

Measurement of dissolved oxygen (DO), pH, ferrous iron and total iron were completed in the field. pH was measured on unfiltered samples with a Thermo Orion low maintenance triode (Model 9107). DO measurements were also completed on unfiltered samples using either an Orion (835) DO meter or CHEMetrics colorimetric ampoules. Ferrous iron and total iron were measured from samples filtered through an in-line 0.45μm filter using CHEMetric colorimetric

ampoules. Given the necessity of purging small volumes of water to prevent alteration of the injectate plumes' migrations through the aquifer, it was difficult to monitor pH with the Thermo Orion pH probe. The probe had significant "drift" if not given time to stabilize (on the order of 5-10 minutes). Unfortunately, "snapshot" pH measurements were needed. Because of the complications with drift, the Thermo Orion probe used for this fieldwork did not seem capable of providing an accurate or precise snapshot pH measurement. As a result, pH data is sparse. Future fieldwork will require use of an instrument that can yield accurate snapshot measurements of pH.

Table 3-4 describes the preservation technique, glassware, and field filtering used for the various samples. Samples for inorganic analyses (major ions, metals and dissolved ammonia) as well as dissolved organic carbon (DOC) were analyzed by ALS Laboratories. Table 3-5 outlines their methods for these analyses. Immediately after collection, all samples were placed in coolers on ice. If samples were not brought to the ALS Laboratory in Fort McMurray at the end of each day, they were placed in refrigerators in Suncor's Geotechnical/Environmental building until they were delivered to the lab.

Benzene, toluene, ethylbenzene, xylenes (BTEX), trimethylbenzenes (TMB), polyaromatic hydrocarbons (PAHs), naphthenic acids (NAs), acetate and bromide samples were analyzed at the University of Waterloo Organic Geochemistry Laboratory. All samples analyzed at the University of Waterloo were packed in coolers on ice and shipped via a commercial courier for the fastest arrival time. An Orion model 9635 ionplus$^{TM}$ Series bromide ion selective electrode probe connected to an Orion model 290A meter was used for bromide analysis. Acetate was analyzed using a Dionex ICS-2000 ion chromatograph with an ion-eluent generator and conductivity detector and the Dionex IonPac AS18 column. BTEX, TMB and PAHs were analyzed using a gas chromatograph and flame ionization detector (GC-FID) with the results analyzed following the methods of Henderson et al. (1976). Fourier transform infrared spectroscopy (FT-IR) was used to determine total naphthenic acid concentration according to the methods of Jivraj et al. (1995). NA signature was characterized using gas chromatography-mass spectrometry (GC-MS) as described by St. John et al. (1998) and Holowenko et al. (2002). NA signature was also characterized at the University of Alberta's Division of Analytical & Environmental Toxicology using the high performance liquid chromatography/high resolution

mass spectrometry (HPLC/HRMS) method described by Bataineh et al. (2006). Differences in the results produced by these methods are discussed in greater detail in Section 4.6.2.

## 3.4 Sediment Sampling and Analysis

### 3.4.1 Sediment Collection

Sediment samples for extractable elements, FOC and total carbonate analysis were collected during installation of monitoring well nest STP-08-159A. Sediment core for these analyses was collected from three different depths in the WCSC (15.25-16.75 m bgs, 23.75-24.4 m bgs and 31.0-31.5 m bgs). Field handling of the core material is described in Section 3.1.1. The frozen soil cores were transferred from the freezers in Suncor's Geotechnical/Environmental to University of Alberta for storage at -20°C. All subsequent cutting and transfer of core materials was conducted in anaerobic gloveboxes.

### 3.4.2 Trace Element Extractions

The introduction of PA water injectate, with elevated levels of DOC, to the WCSC had the potential to shift the redox conditions of the aquifer system and mobilize trace elements from the aquifer solids. As such, sequential extractions were completed on WCSC sediments to quantify the concentration of extractable trace elements and identify the solid-phases with which they associate.

Sequential extraction of trace elements was completed at the University of British Columbia's Department of Earth and Ocean Sciences. The goal of the extractions was to quantify the concentrations of trace elements associated with five different fractions of the WCSC sediment (easily exchangeable, amorphous and poorly crystalline Fe/Mn/Al oxides and oxyhydroxides, well crystallized Fe/Mn/Al oxides and oxyhydroxides, organic matter and silicates/residual minerals) by progressively exposing the sediment to harsher reagents. The procedure used for these extractions was adapted primarily from the methods described by Herbert (2006), along with procedures outlined by Haque et al. (2008), Tang et al. (2004) and Tessier et al. (1979).

One gram of air-dried sediment from each of the sampled intervals was used for the extractions. The first extraction targeted easily exchangeable trace elements. The 1.0 g sample aliquot was mixed with 10 mL of 1 M magnesium chloride ($MgCl_2$) in a 50 mL polypropylene centrifugation tube and continuously agitated on a shaker for 1 hour at room temperature (20°C). The resulting

mixture was then centrifuged for 45 minutes to separate the supernatant from the sediment residue. The supernatant was placed in polythene bottles and preserved by reducing the pH to less than 2 with nitric acid and storing at 4°C. The sediment residue was washed with 8 mL of deionized water for 15 minutes in a centrifuge.

The second extraction targeted trace elements associated with poorly crystalline Fe/Mn/Al oxides and oxyhydroxides. The sediment residue from the first extraction was placed in a centrifugation tube with 25 mL of 0.25 M hydroxylammonium chloride ($NH_2OH \cdot HCl$) and 0.25 M HCl and kept in a 50°C water bath for 30 minutes with occasional agitation. The mixture was then centrifuged with the resulting supernatant preserved and the residue washed as described above.

The washed residue from the second extraction was then mixed with 20 mL of 0.20 M $NH_2OH \cdot HCl$ and 25% acetic acid ($CH_3COOH$) in a centrifugation tube and placed in a 90°C water bath for 18 hours with occasional agitation. This extraction targeted trace elements associated with well crystallized Fe/Mn/Al oxides and oxyhydroxides. Preservation and storage of the supernatant was as described above. The sediment residue was washed by centrifuging with 8 mL of 25% acetic acid for 15 minutes.

As previously, the washed residue from the third extraction was used for the fourth, which targeted trace elements associated with the sediment's organic fraction and sulfide minerals. In this extraction, the sediment was mixed with 10 mL of 30% hydrogen peroxide ($H_2O_2$) in 0.5 M $HNO_3$ in a centrifugation tube and placed in a water bath at 85°C for 5 hours with occasional agitation. After cooling, 5 mL of 3.2 M ammonium acetate ($CH_3COONH_4$) in 20% $HNO_3$ and 5 ML of deionized water was added and agitated for 30 minutes at room temperature. Again, the supernatant was separated and preserved and the residual soil was washed with deionized water.

For the final extraction, targeting the trace elements associated with silicate and other primary minerals, the remaining sediment residue was placed in a 50 mL Teflon beaker where it was digested with aqua regia (a 1:3 volumetric mixture of analytical grade concentrated $HNO_3$ and HCl) for 1 hour. After evaporating the mixture to near dryness, the residue was re-dissolved and diluted with deionized water. Again, the mixture was centrifuged and the supernatant preserved.

The supernatant produced by each of the five extraction steps was analyzed for Fe, Mn, Al, Zn, Cu, Ag, Ni, Co, Sr, Ba, Cd, Sb, Pb, V, Cr, and As using inductively coupled plasma opitical emission spectrometry (ICP-OES).

### 3.4.3 FOC and TIC

Fraction organic carbon (FOC) and total inorganic carbon (TIC) were analyzed at the University of Waterloo Organic Geochemistry Laboratory. FOC was analyzed using a Lindberg quartz tube furnace and Beckman non-dispersive infrared analyzer based on the method of Churcher and Dickhout (1987). TIC was determined using the technique described by Barker and Chatten (1982). Samples were acidified and the evolved $CO_2$ was measured with a modified headspace gas-chromatographic technique.

## 3.5 Hydraulic Conductivity Measurements

Hydraulic conductivity of the sediment samples was determined using the falling head permeameter at the University of Waterloo following procedures described by Oldham (1998). Sediment samples were collected at 20 to 50 cm intervals in the WCSC from the soil cores generated during the monitoring well installations. Additional discrete samples were collected from zones where grain size distribution appeared different from the WCSC's typical fine to medium sand. Samples were placed in Ziploc bags and shipped back to the University of Waterloo for testing.

For the tests, approximately 80 g of sample was dried, homogenized and repacked into the permeameter for each test. Once in the permeameter, $CO_2$ gas was used to purge air from the sediments' pore space to improve wetting of the soil. Because oxygen does not dissolve well in water, any air left in the samples could potentially occupy pore space and impact the results. Each sample was gradually wetted from the bottom up to further aid in the displacement of air from the pore spaces. Care was taken in wetting the samples so that fines were not forced out of the samples as they were wetted. Once the air was displaced from the sediment, the permeameter was connected to a manometer. Water was then pumped into the manometer to a set head level and all lines were checked for air bubbles. Finally, the valve beneath the permeameter was opened allowing water to drain from the system through the sediment. The time needed for the water level in the manometer to move from an upper head level to a lower

head level was recorded as the system drained. Each sediment sample was tested three times. With this information, the hydraulic conductivity was analyzed with the following equation:

$$K = \frac{aL}{At}\ln\left(\frac{H_o}{H_1}\right) \quad (1)$$

Where K denotes hydraulic conductivity, a is the cross-sectional area of the manometer, L is the length of soil in the permeameter, A is the cross-sectional area of soil in the permeameter, t is the time for the water level in the manometer to move from $H_o$ to $H_1$, $H_o$ is the original height of water in the manometer, and $H_1$ is the final height of water in the manometer.

### 3.6 Development of Visual MODFLOW Groundwater Model

Complications associated with determination of the groundwater flow direction necessitated development of a three-dimensional model with which to evaluate flow scenarios. Visual MODFLOW version 3.0.0 was used for this purpose. Within the software package, the MODFLOW 2000 numeric engine was used to solve groundwater flow with the WHS Solver selected to solve the numeric equations for the flow simulations. Based on the flow solution generated by MODFLOW 2000, the MT3DMS numeric engine was used to solve the advection-dispersion equation in order to model solute/contaminant transport (Waterloo Hydrogeologic Inc., 2006). The upstream finite difference method was used for simulating contaminant transport because it produces a stable solution with relatively short run times. The goal of the model was to develop various flow scenarios that could explain the observed distributions of the chloride tracer. As such, dispersivity, hydraulic conductivity and hydraulic gradient within the model domain were adjusted until the modelled chloride concentration trends matched observed trends. A curved row of "down-gradient" well nests were placed within the model domain to understand the degree to which flow direction could be misinterpreted with injectate still arriving at the wells.

# 4 Results and Discussion

## 4.1 Preliminary Injection Experiments

Previous laboratory studies found naphthenic acids recalcitrant to biodegradation under anaerobic conditions (Holowenko, et al., 2001; Gervais, 2004). From information available, it seemed that an anaerobic microbial community without previous exposure to naphthenic acids would have limited ability to metabolize NAs from PA water. As such, preliminary injections were designed to assess the capacity of the WCSC aquifer's microbes to metabolize a simple organic compound, acetate.

### 4.1.1 Passive Monitoring of Injectate Migration at the Injection Wells - Conductivity

Conductivity, temperature, and water level measurements recorded by the CTD Divers during post-injection monitoring at STP-07-158-SS and STP-07-159-SS are provided in Appendices E and F, respectively. The data is graphically summarized in Figures 4-1 and 4-2. The water pressure function on the Diver deployed at STP-07-159-SS malfunctioned so groundwater elevation data from that instrument during this period is not available.

Conductivity provided a straightforward means to passively monitor the migration of the injectate. The addition of tracers increased the injectate's concentration of total dissolved solids (TDS), elevating the water's conductivity relative to the aquifer porewater. Detection of elevated conductivity was then considered indicative of the presence or arrival of injectate at a well. Increases in conductivity triggered sampling events to confirm plume arrival.

The results of the preliminary injections demonstrated an additional utility of conductivity measurements. When compared to conservative tracer trends, conductivity measurements can provide evidence of reaction between the injectate and aquifer. Because water's electrical conductivity is a function of its TDS, changes in conductivity reflect changes in TDS. Oxidation/reduction and dissolution/precipitation reactions between the aquifer and the injectate could disproportionately change the injectate's TDS relative to the conservative tracer causing an equivalent shift in conductivity. Conversely, without reaction, the dissolved constituents of the injectate would be conservative and conductivity trends would mimic conservative tracer concentrations.

Figures 4-3a and 4-4a show that groundwater conductivity trends deviated from the conservative tracer trends following the preliminary injections at STP-07-158-SS and STP-07-159-SS. This is likely because reaction between the aquifer and injectate caused a net removal of dissolved species.

After the first six to eight days, however, the conductivity and bromide concentration trends match (Figures 4-3b and 4-4b). Once the conductivity trends mimicked the conservative, non-reactive tracer, it can be assumed that TDS was behaving conservatively and therefore, the reactions that initially influenced the concentrations of dissolved constituents had ceased. Because bromide is conservative in most aquifer settings, declines in its concentration are singularly attributed to dilution via dispersion. As such, the similarity of the later time bromide and conductivity curves indicates that dilution drove the later time decreases in TDS, not reaction. Therefore, in the shallow portion of the aquifer tested via injection at STP-07-158-SS, conductivity trends indicate reactions between the injectate and WCSC aquifer removed dissolved constituents for roughly 8 days and then stopped. Likewise, in the deep portion of the aquifer tested by the injection at STP-07-159-SS, significant reaction between the aquifer and injectate appear to have removed dissolved constituents for 6 days and then came to a halt.

Reaction of acetate appears to be the catalyst for these conductivity/TDS trends. Acetate utilization will be discussed in greater detail in Section 4.1.3 but the significant finding related to this discussion was that declines in acetate concentrations not attributable to dilution were observed for roughly 6 days after the injection in the deep part of the aquifer and 8 days following the injection in the shallow part of the aquifer. Acetate concentrations then stabilized (Figures 4-5a and 4-6a). As such, acetate removal occurred at the same time conductivity and bromide concentration trends deviated from one another. This suggests that the reaction that removed acetate from solution drove a net decrease in the TDS of the injectate. At later times, when conductivity trends mimicked bromide concentrations, the TDS concentrations appear to have been controlled by dilution only.

Microbial oxidation of acetate coupled to dissimilatory Fe(III) and/or Mn(IV) reduction was the most probable pathway of acetate degradation in the aquifer (discussion of enzymatic Fe(III) and Mn(IV) reduction over nonenzymatic reduction is presented in Section 4.6.1). If the reaction of

acetate with manganese dioxide ($MnO_2$) is considered, a net decrease in TDS is certainly possible:

$$CH_3COO^- + 4MnO_{2(s)} + 2HCO_3^- + 3H^+ \leftrightarrow 4MnCO_{3(s)} + 4H_2O$$

In lab microcosm studies, Lovely and Phillips (1988) observed that a consortium of microorganisms (GS-15) could oxidize acetate under anaerobic conditions, using Mn(IV) from $MnO_2$ precipitate as the terminal electron acceptor. In those cultures, they observed a conversion of the $MnO_2$ to rhodochrosite ($MnCO_3$), as outlined in the above reaction. Given this reaction pathway, the oxidation of 1 mole of acetate would result in the removal of 2 moles of bicarbonate from the TDS load. Additionally, the removal of acidity in this reaction should function to decrease conductivity. Similar reaction pathways would be expected for Fe(III), but the stoichiometry of the reaction would be dependent on the Fe(III) mineral phase.

Precipitation of siderite ($FeCO_3$) or rhodochrosite ($MnCO_3$) concomitant with the reductive dissolution of Fe(III) or Mn(IV) oxyhydroxides or oxides is crucial in driving the net decline in TDS predicted from the observed conductivity trends. Consider the following reactions:

$$CH_3COO^- + 8Fe^{3+} + 4H_2O \leftrightarrow 8Fe^{2+} + 2HCO_3^- + 9H^+$$

$$CH_3COO^- + 4Mn^{4+} + 4H_2O \leftrightarrow 4Mn^{2+} + 2HCO_3^- + 9H^+$$

where the Fe(III) and Mn(IV) ions would not exist as dissolved species, but instead, would be derived from manganese or iron oxide or oxyhydroxide minerals on the aquifer solids. Reductive dissolution of solid phase Fe(III) and Mn(IV) minerals via oxidation of acetate would therefore mobilize 8 moles of Fe(II) and 4 moles of Mn(II) from the aquifer solids and generate 2 moles of bicarbonate. In this scenario, the metabolism of acetate would increase the TDS and drive up groundwater conductivity.

The groundwater conductivity trends therefore suggest that the oxidation of acetate via dissimilatory reduction of Mn(IV) or Fe(III) causes precipitation of rhodochrosite and/or siderite, resulting in a net decrease in the groundwater's TDS due to removal of bicarbonate from solution. Unfortunately, following the preliminary injections, groundwater samples were only analyzed for acetate and bromide so changes in iron, manganese and bicarbonate concentrations that could further elucidate the reactive processes were not monitored. Previous studies provide

useful analogues for this hypothesis, however. Notably, Nicholson et al. (1983) found that dissolved iron concentrations in the Borden landfill leachate plume were controlled by the precipitation of siderite. There, reductive dissolution of ferric oxyhydroxide mineral coatings mobilized Fe(II) ions into solution, causing siderite supersaturation and precipitation of the mineral. Baedecker et al. (1993) also reported the formation of siderite and ferroan calcite coatings on mineral grains in the anoxic zone of the Bemidji hydrocarbon spill site in Minnesota. Fe(III) reduction was one of the primary mechanisms of hydrocarbon oxidation in the anoxic zone of that spill, providing the Fe(II) for the formation of the mineral coatings. At the Vejen, Denmark landfill leachate plume, Heron and Christensen (1995) examined the distribution of Fe(II) ions mobilized by reductive dissolution of Fe(III) minerals within the substantial Fe(III)/Mn(IV) reducing zone of that plume. In their study less than 2% of the Fe(II) in the aquifer was identified as dissolved Fe(II). The rest was associated with the aquifer solids with nearly 20% sorbed and more than 80% present as ill-defined solid-phase Fe(II) extractable with 5 M HCl. This demonstrated that the majority of Fe(II) mobilized via reductive dissolution did not stay in solution, but instead sorbed or was re-precipitated.

Overall, the strong correlation between the time of acetate degradation and deviation of conductivity and conservative tracer trends suggests groundwater conductivity can function as a simple means to evaluate reaction within the aquifer if the conductivity trends can be compared to conservative tracer breakthrough curves.

### 4.1.2 Passive Monitoring of Injectate Migration at the Injection Wells - Temperature

Temperature signature was also evaluated as a means of monitoring the injectate's migration through the aquifer. The injectate began to equilibrate with air temperatures during storage in the holding tank, increasing its temperature. At STP-07-158-SS, 15.5°C injectate was released into 3.4°C groundwater. Likewise, at STP-07-159-SS, 12°C injectate was released into 3.2°C groundwater. Although the core of the plumes may maintain elevated temperatures for longer time periods, Figures 4-1a and 4-2 show that convection dissipates the heat from the outer portions of the plume, causing temperatures to return to the aquifer's background levels within 10 to 14 days. Therefore, temperature can be used to identify and track the plumes, but only within the first few weeks of injection.

### 4.1.3 Acetate Utilization

Acetate and bromide concentrations from post-preliminary injection samples are provided in Table 4-1. The acetate level reported for sample STP07159-GW24 exceeded the concentration achievable from the mass of sodium acetate added to the injectate and was therefore considered an outlier and excluded from the data evaluation. Samples STP07159-GW27 and STP07159-GW27D (a duplicate sample) were averaged against one another for data analysis. Alternatively, only the reported value from STP07158-GW13 was used in analysis as acetate was not detected in the duplicate sample (STP07158-GW13D).

Acetate concentrations declined to approximately 20% of initial levels within 7-8 days of the injections while bromide levels remained near initial concentrations (Figure 4-5a and 4-6a). After the early decline, acetate concentrations stabilized and did not fall off until the dispersed portion of the plume - as defined by the bromide breakthrough curve - arrived at the well. There were three primary mechanisms by which the acetate concentration could have declined: degradation, adsorption, and dilution. The impact of dilution was accounted for by normalizing concentrations against the bromide conservative tracer with the following equation:

$$C_r = \frac{Acetate\ \ Concentration\ \ \left(\frac{mg}{L}\right) \div Initial\ \ Acetate\ \ Concentrati\ on\ \left(\frac{mg}{L}\right)}{Bromide\ \ Concentration\ \ \left(\frac{mg}{L}\right) \div Initial\ \ Bromide\ \ Concentration\ \ \left(\frac{mg}{L}\right)} = \frac{Ac\ C \div Ac\ C_o}{Br\ C \div Br\ C_o} \quad (1)$$

Plots of normalized acetate concentration and bromide $C/C_o$ are provided in Figures 4-5b and 4-6b. Following typical convention, the initial concentrations ($C_o$) used in these calculations were those reported from the first groundwater samples collected immediately after injection. From the plots of normalized acetate concentrations it is clear that dilution was not the cause of the initial acetate mass loss. If it was, the normalized acetate concentration would be a line with $C_r$=1.

Based on previous studies of acetate adsorption on marine sediments, partitioning of acetate to the aquifer solids would be unlikely to contribute significantly to acetate mass loss. Sansone et al. (1987) completed batch reactor studies using three different marine sediments (an anoxic clastic mud, a fine carbonate beach sand, and a lateritic muddy sand) and found the mean percentages of acetate sorbed from solution to the sediments were 9%, 10%, and 24% for the fine carbonate beach sand, the lateritic muddy sand, and the clastic mud, respectively. The carbonate

beach sand had the lowest percentage of organic carbon and clay while the clastic mud had the highest. They also determined that sorption of the acetate was not limited by the available sorption sites on the sediments. In similar sorption experiments with sediment from Skan Bay, Alaska, Shaw et al. (1984) found 10 to 40% of acetate from solution sorbed to the sediments. The authors do not provide details on the grain size distribution, but note that kelp functions as a major source of carbon to the sediments. Wang and Lee (1993) studied sandy sediments from Flax Pond, a marine marsh connected to Long Island Sound which contained 7% clay and 2.8% carbon by weight to determine adsorption partitioning coefficient ($K_{ads}$) for acetate to these sediments. Plotting the adsorbed acetate concentration (nmol/g) against the dissolved acetate concentration (μM) yielded a linear isotherm whose slope (4.2 ml/g) was the $K_{ads}$. After treating the sediments with peroxide to remove the organic carbon, they found the adsorption partitioning coefficient for acetate was <0.5 ml/g.

After correcting for dilution, there was an approximate 83% acetate mass loss observed at STP-07-158-SS within 6 days of the shallow injection and an approximate 76% acetate mass loss at STP-07-159-SS within 7 days of the deep injection. These percentage losses are much higher than the maximum acetate sorption (40%) observed in the studies discussed above in sediments with greater organic carbon contents than the WCSC (WCSC sediments collected from the STP-08-159A soil core contained only 0.05 to 0.10% FOC by weight – Table 4-43). From Wang and Lee's (1993) results, mass removal via adsorption seems unlikely given these low FOCs.

Researchers have also found that acetate adsorption kinetics are rapid, with equilibrium between the sorbed and non-sorbed phases obtained in 20 minutes or less (Michelson et al., 1989; Sansone et al., 1987). As such, if sorption to WCSC sediments removed acetate from solution, equilibrium should have been achieved between the time the injections were completed and the first groundwater samples were collected. For the shallow injection, the reported acetate concentration of the injectate (sample STP07158-IJ01) was 22.26 mg/L while the concentration of the first groundwater sample (STP07158-GW02 - collected 38 minutes after the injection was finished) was roughly 20% less at 18.01 mg/L (Table 4-1). This 20% decline in concentration in less than an hour is potentially from adsorption. Conversely, adsorption does not appear to be significant in the deeper portion of the aquifer. There, the injectate had an acetate concentration of 23.73 mg/L (sample STP07159-IJ06), while the first groundwater sample (STP07159-GW25 -

the first sample not considered a sample outlier - collected 18.5 hours after the injection was finished) had an acetate concentration only 2% less than the injectate at 23.27 mg/L. Overall, the data indicate sorption may have removed up to 20% of the acetate from the injectate in the shallow portion of the WCSC. However, given the low FOC in WCSC sediments, it would have been unlikely for 20% of the acetate to partition to the aquifer solids. In the deeper portion of the aquifer, acetate mass removal via sorption did not appear significant.

Because acetate adsorption kinetics are rapid, declines in dilution corrected concentrations after 20 minutes can be attributed to degradation. At both injection depths, the largest declines in acetate concentrations were observed over the 5 to 6 days after the first groundwater samples were collected such that the majority of acetate mass loss was likely via degradation. At STP-07-158-SS, when corrected for dilution, the acetate concentration decreased nearly 80%, from 18.01 mg/L to 3.76 mg/L over the 5.6 days between the collection of the first groundwater sample, STP07158-GW02, and the collection of sample STP07158-GW08. Likewise, at STP-07-159-SS, when corrected for dilution, the acetate concentration decreased nearly 75% over the 6 days between collection of STP07159-GW25 and STP07159-GW29 from 23.27 mg/L to 5.79 mg/L.

In the WCSC, acetate was most likely degraded by microbial oxidation coupled to dissimilatory Mn(IV) and/or Fe(III) reduction. Mn(IV) and Fe(III) were available in the aquifer from coatings on the mineral grains as Mn(IV) and Fe(III) oxides and oxyhydroxides. Solid-phase geochemistry is discussed in Section 4.8 and evidence for Mn(IV) and Fe(III) reducing conditions was presented in Section 2.3.

Several studies on landfill leachate plumes found that substantial attenuation of volatile organic compounds (VOCs) and non-volatile organic compounds (NVOCs) occurred within the iron-reducing portions of the plumes (Heron, et al., 1994; Heron and Christensen, 1995; Lyngkilde, et al., 1992; Rugge, et al. 1995). As discussed above, Lovely and Phillips (1988) identified a consortium of Fe(III) and Mn(IV)-reducing microorganisms able to completely oxidize organic substrate to $CO_2$. They outlined the following reaction pathways for acetate oxidation with concomitant Fe (III) or Mn (IV) reduction:

$$CH_3COO^- + 8Fe^{3+} + 3H_2O \leftrightarrow 8Fe^{2+} + HCO_3^- + CO_2 + 8H^+ \qquad \Delta G^o = -814 \text{ kJ/reaction}$$

$$CH_3COO^- + 4MnO_2 + 2HCO_3^- + 3H^+ \leftrightarrow 4MnCO_3 + 4H_2O \qquad \Delta G° = -737 \text{ kJ/reaction}$$

The Fe(III) reaction and standard energy ($\Delta G^o$) available from the reaction, of course, would differ depending on the type of Fe(III) mineral coating the aquifer solids and on temperature. Regardless, the standard energies demonstrate that microbes can gain significant energy for growth by catalyzing the reactions.

As mentioned earlier, groundwater samples were only analyzed for acetate and bromide during this phase of the project. As such, direct geochemical evidence is not available to demonstrate Mn(IV) or Fe(III) reduction. However, dissolved oxygen levels in the aquifer before and after the injections were <1 mg/L and nitrate was not present. The yellow-brown to orange-brown coloration of the aquifer sediments suggests that Fe(III) was available from the aquifer solids. Geochemical evidence from later injections showed an enrichment in dissolved Fe(II) and Mn(II) concentrations following the PA water injections suggesting reductive dissolution of Fe(III) and Mn(IV) minerals occurred in the presence of elevated DOC from the injectate (Figure 4-37).

Acetate utilization rates were determined from the dilution corrected concentration profiles. Figure 4-7 presents acetate concentrations corrected for dilution {(Acetate in mg/L)/($Br/Br_o$)} over the 7-8 day period when significant acetate mass loss was observed. From these plots, the decline in concentration follows a linear trend. The utilization rates would therefore be best characterized as zero-order, where the rate of utilization remains constant and is independent of concentration. Attempts were also made to fit curves typical of first-order and second-order reaction rates to the full dataset. Ultimately, the straight lines typical of zero-order rates were the best fits. From the slope of the best fit lines the acetate utilization rate in the shallow portion of the aquifer was approximately 1.75 mg/L/day, while the rate in the deeper portion of the aquifer was approximately 2.56 mg/L/day.

Following the initial removal of acetate from solution, the concentration trends over the next 30 days show little if any evidence of acetate mass loss aside from that attributable to dilution. With 3-6 mg/L of acetate still present after the initial utilization of the compound, it seems unlikely that availability of organic substrate is the limiting factor in the reaction. Instead, it is more likely the reaction was limited by the availability of nutrients or electron acceptors.

Overall, these results demonstrated the aquifer's microbes had the ability to metabolize an organic substrate, but showed the availability of nutrients or electron acceptors limited the amount of substrate that could be degraded.

## 4.2 Process-Affected Water Injection Experiments

The results above provided evidence of a potentially viable microbial community in the WCSC capable of oxidizing acetate. To directly test the capacity of the microbes in the WCSC to metabolize naphthenic acids, PA water injections were completed. Scott et al. (2005) point out that commercial naphthenic acids are more readily biodegraded than NAs derived from oil sands PA water and therefore are inappropriate to use as surrogates to assess the biodegradability of oil sands NAs. As such, PA water for these injections was extracted directly from the STP. While experiments by Holowenko et al. (2001) and Gervais (2004) found that NAs do not biodegrade in anaerobic microcosms, the goal of the PA injections was to introduce NAs to a natural anaerobic aquifer setting and increase the volume of aquifer material with which the NAs could react to potentially generate a different result.

### 4.2.1 Passive Monitoring of PA Water Injectate Migration at the Injection Wells - Conductivity

The conductivity, temperature, and water level measurements recorded by the CTD Divers during post-injection monitoring at STP-07-158-SS and STP-07-159-SS are provided in Appendices G and H and graphically summarized in Figures 4-8 and 4-9.

Contrary to observations from the preliminary injections, the chloride conservative tracer breakthrough curves and the conductivity trends observed at the injection wells following the PA water injections were similar throughout the duration of post-injection monitoring (Figures 4-10 and 4-11). These trends suggest there was limited, if any, oxidation of organics.

The strong agreement between conductivity and conservative tracer following the PA water injections indicates TDS was conservative such that reactions between the injectate and aquifer, including oxidation of the injectate's DOC, did not occur. Groundwater samples collected following the PA water injection confirmed that DOC and NAs were essentially conservative in the aquifer (this data is presented Section 4.6). In combination with the results from the preliminary experiments, the results of the PA water injections further demonstrated that by

comparing conductivity trends to conservative tracer behaviour, it is possible to gain insight as to whether significant oxidation/reduction and dissolution/precipitation reactions are occurring between the aquifer and injectate to cause shifts in TDS and conductivity.

### 4.2.2 Passive Monitoring of PA Water Injectate Migration at the Injection Wells - Temperature

The temperature of the PA injectate (~23-27°C) was significantly higher than the preliminary injectate (~12-16°C). Along with the larger volumes of water injected, this extended the length of time the plumes maintained easily distinguishable temperature signatures to roughly 30 days. As illustrated in Figures 4-8 and 4-9, the conductivity signatures were still more distinct, and thus a better suited to track the plumes.

## 4.3 Calculation of Groundwater Velocity

The conservative tracer breakthrough curves observed at the injection wells were used to evaluate groundwater velocity through the WCSC. Figure 4-12 shows a conceptual model of the distribution of injectate immediately after injection. Because of the rapid rate of injection, plug flow displacement of the in situ groundwater was assumed, with the injectate displacing groundwater to occupy a cylinder of aquifer material around the well. The dimensions of the cylinder are controlled by the volume of water injected ($V_o$), the porosity of the aquifer (n), and the height of the injection well screen (h). Using these known values, the radial distance (r) the advective portion of the plume extended from the well was calculated with the following equation:

$$r = \left(\frac{V_o/n}{\pi h}\right)^{1/2} \quad (2)$$

The WCSC was assumed to have a porosity of 0.30, a typical value for sandy sediments (Freeze and Cherry, 1979), the injection well screens were 1.5 meters, and injection volumes varied. Using Equation 2, the injectate plumes for the preliminary injections at STP-07-158-SS and STP-07-159-SS had initial radii of 0.81 and 0.84 meters, respectively. For the PA water injections, it was assumed that the successive injections coalesced to form a solid injectate plume equivalent to the total volume of the injection (3,000 or 4,000 Ls), rather than separate, 1,000 L plumes. This assumption should be valid because the time between each injection was small (~15-40

minutes) and the groundwater velocity in the aquifer was slow. Using Equation 2, the injectate plumes for the PA water injections at STP-07-158-SS and STP-07-159-SS had initial radii of 1.46 and 1.68 meters, respectively.

The conservative tracer breakthrough curves were used to determine the time it took the up-gradient advective fronts of the plumes to migrate back to the injection wells. The concentration curves have a Gaussian distribution likely caused by hydrodynamic dispersion. Therefore, it was assumed that the advective front of a plume was defined by the point where the relative concentration of the conservative tracer was 0.5. These points are illustrated on Figure 4-13. It took 31.4 days for natural groundwater flow in the shallow portion of the WCSC to force the up-gradient advective front of the preliminary injectate plume back to injection well STP-07-158-SS. In the deeper portion of the aquifer, 16.0 days were needed for groundwater flow to drive the up-gradient advective front of the preliminary injectate plume back to injection well STP-07-159-SS. By dividing the radii of the plumes by these times, groundwater velocities of 2.6 and 5.3 cm/day were calculated for the shallow and deeper portions of the WCSC, respectively. The velocities calculated from the PA water injections were significantly higher. While larger volumes were injected at both depths, it took 31.4 days for the up-gradient advective front of the shallow PA injectate plume to migrate back to STP-07-158-SS and 16.4 days for the up-gradient advective front of the deep PA injectate plume to migrate back to STP-07-159-SS. Dividing the radii of the PA plumes by these times yielded groundwater velocities of 4.7 and 10.3 cm/day for the shallow and deeper portions of the WCSC, respectively.

From the groundwater elevation data (Table 2-1 and Figures 4-1b, 4-8b, and 4-9b), the increase in velocity from June through July and August was likely the result of increased hydraulic gradients caused by recharge or pressurization of the aquifer. Water levels increased from the beginning of June (the time of the preliminary injections) through mid-July and early-August (the time of the PA water injections). If the increased elevations were from recharge to the WCSC, the recharge presumably occurred through windows or thinned portions of the glacial till. As a consequence of the non-uniform distribution of infiltration, the recharge should have increased gradients from the recharge areas to the rest of the aquifer and in turn drove up groundwater velocities. If the increase in groundwater elevations was related to pressurization of the aquifer as the STP filled, the highest pressures should have been exerted on the aquifer

materials below the pond. The discharge of tailings to the STP would then increase the pressure/hydraulic gradients from the area of higher hydraulic pressure (beneath the STP) to areas of lower hydraulic pressure (away from the STP), driving an increase in groundwater velocity.

### 4.3.1 Calculation of Longitudinal Dispersivity

Groundwater modeling will play a central role as research at the ISATF evolves. Often, in groundwater models, longitudinal dispersivity is used as a "fitting" parameter and is adjusted to meet monotonicity conditions. This is often necessary because of difficulties in quantifying an aquifer's dispersivity so that "real" values are rarely available. Using simplifying assumptions, the longitudinal dispersivity of the WCSC was calculated based on the conservative tracer breakthrough curves from the injection wells. This work should supply well constrained values of the aquifer's longitudinal dispersivity on the 1 to 10 meter scale of these injection experiments such that other parameters that are more difficult to constrain can be altered to fit observed conditions.

The longitudinal hydrodynamic dispersion coefficient ($D_l$) for solute in a given porous medium is defined by the equation:

$$D_l = \alpha_l \cdot v + D_d \quad (3)$$

Where $\alpha_l$ denotes longitudinal dispersivity, v is groundwater velocity, and $D_d$ represents the effective molecular diffusion coefficient of the solute. Sudicky et al. (1983) state it is acceptable to ignore the effective molecular diffusion coefficient if the diffusive spreading of the solute is significantly less than the spreading driven by mechanical dispersion. Mechanical dispersion will overwhelm molecular diffusion in settings with high groundwater velocities. As discussed in the previous section, the groundwater velocity through the WCSC as driven by natural gradients is slow (2-10 cm/day). However, the plumes were introduced to the WCSC through high velocity injections where the injectate would have moved through the aquifer at rates of 9.5 to 12.4 m/day on average. Therefore, dispersion during injection should have been the primary force distributing solute into the aquifer and the main control on the conservative solute breakthrough curves. This assumption will be discussed in greater detail later in this section. At

these high rates of injection, molecular diffusion will have little influence on the overall hydrodynamic dispersion, so equation 3 simplifies to:

$$D_l = \alpha_l \cdot v \quad (4)$$

Following the time period in which relatively undiluted injectate flowed back to the injection wells, the concentration patterns of the tracers in the dispersive fronts of the injectate plumes took on a Gaussian form. From Sudicky et al. (1983), the Gaussian curve can be used to calculate the longitudinal hydrodynamic dispersion by:

$$D_l = \frac{{\sigma_l}^2}{2t} \quad (5)$$

where $\sigma_l$ is one standard deviation beneath the Gaussian curve of the injectate plumes' dispersive fronts as illustrated in Figure 4-14 and t refers to the length of time the injectate flowed through the aquifer to cause the dispersion. In this instance, t equals the total duration of the injections. The area of 68% of the dispersive front (equivalent to one standard deviation) was calculated and projected onto the relative concentration plots to determine the time required for a single standard deviation to migrate past the injection wells. At STP-07-158-SS, one standard deviation migrated past the injection well in 12.3 days following the preliminary injection and 22.4 days following the PA water injection. At STP-07-159-SS it took 13.0 days for one standard deviation of the preliminary injectate to flow past the injection well and 12.8 days for the PA water injectate. These time values were multiplied by the groundwater velocity (calculated in Section 4.3) to determine a length of each standard deviation ($\sigma_l$). Values are provided on Figure 4-14. The $\sigma_l$ and t values were then plugged into equation 5 to calculate the longitudinal hydrodynamic dispersion coefficients ($D_l$) from each injection. These values are listed in Table 4-2.

Equation 4 states that the magnitude of hydrodynamic dispersion will be a function of the aquifer's longitudinal dispersivity and the groundwater velocity. For these experiments, the highest groundwater velocities were attained during the injection phase and as such, the magnitude of the hydrodynamic dispersion coefficient should be primarily a function of the injection velocities, not the natural groundwater flow. Because injection velocities were 2 orders of magnitude greater than groundwater velocities, the longitudinal hydrodynamic dispersion

resulting from natural flow through the aquifer would be 2 orders of magnitude less than the longitudinal hydrodynamic dispersion from the injections. Therefore, hydrodynamic dispersion from the natural flow of the injectate through the aquifer post-injection would have little if any impact on the shape of the conservative tracer breakthrough curves established during injection. As such, by rearranging Equation 4, longitudinal dispersivity, which is a property of the aquifer's heterogeneities, can be calculated by dividing the hydrodynamic dispersion coefficient by the velocity at which the injectate travelled through the aquifer during the injections.

Injectate velocities obviously varied based on distance travelled from the injection well, with the highest velocities at the well screen and the lowest velocities at the plume front. For ease of calculation, an average injectate velocity was computed by dividing the distance the advective front of the injectate travelled from the well (based on the previously presented conceptual model) by the time it took to complete the injections. These velocities and the longitudinal dispersivities calculated from these values are presented in Table 4-2.

This solution of longitudinal dispersivity is based on the assumption that the concentration profiles were created by mechanical dispersive forces during the injections and that natural groundwater flow is too slow relative to the injection velocities to cause significant alteration of the initial concentration profile over the duration of the monitoring. These assumptions were validated with the use of a one-dimensional analytical model developed by Neville (2001) that solves the advection-dispersion equation to output solute concentration profiles. The model was set up to determine the shape of the concentration profiles immediately after the injections. Model inputs are listed in Table 4-3. Molecular diffusion and first order decay coefficients were set to zero and the retardation factor was set at 1 to eliminate the influence of these parameters on the solute distribution. Figure 4-15 shows a comparison of the modelled and observed concentration profiles. For the observed data, time was multiplied by groundwater velocity to convert the x-axis to length units. The similarity of the profiles validates the dispersivity values calculated with the methods above, demonstrates that the concentration profile is established by the injection process, and illustrates that groundwater transport of the injectate back to the well does little to alter the initial distribution of the solute. Further, the conversion of the observed time units via the estimated groundwater velocities to yield lengths that match the x-axis of the

modelled data provides additional support that the assumptions made in calculating the groundwater velocities were correct.

The increase in longitudinal dispersivity from the preliminary to PA water injections is consistent with the observations of Sudicky et al. (1983) that longitudinal dispersivity is scale dependent. Dispersivity increases with distance travelled because of increased interaction with aquifer heterogeneities. Because the volumes of the PA water injections were greater than the preliminary injections, the injectate plumes traveled greater lengths through the aquifer, increasing the longitudinal dispersivities. Significantly, the results of this study indicate that injection velocity does not influence the magnitude of the longitudinal dispersivity. At STP-07-158-SS, the velocity of the PA water injection was twice that of the preliminary injection and the longitudinal dispersivity was more than six times greater. Conversely, the average velocity of the preliminary injection at STP-07-159-SS was nearly twice that of the PA water injection but the longitudinal dispersivity calculated from the higher velocity preliminary injection data was roughly half that of the lower velocity PA water injection.

The longitudinal dispersivities determined from these injections (0.06-0.51 m) are similar to those observed by Sudicky et al. (1983) (0.01-0.08 m) and Freyberg (1986) (0.36 m) during natural gradient tracer experiments at the Borden aquifer. Grain size distribution of the sediments tested at Borden was similar to the WCSC. For the Borden aquifer, Freyberg (1986) projected the asymptotic value of longitudinal dispersivity was 0.49 m. This value was exceeded in the deeper portion of the aquifer during the PA water injection. It may be coincidental that the dispersivities from this project were so similar to those observed at Borden. The injections share similarities with forced-advection experiments that have found significantly higher longitudinal dispersivity values (1.0-15.0 m) than natural gradient tracer experiments (Anderson, 1979). For future injections, it would be informative to increase the injection volume to determine the asymptotic value of longitudinal dispersivity. This would provide insight as to whether these injections yield results closer to natural gradient tracer experiments or forced-advection tests.

## 4.4 Evaluation of Flow Direction and Hydraulic Gradients

### 4.4.1 Groundwater Flow Direction

As discussed in Section 3.1.1, KCB determined regional flow in the WCSC is from the Southeast to Northwest. In contrast, groundwater elevations measured at the ISATF's injections wells and monitoring well STP-04-40-SS on March 10, May 26, June 2 and June 3, 2008 showed local flow at the ISATF was to the south-southwest (Figures 4-17 – 4-19). Because flow on the scale of meters (the ISATF site scale) often deviates from regional flow, the down-gradient monitoring well nests were positioned south-southwest of the injection wells.

Based on this groundwater elevation data, the hydraulic gradient across the site was 0.03 m/m on March 10. On May 26, June 2, and June 3 the gradient was significantly smaller, at 0.004 m/m. Because the site's gradient is relatively flat, measurement uncertainty could significantly impact calculation of the gradient and determination of flow direction. Measurement of groundwater level with a depth-to-water (DTW) meter could introduce uncertainty of +/- 1 cm. With an additional +/- 1 cm uncertainty from surveying the well casings, the total error associated with determining groundwater elevation at each well was +/- 2 cm. By varying the groundwater elevations measured at these 3 wells on June 3, 2008 by +/- 2 cm, it is possible to generate a maximum hydraulic gradient of 0.006 m/m or a minimum gradient of 0.003 m/m. More significantly, by changing elevations +/- 2 cm, it is possible to shift the flow direction between a bearing of 180° and 220°. Overall, the flat gradient at the site exacerbates the impact of uncertainty in measurements and makes it extremely difficult to determine flow direction.

The PA water injections proved the initial interpretation of the ISATF's flow direction was incorrect. Arrival of the core of the PA water plume was not observed at the STP-08-158A well cluster. Injectate may have reached the STP-08-159A well cluster and this evidence will be discussed in Section 4.9. Fortunately, the well nests provided additional data points with which to evaluate groundwater flow direction, supplying further insight as to why injectate may have arrived at STP-08-159A, but not STP-08-158A. Figures 4-20 through 4-26 show groundwater contours from elevations measured at various times between July 2008 and June 2009. To simplify contouring, the groundwater elevations from the 3 wells in each nest were averaged to provide a single data point for the well clusters. Using any single elevation from the well nests would not have significantly altered the layout of the contours. From these figures, it appears

there is a groundwater ridge or divide that strikes from the southwest to northeast though the site with the top of the divide running through well nest STP-08-158A and injection well STP-07-159-SS. Northwest of the divide flow is to the northwest. Southeast of the divide flow is to the southwest. This flow regime would explain the evidence of injectate arrival at STP-08-159A and the absence of injectate detection at STP-08-158A.

Because the wells are screened at different depths in the WCSC, the possibility of different flow systems, and subsequently flow directions, as a function of depth was examined. It was considered possible that interbeds of silt/clay identified during the installations of well nests STP-08-158A and STP-08-159A were laterally extensive and functioned as aquitards hydraulically disconnecting the portion of WCSC screened by the 158-series wells from WCSC screened by the 159-series wells. If this were the case, groundwater flow direction could certainly vary with depth, complicating the evaluation of the site's hydraulic gradients. However, there are several lines of evidence that would suggest this is not the case. First, the silt/clay lenses identified during drilling were generally less than 10 cm and their lateral continuity could not be definitely determined. Additionally, the similarity of the groundwater elevations between the various wells suggested vertical gradients were minimal and pressure was transmitted uniformly through the entire aquifer. The strongest evidence that the deep injection interval was not isolated from the shallow injection depth was the similar response of all ISATF wells to an injection stressor. On August 9, 2008, Foundex completed installation of a depressurization well located roughly 100 m northeast of the ISATF. In finishing the borehole, Foundex flushed a significant volume of water (the volume was not specified) down-hole from approximately 14:30 to 17:00. The well's at the ISATF, regardless of depth, responded to this injection stressor, with elevations abruptly increasing 5-10 cm around 16:00 (Figure 4-27). This response was demonstrative of a strong hydraulic connection across the length of WCSC aquifer screened by these wells.

### 4.4.2 Vertical Hydraulic Gradient and Flow Direction

Installation of multi-level groundwater monitoring well nests provided an opportunity to closely examine the vertical hydraulic gradient at the site. Water levels at STP-08-158A3 responded slowly to the removal or re-introduction of the CTD Diver and depth-to-water meter, presumably because of the damage sustained during installation. Because groundwater elevations measured

at that well were not as precise, the data was excluded from the evaluation of the vertical gradient in the STP-08-158A well nest. Any inaccuracy in groundwater elevation measurements would be especially problematic in this instance where the vertical gradients were small.

Groundwater elevations measured by DTW meter and used in this evaluation are provided in Table 2-1. Groundwater elevations within the well clusters showed vertical flow was downward. At STP-08-158A, on average, the groundwater elevation in the shallow well (STP-08-158A1) was 2 cm greater than the intermediate well (STP-08-158A2) for a downward gradient of 0.011 m/m. Figure 4-28a depicts the groundwater elevations recorded by the CTD Divers at STP-08-158A1 and STP-08-158A2. This figure highlights the similarity of elevations at the wells and the identical trends over the course of nearly a year of monitoring.

In the STP-08-159A well cluster, the groundwater elevation in the shallow well (STP-08-159A1) was approximately 1 cm greater than the deep well (STP-08-159A3), for a downward vertical gradient of 0.003 m/m. The elevations at STP-08-159A1 and STP-08-159A2 were within 1-6 mm and the elevation at one well was not typically higher than the other. As such, the elevations were considered equal. Figure 4-28b depicts the groundwater elevations recorded by the CTD Divers at STP-08-159A well cluster. Unfortunately, the Divers deployed at STP-08-159A2 and STP-08-159A3 began to malfunction in the Fall 2008, so the data sets are not as extensive as those for STP-08-158A. Nonetheless, the figure shows elevations were similar for each of the wells in the cluster and the overall trends were identical for the time period monitored.

It would be inappropriate to draw definitive conclusions about the vertical gradient from any of these measurements as inaccuracies of 1-2 cm in surveying the monitoring wells and measuring water levels should be anticipated. Overall, the groundwater elevations indicate that the lateral and vertical gradients in the WCSC are very small and difficult to definitively discern.

The CTD Divers were extremely useful for recording data at times when it was not practical or possible to make measurements by hand. Due to the frequency at which the Divers recorded data, the readings provided insight into elevation trends over the course of a year that could not be attained from hand recorded measurements. However, the data collected by the Divers was not used to draw further conclusions about vertical or lateral hydraulic gradients at the site. Levels recorded by the Divers were converted to elevations based on initial elevation

measurements made with a DTW meter. Because the Divers deployed in the well clusters were suspended in the wells with strings, consistent redeployment could not be expected after data downloads because of knotting, twisting and/or stretching of the string. As such, deployment and redeployment of the Divers added additional error to the measurements so that it would be inappropriate to draw conclusions about hydraulic gradients with the data.

## 4.5 Hydraulic Conductivity

Sediment hydraulic conductivities (K) from the STP-08-158A and STP-08-159A soil core samples determined by falling head permeameter are listed in Tables 4-4 and 4-5. A hydraulic conductivity/depth profile is presented in Figure 4-29. The fine to medium sand that dominated the profile had a hydraulic conductivity near 1.0x10-4 m/s, while the silt/clay interbeds had K-values of $1x10^{-6}$ to $2x10^{-8}$ m/s. These values are within the range of hydraulic conductivities expected for the grain size distributions observed (Freeze and Cherry, 1979). The permeameter results are consistent with observations made while logging lithology that the Wood Creek Sand Channel is a relatively homogeneous fine to medium sand with trace to little silt that is interrupted by silt/clay seams. The increase in hydraulic conductivity near the base of the profile is also in-line with observations of increased occurrence of coarse sand and gravel with depth.

A low permeability seam with a hydraulic conductivity less than $1.00x10^{-6}$ m/s was observed between 349 and 350 m amsl at both soil boring locations, suggesting this seam extends laterally at least 25 meters (the distance between the borings). Conversely, a low permeability seam was observed at 351 m amsl at boring STP-08-158A that was not evident from the core materials collected at STP-08-159A. Based on these results, a definitive conclusion as to the lateral continuity of the low permeability seams is not possible.

Injection wells STP-07-158-SS and STP-07-159-SS were slug tested by Klohn Crippen Berger. KCB completed three falling head and three rising head slug tests at each well. The results are provided in Table 4-6 and the geometric mean of the K-values from the tests are plotted on Figure 4-29 at the elevation of the mid-point of the well screens. The geometric mean was used in averaging the values from the six tests to minimize the influence of data outliers. Predictably, the K-values produced from the slug tests were higher than those calculated with the falling head permeameter. This is due to the scale dependence of K as a function of the volume of aquifer

material tested. Slug tests consistently yield higher hydraulic conductivities than permeameter tests because they force water through a greater volume of aquifer material, increasing the likelihood of encountering preferential flow paths (Carrera, 1993; Nieman and Rovey, 2009; Schulze-Makuch et al., 1999). As such, the K-values calculated from the falling head permeameter are not representative of the K-values at the field scale of the injection experiments. The usefulness of the permeameter data lies in the ability to test hydraulic conductivity across small intervals (<1 m) and develop a detailed depth vs. K profile that shows the relative variability of hydraulic conductivity with depth.

## 4.6 Investigation of Naphthenic Acid Natural Attenuation

### 4.6.1 Total Naphthenic Acid Concentration Trends

Total naphthenic acid concentrations for the PA water injection samples and post-injection groundwater samples are provided in Table 4-7. Figure 4-30 compares relative concentrations of DOC and total NAs to the chloride conservative tracer. A full summary of the water sample analyses is provided in Tables 4-10 through 4-42.

The strong overall agreement between NA and chloride concentration trends in Figure 4-30 suggests NAs were conservative in the WCSC with dispersive dilution causing the majority of the reduction in NA concentrations. The data from STP-07-158-SS does, however, provide some evidence that microbes in the WCSC may have a limited ability to breakdown the more complex structures of naphthenic acids. As with acetate, the evidence of NA reaction is from samples collected shortly after injection. Also consistent with the observations from the preliminary injections, the later time data shows no evidence of removal of dissolved organics, suggesting nutrient, electron acceptor, and/or substrate availability prevented perpetuation of the reactions.

Between July 23 and August 27, 2008 (6 to 41 days after the injection) the relative concentrations ($C/C_o$) of NAs observed at STP-07-158-SS deviated below the chloride breakthrough curve indicating potential NA mass removal via adsorption or degradation (Figure 4-30a). The NA concentrations for the samples collected over this time period (STP07158-GW15 - STP07158-GW19) were divided by the chloride $C/C_o$ to correct for dilution such that any changes in the "corrected" values could only be from adsorption or degradation. The

dilution corrected concentrations declined from 49.4 mg/L to 38.3 mg/L 20 days after the injection and stabilized near that level for an additional 20 days (Table 4-8 and Figure 4-31).

Consideration of the uncertainty of data presented in Figures 4-30 and 4-31 brings into question whether these declines in NA concentration were from NA mass removal or were simply an artefact of analytical uncertainty. The standard deviation of replicate samples for the FTIR analytical method used to quantify NA concentrations was +/- 3.5 mg/L. That uncertainty was compounded when the NA concentration of each sample was divided by the Co concentration and it's +/- 3.5 mg/L uncertainty. Bevington and Robinson (1992) state that when multiplying two values with uncertainties, the total uncertainty for the product of the multiplication is the square root of the sum of the squares of each uncertainty. For example, if multiplying Sample A with an uncertainty of x by Sample B with and uncertainty of y, the equation for total uncertainty would be as follows:

$$\text{Total Uncertainty} = (x^2 + y^2)^{1/2} \qquad (6)$$

While Bevington and Robinson (1992) apply this analysis to the multiplication of values, the principle should apply to division as well. As such, by dividing a given NA concentration which has an uncertainty of +/-3.5 mg/L by the Co concentration which also has an uncertainty of +/-3.5 mg/L, a total uncertainty of +/-5 mg/L is introduced to the analysis. For the dilution corrected naphthenic acid concentrations, the uncertainty associated with the naphthenic acid concentration was further compounded by dividing that value by the quotient of two other uncertain concentrations, chloride C/Co. Given these complications, naphthenic acid signature analysis with HPLC/HRMS will be needed to verify whether NA degradation occurred post-injection to reduce NA concentrations or if the apparent decline in NA C/Co is simply a consequence of uncertainty.

With the limited number of data points and the uncertainty associated with the analytical methods, definitive conclusions about apparent NA utilization rates are not possible. From the dilution corrected data, on average, 0.4 mg/L/day of naphthenic acids were removed from solution from the end of the injection on July 17 until August 21, roughly 35 days later. A greater NA mass loss would be needed to be confident that the observed trends were truly a consequence of NA utilization.

If the observed deviation of the NA trends from the chloride conservative tracer were in fact from degradation, the results of previous investigations and the observed trends in dissolved chemistry indicate microbial oxidation as the most likely cause of the apparent mass loss. Gervais (2004) did not observe measurable partitioning of NAs to soils at various field sites with similar conditions, so it is unlikely that sorption was significant. Dissolved iron and manganese concentrations gradually increased following the PA water injections (Figure 4-37) indicating Fe(III) and Mn(IV) from oxide and oxyhydroxide mineral coatings on the aquifer solids were reductively dissolved to release Fe(II) and Mn(II) to solution. Dissolved organics from the injectate were the most likely reductants and because naphthenic acids were the primary dissolved organic component in the injectate, it stands to reason they functioned as electron donors.

Previous studies demonstrate the importance of microbes in facilitating oxidation under manganese and iron reducing conditions. Lovely et al. (1991) investigated enzymatic and nonenzymatic mechanisms for Fe(III) reduction coupled to the oxidation of several different organic substrates and found that at circumneutral pH typical of aquifers, microbes enzymatically catalyze the reduction of the majority of Fe(III) in oxidizing organics. Most of the organic compounds studied were unable to reduce Fe(III) nonenzymatically and for those that could, the amounts reduced were smaller, the rate and extent of reduction was less than that observed for the enzymatic pathways, and often conditions not typical of an aquifer (e.g. low pH) were required for the reaction. The authors concluded that most Fe(III) reduction in aquatic sediments coupled to the oxidation of organic matter is from enzymatically catalyzed reactions.

Deng and Stumm (1993) identified abiotic mechanisms for the reduction of Fe(III) oxyhydroxides with concomitant oxidation of fulvic acid. However, their study examined Fe(III) reduction at the oxic/anoxic boundary and found that Fe(III) oxyhydroxides functioned as "electron-transfer mediators" in the oxidation of fulvic acid by molecular oxygen, not as the terminal electron acceptors. The absence of dissolved oxygen in the WCSC would prevent this reaction from occurring. Further, they found aged fulvic acid had significantly less reducing power than freshly prepared fulvic acid, likely due to gradual oxidation of the easily oxidized functional groups. Naphthenic acids from the STP PA water have been aged over millions of years and have limited reducing power. So, even if enough DO for reaction was introduced

during injection, the likelihood of abiotic oxidation of the naphthenic acids seems unlikely because of their minimal reducing power.

Albrechtsen and Christensen (1994) studied sediments from a landfill leachate polluted aquifer and found significant oxidation of organics occurred in conjunction with iron reduction in medium with active bacteria. Reaction was limited when the medium was treated with formaldehyde, chloroform or pasteurization to kill the bacteria. Baedecker et al. (1993) observed degradation of benzene and toluene in microbially active microcosms under Mn(IV) and Fe(III) reducing conditions, but saw no reaction in sterilized controls. Others have attributed the presence of large iron-reducing zones in groundwater systems and landfill leachate plumes to microbial oxidation of organic matter in the leachate with Fe(III) functioning as the terminal electron acceptor (Chapelle and Lovely, 1992; Lyngkilde and Christensen, 1992; Lyngkilde et al., 1992; Rugge et al., 1995).

In summary, the increasing dissolved iron and manganese trends demonstrated reductive dissolution of Fe(III) and/or Mn(IV) occurred post injection. The results of previous investigations show that the oxidation of organic matter coupled to the reduction of Fe(III) and Mn(IV) is generally enzymatic. Therefore, if NAs were removed from the PA water injectate in the WCSC, biodegradation was the most likely cause of the NA mass removal.

Nitrate may have played a role as an electron acceptor if the NAs did in fact undergo microbial oxidation. The potential importance of nitrate for the degradation of NAs is highlighted in Figure 4-32, which shows dilution corrected naphthenic acid concentrations declined when nitrate was present and stabilized once nitrate was no longer available. Nitrate was not identified above laboratory detection limits in the background groundwater samples collected before injection but was present in the injectate at concentrations of 0.4 – 0.6 mg/L (Table 4-9). Therefore, if nitrate was needed as an electron acceptor for biodegradation of naphthenic acids, the aquifer itself could not supply it. Once the nitrate supply from the injectate was exhausted, the reaction could not proceed. Dispersion during injection would have diluted the nitrate concentrations at the outer portion of the injectate plumes, such that nitrate may not have been available at the levels required for the metabolic reactions to biodegrade the NAs. This would explain why the later time chloride and naphthenic acid concentration trends plot on essentially the same curve. While this evidence indicates nitrate may play a role in the degradation of NAs,

the dissolved iron and manganese trends still show an apparent mobilization of Mn(II) and Fe(II) following the injections (Figure 4-37a). This suggests, Mn(IV) and Fe(III) still functioned as electron acceptors for the oxidation of dissolved organics in the injectate.

Similar NA concentration trends were not apparent following the PA water injection at STP-07-159-SS. Figure 4-30b shows an immediate deviation between NA and chloride concentrations 14 hours after the injection was completed. Thereafter, concentration trends indicate NAs behaved conservatively. With only one data point showing evidence of reaction, it would be tenuous to use this data to conclude NA degradation occurred in the deep portion of the aquifer or to hypothesize mechanisms of that mass loss. Interestingly, it appears that nitrate in the PA injectate was rapidly utilized in the deeper portion of the aquifer, and similar to the shallow injection, its absence may have been inhibitory to the propagation of NA degradation reaction(s). The PA injectate at STP-07-159-SS had 0.4-0.5 mg/L of nitrate. Nitrate was not detected in sample STP07159-GW35, the groundwater sample collected roughly 14 hours after injection (Table 4-9). So, the short timeframe immediately after the injection during which naphthenic acid concentration trends deviated from the conservative tracer coincided with the period when nitrate was still available for reaction from the injectate.

Overall, the evidence of NA utilization from the total NA concentration trends is limited at both depths. Other lines of evidence are needed to show whether NA degradation occurred.

### 4.6.2 Naphthenic Acid Signature Analysis – Gas Chromatography – Electron Impact Mass Spectrometry

Naphthenic acids are complex mixtures of alkyl-substituted acyclic and cycloaliphatic carboxylic acids whose isomer composition varies depending on source. This complicates the characterization of samples. St. John et al. (1998) developed a method by which gas chromatography – electron impact mass spectrometry of *tert*-butyldimethylsilyl derivatives of NAs can be used to determine relative percentages of isomer classes of an NA sample. The isomer classes are defined by carbon number (n) and cyclization (z). Holowenko et al. (2002) used these methods to analyze naphthenic acids from different sources, listing the relative proportion of the isomers in matrices and graphing the outputs on three-dimensional plots for greater ease of comparison. An example matrix and three-dimensional plot is provided in Figure 4-33. From these plots, they observed changes in the relative proportion of NA "clusters"

(groups of NA isomer classes divided based on carbon number) as samples aged. Specifically, they reported an increase in the relative proportion of NAs in the C22+ cluster (NAs with 22 or more carbon atoms), a shift accompanied by a decrease in toxicity of the water. They hypothesized the increase of the C22+ cluster was a consequence of microbes biodegrading NAs with C≤21. As the lower molecular weight NAs were degraded over time, the relative proportion of the C22+ cluster increased. This led the authors to conclude that higher carbon number NAs were more recalcitrant to biodegradation. Additionally, because the toxicity decreased with aging and the apparent removal of low carbon number NAs, they concluded that low molecular weight NAs contributed more to the toxicity of PA water than heavier NAs.

Clemente et al. (2003) developed a statistical approach to determine if the signatures of naphthenic acids from different sources were significantly different. For a given sample they calculated the relative proportion of NAs in three different carbon number groups: NAs with 5-13 carbons were placed in Group 1; 14-21 carbon NAs were placed in Group 2; and the C22+ cluster (C22 to C33) was considered Group 3. They divided the relative proportion of each isomer class by 100 and took the arcsine of that quotient for variance stabilization. The arcsine-transformed data for Groups 1, 2, and 3 of one sample were compared to the arcsine-transformed data for Groups 1,2, and 3 of a second sample using a two-sample t-test. If the P value of a group from the t-test comparison of two samples was <0.05, the group, and in turn, the samples were considered statistically different. Figures 4-34 and 4-35 are example t-test matrices.

Using the t-test method described above, Gervais (2004) found that adsorption did not cause statistically significant changes in NA signature. Therefore, if a change in NA signature for samples collected from the same source at different times was observed, the change in signature could be attributed singularly to degradation. She then used the t-test method to verify whether NA mixtures had undergone biotransformations under various aerobic and anaerobic conditions.

Using a high performance liquid chromatography/high resolution mass spectrometry (HPLC/HRMS) analytical method to analyze naphthenic acids researchers have since determined the foundation of the above conclusions is incorrect (Bataineh et al., 2006; Han et al., 2008). They found low-resolution GC-MS techniques misclassified NAs, incorrectly assigning compounds to either low or high carbon number NA isomer groups. For instance, Han et al. (2008) found GC/MS misclassified hydroxylated $C_{14}$, $C_{15}$, and $C_{16}$ NAs with Z=-4 as $C_{22}$, $C_{23}$,

and $C_{24}$ NAs with Z=0. Significantly, hydroxylated NAs are likely by-products of biodegradation of NAs. Therefore, the shift to higher carbon numbers with aging was actually the result of misclassification of degraded NAs, not from recalcitrance of the higher carbon number compounds. Additional research has found cyclization (z number), the arrangement of the functional groups on the ring structures (stereoisomerism), and the amount of branching on the alkyl and/or the carboxyl functional groups are the primary factors controlling NA biodegradation, while carbon number has little if any influence on the degradability of an NA (Bataineh et al., 2006; Han et al., 2008; Smith et al., 2008).

Although low resolution GC-MS will misclassify certain isomer classes, the t-test statistical analysis of low resolution GC-MS data is still useful in evaluating whether two samples are statistically different. So long as the same technique is used to analyze both samples, the technique should misidentify/misclassify NAs consistently. A statistically significant difference in the low resolution GC-MS signature of samples from the same source will then show evolution of the NAs, although the changes should not be used to speculate on the mechanisms of degradation or structural features limiting/preventing degradation.

For this project, any sample with a total naphthenic acid concentration above the FT-IR method detection limit was also analyzed with gas chromatography – electron impact mass spectrometry at University of Waterloo to determine the NA signature. The signature for each groundwater sample (designated by GW in the sample I.D.) was compared to the injectate samples' (designated by IJ in the sample I.D.) signature using the T-Test method. Two groundwater samples were found to be statistically significantly different from the initial signature of the injectate. The relative proportion of the C22+ cluster of sample STP07158-GW16 was greater than injectate sample STP07158-IJ03. Similarly, the relative proportion of the C22+ cluster of groundwater sample STP07159-GW36 was greater than that of the injectate sample STP07159-IJ11. These t-test results are presented in Figures 4-34 and 4-35. The shift in the C22+ cluster is similar to the observations of Holowenko et al. (2002) where aged samples had a higher relative proportion of the C22+ cluster.

Samples STP07158-GW16 and STP07159-GW36 were the second groundwater samples collected after the injections. It is logical that they would show evidence of a change in signature when the first groundwater samples did not because the injectate had more time to react in the

aquifer (STP07158-GW16 was collected approximately 1 week after the shallow injection and STP07159-GW36 was collected roughly 2 weeks after the deep injection). The absence of similar shifts in the relative proportion of the C22+ cluster in later samples is difficult to explain. Given the fact that the later samples represent injectate that was in the aquifer for even longer periods of time, NAs in these samples should be equivalently or more degraded than samples STP07158-GW16 and STP07159-GW36. The absence of a similar change in NA signature for the later samples can be explained in two ways. Either degradation of NAs was not spatially uniform throughout the volume of the aquifer or the change in signature for STP07158-GW16 and STP07159-GW36 is not actually from a degradation reaction. A set of samples were selected and have been shipped to University of Alberta to be analyzed with HPLC/HRMS with the hope that this scan can clarify whether significant reaction is occurring within the WCSC to degrade naphthenic acids.

As mentioned above, dissolved manganese and iron concentrations gradually increased following the injections (Figure 4-37), and continued to increase until the end of the monitoring period at both injection depths. This suggests Mn(IV) and Fe(III) minerals from the aquifer solids underwent reductive dissolution to release Mn(II) and Fe(II) to solution. With the limited evidence of NA degradation, a question surfaces as to what functioned as the electron donor in these redox reactions. Oiffer (2006) observed reduction of Mn(IV) and Fe(III) in a shallow groundwater plume emanating from one of Syncrude's tailings ponds without identifying an electron donor capable of driving the reduction. Figure 4-30 shows evidence of mass removal/reaction of NAs and DOC shortly after injection at STP-07-158-SS, but not at later times, and there is little evidence of any reaction of DOC or NAs in the deep injection interval (STP-07-159-SS). If NAs and/or the DOC functioned as the electron donors, the reactions must have occurred without changing their total concentrations. This could occur if the NAs in the injectate underwent a partial biotransformation that supplied electrons for the reductive dissolution of Mn(IV) and Fe(III) minerals. Because the biotransformation would have been incomplete, it would not manifest as a change in total DOC or NA concentrations. More specifically, the NAs could have undergone β-oxidation, cleaving the carboxyl functional group from the cycloalkane and leaving behind the recalcitrant ring structure with the alkyl functional group still attached. Transformations in signature from this type of reaction may not have been apparent with the analytical techniques applied at the University of Waterloo. HPLC/HRMS

analysis should aid in confirmation of these hypotheses. Unfortunately, results of the HPLC/HRMS sample analysis were not ready in time for inclusion in this document.

### 4.6.3 BTEX Compounds as Potential Electron Donors

With limited evidence of naphthenic acid oxidation to drive dissimilatory Mn(IV) and Fe(III) reduction, other dissolved organics in the injectate must be considered as potential electron donors. Benzene, toluene, ethylbenzene, p+m-xylenes, and o-xylene were present in the PA water injectate released at STP-07-158-SS and STP-07-159-SS, but at concentrations less than 25 µg/L (Tables 4-17 and 4-20). At STP-07-158-SS, concentrations of benzene, ethylbenzene and xylenes dropped below or near laboratory detection limits in the first groundwater sample collected post-injection (STP07158-GW15) and remained at those levels for the remainder of the monitoring period (Table 4-23). Toluene, which was reported at concentrations of 18 and 7 µg/L in injectate samples STP07158-IJ02 and STP07158-IJ03, respectively, was detected at 73 µg/L in the first groundwater sample, and then dropped to levels between 3 and 13 µg/L for the duration of post-injection monitoring. The injectate sample (STP07158-IJ04) from the final 1,000 litres injected was not analyzed for BTEX, so it is possible toluene was released into the aquifer at a concentration near 72.9 µg/L in the final injection. However, each of the 3, 1,000 L injections came from the same vacuum truck load so it seems unlikely that the dissolved concentrations of BTEX would be that different. More likely, the toluene concentration for STP07158-GW15 is erroneously elevated due to analytical uncertainty or sampling error.

Because the majority of BEX mass was absent from the STP-07-158-SS plume when the first groundwater sample was collected, the removal of these compounds cannot be confidently attributed to reaction within the aquifer. Given the method of injection, the water was certainly agitated during injection such that much of the BEX mass could have volatilized. Toluene, however, did persist in the plume, and provides a means to evaluate utilization of an aromatic hydrocarbon within the WCSC at the shallow injection depth. Omitting sample STP07158-GW15, relative concentrations of chloride and toluene reported at STP-07-158-SS following the PA water injection are plotted on Figure 4-36a. By July 23, the relative concentration of toluene deviated well below chloride levels, suggesting mass removal. As with BEX, volatilization during injection could certainly account for much of the mass lost. However, by August 21, the relative concentration of toluene was greater than chloride and remained so for the duration of

post-injection monitoring. This suggests that initially, toluene sorbed to the aquifer solids, reducing its dissolved concentration relative to the chloride conservative tracer. As the dilute outer portions of the injectate plume migrated back through STP-07-158-SS, desorption released toluene from the aquifer solids into solution and elevated the relative concentration of toluene to levels above chloride. These trends provide no evidence to suggest toluene was oxidized in the shallow portion of the WCSC and indicate that sorption/desorption was the primary control on dissolved concentrations. Therefore, it seems unlikely that toluene functioned as an electron donor in the reduction of Mn(IV) and Fe(III). The possibility remains that the removal of BEX was via an oxidation reaction coupled to dissimilatory Mn(IV) and Fe(III) reduction. However, this could only explain an initial mobilization of Mn(II) and Fe(II), not the consistent increase in dissolved Mn(II) and Fe(II) concentrations observed over the duration of post-injection monitoring. Further, previous studies of aromatic hydrocarbon biodegradation under anaerobic conditions found toluene more likely to degrade than benzene, ethylbenzene, or xylenes (Acton and Barker, 1992; Reinhard et al., 1995). As such, toluene's persistence suggests that biodegradation was not the process by which BEX was removed from the injectate and that oxidation of aromatic hydrocarbons was limited in the shallow portion of the WCSC.

Benzene, toluene, ethylbenzene, p+m-xylenes, and o-xylenes, were all detected in post-injection samples from STP-07-159-SS (Table 4-26). Relative concentrations of chloride and BTEX observed following the PA water injection at STP-07-159-SS are presented in Figure 4-36b. In general, the BTEX concentration trends in the deeper portion of the aquifer were similar to the toluene trends observed at STP-07-158-SS. The relative concentrations initially deviated below chloride, but within a month of injection were at levels greater than chloride. As above, this suggests an initial period where sorption reduced dissolved BTEX concentrations relative to the chloride conservative tracer. This was followed by a desorption phase that released BTEX from the aquifer solids back into solution, elevating their relative concentrations to levels above that of chloride. As with the shallow portion of the WCSC, there is no evidence to suggest that the oxidation of aromatic hydrocarbons occurred to supply electrons for the reduction of Mn(IV) or Fe(III).

## 4.7 Mobilization of Trace Metals

Because the pH of the WCSC aquifer is circumneutral, the Eh of the system had to be reduced to mobilize Mn(II), Fe(II) and associated trace metals from the aquifer solids. A reduction in Eh of the system was facilitated by the introduction of injectate with elevated DOC. Trends in dissolved metals concentrations indicate manganese and iron reducing reactions were stimulated in the WCSC following the PA water injections. Dissolved Mn(II) and Fe(II) concentrations increased consistent with typical reductive dissolution of Mn(IV) and Fe(III) oxide and oxyhydroxide minerals (Figure 4-37). In all likelihood, at background conditions, organic substrate availability limited the microbial redox reactions in the WCSC. With an increase in DOC from the injectate, dissimilatory Mn(IV) and Fe(III) reduction reactions were stimulated.

Figure 4-37 shows dissolved iron and manganese concentrations gradually increased following the PA water injections at both depth intervals. Over the same period of time, levels of the chloride conservative tracer declined as the up-gradient side of the injectate plume and its dispersive front migrated back through the injection wells (Figure 4-30). Concentrations of iron and manganese could increase concomitant with a drop in chloride concentrations without reaction if their dissolved concentrations were lower in the injectate than the aquifer. In such a scenario, the increase of dissolved iron and manganese would not represent a mobilization of Fe(II) or Mn(II) from the aquifer solids, but a return to background conditions. To rule out this possibility, background Fe and Mn groundwater and injectate concentrations were added to the plots. Dissolved iron concentrations in the injectate were higher than initial groundwater levels at both depth intervals. As such, the increase in iron concentrations is almost certainly representative of a mobilization. Conversely, dissolved manganese concentrations were higher in the groundwater than the injectate. However, manganese concentrations increased to levels well above background at both injection depths, suggesting manganese was also mobilized.

As a note, the injectate samples collected from the STP-07-158-SS injectate were not field filtered. The addition of nitric acid as preservative to the unfiltered samples mobilized metals from the suspended particulates that remained in the water. As such, the concentrations of metals for these samples presented in Table 4-16 do not represent the true dissolved concentrations. Instead of using this distorted data, the dissolved metals concentrations from the

STP-07-159-SS injectate samples, which were field filtered prior to sample collection, were considered representative of the STP-07-158-SS injectate's dissolved metals load as well.

Iron concentrations observed at STP-07-158-SS and STP-07-159-SS dropped off dramatically roughly a month after the injections. This does not necessarily indicate a discontinuation of the reductive dissolution reactions. Similar declines in iron concentration observed by others have been attributed to concomitant sulfate and Fe(III) reduction where reaction between reduced Fe(II) and $H_2S$ led to precipitation of iron sulfide minerals (Chapelle and Lovely, 1992; Heron and Christensen, 1995; Heron et al., 1994; Hunter et al., 1998)). Lovely and Goodwin (1988) state this is likely to occur as Fe(III) reduction reactions use up readily available Fe(III) from the aquifer solids. As Fe(III) availability declines, Fe(III) reducing organisms are no longer able to outcompete sulfate reducers for hydrogen and electron donors (normally organic carbon). As a result, Fe(III) and sulfate reduction begin to occur simultaneously. However, comparison of sulfate trends to chloride following the PA water injections indicates sulfate was conservative at both aquifer depths (Figure 4-38). Groundwater was not analyzed for sulfide, so the presence of the reduced species cannot be used to confirm if sulfate-reduction occurred but the conservative sulfate trends suggest it did not.

Depending on pH, oxidation-reduction potential, and aqueous and solid-phase geochemistry, Fe(II) could also have been removed from solution in other ways including adsorption or precipitation as carbonate or oxide minerals (Baedecker et al., 1993; Heron and Christensen, 1995; Heron et al., 1994; Hunter et al., 1998). A more detailed understanding of the WCSC's geochemistry would be needed to determine the most likely pathway by which the Fe(II) was removed from solution. Ultimately, the consistent increase in Mn concentrations during this time period suggests oxidation of organic matter continued.

Manganese and iron reducing conditions in the WCSC have problematic implications for the mobilization of trace metals. In laboratory microcosm experiments, Grantham et al. (1997) showed dissimilatory reduction of Fe(III) oxyhydroxides coatings on quartz surfaces created iron dissolution features on the mineral grains and increased the concentration of ferrous iron in solution. Trace metals co-precipitate with Mn and Fe oxides and oxyhydroxides so that the precipitation/dissolution of these mineral coatings largely controls trace metal mobility. Reductive dissolution of Mn and Fe oxides and oxyhydroxides under anaerobic conditions

releases Mn, Fe, and any co-precipitated trace metals to the aqueous phase (Stumm and Sulzberger, 1992; Suarez and Langmuir, 1976; Zachara et al., 2001). In their study of the solubilzation of co-precipitated Co(III) and Ni(II), from goethite (α-FeOOH) Zachara, et al. (2001) found that the presence of cobalt and nickel at 1 mol.% did not impact microbes ability to reduce the goethite. They also point out that depending on an aquifer's geochemical conditions, adsorption to the residual coatings on the aquifer solids and re-precipitation will in large part control the levels of the trace metals that ultimately mobilize into solution.

Metal cations and anions will also adsorb to Fe(III) oxide and oxyhydroxide coatings, complexing with surficial hydroxyl groups. As such, reductive dissolution of the oxides or oxyhydroxides or a drop in pH can mobilize trace metals adsorbed to the mineral surfaces as well (Bruno et al., 1998; Stumm and Sulzberger, 1992; Zachara et al., 2001).

Following the injections, there was an apparent enrichment in the dissolved concentration of trace metals as would be predicted given the iron and manganese-reducing conditions. At STP-07-158-SS dissolved strontium and zinc concentrations increased well above levels reported for un-impacted groundwater and the injectate. Barium and cobalt concentrations also increased to levels above background by the end of the monitoring period (Figure 4-39). Significantly, the concentrations of all four metals trended upward over the course of monitoring while the conservative tracer trends decreased (Figure 4-30a), suggesting the reductive dissolution reactions mobilizing Mn(II) and Fe(II) were also releasing these metals.

Strontium concentrations increased to levels above background at the deeper injection interval (STP-07-159-SS) as well, while barium concentrations for the final month of sampling were above background groundwater levels (Figure 4-40). Post-injection cobalt concentrations never exceeded levels reported for the injectate, but showed a consistent upward trend from the end of August through November 1, 2008. Over this same time period, the conservative tracer concentration dropped significantly (Figure 4-30b) and because cobalt was not detected in the background groundwater samples, the increasing trends suggest it was mobilized from the aquifer solids. As with the shallow injection depth, the upward concentration trends for strontium, barium and cobalt with a simultaneous decrease in chloride concentrations suggests the metals were mobilized from the aquifer solids as Mn(IV) and Fe(III) mineral coatings were reductively dissolved.

Researchers have identified associations between these elements and Fe-and Mn-containing minerals. Metal cations with $2^+$ and $3^+$ valences can substitute in crystalline Fe(III) oxide structures (Zachara, et al., 2001). In their study of mine tailings at Stekenjokk in Sweden, Holmstrom and Ohlander (2001) found layers rich in Fe- and Mn- oxyhydroxides functioned as traps for trace metals including cobalt and zinc, where the metals were adsorbed and/or co-precipitated with the oxyhydroxides. Herbert (1997) found that depending on soil horizon, adsorption and co-precipitation with Fe oxides was a significant sink for zinc in haplic podzol soils impacted by acid mine drainage. Bradl (2004) states that cobalt is found to accumulate in Fe and Mn hydrous oxides and that Mn minerals are especially important sinks of cobalt in soils. In their study of hydrous amorphous aluminum, iron and manganese oxides, Axe and Trivedi (2002) found significant sorption of zinc and strontium to the minerals' internal micropores. Huisman et al. (1997) determined that in general heavy metal concentrations could be correlated to clay content of soils in the Southern Netherlands, but outlying samples with high concentrations of heavy metals, including barium and zinc, were associated with zones of hydromorphic iron-oxide accumulations.

It is important to point out that metal sorption generally increases with pH (Bradl, 2004) due to the association of hydroxyl groups with mineral surfaces that creates negatively charged surface sites. Therefore, the enrichment in iron, manganese, barium, cobalt, strontium and zinc concentrations following the PA water injection was probably not pH driven desorption because the PA water had a higher pH (~8-9.5) than the WCSC porewater (~6.5-7.5). This suggests that reductive dissolution of the Mn(IV) and Fe(III) oxide and oxyhydroxide minerals or other Mn and Fe-containing minerals was the key mechanism by which the metals were released.

It was also possible that suspended particulates in the highly turbid PA water injectate were the source of the trace elements that appeared to mobilize into solution following the injections. The failure to field filter the STP-07-158-SS injectate samples provided an opportunity to gain insight into the solid-phase geochemistry of the suspended particulates in the STP PA water and evaluate this possibility. The addition of nitric acid to the unfiltered samples had the potential to mobilize trace elements that could have been easily scavenged from these particulates. For the STP-07-158-SS injectate samples, the average concentrations of Ba, Co, Sr, and Zn were 0.121, 0.024, 0.316, and 0.044 mg/L, respectively (Table 4-16). Dissolved concentrations of Ba, Sr and

Zn exceeded these levels in post-injection samples collected from both STP-07-158-SS and STP-07-159-SS (Tables 4-22 and 4-25). This suggests that at least a portion of the Ba, Sr and Zn was mobilized from the aquifer solids. While dissolved Co concentrations in the post-PA injection samples did not exceed the levels reported from the unfiltered STP-07-158-SS injectate samples, it is still possible that the increase in concentration was the result of mobilization from the aquifer solids, there is simply less conclusive evidence.

## 4.8 Trace Element Extractions and Solid-Phase Geochemistry

Trace element concentrations reported from the sequential extractions along with FOC and TIC data for the WCSC sediments are reported in Table 4-43. Sediment samples for these analyses were collected from the STP-08-159A soil core at three depth intervals in the WCSC; 51-53 feet bgs (15.5-16.2 m bgs), 78-80 feet bgs (23.8-24.4 m bgs), and 102-104 feet bgs (31.1-31.7 m bgs). The samples from 51-53 feet bgs and 102-104 feet bgs correspond roughly to the injection intervals of STP-07-158-SS and STP-07-159-SS, respectively. The intermediate sample was collected to determine whether the WCSC's solid-phase geochemistry is vertically heterogeneous. Samples were collected after the preliminary injection, but before the process-affected water injections.

Of primary interest for this study were the trace elements associated with the amorphous and poorly crystalline Fe and Mn oxides and oxyhydroxides (F2 on Table 4-43). The aqueous geochemistry has indicated dissimilatory manganese and iron reduction occurred in the WCSC following the PA water injections. As such, trace elements extracted from the amorphous and poorly crystalline iron and manganese oxides and oxyhydroxides would be those expected to mobilize from the aquifer solids as oxidation of dissolved organics reductively dissolved these minerals. In the extraction phase targeting the amorphous and poorly crystalline Fe/Mn/Al oxides and oxyhydroxides (F2), iron, aluminum, zinc and strontium were extracted at concentrations greater than 1 mg/kg from each depth interval (Table 4-43). Additionally, more than 2 mg/kg of manganese were extracted from the sediment samples from 78-80 and 102-104 feet bgs. Aside from the 0.15 mg/kg manganese concentration from 51-53 feet bgs, the elevated levels of Mn (2.1 to 2.4 mg/kg) and especially Fe (48 to 100 mg/kg) indicate amorphous and poorly crystalline Fe and Mn oxides and oxyhydroxides were available from the aquifer solids to undergo dissimilatory reduction in the oxidation of injectate DOC. Also of significance, the

extraction data suggests that zinc and strontium, two of the trace elements whose dissolved concentrations increased above background levels following the PA water injections (zinc at the shallow injection depth and strontium at both injection depths), were associated with the Fe/Mn/Al oxides and oxyhydroxides. As such, mobilization of these elements into solution would be a predicted consequence of the reductive dissolution of the Fe and Mn oxides and oxyhydroxides. Therefore, the solid-phase data supports the hypothesis from Section 4.7 that dissimilatory reduction of Fe and Mn oxides and oxyhydroxides is releasing Fe(II), Mn(II) and trace elements sorbed or co-precipitated with these minerals into solution.

The high levels of Al extracted during the F2 phase suggests that poorly crystalline and amorphous aluminum oxides and oxyhydroxides are also present on the WCSC sediments. However, because Al does not function as a terminal electron acceptor, reductive dissolution of these minerals would not be expected. Therefore, aluminum would be unlikely to mobilize from the aquifer solids in conjunction with oxidation of the injectate's organics. As such, the absence of evidence of aluminum mobilization into solution following the PA water injections is compatible with the results of the sequential extractions. In laboratory microcosm studies, Grantham et al. (1997) observed iron dissolution features on Fe(III) oxyhydroxide mineral coatings as a result of dissimilatory Fe(III) reduction by microbes. Similar dissolution features were not apparent on aluminum oxyhydroxide coatings in parallel experiments. This demonstrates that microbial redox reactions could occur within the WCSC to release iron, manganese and associated trace elements from iron and manganese oxides and oxyhydroxides without releasing aluminum from aluminum oxides and oxyhydroxides.

WCSC sediments around the injection wells have now been exposed to PA water. It would be informative to collect new sediment cores from injectate-impacted portions of the aquifer to determine if reactions with the injectate caused significant changes to the WCSC's solid-phase geochemistry.

## 4.9 Results of Down-Gradient Monitoring

### 4.9.1 Groundwater Elevation Trends

Groundwater elevation, conductivity and temperature data from the CTD Divers deployed in the down-gradient monitoring wells are provided in Figures 4-41 through 4-44 and a full listing of

the data is provided in Appendices I through N. An increase in groundwater elevation over the course of the monitoring period is apparent at the monitoring (Figures 4-41 and 4-43) and injection wells (Figures 4-8 and 4-9). This consistent increase in elevation was not predicted. Over the course of a year, elevations were expected to rise when the aquifer recharged (e.g. the spring melt) and drop during periods when infiltration was limited (e.g. the winter months when the ground is frozen) with the fluctuations oscillating above and below a mean elevation. Instead, there was an overall increase in groundwater elevation at each of the wells. This may be from pressurization of the WCSC as the STP is filled. As PA water is added to the STP, the head pressure is transferred to the WCSC. If the increase in pressure/elevation in the WCSC is in fact from filling the STP, groundwater elevations will continue to increase until the STP is at full capacity. This also has important consequences for containment of PA water that infiltrates to the WCSC. If the STP is pressurizing the WCSC, the highest head in the WCSC will be beneath the pond. This would drive groundwater flow laterally away from the pond. As a consequence, flow in the WCSC southeast of the STP could switch from northeast to the southeast where currently, there is no containment (i.e. pumping wells or cut-off walls). KCB expects new depressurization wells installed southeast of the STP to prevent this reversal of flow. However, these wells are currently in place between the STP and the ISATF and head levels in the ISATF's wells still show a pressurization of the WCSC. However, groundwater elevations at the ISATF do not indicate a switch in groundwater flow direction. Alternatively, the increase in elevations may be from the completion of the bentonite slurry wall across the southwestern branch of the WCSC (Zone 2 in Figure 2-2) during the summer of 2008 which could have caused a "back-up" of water through the rest of the WCSC. This could cause groundwater elevations to increase throughout the aquifer without causing a switch in hydraulic gradients.

### 4.9.2 Evidence of Injectate Arrival

Conductivity readings recorded by the CTD Divers in the down-gradient monitoring wells were checked on a weekly basis through November 2008. An increase in conductivity to 0.50 mS/cm (background in the wells ranged between 0.40 and 0.47 mS/cm) was considered potentially indicative of the arrival of the injectate plumes (the STP-07-158-SS injectate had a conductivity of ~2.0 mS/cm and the STP-07-159-SS injectate had a conductivity of ~3.4 mS/cm) and triggered confirmatory sampling. Conductivity in the STP-08-158A well cluster never deviated from background levels. Groundwater elevations and contours plotted in Figures 4-20 through

4-26 indicate this is probably because STP-08-158A was not positioned down-gradient of injection well STP-07-158-SS.

Groundwater conductivity in STP-08-159A1 remained below 0.50 mS/cm throughout the duration of post-injection monitoring. At STP-08-159A2, the groundwater conductivity increased to 0.50 mS/cm on September 6, 2008 (Figure 4-44b), triggering sample collection on September 12. The drop in conductivity between September 12 and October 2 is likely from redeployment of the CTD diver that left the logger dangling above the well screen. The level data from that time period indicate this may be the case (the length of water column measured above the Diver was significantly shorter over the period of time between removal of the Diver and redeployment). In all likelihood, there was a tangle or knot in the line attached to the Diver that prevented the instrument from reaching full depth within the well screen.

At STP-08-159A3, groundwater conductivity increased to 0.50 mS/cm on August 8, 2008 (Figure 4-44c), triggering sample collection during the next sampling event on August 21. Groundwater conductivity increased to 0.57 mS/cm by September 6, and remained near that level for the remainder of the monitoring period.

In the confirmatory groundwater samples collected at STP-08-159A2 and STP-08-159A3, chloride concentrations were elevated relative to the background from STP-07-159-SS (33-38 mg/L from Table 4-15), ranging between 47 and 52 mg/L at STP-08-159A2 (Figure 4-45a and Table 4-30) and 60 and 68 mg/L at STP-08-159A3 (Figure 4-45b and Table 4-33). These elevated levels were considered a potential indication of the arrival of injectate. However, the injectate chloride concentration was between 520 and 676 mg/L (Table 4-21). Therefore, if these chloride detections represented arrival of the plume, it was significantly diluted.

The DOC concentration in the background sample from the deep injection interval (STP-07-159-SS) was 13 mg/L (Table 4-14). This sample was collected by KCB shortly after monitoring well installation and seems somewhat elevated given other observations of DOC at this depth. Namely, post-PA water injection monitoring at STP-07-159-SS showed DOC concentrations dropped to 4 mg/L after the injectate plume and its dispersion front migrated through the well (Table 4-26). Regardless of the "true" background DOC concentration, elevated levels of DOC, greater than 13 mg/L, were identified in monitoring wells STP-08-159A2 and STP-08-159A3

following the PA water injection. The highest DOC concentrations at STP-08-159A2 (26 mg/L) and STP-08-159A3 (21 mg/L) were both reported from samples collected on September 12, 2008 (Tables 4-29 and 4-32). As presented in Figure 4-45, DOC concentrations declined from these peaks, dropping to levels between 5 and 6 mg/L by November 1 at STP-08-159A2 and between 5 and 7 mg/L at STP-08-159A3 by September 30.

BTX, especially benzene and toluene, were also identified in the confirmatory samples from STP-08-159A2 and STP-08-159A3 (Tables 4-29 and 4-32). The peak toluene and benzene concentrations exceeded those reported for the injectate, making these detections difficult to reconcile considering chloride concentrations indicated arrival of diluted injectate. However, given the absence of other known BTEX sources and the concurrent increase in DOC, the injectate remains a likely source of the aromatic hydrocarbons. Combined with the chloride and conductivity data, the detection of elevated DOC and BTEX at STP-08-159A2 and STP-08-159A3 suggests at least a portion of the injectate plume passed through these wells.

Naphthenic acids, however, were not detected at STP-08-159A2. They were detected at STP-08-159A3, but only in the first groundwater sample at a concentration just above the method detection limit and below the limit of quantification (Tables 4-29 and 4-32). Total naphthenic acid concentration trends discussed in Section 4.6.1 indicated naphthenic acids behaved conservatively in the WCSC, with dilution functioning as the main force decreasing concentration. Because naphthenic acids comprised the majority of the DOC in the injectate, NA concentrations near 20 mg/L were anticipated in the samples with elevated DOC. This was not the case.

There are two scenarios that could account for the concentration trends observed at the down-gradient wells. The first is that the injectate plume simply did not arrive at the down-gradient well nest and the chloride, DOC and BTX identified at elevated concentrations originated from another source. The second explanation is that the NAs biodegraded between the injection well and the down-gradient well nest such that the elevated chloride, DOC and BTX concentrations marked the arrival of the injectate plume devoid of naphthenic acids. This explanation would require BTX compounds to persist in an aquifer capable of degrading naphthenic acids. Given the recalcitrance of NAs to biodegradation relative to BTX, this scenario seems unlikely.

The dissolved iron trends at STP-08-159A2 and STP-08-159A3 could be used to justify the alternate contaminant source scenario. Figure 4-45 shows dissolved iron concentrations increased dramatically to levels between 6 and 10 mg/L at STP-08-159A2 and STP-08-159A3 while DOC concentrations decreased from near 20 mg/L to around 6 mg/L. The decrease in DOC could be attributed to oxidation coupled to dissimalotry Fe(III) and Mn(IV) reduction. Because chloride concentrations remained elevated throughout the monitoring period, it can be reasonably asserted that DOC concentrations had to decrease via reaction rather than a return to background conditions. These iron, manganese and DOC trends are quite different from those observed at STP-07-159-SS. There, dissolved iron concentrations only increased to 0.5 mg/L after the PA water injection. Additionally, the strong agreement between DOC and chloride trends at that well indicated the decrease in DOC was mainly from a return to background conditions (Figure 4-30b). In combination, these results suggest the DOC detected at the down-gradient points may have been in a more easily oxidized form than injectate DOC and therefore, from a different source.

More likely, the elevated dissolved iron and manganese concentrations in the down-gradient points resulted from sampling technique. The injection wells were sampled with dedicated submersible pumps. Operation of the pump caused minimal agitation of the formation and produced clear sample water. The monitoring wells were sampled with tubing and a foot-valve, a process that agitated the formation and produced cloudy/turbid purge and sample water. All dissolved metals samples were field filtered, but a yellow-orange tint was notable post-filtering in the monitoring well samples suggesting some particulates remained suspended in the sample water. Samples collected with the submersible pump were clear after filtering. Therefore, the elevated iron concentrations in the samples collected with the foot-valve may be a result of acid preservative mobilizing iron from particulates that passed through the filter. A final round of groundwater samples collected on June 20 and 21, 2009 from each of the wells at the ISATF supports this hypothesis. In this round of sampling, the concentration of dissolved iron at STP-08-159A2 approached 10 mg/L (Table 4-28) while at STP-08-159A3 the iron concentration remained around 6 mg/L (Table 4-31). Dissolved iron concentrations at STP-08-158A1, STP-08-158A2 and STP-08-159A1 - where there was no previous evidence to suggest arrival of injectate – were 3.8, 9.1, and 9.7 mg/L, respectively (Tables 4-37, 4-40, and 4-34). At the same time, iron concentrations at the injection wells remained below 0.4 mg/L (Tables 4-22 and 4-25).

Chloride concentrations at STP-08-159A2 and 159A3 remained elevated at levels between 50 and 60 mg/L in the samples collected on June 21, 2009 (Tables 4-30 and 4-33). This casts further doubt on the possibility that the anomalous chloride, BTX and DOC concentrations at these wells were from the arrival of injectate. To insure representative samples were collected during this event, nearly 20 Ls were purged from each well prior to sample collection. As such, it is unlikely that the elevated concentrations resulted from failure to remove stagnant water from the sample tubing and well. At velocities of 10 cm/day, the entire body of the injectate plume should have migrated by the monitoring points in the 10.5 months that passed between injection and collection of these samples. Even if the velocity were slow enough that the plume had not migrated by the wells in this amount of time, dispersion and diffusion should have reduced the chloride concentrations to near the 30 mg/L background level. Interestingly, the chloride concentration at STP-08-159A1 – screened just half a meter above STP-08-159A2 – was only 31 mg/L (Table 4-36), nearly identical to the background levels identified at STP-07-159-SS. Given the glaciofluvial origins of the unit, it seems unlikely there could be a natural cause of a 20 mg/L increase in chloride concentration across 0.5 meters of aquifer. These factors point back to the possibility of an alternate source. Perhaps there is preferential flow within the gravel and coarse sand observed below 29.0 m bgs that is functioning to distribute contaminants from another source area to STP-08-159A2 and STP-08-159A3. However, given the location of the ISATF, there are few possible source areas aside from the STP. If infiltration from the STP were the source of the elevated dissolved constituents, naphthenic acids should be detected as well. Additionally, the shallow portions of the aquifer should also be impacted.

Overall, it is not clear the plume from either injection reached the down-gradient well nests. While the elevated concentrations of iron and manganese can be accounted for based on sampling technique, the elevated concentrations of BTX, DOC and chloride at STP-08-159A2 and STP-08-159A3 remain difficult to explain.

## 4.10 Results of Groundwater Modelling

Given the confusion from the results of the down-gradient monitoring, groundwater modelling was used to simulate the PA water injections in an attempt to understand flow conditions in the WCSC. The primary goal of the model was to further quantify the WCSC's longitudinal dispersivity and hydraulic conductivity and to understand the accuracy with which flow direction

must be identified in order to install down-gradient monitoring points that will intercept injected plumes.

### 4.10.1 Shallow Injection Depth: Validation of Longitudinal Dispersivity and Investigation of Impact of Uncertainty in Interpreting Flow Direction

For the shallow injection, the chloride breakthrough curve at STP-07-158-SS was used to calibrate the model. Using the groundwater elevation at STP-07-158-SS as a reference, the up-gradient and down-gradient constant head boundary conditions were programmed to drive groundwater flow at a velocity of 5 cm/day with the aquifer porosity programmed at 0.3 and the hydraulic conductivity set near $10^{-3}$ m/s. The background chloride concentration through the model domain was set at 10 mg/L. Within the model, a point source boundary was created and connected to the injection well, releasing water with a chloride concentration of 537 mg/L at a rate of 19.9 $m^3$/day for 0.155 days at the start of the model run. Hydraulic conductivity and dispersivity were then varied until the chloride concentration curve modelled at the injection well matched the observed concentrations. Table 4-44 lists the model inputs and provides justifications of the values. Figure 4-46 shows a plan view of the grid discretization along with the position of the injection well and the arc of down-gradient monitoring points. The up-gradient and down-gradient constant head boundaries and the head equipotentials are also shown. Figure 4-47 depicts the grid layout in cross-section. The grid was set up to extend from ground surface to the base of the WCSC. In MODFLOW, unless otherwise specified, the lower boundary is no flow. This was acceptable in this model as the WCSC overlies the Clearwater Formation, a significantly less permeable bedrock unit.

The model was run for 115 days, the length of time between the July 17, 2008 injection and collection of groundwater sample at STP-07-158-SS (November 8, 2008). Figure 4-48 shows the agreement between the observed and modelled chloride concentration breakthrough curves at STP-07-158-SS. This match was achieved by setting the hydraulic conductivity at $2.25 \times 10^{-3}$ m/s and decreasing the longitudinal dispersivity to 0.06 m. This is identical to the longitudinal dispersivity calculated from the breakthrough curve of the preliminary injection using analytical methods, but roughly a factor of 6 less than the value computed from the PA water injection data (Table 4-2). Regardless, the results of both the numeric modelling and analytical analysis found low values of longitudinal dispersivity, all of which were within an order of magnitude. This has

important implications as research at the ISATF shifts towards treating PA water with chemical oxidants. Because the dispersivities at the scale of these injections are low, the mechanical mixing forces needed to distribute the oxidant(s) to the plume will be minimal.

The modelled movement of the chloride plume at the injection depth (352.5-353.0 m amsl) is illustrated in Figure 4-49. At 60 days, when the core of the plume passed the arc of down-gradient points, injectate was still detected in the fifth well offset from the line of the plume's flowpath. Based on this model output, estimates of flow direction must then be within 30° of the true flow path for injectate to reach a monitoring well installed just 4 meters from the injection point. While elevated chloride was still detected in the fifth well offset from the plume's flow path, the injectate that reached the well was extremely dilute, with chloride concentrations of only 15-20 mg/L.

### 4.10.2 Deep Injection Depth: Validation of Longitudinal Dispersivity and Investigation of Impact of Uncertainty in Interpreting Flow Direction – No Vertical Flow Components

The evidence of injectate arrival at STP-08-159A2 and STP-08-159A3 provided additional data points with which to calibrate the model of injectate migration through the deeper test interval. However, because the geochemical evidence of injectate at the down-gradient points is somewhat tenuous, several different scenarios were modelled.

The first simulation was created with the up-gradient and down-gradient constant head boundaries programmed to drive horizontal flow through the WCSC without vertical flow components or variability in hydraulic conductivity in the WCSC. The groundwater elevation at STP-07-159-SS was used as a reference to calculate up-gradient and down-gradient constant head boundary conditions that would drive groundwater flow at a velocity of approximately 10 cm/day with a porosity of 0.3 and a hydraulic conductivity near $10^{-3}$ m/s. For the deep injection, the point source boundary was created to release water with a chloride concentration of 583 mg/L at a rate of 30.9 $m^3$/day for 0.136 days at the start of the model run. The background chloride concentration was set at 35.5 mg/L. As above, hydraulic conductivity and dispersivity were then varied until the chloride concentration curve modelled at the injection well matched the observed concentrations. For this simulation, there was no attempt to match the modelled

and observed chloride concentrations at the down-gradient points. Table 4-45 lists the model inputs and provides justifications of the values. Figure 4-50 shows a plan view of the grid discretization along with the position of the injection well and the arc of down-gradient monitoring points. The up-gradient and down-gradient constant head boundaries and the head equipotentials are also shown. Figure 4-51 depicts the grid layout in cross-section.

The simulation was run for 164 days, from the date of injection on August 7, 2008 until January 17, 2009, when groundwater samples were collected from STP-08-159A2 and STP-08-159A3. Figure 4-52 depicts the migration of the injectate through the WCSC at the depth of injection (340.5-341.0 m amsl). By day 164, the entire body of injectate had moved beyond the bounds of the model domain. Around day 80, the core of the plume reached the arc of down-gradient wells. In this simulation, injectate was still detected in the fifth well offset from the line of the plume's flowpath, but at a concentration only slightly above background. Based on this model, injectate would not be observed at a monitoring point placed more than 20° from the true flow line at a distance of 8 meters from the injection point.

There was excellent agreement between the observed and simulated chloride breakthrough curve at STP-07-159-SS using a WCSC hydraulic conductivity of $2.5 \times 10^{-3}$ m/s and a dispersivity of 0.51 m (Figure 4-53). This is identical to the longitudinal dispersivity calculated via analytical methods (Table 4-2). As above, this low value of longitudinal dispersivity may have problematic implications for the delivery of oxidants to a PA water plume within the WCSC.

### 4.10.3 Deep Injection Depth: Use of Breakthrough Curves at Down-Gradient Monitoring Points for Additional Model Calibration

As stated previously, the evidence of injectate arrival at STP-08-159A2 and STP-08-159A3 provided additional data points to use for model calibration. The higher chloride concentrations observed at STP-08-159A3 suggested the flow regime in the WCSC distributed injectate vertically as well as horizontally. Additionally, coarser materials with potentially higher permeabilities were observed near the base of the STP-08-159A borehole. As such, a model simulation was developed with vertical components of flow and variable hydraulic conductivity in the WCSC.

As before, the groundwater elevation at STP-07-159-SS was used as a reference to calculate up-gradient and down-gradient constant head boundary conditions that would drive a groundwater velocity of approximately 10 cm/day. However, the higher chloride concentrations observed at STP-08-159A3 (Table 4-33) relative to STP-08-159A2 (Table 4-30) indicated vertical flow in the aquifer may have distributed the injectate down. As such, the up-gradient and down-gradient boundary conditions were manipulated to create vertical flow. At the up-gradient boundary, the constant head boundary condition was set at 355.363 m amsl from 355.5 m amsl (the base of the till) to 343.5 m amsl. From 343.5 m amsl to the base of the model domain, the constant head boundary condition was programmed at an elevation 355.362 m amsl. At the down-gradient boundary, a constant head boundary condition was not specified from 355.5 m amsl to 343.5 m amsl. By not specifying the boundary across this interval, Modflow created a no flow boundary. While this is not physically true within the aquifer, it was the best way to create the desired vertical flow. From 343.5 m amsl to the base of the model, the down-gradient constant head boundary condition was set at 355.358 m amsl. The initial head equipotentials created by these boundary conditions are shown in Figure 4-54.

In Figure 4-54, the injection well and down-gradient points are offset relative to their positions in Figure 4-51. While the distance between the wells is the same, the entire set of wells was moved up-gradient in the model domain so the monitoring points would be further from the down-gradient boundary. This was necessary because of the amplified components of vertical flow at the boundaries. Aside from dispersivity and hydraulic conductivity, all other model inputs were the same as listed in Table 4-45.

The observed chloride concentrations at both down-gradient points increased to a "peak" around day 50, dropped off to a low point near day 70, and then increased to a second peak between days 80 and 100 (Figures 4-55b and 4-55c). The goal of this model run was to vary the parameters to achieve the closest possible match between the modelled and observed data over the first 70 days. The best approximation was achieved when the hydraulic conductivity and dispersivity from 336.5 to 339.5 m amsl (this includes the STP-08-159A3 screened interval) were programmed at $3.2 \times 10^{-3}$ m/s and 1.35 m, respectively. Hydraulic conductivity and dispersivity through the rest of the WCSC were left at $2.5 \times 10^{-3}$ m/s and 0.51 m. Figure 4-55 compares the modelled and observed chloride concentrations. As in Section 4.10.2, there was

excellent agreement between the observed and simulated chloride breakthrough curve at STP-07-159-SS. While the quality of the match between the data at STP-08-159A2 and STP-08-159A3 was not as good, by introducing a vertical flow component and creating a layer with higher conductivity and dispersivity, it was possible to achieve relatively good agreement at the down-gradient monitoring points over the first 70 days post-injection.

As with the previous simulation, the model was run for 164 days. Figure 4-56 depicts the migration of the injectate through the WCSC in cross-section. The injectate's velocity increased as a result of the higher hydraulic conductivity from 336.5 to 339.5 m amsl. By day 150, the entire body of injectate had moved beyond the bounds of the model domain.

The difference in chloride concentration between the "peaks" and "valley" at STP-08-159A2 and STP-08-159A3 was less than 10 mg/L so the drop in concentration may not represent a real change and instead may be the result of sampling error or analytical uncertainty. As such, a final scenario was modelled in which the dispersivity was increased in an attempt to create constant, elevated chloride concentrations at the down-gradient points. Aside from hydraulic conductivity, dispersivity, and the constant head boundary conditions, all model inputs were the same as described in Table 4-45. The constant head boundaries were programmed to drive the vertical flow shown in Figure 4-54. Dispersivity throughout the entire length of WCSC was programmed at 1.5 m and the hydraulic conductivity was set at $2x10^{-3}$ m/s.

The observed and modelled breakthrough curves for this model run are shown in Figure 4-57. By increasing the dispersivity, it was possible to simulate the duration of elevated concentrations observed at the down-gradient points. However, the increased dispersivity drove greater dilution such that the modelled concentrations at STP-08-159A2 and STP-08-159A3 did not approach the same levels as the observed concentrations. Additionally, the quality of the match between the breakthrough curves at STP-07-159-SS was degraded by these changes.

### 4.10.4 Summary of Findings from Groundwater Modelling

Results of the groundwater modelling were in agreement with the analytical solutions of longitudinal dispersivities, indicating dispersivities at the scale of the ISATF injections are small. Within the shallow injection interval, the best match between the observed and modelled breakthrough curves at STP-07-158-SS was achieved when the longitudinal dispersivity was set

at 0.06 m. For the deeper interval, a longitudinal dispersivity of 0.51 m generated the best agreement between the observed and modelled data at STP-07-159-SS. Critically, these dispersivities produced the best match to the observed data when the hydraulic conductivities were programmed near $2x10^{-3}$ m/s, similar to the K-values calculated for the WCSC from slug tests.

With these low values of dispersivity, accurate estimation of flow direction becomes critical in positioning down-gradient monitoring points. At the shallow depth, a 3,000 L injectate plume will not be observed in a monitoring well point positioned more than 30° off from the true direction of groundwater flow at a distance of 4 meters from the injection well. At the deep injection depth, a 4,000 L injectate plume will not be observed in a monitoring point installed more than 20° deviant from the true groundwater flow direction at a distance of 8 meters from the injection well. Estimation of flow direction to this degree of accuracy will likely require the installation of additional wells around each injection point.

# 5 Conclusions

Injection experiments completed at the ISATF during the summer of 2008 facilitated the quantification of properties of the WCSC aquifer, provided insight into its capacity to metabolize naphthenic acids and identified trace metal mobilization as a potential consequence of the infiltration of PA water to the aquifer. Additionally, analysis of data from these injections identified simple observations that can provide preliminary evidence of reaction (or the absence of reaction) as well as the best means to passively track injectate in the aquifer.

Groundwater conductivity proved superior to temperature as a parameter to passively monitor plume movement within the WCSC. In addition, comparison of groundwater conductivity trends to conservative tracer breakthrough curves provided a preliminary indication of microbial oxidation of acetate. Conductivity trends deviated from the conservative tracer breakthrough curves when the reaction of acetate drove an apparent removal of TDS from the plume. During the PA water injections, where reaction between injectate and the aquifer was limited, groundwater conductivity and conservative tracer trends were identical. These results suggest that because groundwater conductivity is a function of TDS, comparison of conductivity to conservative tracer breakthrough curves reveals the absence of reaction when conductivity trends show TDS is conservative or the occurrence of reaction when conductivity trends indicate TDS is added or removed.

In the shallow portion of the aquifer, the groundwater velocity was estimated between 2.6 and 4.7 cm/day. At the deeper injection depth, the velocities were between 5.3 and 10.3 cm/day. Considering hydraulic conductivities calculated from slug tests were on the order of $10^{-3}$ m/s, these slow velocities were a consequence of the relatively flat hydraulic gradient across the ISATF. Because of the flat gradients, attempts to use groundwater elevations from wells within and near the ISATF to determine groundwater flow direction proved difficult. Installation of monitoring well nests in June 2008 provided additional data points to contour groundwater elevation and improved understanding of the flow system. A groundwater ridge appears to run through the site so that injectate released at STP-07-158-SS would flow northwest and injectate introduced at STP-07-159-SS would flow southwest. However, because of the flat gradient and water level measurement uncertainties, it is difficult to define flow direction at the site with certainty.

Accurate estimation of flow direction will be critical in positioning monitoring wells that intercept injected plumes. Simulations of the 3,000 L PA water injection at STP-07-158-SS found that injectate will not be detected at a well positioned more than 30° from the plume's flowpath at a 4 meter distance from the injection point. Likewise, simulations of the 4,000 L PA water injection at STP-07-159-SS found that injectate will not be detected at a well positioned more than 20° from the plume's flowpath at an 8 meter distance from the injection well.

At the scale of the ISATF injections (<10 m travel distance through the aquifer), the longitudinal dispersivity of the WCSC was between 0.06 and 0.37 m at the shallow injection depth and 0.28 and 0.51 m at the deep injection depth. These dispersivity values were initially calculated with analytical methods and confirmed with a three-dimensional numeric model.

Groundwater elevations at each of the ISATF wells consistently increased over nearly a year of monitoring. Instead of fluctuating about a single mean elevation, the general trend of the elevations was upward. Small fluctuations at the scale of days or weeks were apparent, but larger seasonal fluctuations were not. This may reflect a pressurization of the WCSC as the STP is filled. As PA water is added to the STP, the head pressure is transferred to the WCSC. If the increase in elevation in the WCSC is in fact from filling the STP, groundwater elevations will continue to increase until the STP is at full capacity. This pressurization of the WCSC could set up hydraulic gradients that drive groundwater flow to the southeast towards a section of the channel where hydraulic controls are not in place. However, groundwater elevations at the ISATF do not indicate the direction of groundwater flow has changed. Therefore, the increase in elevations may be from the completion of the bentonite slurry wall across the southwestern branch of the WCSC during the summer of 2008 which caused a "back-up" of water through the rest of the WCSC. This could drive increases in groundwater elevations throughout the aquifer without causing a switch in hydraulic gradients.

Acetate mass was partially removed from the plumes released in the preliminary injections. While dilution and adsorption caused some of the decrease in acetate concentration, these processes could not account for the significant reduction in concentration observed over the six to eight days after injection. Given the aquifer conditions and degradability of acetate, microbial oxidation coupled to dissimilatory Fe(III) and Mn(IV) reduction was the most likely degradation pathway. These findings were significant in that they provided evidence of an active microbial

population in the WCSC capable of metabolizing organic substrate. The incomplete acetate removal suggested availability of nutrients or electron acceptors prevented complete degradation.

Naphthenic acid concentration trends following the PA water injections show dilution accounted for the majority of NA concentration reduction within the WCSC. Early deviations between total NA and conservative tracer breakthrough curves at STP-07-158-SS indicate degradation reactions may have removed some NA mass, possibly via microbial oxidation. Despite the predominant manganogenic and ferrogenic redox conditions in the WCSC, it appears nitrate may have played a role as an electron acceptor in this suspected degradation. However, the majority of evidence points to dispersive dilution as the primary force reducing NA concentrations in the aquifer with NAs generally recalcitrant.

Despite the recalcitrance of NAs within the WCSC, there was an apparent enrichment in the concentrations of dissolved Fe(II) and Mn(II) in post-PA water injection groundwater samples. This mobilization was likely the result of reductive dissolution of Mn(IV) and Fe(III) oxide and oxyhydroxide mineral coatings on the WCSC aquifer solids coupled to the oxidation of DOC in the PA water injectate. While naphthenic acids comprised the majority of DOC in the injectate, other organics must have functioned as the electron donors in the reaction(s) given naphthenic acids apparent recalcitrance. BTEX were considered possible electron donors, but these compounds also appeared to persist in the aquifer.

Increases in the dissolved concentrations of barium cobalt, strontium and zinc post-injection were likely a result of the reductive dissolution of the Mn(IV) and Fe(III) oxide and oxyhydroxide minerals. Trace metals associate with Mn(IV) and Fe(III) minerals through sorption or co-precipitation and as a result, mobilization of trace metals is a frequent consequence of dissimilatory Fe(III) and Mn(IV) reduction. The results of the solid-phase sequential extractions indicated that relatively high levels of Fe, Mn, Sr, and Zn were associated with the poorly crystalline Fe/Mn/Al oxides and oxyhydroxides in the WCSC sediments such that the release of these elements would be a predicted consequence of their reductive dissolution. Because the pH of the injectate was elevated relative to the aquifer porewater, changes in pH from the injectate were unlikely to have caused desorption of these cations. This underscores the likelihood that reductive dissolution released Mn(II) and Fe(II) into solution along with Ba, Co, Sr and Zn.

# 6 Recommendations

The results from this project should supply researchers with guidance on the best methods for successful implementation of projects at the ISATF and insight into potential difficulties that could develop due to the set up of the research facility and conditions in the WCSC. A few important points from experience gained at the research facility follow.

All future injections at the ISATF should be marked with a conservative tracer not detected in WCSC porewater (e.g. bromide, boron). Although chloride is present at high concentrations in PA water, its use as a tracer complicated interpretation of data because of its natural occurrence in WCSC groundwater.

Extra lengths of garden hose should be added to the injection system so that injectate cannot free-fall from the outlet of the hose to the water column. This set up caused agitated flow of the injectate into the aquifer which could have entrained air within the pores of the aquifer and ultimately reduced the hydraulic conductivity of the WCSC around the injection wells. This in turn may have influenced the flow of the injectate back through the aquifer. By adding lengths of hose to the injection system it will be possible to place the injection outlet into the well's water column and eliminate the entrenchment of air bubbles during injection.

In this project, the most significant geochemical changes occurred within a week of injection. Therefore, the majority of post-injection samples should be concentrated within this time period, with decreased sampling frequencies thereafter. Evidence in this study indicated microbial processes were involved in the degradation of organics and mobilization of metals. However, considering the significant differences between the geochemistry of the injectate and the WCSC's porewater, it would be prudent to evaluate whether these geochemical differences could drive dissolution of the aquifer solids without microbial processes. Studies of Aquifer Storage Recovery (ASR) wells could provide valuable analogues to evaluate this possibility.

Quantitative and qualitative analysis of the behaviour of injectate in the WCSC indicated that longitudinal dispersity in the aquifer is small. This has important consequences as researchers at the ISATF begin to investigate in situ chemical oxidation treatments. It will be difficult to deliver oxidant to the PA water plumes via injection because of the limited advective mixing. If

chemical oxidants are found to effectively degrade naphthenic acids, methods of delivery will have to be carefully evaluated.

Development of an alternate conceptual model that accounts for the influence of aquifer heterogeneity on the distribution of injectate should be considered. The conceptual model used for this project assumed the aquifer was homogeneous across the screened intervals of the injection wells so that injectate occupied a cylinder whose geometry could be understood based on the volume of water injected, the length of the injection well screens and the porosity of the aquifer. In contrast to this conceptualization, in a heterogeneous system, injectate will flow preferentially into the higher hydraulic conductivity zones, significantly distorting the cylindrical shape of the plume around the injection well. Migration of injectate from the lower permeability sediments will extend the tail of breakthrough curves observed at injection points. At down-gradient points, the injectate may arrive in pulses as the plume moves at various rates through different portions of the aquifer as a consequence of the variable permeability of the sediments. Therefore, an alternate conceptual model that accounts for this heterogeneity would be extremely useful. The complication will be developing a method to quantify those heterogeneities at a field scale. This may require the use of a packer system that facilitates the completion of slug or pump tests across 10 to 30 cm lengths of the injection well screens.

Understanding groundwater flow direction will also be central to the effective delivery of oxidant. If proposed geophysical methods are unable to definitively discern the groundwater flow direction, installation of a third monitoring well/well nest at each of the injection intervals should be considered. Numeric modelling demonstrated that the main body of injectate will not be detected at monitoring points positioned more than 30° from the injectate's flowpath at distances of only 4 to 8 meters from injection wells. In addition, future geotechnical activities may significantly alter the groundwater flow direction in the ISATF and researchers need to track such activity before initiating long-term experiments. Given these complications in understanding flow direction, it may be necessary to install pumping/capture wells to control the movement of injectate within the aquifer. Because the site's hydraulic gradient is so flat, relatively little pumping would be needed to set up gradients to control flow through the aquifer.

WCSC sediments around the injection wells have now been exposed to PA water. It would be informative to collect new sediment cores from injectate-impacted portions of the aquifer to

determine if reactions with the injectate caused significant changes to the WCSC's solid-phase geochemistry.

Until this project, biota in the WCSC had not been exposed to naphthenic acids. The duration of exposure from these injections may not have been sufficient for the aquifer's microbial community to acclimate to the changes in geochemistry and initiate metabolism of NAs. Therefore, researchers should consider generating a continuous plume through repeated injections, exposing WCSC microbes to PA water and naphthenic acids over longer time periods (>3 months). Given continuous exposure, biodegradation under the anaerobic conditions may be stimulated after an acclimatization period.

The results of this study suggest monitored natural attenuation will not address naphthenic acid impacts to the WCSC. Depending on the degree of restoration deemed necessary, treatment of NA-impacted portions of the WCSC will require active remediation. Because portions of the WCSC are Mn(IV) and Fe(III)-reducing, Suncor should expect the oxidation of labile DOC in the infiltrating PA water to mobilize trace metals from the aquifer solids. Whether the mobilization of these metals increases concentrations to levels above Alberta groundwater quality criteria will be in large part a function of the aquifer's solid-phase geochemistry. Considering the potential spatial heterogeneity of the WCSC's solid-phase geochemistry, it would be advisable for Suncor to characterize extractable trace metals and redox conditions in other portions of the WCSC in order to anticipate which metals are likely to mobilize and the risk these metals pose to various environmental receptors.

# Tables

## Table 2-1: Groundwater Elevations – November 6, 2007 – June 24, 2009

| | Groundwater Elevation (m amsl) | | | | | | | | |
|---|---|---|---|---|---|---|---|---|---|
| | STP-07-158-SS | STP-07-159-SS | STP-08-158A1 | STP-08-158A2 | STP-08-158A3 | STP-08-159A1 | STP-08-159A2 | STP-08-159A3 | STP-04-40-SS |
| November 6, 2007 | 354.71 | 354.77 | NM | NM | NM | NM | NM | NM | NM |
| May 23, 2008 | 355.089 | 355.143 | NM | NM | NM | NM | NM | NM | NM |
| May 26, 2008 | 355.104 | 355.163 | NM | NM | NM | NM | NM | NM | 355.043 |
| June 2, 2008 | 355.281 | 355.381 | NM | NM | NM | NM | NM | NM | 355.221 |
| June 3, 2008 | 355.350 | 355.495 | NM | NM | NM | NM | NM | NM | 355.298 |
| July 11, 2008 | 355.324 | 355.370 | 355.366 | 355.338 | 355.357 | 355.374 | 355.378 | 355.363 | NM |
| July 15, 2008 | 355.300 | 355.347 | 355.337 | 355.312 | 355.354 | 355.347 | 355.349 | 355.336 | NM |
| July 16, 2008 | 355.264 | NM | 355.302 | 355.277 | 355.331 | NM | NM | NM | NM |
| July 17, 2008 | 355.281 | NM | 355.317 | 355.291 | 355.313 | NM | NM | NM | NM |
| July 18, 2008 | NM | 355.377 | 355.368 | 355.342 | 355.361 | 355.376 | 355.379 | 355.366 | NM |
| July 19, 2008 | NM | NM | 355.392 | 355.369 | 355.389 | NM | NM | NM | NM |
| July 20, 2008 | NM | NM | 355.405 | 355.381 | 355.416 | NM | NM | NM | NM |
| July 21, 2008 | NM | 355.450 | 355.434 | 355.410 | 355.430 | 355.448 | 355.450 | 355.439 | NM |
| July 22, 2008 | NM | 355.387 | 355.375 | 355.352 | 355.429 | 355.386 | 355.390 | 355.373 | NM |
| July 23, 2008 | NM | 355.371 | 355.366 | 355.345 | 355.410 | 355.378 | 355.381 | 355.367 | NM |
| July 24, 2008 | NM | 355.377 | 355.372 | 355.349 | 355.403 | 355.383 | 355.385 | 355.370 | NM |
| August 4, 2008 | NM | 355.400 | 355.387 | 355.367 | 355.454 | 355.403 | 355.405 | 355.391 | NM |
| August 5, 2008 | NM | 355.344 | 355.332 | 355.311 | 355.413 | 355.345 | 355.35 | 355.336 | NM |
| August 6, 2008 | NM | 355.335 | 355.322 | 355.304 | 355.471 | 355.338 | 355.343 | 355.329 | NM |
| August 7, 2008 | NM | NM | 355.437 | 355.417 | 355.319 | 355.454 | 355.457 | 355.442 | NM |
| August 8, 2008 | NM | NM | 355.439 | 355.420 | 355.547 | 355.453 | 355.458 | 355.444 | NM |
| August 9, 2008 | NM | NM | 355.450 | 355.430 | 355.481 | 355.462 | 355.468 | 355.451 | NM |
| August 10, 2008 | NM | NM | 355.504 | 355.486 | 355.509 | 355.518 | 355.522 | 355.507 | NM |
| August 11, 2008 | NM | NM | 355.482 | 355.465 | 355.481 | 355.495 | 355.500 | 355.482 | NM |
| August 21, 2008 | NM | NM | 355.538 | 355.518 | 355.545 | 355.556 | 355.562 | 355.547 | NM |
| August 27, 2008 | NM | NM | 355.643 | 355.628 | 355.640 | 355.666 | 355.667 | 355.657 | NM |
| September 3, 2008 | NM | NM | 355.493 | 355.473 | 355.485 | 355.506 | 355.512 | 355.492 | NM |
| September 12, 2008 | NM | NM | 355.623 | 355.608 | 355.625 | 355.641 | 355.642 | 355.617 | NM |
| September 17, 2008 | NM | NM | 355.570 | 355.557 | 355.548 | 355.588 | 355.586 | 355.573 | NM |
| September 25, 2008 | NM | NM | 355.575 | 355.556 | 355.566 | 355.589 | 355.590 | 355.573 | NM |
| September 30, 2008 | NM | NM | 355.533 | 355.513 | 355.530 | 355.516 | 355.552 | 355.532 | NM |
| October 16, 2008 | NM | NM | 355.673 | 355.653 | 355.660 | 355.696 | 355.692 | 355.667 | NM |
| October 23, 2008 | NM | NM | 355.778 | 355.757 | 355.778 | 355.793 | 355.790 | 355.776 | NM |
| November 1, 2008 | NM | NM | 355.607 | 355.586 | 355.607 | 355.623 | 355.627 | 355.607 | NM |
| November 8, 2008 | NM | NM | 355.578 | 355.559 | 355.560 | 355.601 | 355.596 | 355.585 | NM |
| November 15, 2008 | NM | NM | 355.563 | 355.548 | 355.575 | 355.596 | 355.592 | 355.587 | NM |
| November 22, 2008 | NM | NM | 355.783 | 355.763 | 355.770 | 355.796 | 355.802 | 355.787 | NM |
| January 17, 2009 | NM | NM | 355.723 | 355.703 | 355.715 | 355.736 | 355.732 | 355.717 | NM |
| June 20, 2009 | 356.154 | 356.209 | 356.181 | 356.167 | 356.193 | 356.201 | 356.202 | 356.188 | NM |
| June 24, 2009 | 356.14 | 356.189 | 356.166 | 356.15 | 356.166 | 356.181 | 356.187 | 356.171 | 356.072 |

Notes:
NM - Not Measured

## Table 2-2: Redox Indicator Parameters for Background Samples Collected at STP-07-158-SS and STP-07-159-SS

| | Range of Background Concentrations in WCSC[1] | | Range of Expected Concentrations for Redox Zones[1,2] | |
|---|---|---|---|---|
| Parameter | STP-07-158-SS | STP-07-159-SS | Manganogenic | Ferrogenic |
| Oxygen | <1.0 | <1.0 | 0.0 - 0.5 | 0.0 - 0.9 |
| Nitrate | <0.1 - 0.3 | <0.1 - 0.1 | 0.0 - 0.80 | 0.0 - 0.48 |
| Nitrite | <0.05 | <0.05 - 0.07 | 0.0 - 0.14 | 0.0 - 0.03 |
| Mn(II) | 0.069 - 0.176 | 0.11 - 0.19 | 0.3 - 0.9 | 0.0 - 1.2 |
| Fe(II) | 0.011 - 0.2 | 0.018 - 0.212 | 0.0 - 1.4 | 1.5 - 39.0 |
| Sulfate | 19.7 - 65.3 | 13.5 - 115 | 6 - 70 | 6 - 155 |

Notes:

1) All concentrations in mg/L

2) Concentrations observed by Lyngkilde and Christensen (1992) in redox zones of a landfill leachate plume

## Table 2-3: Major Ion Concentrations for Process-Affected Water Injectate Samples from the South Tailings Pond

| | STP07158-IJ02 | STP07158-IJ03 | STP07159-IJ07 | STP07159-IJ11 |
|---|---|---|---|---|
| **Parameter** | July 17, 2008 | July 17, 2008 | August 7, 2008 | August 7, 2008 |
| Chloride (Cl) | 537 | 414 | 554 | 676 |
| Calcium (Ca) | 11.9 | 10.7 | 7.9 | 8.8 |
| Potassium (K) | 9 | 8.9 | 8.9 | 9.9 |
| Magnesium (Mg) | 6 | 5.5 | 4.4 | 4.7 |
| Sodium (Na) | 670 | 686 | 606 | 707 |
| Sulfate ($SO_4$) | 190 | 183 | 169 | 169 |
| Bicarbonate ($HCO_3$) | 637 | 515 | 623 | 625 |
| TDS (Calculated) | 1750 | 1760 | 1680 | 1900 |

Notes:

All Concentrations in mg/L

## Table 3-1: STP-07-158-SS Groundwater Parameters

| STP-07-158SS - Field Parameters during June 3, 2008 Pumping Event | | | | |
|---|---|---|---|---|
| Time | Volume Pumped (L) | pH | Temperature °C | DTW (m) |
| 15:27 | 0 | 7.17 | 4.8 | 14.72 |
| 15:32 | 37.85 | 6.85 | 4.9 | 14.78 |
| 15:37 | 60 | 6.79 | 4.9 | 14.78 |
| 15:42 | 90 | 6.83 | 4.9 | 14.81 |
| 15:47 | 128 | 6.82 | 4.9 | 14.81 |
| 15:52 | 166 | 6.71 | 4.9 | 14.81 |
| 15:57 | 180 | 6.80 | 4.9 | 14.81 |
| 16:02 | 200 | 6.85 | 5 | 14.81 |
| 16:07 | 240 | * | 4.9 | 14.81 |
| 16:12 | 280 | * | 4.9 | 14.81 |
| 16:17 | 320 | * | 4.9 | 14.81 |
| 16:22 | 360 | 6.56 | 4.8 | 14.81 |
| 16:27 | 380 | 6.66 | 4.9 | 14.81 |
| 16:32 | 420 | 6.77 | 4.9 | 14.81 |
| 16:37 | 460 | 6.82 | 4.9 | 14.81 |
| 16:42 | 500 | 6.86 | 4.9 | 14.81 |
| 16:47 | 530 | 6.88 | 4.8 | 14.81 |
| 16:52 | 560 | 6.90 | 4.7 | 14.82 |
| 16:57 | 590 | 6.92 | 4.7 | 14.66 |
| 17:02 | 630 | 6.94 | 4.7 | 14.82 |
| 17:07 | 660 | 6.95 | 4.7 | 14.82 |
| 17:12 | 690 | * | 4.7 | 14.82 |
| 17:17 | 720 | * | 4.7 | 14.82 |
| 17:22 | 750 | * | 4.7 | 14.82 |
| 17:27 | 780 | * | 4.7 | 14.82 |
| 17:32 | 820 | 6.80 | 4.8 | 14.82 |
| 17:37 | 850 | 6.88 | 4.8 | 14.82 |
| 17:42 | 880 | 6.85 | 4.7 | 14.82 |
| 17:47 | 920 | 6.95 | 4.8 | 14.83 |
| 17:52 | 950 | 6.97 | 4.8 | 14.83 |
| 17:57 | 980 | 6.99 | 4.7 | 14.83 |
| 18:02 | 1110 | 7.01 | 4.7 | 14.82 |
| 18:05 | | 7.01 | 4.7 | 14.81 |

| Notes: | | | |
|---|---|---|---|
| * | pH Meter Shut-Off - Took ~20 minutes to return to previous levels | | |
| DO: | Used CHEMetrics Kit to Measure DO at 16:42 | | |
| | Reading: <1 mg/L | | |
| Ferrous Iron: Used CHEMetrics Kit to Measure Ferrous Iron at 16:49 | | | |
| | Reading: <0.1 mg/L | | |
| Total Iron: Used CHEMetrics Kit to Measure Total Iron at 16:56 | | | |
| | Reading 0.0 - 0.1 mg/L | | |

## Table 3-2: STP-07-159-SS Groundwater Parameters

| STP-07-159SS - Field Parameters during June 5, 2008 Pumping Event | | | | |
|---|---|---|---|---|
| Time | Volume Pumped (L) | pH | Temperature °C | DTW (m) |
| 8:43 | 0 | 7.60 | 4.3 | 14.86 |
| 8:48 | 25 | 7.36 | 4.7 | 14.86 |
| 8:53 | 50 | 7.30 | 4.9 | 14.86 |
| 8:58 | 100 | 7.29 | 5.1 | 14.86 |
| 9:03 | 150 | 7.30 | 5 | 14.85 |
| 9:08 | 190 | 7.32 | 5 | 14.85 |
| 9:13 | 230 | 7.35 | 5 | 14.85 |
| 9:18 | 270 | 7.36 | 5.1 | 14.85 |
| 9:23 | 310 | 7.38 | 5.2 | 14.85 |
| 9:28 | 360 | 7.39 | 5.2 | 14.85 |
| 9:33 | 400 | 7.41 | 5.3 | 14.85 |
| 9:38 | 440 | * | 5.3 | 14.85 |
| 9:43 | 470 | * | 5.3 | 14.85 |
| 9:48 | 510 | * | 5.4 | 14.85 |
| 9:53 | 550 | 7.39 | 5.4 | 14.85 |
| 9:58 | 580 | 7.35 | 5.5 | 14.85 |
| 10:03 | 620 | 7.31 | 5.6 | 14.85 |
| 10:08 | 660 | 7.30 | 5.7 | 14.85 |
| 10:13 | 700 | 7.31 | 5.7 | 14.85 |
| 10:18 | 740 | 7.30 | 5.7 | 14.85 |
| 10:23 | 780 | 7.30 | 5.8 | 14.85 |
| 10:28 | 820 | 7.29 | 5.9 | 14.85 |
| 10:33 | 860 | 7.29 | 6 | 14.85 |
| 10:38 | 900 | 7.21 | 6 | 14.85 |
| 10:43 | 940 | 7.17 | 6.1 | 14.85 |
| 10:48 | 980 | 7.14 | 6.1 | 14.85 |
| 10:53 | 1020 | 7.07 | 6 | 14.85 |

| Notes: | | |
|---|---|---|
| * | Checked Calibration of pH Meter | |
| DO: | Used CHEMetrics Kit to Measure DO at 9:50 | |
| | Reading: <1 mg/L | |
| Ferrous Iron: Used CHEMetrics Kit to Measure Ferrous Iron at 9:57 | | |
| | Reading: 0.2 mg/L | |
| Total Iron: Used CHEMetrics Kit to Measure Total Iron at 10:01 | | |
| | Reading: 0.2 mg/L | |

**Table 3-3: Process-Affected Water Injection Information**

| STP-07-158-SS: Process-Affected Water Injection - July 17, 2008 | | | | | | | | | | | |
|---|---|---|---|---|---|---|---|---|---|---|---|
| Injection | Volume (L) | Start Injection | Finish Injection | Injection Rate (L/m) | Tracer | Tracer Salt | Mass of Salt Added (g) | Mass of Tracer Added (g) | Tracer Concentration (mg/L) | ph | DO (mg/L) |
| Injection #1 | 1041 | 12:40 | 13:52 | 14.46 | Chloride | NaCl | 329.7 | 200 | 192 | 8.20 | 2 |
| Injection #2 | 1020 | 14:31 | 15:36 | 15.69 | Boron | $Na_2B_4O_7$ | 465.3 | 100 | 98 | 9.17 | 2-3 |
| Injection #3 | 1020 | 16:22 | 17:48 | 11.86 | Bromide | NaBr | 321.9 | 250 | 245 | 8.53 | 2-3 |
| **STP-07-159-SS: Process-Affected Water Injection - August 7, 2008** | | | | | | | | | | | |
| Injection #1 | 1060 | 15:30 | 16:16 | 23.04 | Chloride | NaCl | 329.7 | 200 | 189 | 8.20 | 2-3 |
| Injection #2 | 1040 | 16:25 | 17:14 | 21.22 | Bromide | NaBr | 193.2 | 150 | 144 | 8.22 | 2-3 |
| Injection #3 | 946 | 17:27 | 18:11 | 21.50 | Boron | $Na_2B_4O_7$ | 465.3 | 100 | 106 | pH Probe Malfunctioned | 2-3 |
| Injection #4 | 1050 | 18:24 | 19:21 | 18.42 | Bromide | NaBr | 64.4 | 50 | 48 | | 2-3 |
| | | | | | Chloride | NaCl | 329.7 | 200 | 190 | | |

## Table 3-4: Bottles, Preservative and Field Filtering in Accordance with Parameters to be Analyzed

| Parameter | Bottle Requirement | Preservative | Field Filtered? |
|---|---|---|---|
| Major Ions Package | 500 ml Plastic | None | No |
| Dissolved Metals | 250 ml Plastic | 5 ml of 20% Nitric Acid | Yes |
| Dissolved Ammonia | 500 ml Plastic | 2 ml of 1:1 $H_2SO_4$ | Yes |
| DOC | 100 ml Amber (Glass) | 1 ml of 1:1 $H_2SO_4$ | Yes |
| BTEX and PAHs | 3 – 40 mL VOAs | 0.4 ml of 10% Sodium Azide | No |
| Naphthenic Acids | 2 – 1 litre Amber (Glass) | None | No |
| Acetate | 1 – 20 ml Plastic Jar | 0.2 ml of 10% Sodium Azide | No |
| Bromide | 20 ml Plastic Jar | None | No |

## Table 3-5: Laboratory Analytical Method – ALS Laboratories

| Analysis | Reference Method | Instrument |
|---|---|---|
| DOC | APHA 5310 B-INSTRUMENTAL | Infra-red Carbon Analyzer |
| CHLORIDE | APHA 4500 CL E-COLORIMETRY | Konelab Colorimeter |
| ICP metals and SO4 for routine water | APHA 3120 B-ICP-OES | ICP/OES[1] |
| Iron (Fe)-Dissolved | APHA 3120 B-ICP-OES | ICP/OES[1] |
| Dissolved Trace Metals (Low Level) | APHA 3125-ICP-MS | ICP/MS[2] |
| Manganese (Mn)-Dissolved | APHA 3120 B ICP-OES | ICP/OES[1] |
| Nitrate+Nitrite-N | APHA 4500 NO3-H - COLORIMETRY | Technicon Colorimeter |
| Ammonia-N, Dissolved | APHA4500NH3F | Aquakem Discrete (automated Spectrophotometer) |
| Nitrite-N | APHA 4500 NO2B-COLORIMETRY | Technicon Colorimeter |
| Nitrate-N | APHA 4500 NO3H-COLORIMETRY | Technicon Colorimeter |
| pH, Conductivity, and Total Alkalinity | APHA 4500-H, 2510, 2320 | pH - pH meter, Conductivity - Conductance meter, Alkalinity by titration/pH meter. |
| Notes: | | |
| 1) ICP/OES: Inductively Coupled Plasma Optical Emission Spectrometry | | |
| 2) ICT/MS: Inductively Coupled Plasma Mass Spectrometry | | |

**Table 4-1: Bromide and Acetate Concentrations from Preliminary Injection Samples**

| Sample ID | Sample Time | Bromide Concentration (mg/L) | Acetate Concentration (mg/L) | Acetate Concentration - Corrected for Dilution[1] (mg/L) |
|---|---|---|---|---|
| **STP-07-158-SS** | | | | |
| STP07158-IJ01 | 04/06/2008 10:59 | 255 | 22.26 | NA |
| STP07158-GW02 | 04/06/2008 17:12 | 252 | 18.01 | 18.01 |
| STP07158-GW03 | 05/06/2008 8:16 | 255 | 16.23 | 16.05 |
| STP07158-GW04 | 05/06/2008 13:55 | 253 | 17.00 | 16.93 |
| STP07158-GW05 | 06/06/2008 8:22 | 248 | 10.04 | 10.19 |
| STP07158-GW06 | 07/06/2008 8:34 | 240 | 14.84 | 15.59 |
| STP07158-GW07 | 08/06/2008 9:19 | 233 | 13.82 | 14.97 |
| STP07158-GW08 | 10/06/2008 8:52 | 243 | 3.62 | 3.76 |
| STP07158-GW09 | 12/06/2008 8:57 | 239 | 4.90 | 5.18 |
| STP07158-GW10 | 16/06/2008 9:55 | 230 | 4.66 | 5.10 |
| STP07158-GW11 | 20/06/2008 10:26 | 248 | 3.89 | 3.97 |
| STP07158-GW12 | 25/06/2008 16:53 | 230 | 4.67 | 5.13 |
| STP07158-GW13 | 10/07/2008 8:39 | 84 | 3.20 | 9.60 |
| STP07158-GW13D | 10/07/2008 8:39 | 82 | ND | ND |
| STP07158-GW14 | 15/07/2008 10:45 | 38 | 0.45 | 2.96 |
| **STP-07-159-SS** | | | | |
| STP07159-IJ06 | 05/06/2008 12:04 | 261 | 23.73 | NA |
| STP07159-GW24 | 05/06/2008 14:06 | 258 | 114.24 | 113.38 |
| STP07159-GW25 | 06/06/2008 8:17 | 256 | 23.27 | 23.27 |
| STP07159-GW26 | 07/06/2008 8:19 | 251 | 16.24 | 16.56 |
| STP07159-GW27 | 08/06/2008 9:02 | 249 | 11.30 | 11.61 |
| STP07159-GW27D | 08/06/2008 9:02 | 245 | 23.78 | 24.89 |
| STP07159-GW28 | 10/06/2008 8:37 | 246 | 12.84 | 13.37 |
| STP07159-GW29 | 12/06/2008 8:44 | 241 | 5.46 | 5.79 |
| STP07159-GW30 | 16/06/2008 9:43 | 199 | 5.79 | 7.47 |
| STP07159-GW31 | 20/06/2008 10:05 | 142 | 5.88 | 10.59 |
| STP07159-GW32 | 25/06/2008 16:53 | 80 | 0.59 | 1.90 |
| STP07159-GW33 | 10/07/2008 9:23 | 29 | 0.48 | 4.16 |
| STP07159-GW34 | 15/07/2008 12:27 | 16 | 0.26 | 4.25 |

Notes:

ND - Not Detected

NA - Not Applicable

1) Corrected for dilution by dividing the acetate concentration by the bromide C/Co
STP-07-158-SS Co Sample: STP07158-GW02
STP-07-159-SS Co Sample: STP07159-GW25

**Table 4-2: Data Used to Calculate Longitudinal Dispersivities and the Resulting Values**

| Injection | Well | Length of Injection: t (days) | Standard Deviation: σ (m) | Hydrodynamic Dispersion Coefficient: $D_l$ ($m^2$/day) | Injectate Velocity: v (m/day) | Longitudinal Dispersivity: $\alpha_l$ (m) |
|---|---|---|---|---|---|---|
| Preliminary Injections | STP-07-158-SS | 0.22 | 0.32 | 0.23 | 3.75 | 0.06 |
| | STP-07-159-SS | 0.05 | 0.68 | 5.19 | 18.67 | 0.28 |
| PA Water Injections | STP-07-158-SS | 0.15 | 1.04 | 3.53 | 9.46 | 0.37 |
| | STP-07-159-SS | 0.14 | 1.32 | 6.37 | 12.38 | 0.51 |

**Table 4-3: Parameters Input for Modelling One-Dimensional Advection-Dispersion of Solute During Injections. Solute Distribution Modelled with Oned_1 Analytical Solution (Neville, 2001)**

| Injection | Well | Darcy Flux (m/day) | Porosity | Longitudinal Dispersivity (m) | Molecular Diffusion Coefficient ($m^2$/day) | Retardation Factor | First Order Decay Coefficient ($day^{-1}$) | Initial Concentration (C/Co) | Inflow Concentration (C/Co) | Initial Time (Days) | Final Time (Days) |
|---|---|---|---|---|---|---|---|---|---|---|---|
| Preliminary Injections | STP-07-158-SS | 1.1237 | 0.3 | 6.2152E-02 | 0 | 1 | 0 | 0 | 1 | 0 | 0.21597 |
| | STP-07-159-SS | 5.6007 | 0.3 | 0.27790 | 0 | 1 | 0 | 0 | 1 | 0 | 4.5139E-02 |
| PA Water Injections | STP-07-158-SS | 2.8372 | 0.3 | 0.37277 | 0 | 1 | 0 | 0 | 1 | 0 | 0.15486 |
| | STP-07-159-SS | 3.7134 | 0.3 | 0.51459 | 0 | 1 | 0 | 0 | 1 | 0 | 0.13611 |

**Table 4-4: Hydraulic Conductivity of Sediment Samples from STP-08-158A Soil Core as Determined with Falling Head Permeameter**

| STP-08-158A Soil Core Hydraulic Conductivities | | |
|---|---|---|
| Elevation of Top of Sample (m amsl) | Elevation of Base of Sample (m amsl) | Hydraulic Conductivity (m/s) |
| 353.63 | 353.40 | 3.51E-05 |
| 353.40 | 353.18 | 2.58E-05 |
| 353.18 | 352.95 | 4.82E-05 |
| 352.95 | 352.73 | 9.88E-05 |
| 352.73 | 352.50 | 1.34E-04 |
| 352.50 | 352.28 | 6.83E-05 |
| 352.28 | 352.06 | 8.06E-05 |
| 352.06 | 351.83 | 1.16E-04 |
| 351.83 | 351.61 | 9.38E-05 |
| 351.61 | 351.38 | 1.33E-04 |
| 351.38 | 351.16 | 1.21E-04 |
| 351.16 | 350.94 | 1.81E-05 |
| 351.11 | 350.89 | 1.05E-07 |
| 350.94 | 350.71 | 8.93E-05 |
| 350.58 | 350.20 | 6.33E-05 |
| 350.20 | 349.82 | 1.59E-05 |
| 349.82 | 349.43 | 2.17E-06 |
| 349.43 | 349.34 | 1.00E-06 |
| 349.34 | 349.05 | 3.64E-06 |

**Table 4-5: Hydraulic Conductivity of Sediment Samples from STP-08-159A Soil Core as Determined with Falling Head Permeameter**

| STP-08-159A Soil Core Hydraulic Conductivities | | |
|---|---|---|
| Elevation of Top of Sample (m amsl) | Elevation of Base of Sample (m amsl) | Hydraulic Conductivity (m/s) |
| 354.40 | 354.32 | 2.21E-05 |
| 352.19 | 351.81 | 7.64E-05 |
| 351.81 | 351.42 | 9.95E-05 |
| 351.42 | 351.04 | 3.91E-05 |
| 351.04 | 350.66 | 5.95E-05 |
| 350.66 | 350.12 | 6.81E-05 |
| 350.03 | 349.94 | 2.60E-07 |
| 350.12 | 349.59 | 4.42E-05 |
| 349.59 | 349.05 | 6.15E-05 |
| 349.05 | 348.51 | 1.36E-04 |
| 348.51 | 347.97 | 1.28E-04 |
| 347.97 | 347.43 | 9.05E-05 |
| 347.61 | 347.16 | 6.53E-05 |
| 347.06 | 347.00 | 2.21E-08 |
| 347.16 | 346.70 | 6.35E-05 |
| 346.70 | 346.24 | 8.32E-05 |
| 346.27 | 346.19 | 8.81E-05 |
| 346.24 | 345.94 | 6.10E-05 |
| 345.94 | 345.79 | 4.67E-07 |
| 345.79 | 345.46 | 6.90E-05 |
| 345.46 | 345.14 | 1.27E-04 |
| 345.36 | 345.30 | 1.18E-04 |
| 344.49 | 344.01 | 1.04E-04 |
| 344.01 | 343.58 | 1.04E-04 |
| 343.58 | 343.50 | 1.98E-07 |
| 343.50 | 343.39 | 9.01E-05 |
| 343.39 | 343.04 | 5.01E-05 |
| 339.99 | 339.89 | 1.71E-03 |
| 339.89 | 339.78 | 2.09E-04 |
| 339.78 | 339.35 | 1.29E-04 |
| 339.35 | 338.86 | 1.11E-04 |
| 338.86 | 338.38 | 1.58E-04 |
| 338.38 | 337.90 | 1.13E-04 |

**Table 4-6: Hydraulic Conductivities Determined By KCB Slug Tests of Injection Wells STP-07-158-SS and STP-07-159-SS**

| Test Type | Test Number | K-Values (m/s) | |
|---|---|---|---|
| | | STP-07-159-SS | STP-07-158-SS |
| Falling Head | 1 | 4.60E-03 | 2.60E-03 |
| | 2 | 9.90E-04 | 2.60E-03 |
| | 3 | 2.60E-03 | 3.90E-03 |
| Rising Head | 1 | 1.90E-03 | 5.70E-03 |
| | 2 | 2.30E-03 | 7.70E-03 |
| | 3 | 2.10E-03 | 1.60E-02 |
| Geometric Mean: | | 2.18E-03 | 5.14E-03 |

**Table 4-7: Naphthenic Acid Concentrations for PA Water Injection Samples and Post-Injection Groundwater Samples at STP-07-158-SS and STP-07-159-SS**

| Sample ID | Date Sampled | NA Concentration (mg/L) |
|---|---|---|
| **STP-07-158-SS** | | |
| STP07158-IJ02 | July 17, 2008 | 41.4 |
| STP07158-IJ03 | July 17, 2008 | 44.8 |
| STP07158-GW15 | July 18, 2008 | 49.4 |
| STP07158-GW16 | July 23, 2008 | 41.9 |
| STP07158-GW17 | August 6, 2008 | 32.6 |
| STP07158-GW18 | August 21, 2008 | 14.4 |
| STP07158-GW19 | August 27, 2008 | 8.9 |
| STP07158-GW20 | September 3, 2008 | 8.0 |
| STP07158-GW21 | September 12, 2008 | 4.3 |
| STP07158-GW22 | September 17, 2008 | 4.1 |
| STP07158-GW23 | September 25, 2008 | 2.7 |
| STP07158-GW24 | September 30, 2008 | 2.3 |
| STP07158-GW25 | October 8, 2008 | 1.7 |
| STP07158-GW25D | October 8, 2008 | 1.6 |
| STP07158-GW26 | October 16, 2008 | 1.1 |
| STP07158-GW27 | October 23, 2008 | 1.3 |
| STP07158-GW28 | November 1, 2008 | <1.0 |
| STP07158-GW29 | November 8, 2008 | <1.0 |
| **STP-07-159-SS** | | |
| STP07159-IJ07 | August 7, 2008 | 43.9 |
| STP07159-IJ11 | August 7, 2008 | 41.3 |
| STP07159-GW35 | August 8, 2008 | 32.4 |
| STP07159-GW36 | August 21, 2008 | 31.5 |
| STP07159-GW37 | August 27, 2008 | 10.1 |
| STP07159-GW38 | September 3, 2008 | 6.6 |
| STP07159-GW39 | September 12, 2008 | 5.3 |
| STP07159-GW40 | September 17, 2008 | 2.8 |
| STP07159-GW41 | September 25, 2008 | 1.2 |
| STP07159-GW42 | September 30, 2008 | 1.5 |
| STP07159-GW43 | October 8, 2008 | 1.1 |
| STP07159-GW44 | October 16, 2008 | <1.0 |
| STP07159-GW45 | October 23, 2008 | <1.0 |
| STP07159-GW46 | November 1, 2008 | <1.0 |

**Table 4-8: Dilution Corrected Naphthenic Acid Concentrations at STP-07-158-SS from July 18 – August 27, 2008**

| Sample ID | Date Collected | Chloride (C/Co) | Naphthenic Acids (mg/l) | Dilution Corrected NA Concentration (mg/L)[1] |
|---|---|---|---|---|
| STP07158-GW15 | 18/07/2008 8:42 | 1.0 | 49.4 | 49.4 |
| STP07158-GW16 | 23/07/2008 9:32 | 1.0 | 41.9 | 43.0 |
| STP07158-GW17 | 06/08/2008 11:13 | 0.9 | 32.6 | 38.3 |
| STP07158-GW18 | 21/08/2008 13:00 | 0.4 | 14.4 | 36.2 |
| STP07158-GW19 | 27/08/2008 13:30 | 0.2 | 8.9 | 38.8 |
| | | | | |
| Notes: | | | | |
| 1) Corrected for dilution by dividing the NA concentration in mg/L by the chloride C/Co | | | | |

**Table 4-9: Nitrate Concentrations for Background Groundwater, PA Water Injectate, and Post-Injection Groundwater Samples at STP-07-158-SS and STP-07-159-SS**

| Sample Type | Sample ID | Date Sampled | Nitrate Concentration (mg/L) |
|---|---|---|---|
| **STP-07-158-SS** | | | |
| **Background Samples** | MW07-035 | April 25, 2007 | 0.3 |
| | STP07158-GW01 | May 30, 2008 | <0.1 |
| **Injection Samples** | STP07158-IJ02 | July 17, 2008 | 0.6 |
| | STP07158-IJ03 | July 17, 2008 | 0.6 |
| **Post-Injection Samples** | STP07158-GW15 | July 18, 2008 | 0.4 |
| | STP07158-GW16 | July 23, 2008 | 0.3 |
| | STP07158-GW17 | August 6, 2008 | 0.3 |
| | STP07158-GW18 | August 21, 2008 | <0.1 |
| | STP07158-GW19 | August 27, 2008 | <0.1 |
| | STP07158-GW20 | September 3, 2008 | <0.1 |
| | STP07158-GW21 | September 12, 2008 | <0.1 |
| | STP07158-GW22 | September 17, 2008 | <0.1 |
| | STP07158-GW23 | September 25, 2008 | <0.1 |
| | STP07158-GW24 | September 30, 2008 | <0.1 |
| | STP07158-GW25 | October 8, 2008 | 0.1 |
| | STP07158-GW25D | October 8, 2008 | <0.1 |
| | STP07158-GW26 | October 16, 2008 | <0.1 |
| | STP07158-GW27 | October 23, 2008 | <0.1 |
| | STP07158-GW28 | November 1, 2008 | <0.1 |
| | STP07158-GW29 | November 8, 2008 | <0.1 |
| **STP-07-159-SS** | | | |
| **Background Samples** | MW07-034 | April 25, 2007 | 0.1 |
| | STP07159-GW23 | May 30, 2008 | <0.1 |
| **Injection Samples** | STP07159-IJ07 | August 7, 2008 | 0.5 |
| | STP07159-IJ11 | August 7, 2008 | 0.4 |
| **Post-Injection Samples** | STP07159-GW35 | August 8, 2008 | <0.1 |
| | STP07159-GW36 | August 21, 2008 | <0.1 |
| | STP07159-GW37 | August 27, 2008 | <0.1 |
| | STP07159-GW38 | September 3, 2008 | <0.1 |
| | STP07159-GW39 | September 12, 2008 | <0.1 |
| | STP07159-GW40 | September 17, 2008 | <0.1 |
| | STP07159-GW41 | September 25, 2008 | 0.4 |
| | STP07159-GW42 | September 30, 2008 | 0.2 |
| | STP07159-GW43 | October 8, 2008 | 0.1 |
| | STP07159-GW44 | October 16, 2008 | <0.1 |
| | STP07159-GW45 | October 23, 2008 | <0.1 |
| | STP07159-GW46 | November 1, 2008 | <0.1 |

## Table 4-10: Background Metals Concentrations in Groundwater at STP-07-158-SS

| | | | Aluminum (Al) | Boron (B) | Barium (Ba) | Bromide (Br) | Cadmium (Cd) | Cobalt (Co) | Copper (Cu) | Iron (Fe) | Lithium (Li) | Manganese (Mn) | Nickel (Ni) | Antimony (Sb) | Selenium (Se) | Strontium (Sr) | Titanium (Ti) | Thallium (Tl) | Uranium (U) | Zinc (Zn) |
|---|---|---|---|---|---|---|---|---|---|---|---|---|---|---|---|---|---|---|---|---|
| **Alberta Tier 1 Groundwater Remediation Guidelines for Natural Area with Coarse Soil Type (mg/L)** | | | 0.1 | 5 | 1 | Not Listed | 0.005 | Not Listed | 0.004 | 0.3 | Not Listed | 0.05 | 0.15 | 0.006 | 0.001 | Not Listed | Not Listed | Not Listed | 0.02 | 0.03 |
| **Sample Location** | **Sample ID** | **Sample Date** | | | | | | | | | | | | | | | | | | |
| **STP07-158-SS** | **MW07-035** | **April 25, 2007** | 0.02 | <0.05 | 0.074 | NA | 0.0001 | 0.003 | <0.001 | 0.02 | 0.019 | 0.176 | 0.015 | 0.0007 | 0.0011 | NA | 0.001 | 0.0001 | 0.0033 | 0.006 |
| **STP07-158-SS** | **STP07158-GW01** | **May 30, 2008** | <0.01 | 0.06 | 0.107 | 0.8 | <0.001 | <0.002 | 0.003 | 0.011 | NA | 0.069 | 0.006 | NA | NA | 0.293 | <0.001 | <0.05 | NA | 0.033 |

Notes:
Only those parameters detected above laboratory detection limits at least once are listed
< - Not Detected Above Numeric Value that Follows
NA - Not Analyzed
*All Concentrations in mg/L

**Table 4-11: Background Dissolved Organics Concentrations in Groundwater at STP-07-158-SS**

| | | | VOCs | | PAHs | | |
|---|---|---|---|---|---|---|---|
| | | | Toluene | p+m-Xylene | Naphthalene | DOC | Naphthenic Acids |
| **Alberta Tier 1 Groundwater Remediation Guidelines for Natural Area with Coarse Soil Type (mg/L)** | | | 0.024 | 0.3 | 0.0011 | Not Listed | Not Listed |
| **Sample Location** | **Sample ID** | **Sample Date** | | | | | |
| **STP07-158-SS** | **MW07-035** | **April 25, 2007** | <0.50 | <0.50 | 0.07 | 6 | <1 |
| **STP07-158-SS** | **STP07158-GW01** | **May 30, 2008** | 1.7 | 1.2 | <2.2 | NA | <1 |
| Notes: | | | | | | | |
| Only those parameters detected above laboratory | | | | | | | |
| detection limits at least once are listed | | | | | | | |
| < - Not Detected Above Numeric Value that Follows | | | | | | | |
| NA - Not Analyzed | | | | | | | |
| *All Concentrations in mg/L unless otherwise noted | | | | | | | |
| 1) VOC, TMB, and PAH for STP07158-GW01 in µg/L | | | | | | | |

## Table 4-12: Background Major Ion Concentrations and Miscellaneous Groundwater Data at STP-07-158-SS

| | | | Chloride (Cl) | Calcium (Ca) | Potassium (K) | Magnesium (Mg) | Sodium (Na) | Sulfate ($SO_4$) | Nitrate+Nitrite-N | Nitrate-N | Fluoride (F) | Ion Balance[1] | TDS (Calculated) | Hardness (as $CaCO_3$) | Conductivity (EC)[2] | Bicarbonate ($HCO_3$) | Alkalinity, Total (as $CaCO_3$) |
|---|---|---|---|---|---|---|---|---|---|---|---|---|---|---|---|---|---|
| **Alberta Tier 1 Groundwater Remediation Guidelines for Natural Area with Coarse Soil Type (mg/L)** | | | 230 | Not Listed | Not Listed | Not Listed | 200 | 500 | - | 13 | 0.12 | Not Listed | 500 | Not Listed | Not Listed | Not Listed | Not Listed |
| **Sample Location** | **Sample ID** | **Sample Date** | | | | | | | | | | | | | | | |
| **STP07-158-SS** | **MW07-035** | **April 25, 2007** | 16 | 78.5 | 2.8 | 21.4 | 25 | 65.3 | 0.3 | 0.3 | 0.48 | 98.6 | 363 | 284 | 597 | 310 | 254 |
| **STP07-158-SS** | **STP07158-GW01** | **May 30, 2008** | 4 | 112 | 1.5 | 33.3 | 4 | 19.7 | <0.1 | <0.1 | NA | 99.9 | 416 | 417 | 712 | 490 | 402 |

Notes:
Only those parameters detected above laboratory detection limits at least once are listed
< - Not Detected Above Numeric Value that Follows
NA - Not Analyzed
*All Concentrations in mg/L unless otherwise noted
1) Values of ion balance are percentages
2) Units of conductivity: µS/cm

## Table 4-13: Background Metals Concentrations in Groundwater at STP-07-159-SS

| | | | Arsenic (As) | Aluminum (Al) | Boron (B) | Barium (Ba) | Bromide (Br) | Iron (Fe) | Lithium (Li) | Manganese (Mn) | Molybdenum (Mo) | Nickel (Ni) | Antimony (Sb) | Selenium (Se) | Strontium (Sr) | Uranium (U) | Vanadium (V) | Zinc (Zn) |
|---|---|---|---|---|---|---|---|---|---|---|---|---|---|---|---|---|---|---|
| **Alberta Tier 1 Groundwater Remediation Guidelines for Natural Area with Coarse Soil Type (mg/L)** | | | 0.005 | 0.1 | 5 | 1 | Not Listed | 0.3 | Not Listed | 0.05 | Not Listed | 0.15 | 0.006 | 0.001 | Not Listed | 0.02 | Not Listed | 0.03 |
| **Sample Location** | **Sample ID** | **Sample Date** | | | | | | | | | | | | | | | | |
| **STP07-159-SS** | **MW07-034** | **April 25, 2007** | 0.0012 | 0.03 | 0.11 | 0.123 | NA | 0.018 | 0.022 | 0.11 | 0.005 | 0.006 | 0.0018 | 0.0041 | NA | 0.0157 | 0.001 | 0.011 |
| **STP07-159-SS** | **STP07159-GW23** | **May 30, 2008** | NA | <0.01 | 0.21 | 0.133 | 1.6 | 0.212 | NA | 0.19 | <0.005 | 0.003 | NA | NA | 0.26 | NA | <0.001 | 0.162 |

Notes:
Only those parameters detected above laboratory detection limits at least once are listed
< - Not Detected Above Numeric Value that Follows
NA - Not Analyzed
*All Concentrations in mg/L

**Table 4-14: Background Dissolved Organics Concentrations in Groundwater at STP-07-159-SS**

| | | | VOCs | | | | PAHs | | | |
|---|---|---|---|---|---|---|---|---|---|---|
| | | | Toluene | p+m-Xylene | o-Xylene | 1,2,3-trimethylbenzene | Naphthalene | Indole+2-methyl naphthalene | DOC | Naphthenic Acids |
| **Alberta Tier 1 Groundwater Remediation Guidelines for Natural Area with Coarse Soil Type (mg/L)** | | | 0.024 | 0.3 | | Not Listed | 0.0011 | Not Listed | Not Listed | Not Listed |
| **Sample Location** | **Sample ID** | **Sample Date** | | | | | | | | |
| **STP07-159-SS** | **MW07-034** | **April 25, 2007** | 0.85 | 0.00073 | | NA | 0.01 | NA | 13 | 2 |
| **STP07-159-SS** | **STP07159-GW23** | **May 30, 2008** | 0.99 | 1.2 | 0.52 | 0.44 | <2.2 | 1.2 | NA | <1 |

Notes:

Only those parameters detected above laboratory detection limits at least once are listed

< - Not Detected Above Numeric Value that Follows

NA - Not Analyzed

*All Concentrations in mg/L unless otherwise noted

1) VOC, TMB, and PAH for STP07159-GW29 in µg/L

## Table 4-15: Background Major Ion Concentrations and Miscellaneous Groundwater Data at STP-07-159-SS

| | | | Chloride (Cl) | Calcium (Ca) | Potassium (K) | Magnesium (Mg) | Sodium (Na) | Sulfate ($SO_4$) | Nitrate+Nitrite-N | Nitrate-N | Nitrite-N | Ammonia | Fluoride (F) | Ion Balance[1] | TDS (Calculated) | Hardness (as $CaCO_3$) | Conductivity (EC)[2] | Bicarbonate ($HCO_3$) | Alkalinity, Total (as $CaCO_3$) |
|---|---|---|---|---|---|---|---|---|---|---|---|---|---|---|---|---|---|---|---|
| **Alberta Tier 1 Groundwater Remediation Guidelines for Natural Area with Coarse Soil Type (mg/L)** | | | 230 | Not Listed | Not Listed | Not Listed | 200 | 500 | - | 13 | 0.06 | 1.37 | 0.12 | Not Listed | 500 | Not Listed | Not Listed | Not Listed | Not Listed |
| **Sample Location** | **Sample ID** | **Sample Date** | | | | | | | | | | | | | | | | | |
| **STP07-159-SS** | **MW07-034** | **April 25, 2007** | 33 | 73.3 | 3.6 | 19.2 | 74 | 115 | 0.2 | 0.1 | 0.07 | 0.55 | 0.33 | 102 | 471 | 262 | 749 | 309 | 253 |
| **STP07-159-SS** | **STP07159-GW23** | **May 30, 2008** | 38 | 81.4 | 2.1 | 23 | 72 | 13.5 | <0.1 | <0.1 | <0.05 | <0.05 | NA | 99.9 | 464 | 298 | 789 | 476 | 390 |

Notes:

Only those parameters detected above laboratory detection limits at least once are listed

< - Not Detected Above Numeric Value that Follows

NA - Not Analyzed

*All Concentrations in mg/L unless otherwise noted

1) Values of ion balance are percentages

2) Units of conductivity: µS/cm

## Table 4-16: Metals Concentrations in STP-07-158-SS PA Water Injectate

| | | | Arsenic (As) | Aluminum (Al) | Boron (B) | Barium (Ba) | Beryllium (Be) | Bromide (Br) | Cobalt (Co) | Chromium (Cr) | Copper (Cu) | Iron (Fe) | Manganese (Mn) | Molybdenum (Mo) | Nickel (Ni) | Lead (Pb) | Selenium (Se) | Strontium (Sr) | Titanium (Ti) | Vanadium (V) | Zinc (Zn) |
|---|---|---|---|---|---|---|---|---|---|---|---|---|---|---|---|---|---|---|---|---|---|
| **Alberta Tier 1 Groundwater Remediation Guidelines for Natural Area with Coarse Soil Type (mg/L)** | | | 0.005 | 0.1 | 5 | 1 | Not Listed | Not Listed | Not Listed | 0.001 | 0.004 | 0.3 | 0.05 | Not Listed | 0.15 | 0.007 | 0.001 | Not Listed | Not Listed | Not Listed | 0.03 |
| **Sample Location** | **Sample ID** | **Sample Date** | | | | | | | | | | | | | | | | | | | |
| **STP07-158-SS** | **STP07158-IJ02** | **July 17, 2008** | 0.0079 | 3.02 | 2.44 | 0.118 | 0.002 | 4.2 | 0.024 | <0.005 | 0.009 | 10.6 | 0.339 | 0.194 | 0.053 | 0.014 | 0.0023 | 0.313 | 0.019 | 0.029 | 0.047 |
| **STP07-158-SS** | **STP07158-IJ03** | **July 17, 2008** | 0.0087 | 3.01 | 98.70 | 0.124 | 0.002 | 2.8 | 0.024 | 0.005 | 0.008 | 10.9 | 0.322 | 0.201 | 0.054 | 0.015 | 0.0024 | 0.318 | 0.025 | 0.031 | 0.041 |
| **STP07-158-SS** | **STP07158-IJ04** | **July 17, 2008** | NA | NA | NA | NA | NA | 297.9 | NA | NA | NA | NA | NA | NA | NA | NA | NA | NA | NA | NA | NA |

Notes:

Only those parameters detected above laboratory detection limits at least once are listed

< - Not Detected Above Numeric Value that Follows

NA - Not Analyzed

*All Concentrations in mg/L

**Samples not field filtered - Results not representative of dissolved concentrations

**Table 4-17: Dissolved Organics Concentrations in STP-07-158-SS PA Water Injectate**

| | | | VOCs | | | | | Trimethylbenzene | | | PAHs | | |
|---|---|---|---|---|---|---|---|---|---|---|---|---|---|
| | | | Benzene | Toluene | EthylBenzene | p+m-Xylene | o-Xylene | 1,3,5-trimethylbenzene | 1,2,4-trimethylbenzene | 1,2,3-trimethylbenzene | Indole+2-methyl naphthalene | DOC | Naphthenic Acids |
| **Alberta Tier 1 Groundwater Remediation Guidelines for Natural Area with Coarse Soil Type** | | | 5 | 24 | 2.4 | 300 | | Not Listed | Not Listed | Not Listed | Not Listed | Not Listed | Not Listed |
| **Sample Location** | **Sample ID** | **Sample Date** | | | | | | | | | | | |
| **STP07-158-SS** | **STP07158-IJ02** | **July 17, 2008** | 7.0 | 17.9 | 5.1 | 21.6 | 8.2 | 1.3 | 2.1 | 13.4 | 2.0 | 41 | 41.4 |
| **STP07-158-SS** | **STP07158-IJ03** | **July 17, 2008** | 4.3 | 7.2 | 18.7 | 8.0 | 3.2 | <1.0 | <1.0 | <1.2 | 5.0 | 40 | 44.8 |

Notes:

Only those parameters detected above laboratory detection limits at least once are listed

< - Not Detected Above Numeric Value that Follows

NA - Not Analyzed

*All Concentrations in mg/L unless otherwise noted

1) VOC, TMB, and PAH concentrations in µg/L including remediaiton guidelines

## Table 4-18: Major Ions and Miscellaneous Data for STP-07-158-SS PA Water Injectate

| | | | Chloride (Cl) | Calcium (Ca) | Potassium (K) | Magnesium (Mg) | Sodium (Na) | Sulfate ($SO_4$) | Nitrate+Nitrite-N | Nitrate-N | Ammonia | Ion Balance[1] | TDS (Calculated) | Hardness (as $CaCO_3$) | Conductivity (EC)[2] | Bicarbonate ($HCO_3$) | Carbonate ($CO_3$) | Alkalinity, Total (as $CaCO_3$) |
|---|---|---|---|---|---|---|---|---|---|---|---|---|---|---|---|---|---|---|
| **Alberta Tier 1 Groundwater Remediation Guidelines for Natural Area with Coarse Soil Type (mg/L)** | | | 230 | Not Listed | Not Listed | Not Listed | 200 | 500 | - | 13 | 1.37 | Not Listed | 500 | Not Listed | Not Listed | Not Listed | Not Listed | Not Listed |
| **Sample Location** | **Sample ID** | **Sample Date** | | | | | | | | | | | | | | | | |
| **STP07-158-SS** | **STP07158-IJ02** | **July 17, 2008** | 537 | 11.9 | 9 | 6 | 670 | 190 | 0.6 | 0.6 | 1 | 102 | 1750 | 54 | 3090 | 637 | 10 | 538 |
| **STP07-158-SS** | **STP07158-IJ03** | **July 17, 2008** | 414 | 10.7 | 8.9 | 5.5 | 686 | 183 | 0.6 | 0.6 | 1.17 | 101 | 1760 | 49 | 2980 | 515 | 199 | 754 |

Notes:

Only those parameters detected above laboratory detection limits at least once are listed

< - Not Detected Above Numeric Value that Follows

NA - Not Analyzed

*All Concentrations in mg/L unless otherwise noted

1) Values of ion balance are percentages

2) Units of conductivity: µS/cm

## Table 4-19: Metals Concentrations in STP-07-159-SS PA Water Injectate

| | | | Arsenic (As) | Aluminum (Al) | Boron (B) | Barium (Ba) | Bromide (Br) | Cobalt (Co) | Iron (Fe) | Manganese (Mn) | Molybdenum (Mo) | Nickel (Ni) | Selenium (Se) | Strontium (Sr) | Titanium (Ti) | Uranium (U) | Vanadium (V) |
|---|---|---|---|---|---|---|---|---|---|---|---|---|---|---|---|---|---|
| **Alberta Tier 1 Groundwater Remediation Guidelines for Natural Area with Coarse Soil Type (mg/L)** | | | 0.005 | 0.1 | 5 | 1 | Not Listed | Not Listed | 0.3 | 0.05 | Not Listed | 0.15 | 0.001 | Not Listed | Not Listed | 0.02 | Not Listed |
| **Sample Location** | **Sample ID** | **Sample Date** | | | | | | | | | | | | | | | |
| **STP07-159-SS** | **STP07159-IJ07** | **August 7, 2008** | 0.006 | 0.7 | 5.21 | 0.04 | 8.1 | 0.003 | 0.159 | 0.033 | 0.332 | 0.014 | 0.008 | 0.218 | 0.013 | 0.006 | 0.01 |
| **STP07-159-SS** | **STP07159-IJ08** | **August 7, 2008** | NA | NA | NA | NA | 151.5 | NA | NA | NA | NA | NA | NA | NA | NA | NA | NA |
| **STP07-159-SS** | **STP07159-IJ09** | **August 7, 2008** | NA | NA | 104 | NA | NA | NA | NA | NA | NA | NA | NA | NA | NA | NA | NA |
| **STP07-159-SS** | **STP07159-IJ10** | **August 7, 2008** | NA | NA | NA | NA | 27.3 | NA | NA | NA | NA | NA | NA | NA | NA | NA | NA |
| **STP07-159-SS** | **STP07159-IJ11** | **August 7, 2008** | 0.006 | <0.1 | 3.32 | 0.044 | 61.3 | 0.002 | 0.052 | 0.033 | 0.265 | 0.013 | 0.041 | 0.216 | <0.003 | 0.006 | 0.01 |

Notes:

Only those parameters detected above laboratory detection limits at least once are listed

< - Not Detected Above Numeric Value that Follows

NA - Not Analyzed

*All Concentrations in mg/L

**Table 4-20: Dissolved Organics Concentrations in STP-07-159-SS PA Water Injectate**

| | | | VOCs | | | | | Trimethylbenzene | | | PAHs | | | | |
|---|---|---|---|---|---|---|---|---|---|---|---|---|---|---|---|
| | | | Benzene | Toluene | EthylBenzene | p+m-Xylene | o-Xylene | 1,3,5-trimethylbenzene | 1,2,4-trimethylbenzene | 1,2,3-trimethylbenzene | Naphthalene | Indole+2-methyl naphthalene | 1-methyl naphthalene | DOC | Naphthenic Acids |
| **Alberta Tier 1 Groundwater Remediation Guidelines for Natural Area with Coarse Soil Type** | | | 5 | 24 | 2.4 | 300 | | Not Listed | Not Listed | Not Listed | 1.1 | Not Listed | Not Listed | Not Listed | Not Listed |
| **Sample Location** | **Sample ID** | **Sample Date** | | | | | | | | | | | | | |
| **STP07-159-SS** | **STP07159-IJ07** | **August 7, 2008** | 2.0 | 6.4 | 2.6 | 15.2 | 7.5 | 3.1 | 7.1 | 20.7 | 5.6 | 6.9 | 4.3 | 52 | 43.9 |
| **STP07-159-SS** | **STP07159-IJ11** | **August 7, 2008** | 2.1 | 7.8 | 3.0 | 16.3 | 7.7 | 1.5 | 6.9 | 7.7 | 5.8 | 4.9 | 4.4 | 48 | 41.3 |

Notes:

Only those parameters detected above laboratory detection limits at least once are listed

< - Not Detected Above Numeric Value that Follows

NA - Not Analyzed

*All Concentrations in mg/L unless otherwise noted

1) VOC, TMB, and PAH concentrations in µg/L including remediation guidelines

## Table 4-21: Major Ions and Miscellaneous Data for STP-07-159-SS PA Water Injectate

| | | | Chloride (Cl) | Calcium (Ca) | Potassium (K) | Magnesium (Mg) | Sodium (Na) | Sulfate ($SO_4$) | Nitrate+Nitrite-N | Nitrate-N | Nitrite-N | Ammonia | Ion Balance[1] | TDS (Calculated) | Hardness (as $CaCO_3$) | Conductivity (EC)[2] | Bicarbonate ($HCO_3$) | Carbonate ($CO_3$) | Alkalinity, Total (as $CaCO_3$) |
|---|---|---|---|---|---|---|---|---|---|---|---|---|---|---|---|---|---|---|---|
| **Alberta Tier 1 Groundwater Remediation Guidelines for Natural Area with Coarse Soil Type (mg/L)** | | | 230 | Not Listed | Not Listed | Not Listed | 200 | 500 | - | 13 | 0.06 | 1.37 | Not Listed | 500 | Not Listed | Not Listed | Not Listed | Not Listed | Not Listed |
| **Sample Location** | **Sample ID** | **Sample Date** | | | | | | | | | | | | | | | | | |
| **STP07-159-SS** | **STP07159-IJ07** | **August 7, 2008** | 554 | 7.9 | 8.9 | 4.4 | 606 | 169 | 0.5 | 0.5 | <0.05 | 1.09 | 90.9 | 1680 | 38 | 2990 | 623 | 21 | 546 |
| **STP07-159-SS** | **STP07159-IJ10** | **August 7, 2008** | 520 | NA | NA | NA | NA | NA | NA | NA | NA | NA | NA | NA | NA | NA | NA | NA | NA |
| **STP07-159-SS** | **STP07159-IJ11** | **August 7, 2008** | 676 | 8.8 | 9.9 | 4.7 | 707 | 169 | 0.4 | 0.4 | <0.05 | 1.61 | 95.1 | 1900 | 41 | 3300 | 625 | 18 | 543 |

Notes:

Only those parameters detected above laboratory detection limits at least once are listed

< - Not Detected Above Numeric Value that Follows

NA - Not Analyzed

*All Concentrations in mg/L unless otherwise noted

1) Values of ion balance are percentages

2) Units of conductivity: µS/cm

## Table 4-22: Post PA Water Injection Dissolved Metals Concentrations at STP-07-158-SS

| | | | Arsenic (As) | Silver (Ag) | Aluminum (Al) | Boron (B) | Barium (Ba) | Bismuth (Bi) | Bromide (Br) | Cadmium (Cd) | Cobalt (Co) | Chromium (Cr) | Copper (Cu) | Iron (Fe) | Manganese (Mn) | Molybdenum (Mo) | Nickel (Ni) | Lead (Pb) | Antimony (Sb) | Selenium (Se) | Tin (Sn) | Strontium (Sr) | Titanium (Ti) | Thallium (Tl) | Uranium (U) | Vanadium (V) | Zinc (Zn) |
|---|---|---|---|---|---|---|---|---|---|---|---|---|---|---|---|---|---|---|---|---|---|---|---|---|---|---|---|
| **Alberta Tier 1 Groundwater Remediation Guidelines for Natural Area with Coarse Soil Type (mg/L)** | | | 0.005 | 0.0001 | 0.1 | 5 | 1 | Not Listed | Not Listed | 0.005 | Not Listed | 0.001 | 0.004 | 0.3 | 0.05 | Not Listed | 0.15 | 0.007 | 0.006 | 0.001 | Not Listed | Not Listed | Not Listed | Not Listed | 0.02 | Not Listed | 0.03 |
| **Sample Location** | **Sample ID** | **Sample Date** | | | | | | | | | | | | | | | | | | | | | | | | | |
| **STP07-158-SS** | **STP07158-GW15** | **July 18, 2008** | 0.0028 | <0.005 | 0.03 | 8.82 | 0.055 | NA | 269.1 | <0.001 | 0.003 | <0.005 | 0.008 | 0.015 | 0.053 | 0.240 | 0.015 | <0.005 | NA | 0.0028 | <0.05 | 0.226 | 0.001 | <0.05 | NA | 0.003 | 0.027 |
| **STP07-158-SS** | **STP07158-GW16** | **July 23, 2008** | 0.0023 | <0.005 | 0.01 | 10.10 | 0.058 | NA | 247.3 | <0.001 | 0.002 | <0.005 | 0.003 | 0.008 | 0.053 | 0.158 | 0.012 | <0.005 | NA | 0.0018 | <0.05 | 0.225 | <0.001 | <0.05 | NA | 0.003 | 0.067 |
| **STP07-158-SS** | **STP07158-GW17** | **August 6, 2008** | 0.0040 | <0.002 | <0.1 | 41.40 | 0.062 | <0.0005 | 83.5 | <0.001 | 0.002 | <0.004 | <0.006 | 0.054 | 0.068 | 0.104 | 0.01 | <0.001 | <0.004 | 0.057 | <0.002 | 0.252 | <0.003 | <0.0005 | 0.008 | 0.006 | 0.11 |
| **STP07-158-SS** | **STP07158-GW18** | **August 21, 2008** | 0.0028 | <0.0002 | 0.07 | 16.20 | 0.055 | <0.00005 | 16.9 | 0.0001 | 0.002 | 0.0029 | 0.0027 | 0.146 | 0.091 | 0.0534 | 0.0072 | 0.0004 | <0.0004 | 0.0007 | <0.0002 | 0.228 | 0.0013 | 0.00013 | 0.0058 | 0.0032 | 0.114 |
| **STP07-158-SS** | **STP07158-GW19** | **August 27, 2008** | 0.0015 | <0.005 | 0.02 | 9.44 | 0.056 | NA | 10.9 | <0.001 | <0.002 | <0.005 | 0.0020 | 0.046 | 0.09 | 0.0350 | 0.006 | <0.005 | NA | 0.0004 | <0.05 | 0.224 | <0.001 | <0.05 | NA | <0.001 | 0.186 |
| **STP07-158-SS** | **STP07158-GW20** | **September 3, 2008** | 0.0012 | <0.0002 | 0.04 | 7.82 | 0.061 | <0.00005 | 7.0 | <0.0001 | 0.0021 | 0.0004 | 0.0025 | 0.016 | 0.123 | 0.0363 | 0.0066 | <0.0001 | <0.0004 | <0.0004 | <0.0002 | 0.270 | 0.0014 | <0.00005 | 0.0051 | 0.0023 | 0.2 |
| **STP07-158-SS** | **STP07158-GW21** | **September 12, 2008** | 0.0014 | <0.0002 | <0.01 | 5.45 | 0.075 | <0.00005 | 4.0 | <0.0001 | 0.0026 | 0.0007 | 0.0012 | 0.007 | 0.17 | 0.0278 | 0.0064 | <0.0001 | <0.0004 | 0.0025 | <0.0002 | 0.320 | <0.0003 | <0.00005 | 0.0052 | 0.0008 | 0.23 |
| **STP07-158-SS** | **STP07158-GW22** | **September 17, 2008** | 0.0015 | <0.0002 | <0.01 | 4.24 | 0.080 | <0.00005 | 2.7 | <0.0001 | 0.0028 | 0.0006 | 0.0013 | 0.012 | 0.182 | 0.0269 | 0.0066 | <0.0001 | <0.0004 | 0.0033 | <0.0002 | 0.358 | 0.0004 | 0.00024 | 0.0044 | 0.0008 | 0.202 |
| **STP07-158-SS** | **STP07158-GW23** | **September 25, 2008** | 0.0014 | <0.0002 | <0.01 | 2.92 | 0.088 | <0.00005 | 0.9 | <0.0001 | 0.0031 | <0.0004 | 0.0009 | 0.008 | 0.256 | 0.0234 | 0.0069 | <0.0001 | <0.0004 | 0.0027 | <0.0002 | 0.389 | 0.0003 | <0.00005 | 0.004 | 0.0009 | 0.251 |
| **STP07-158-SS** | **STP07158-GW24** | **September 30, 2008** | 0.0013 | <0.0002 | <0.01 | 2.56 | 0.088 | <0.00005 | 0.8 | <0.0001 | 0.0031 | 0.0004 | 0.0009 | 0.016 | 0.268 | 0.0193 | 0.0065 | <0.0001 | <0.0004 | 0.0021 | <0.0002 | 0.397 | 0.0004 | <0.00005 | 0.0035 | 0.0007 | 0.242 |
| **STP07-158-SS** | **STP07158-GW25** | **October 8, 2008** | 0.0013 | <0.0002 | <0.01 | 1.97 | 0.089 | <0.00005 | 0.6 | <0.0001 | 0.003 | 0.0007 | 0.0009 | <0.005 | 0.314 | 0.0205 | 0.0063 | <0.0001 | <0.0004 | 0.0015 | <0.0002 | 0.404 | <0.0003 | <0.00005 | 0.0035 | 0.0008 | 0.175 |
| **STP07-158-SS** | **STP07158-GW25D** | **October 8, 2008** | 0.0012 | <0.0002 | <0.01 | 1.92 | 0.090 | <0.00005 | 0.6 | <0.0001 | 0.003 | 0.0006 | 0.0009 | <0.005 | 0.309 | 0.0199 | 0.0061 | <0.0001 | <0.0004 | 0.0015 | <0.0002 | 0.412 | <0.0003 | <0.00005 | 0.0033 | 0.0006 | 0.187 |
| **STP07-158-SS** | **STP07158-GW26** | **October 16, 2008** | 0.0015 | <0.0002 | <0.01 | 1.38 | 0.115 | <0.00005 | 0.3 | <0.0001 | 0.004 | 0.0014 | 0.0008 | 0.049 | 0.452 | 0.0115 | 0.0072 | <0.0001 | <0.0004 | 0.0011 | <0.0002 | 0.563 | 0.0003 | <0.00005 | 0.0028 | <0.001 | 0.32 |
| **STP07-158-SS** | **STP07158-GW27** | **October 23, 2008** | 0.0016 | <0.0002 | <0.01 | 1.15 | 0.143 | <0.00005 | 0.4 | <0.0001 | 0.0058 | 0.0004 | 0.0013 | 0.079 | 0.528 | 0.0054 | 0.0095 | 0.0002 | <0.0004 | <0.0004 | <0.0002 | 0.703 | <0.0003 | <0.00005 | 0.0024 | <0.001 | 0.47 |
| **STP07-158-SS** | **STP07158-GW28** | **November 1, 2008** | 0.0014 | 0.0024 | <0.01 | 0.95 | 0.153 | 0.0003 | 0.3 | <0.0001 | 0.0062 | <0.0004 | 0.0009 | 0.111 | 0.567 | 0.0038 | 0.0104 | 0.0002 | 0.0005 | 0.001 | 0.0006 | 0.691 | 0.0009 | 0.00017 | 0.0024 | <0.0001 | 0.38 |
| **STP07-158-SS** | **STP07158-GW29** | **November 8, 2008** | 0.0012 | <0.0002 | <0.01 | 0.55 | 0.157 | <0.00005 | 0.2 | <0.0001 | 0.0053 | 0.001 | 0.0009 | 0.166 | 0.418 | 0.0022 | 0.0093 | 0.0002 | <0.0004 | <0.0004 | <0.0002 | 0.657 | 0.0006 | 0.00006 | 0.0018 | 0.000 | 0.482 |
| **STP07-158-SS** | **STP07158-GW30** | **June 20, 2009** | 0.0007 | 0.00020 | 0.019 | 0.0903 | 0.188 | <0.00005 | NA | <0.00010 | 0.0022 | 0.00093 | 0.0008 | 0.325 | 0.52 | 0.0011 | 0.0072 | 0.00017 | <0.00040 | <0.0004 | <0.00020 | 0.315 | 0.00059 | <0.00005 | 0.0029 | <0.0001 | 0.309 |

Notes:

Only those parameters detected above laboratory detection limits at least once are listed

< - Not Detected Above Numeric Value that Follows

NA - Not Analyzed

*All Concentrations in mg/L

**Table 4-23: Post PA Water Injection Dissolved Organics Concentrations at STP-07-158-SS**

| | | | VOCs | | | PAHs | | | |
|---|---|---|---|---|---|---|---|---|---|
| | | | Benzene | Toluene | p+m-Xylene | Indole+2-methyl naphthalene | Acenaphthylene | DOC | Naphthenic Acids |
| **Alberta Tier 1 Groundwater Remediation Guidelines for Natural Area with Coarse Soil Type** | | | 5 | 24 | 300 | Not Listed | 46 | Not Listed | Not Listed |
| **Sample Location** | **Sample ID** | **Sample Date** | | | | | | | |
| **STP07-158-SS** | **STP07158-GW15** | **July 18, 2008** | <1.3 | 72.9 | <2.6 | 1.5 | <1.4 | 54 | 49.4 |
| **STP07-158-SS** | **STP07158-GW16** | **July 23, 2008** | <1.3 | 11.6 | 1.3 | 2.6 | <1.4 | 47 | 41.9 |
| **STP07-158-SS** | **STP07158-GW17** | **August 6, 2008** | <1.3 | 10.0 | 1.2 | 4.3 | <1.4 | 45 | 32.6 |
| **STP07-158-SS** | **STP07158-GW18** | **August 21, 2008** | 1.4 | 9.1 | 1.6 | <2.8 | <1.4 | 21 | 14.4 |
| **STP07-158-SS** | **STP07158-GW19** | **August 27, 2008** | <1.3 | 12.8 | 1.4 | 1.7 | <1.4 | 15 | 8.9 |
| **STP07-158-SS** | **STP07158-GW20** | **September 3, 2008** | <1.3 | 9.4 | 1.4 | <2.8 | 5.0 | 13 | 8 |
| **STP07-158-SS** | **STP07158-GW21** | **September 12, 2008** | 1.8 | 10.4 | 1.3 | <2.8 | 5.3 | 10 | 4.3 |
| **STP07-158-SS** | **STP07158-GW22** | **September 17, 2008** | <1.3 | 9.3 | 1.4 | 1.4 | <1.4 | 9 | 4.1 |
| **STP07-158-SS** | **STP07158-GW23** | **September 25, 2008** | <1.3 | 7.4 | 1.3 | 1.2 | 3.9 | 12 | 2.7 |
| **STP07-158-SS** | **STP07158-GW24** | **September 30, 2008** | <1.3 | 7.2 | <2.6 | <2.8 | 4.0 | 6 | 2.3 |
| **STP07-158-SS** | **STP07158-GW25** | **October 8, 2008** | <1.3 | 4.1 | <2.6 | 1.4 | 3.9 | 6 | 1.7 |
| **STP07-158-SS** | **STP07158-GW25D** | **October 8, 2008** | <1.3 | 5.0 | <2.6 | 1.1 | 4.5 | 5 | 1.6 |
| **STP07-158-SS** | **STP07158-GW26** | **October 16, 2008** | <1.3 | 5.7 | 1.2 | <2.8 | 4.4 | 4 | 1.1 |
| **STP07-158-SS** | **STP07158-GW27** | **October 23, 2008** | <1.3 | 3.2 | 1.2 | 4.2 | 2.7 | 5 | 1.3 |
| **STP07-158-SS** | **STP07158-GW28** | **November 1, 2008** | <1.3 | 3.2 | 1.4 | <2.8 | 4.7 | 5 | <1.0 |
| **STP07-158-SS** | **STP07158-GW29** | **November 8, 2008** | 1.2 | 3.1 | 1.5 | <2.8 | 1.4 | 4 | <1.0 |
| **STP07-158-SS** | **STP07158-GW30** | **November 8, 2008** | NA | NA | NA | NA | NA | 2.9 | <0.5 |

Notes:

Only those parameters detected above laboratory detection limits at least once are listed

< - Not Detected Above Numeric Value that Follows

NA - Not Analyzed

*All Concentrations in mg/L unless otherwise noted

1) VOC, TMB, and PAH concentrations in µg/L including remediaiton guidelines

## Table 4-24: Post PA Water Injection Major Ions and Miscellaneous Groundwater Data at STP-07-158-SS

| | | | Chloride (Cl) | Calcium (Ca) | Potassium (K) | Magnesium (Mg) | Sodium (Na) | Sulfate ($SO_4$) | Nitrate+Nitrite-N | Nitrate-N | Nitrite-N | Ammonia | Ion Balance[1] | TDS (Calculated) | Hardness (as $CaCO_3$) | Conductivity (EC)[2] | Bicarbonate ($HCO_3$) | Carbonate ($CO_3$) | Alkalinity, Total (as $CaCO_3$) |
|---|---|---|---|---|---|---|---|---|---|---|---|---|---|---|---|---|---|---|---|
| **Alberta Tier 1 Groundwater Remediation Guidelines for Natural Area with Coarse Soil Type (mg/L)** | | | 230 | Not Listed | Not Listed | Not Listed | 200 | 500 | - | 13 | 0.06 | 1.37 | Not Listed | 500 | Not Listed | Not Listed | Not Listed | Not Listed | Not Listed |
| **Sample Location** | **Sample ID** | **Sample Date** | | | | | | | | | | | | | | | | | |
| **STP07-158-SS** | **STP07158-GW15** | **July 18, 2008** | 538 | 12.7 | 8.3 | 6 | 641 | 181 | 0.5 | 0.4 | 0.14 | 0.83 | 97.2 | 1720 | 56 | 2990 | 652 | 12 | 554 |
| **STP07-158-SS** | **STP07158-GW16** | **July 23, 2008** | 525 | 14.2 | 6.7 | 7.1 | 606 | 180 | 0.3 | 0.3 | <0.05 | 0.87 | 94.2 | 1670 | 65 | 2840 | 668 | <5 | 551 |
| **STP07-158-SS** | **STP07158-GW17** | **August 6, 2008** | 459 | 20.3 | 6.1 | 8.7 | 540 | 154 | 0.3 | 0.3 | <0.05 | 0.5 | 94.7 | 1510 | 87 | 2640 | 636 | 6 | 532 |
| **STP07-158-SS** | **STP07158-GW18** | **August 21, 2008** | 220 | 23.9 | 7 | 10.3 | 367 | 87 | <0.1 | <0.1 | 0.08 | 0.39 | 98.8 | 1030 | 102 | 1760 | 633 | <5 | 519 |
| **STP07-158-SS** | **STP07158-GW19** | **August 27, 2008** | 131 | 26.5 | 5 | 10.6 | 259 | 57.4 | <0.1 | <0.1 | <0.05 | 0.38 | 93 | 781 | 110 | 1410 | 593 | <5 | 486 |
| **STP07-158-SS** | **STP07158-GW20** | **September 3, 2008** | 88 | 35.4 | 6.9 | 14.2 | 227 | 55.3 | <0.1 | <0.1 | <0.05 | 0.42 | 102 | 746 | 119 | 1240 | 603 | <5 | 494 |
| **STP07-158-SS** | **STP07158-GW21** | **September 12, 2008** | 60 | 47.2 | 6.5 | 18.3 | 190 | 54.8 | <0.1 | <0.1 | <0.05 | 0.39 | 100 | 659 | 193 | 1120 | 574 | <5 | 471 |
| **STP07-158-SS** | **STP07158-GW22** | **September 17, 2008** | 48 | 42.2 | 5.7 | 16.7 | 160 | 44.7 | <0.1 | <0.1 | <0.05 | 0.38 | 91.6 | 596 | 174 | 1040 | 566 | <5 | 464 |
| **STP07-158-SS** | **STP07158-GW23** | **September 25, 2008** | 32 | 50.6 | 6.2 | 20.1 | 147 | 38.9 | <0.1 | <0.1 | <0.05 | 0.35 | 98.7 | 570 | 209 | 966 | 559 | <5 | 458 |
| **STP07-158-SS** | **STP07158-GW24** | **September 30, 2008** | 25 | 50.3 | 5.7 | 20.6 | 136 | 36 | <0.1 | <0.1 | <0.05 | 0.34 | 97.6 | 546 | 210 | 938 | 553 | <5 | 454 |
| **STP07-158-SS** | **STP07158-GW25** | **October 8, 2008** | 20 | 47.1 | 5.9 | 18.9 | 137 | 31.1 | 0.1 | 0.1 | <0.05 | 0.36 | 97 | 533 | 195 | 909 | 556 | <5 | 455 |
| **STP07-158-SS** | **STP07158-GW25D** | **October 8, 2008** | 20 | 45.7 | 5.7 | 18.3 | 133 | 30.2 | <0.1 | <0.1 | <0.05 | 0.44 | 94.2 | 527 | 189 | 913 | 557 | <5 | 456 |
| **STP07-158-SS** | **STP07158-GW26** | **October 16, 2008** | 10 | 61.1 | 6.6 | 26.4 | 91 | 24.1 | <0.1 | <0.1 | <0.05 | 0.31 | 95.9 | 489 | 261 | 854 | 547 | <5 | 449 |
| **STP07-158-SS** | **STP07158-GW27** | **October 23, 2008** | 15 | 74.8 | 6.6 | 30.1 | 77 | 31.3 | <0.1 | <0.1 | <0.05 | 0.4 | 97.9 | 501 | 311 | 857 | 541 | <5 | 443 |
| **STP07-158-SS** | **STP07158-GW28** | **November 1, 2008** | 16 | 88.4 | 6.1 | 33 | 56 | 30.4 | <0.1 | <0.1 | <0.05 | 0.43 | 100 | 489 | 357 | 863 | 525 | <5 | 431 |
| **STP07-158-SS** | **STP07158-GW29** | **November 8, 2008** | 7 | 92.4 | 5 | 33.5 | 26 | 22.2 | <0.1 | <0.1 | <0.05 | 0.26 | 95.3 | 438 | 369 | 801 | 512 | <5 | 420 |
| **STP07-158-SS** | **STP07158-GW30** | **June 20, 2009** | 1.61 | 111 | 33.6 | 2.22 | 6.6 | 20.7 | <0.050 | <0.071 | <0.050 | <0.050 | 103 | 414 | 416 | 741 | 484 | <5 | 397 |

Notes:

Only those parameters detected above laboratory detection limits at least once are listed

< - Not Detected Above Numeric Value that Follows

NA - Not Analyzed

*All Concentrations in mg/L unless otherwise noted

1) Values of ion balance are percentages

2) Units of conductivity: µS/cm

## Table 4-25: Post PA Water Injection Dissolved Metals Concentrations at STP-07-159-SS

| | | | Arsenic (As) | Aluminum (Al) | Boron (B) | Barium (Ba) | Bromide (Br) | Cadmium (Cd) | Cobalt (Co) | Chromium (Cr) | Copper (Cu) | Iron (Fe) | Manganese (Mn) | Molybdenum (Mo) | Nickel (Ni) | Lead (Pb) | Antimony (Sb) | Selenium (Se) | Strontium (Sr) | Titanium (Ti) | Thallium (Tl) | Uranium (U) | Vanadium (V) | Zinc (Zn) |
|---|---|---|---|---|---|---|---|---|---|---|---|---|---|---|---|---|---|---|---|---|---|---|---|---|
| **Alberta Tier 1 Groundwater Remediation Guidelines for Natural Area with Coarse Soil Type (mg/L)** | | | 0.005 | 0.1 | 5 | 1 | Not Listed | 0.005 | Not Listed | 0.001 | 0.004 | 0.3 | 0.05 | Not Listed | 0.15 | 0.007 | 0.006 | 0.001 | Not Listed | Not Listed | Not Listed | 0.02 | Not Listed | 0.03 |
| **Sample Location** | **Sample ID** | **Sample Date** | | | | | | | | | | | | | | | | | | | | | | |
| **STP07-159-SS** | **STP07159-GW35** | **August 8, 2008** | 0.006 | <0.1 | 3.75 | 0.063 | 56.3 | <0.001 | 0.002 | <0.004 | <0.006 | 0.01 | 0.037 | 0.255 | 0.012 | <0.001 | <0.004 | 0.043 | 0.208 | <0.003 | <0.0005 | 0.008 | 0.009 | <0.02 |
| **STP07-159-SS** | **STP07159-GW36** | **August 21, 2008** | 0.0016 | 0.13 | 25.90 | 0.052 | 64.2 | 0.0004 | 0.0019 | 0.0031 | 0.002 | 0.387 | 0.045 | 0.188 | 0.0092 | 0.0012 | 0.0011 | 0.0007 | 0.181 | 0.0017 | 0.00006 | 0.0126 | 0.0046 | 0.059 |
| **STP07-159-SS** | **STP07159-GW37** | **August 27, 2008** | 0.0023 | 0.09 | 6.45 | 0.03 | 9.3 | <0.001 | <0.002 | <0.005 | <0.001 | 0.171 | 0.02 | 0.071 | 0.005 | <0.005 | NA | <0.0004 | 0.074 | <0.001 | <0.05 | NA | 0.001 | 0.035 |
| **STP07-159-SS** | **STP07159-GW38** | **September 3, 2008** | 0.0017 | 0.12 | 3.84 | 0.039 | 4.1 | <0.0001 | 0.0008 | <0.0004 | 0.0012 | 0.038 | 0.035 | 0.0349 | 0.0032 | 0.0001 | 0.0008 | <0.0004 | 0.133 | 0.0032 | <0.00005 | 0.0055 | 0.0021 | 0.006 |
| **STP07-159-SS** | **STP07159-GW39** | **September 12, 2008** | 0.0021 | 0.01 | 3.12 | 0.065 | 3.9 | <0.0001 | 0.0008 | 0.0017 | <0.0006 | 0.074 | 0.065 | 0.0267 | 0.0031 | <0.0001 | 0.0006 | 0.0031 | 0.240 | 0.0005 | <0.00005 | 0.0048 | 0.0006 | 0.01 |
| **STP07-159-SS** | **STP07159-GW40** | **September 17, 2008** | 0.0020 | <0.01 | 1.88 | 0.088 | 3.8 | <0.0001 | 0.0009 | 0.001 | <0.0006 | 0.102 | 0.083 | 0.0191 | 0.0032 | <0.0001 | 0.0006 | 0.0036 | 0.354 | <0.0003 | 0.00008 | 0.0035 | 0.0005 | 0.02 |
| **STP07-159-SS** | **STP07159-GW41** | **September 25, 2008** | 0.0018 | <0.01 | 1.33 | 0.105 | 1.3 | <0.0001 | 0.0011 | 0.0006 | <0.0006 | 0.128 | 0.121 | 0.0125 | 0.0035 | <0.0001 | 0.0005 | 0.0019 | 0.434 | <0.0003 | 0.00009 | 0.0027 | 0.0004 | 0.021 |
| **STP07-159-SS** | **STP07159-GW42** | **September 30, 2008** | 0.0017 | <0.01 | 1.05 | 0.124 | 0.9 | <0.0001 | 0.0015 | 0.0005 | <0.0006 | 0.245 | 0.165 | 0.0103 | 0.0039 | <0.0001 | <0.0004 | 0.0016 | 0.529 | <0.0003 | <0.00005 | 0.0024 | 0.0005 | 0.053 |
| **STP07-159-SS** | **STP07159-GW43** | **October 8, 2008** | 0.0019 | <0.01 | 0.73 | 0.132 | 0.8 | <0.0001 | 0.0018 | 0.0007 | <0.0006 | 0.318 | 0.19 | 0.0085 | 0.0041 | <0.0001 | <0.0004 | 0.0009 | 0.598 | <0.0003 | <0.00005 | 0.0021 | 0.0005 | 0.117 |
| **STP07-159-SS** | **STP07159-GW44** | **October 16, 2008** | 0.0021 | <0.01 | 0.65 | 0.140 | 0.5 | <0.0001 | 0.002 | <0.0004 | <0.0006 | 0.425 | 0.207 | 0.0082 | 0.0045 | <0.0001 | <0.0004 | 0.0008 | 0.610 | <0.0003 | <0.00005 | 0.002 | <0.001 | 0.065 |
| **STP07-159-SS** | **STP07159-GW45** | **October 23, 2008** | 0.0019 | <0.01 | 0.50 | 0.146 | 0.5 | <0.0001 | 0.0021 | <0.0004 | <0.0006 | 0.378 | 0.206 | 0.007 | 0.0046 | <0.0001 | <0.0004 | <0.0004 | 0.625 | <0.0003 | <0.00005 | 0.0021 | <0.001 | 0.099 |
| **STP07-159-SS** | **STP07159-GW46** | **November 1, 2008** | 0.0015 | <0.01 | 0.36 | 0.149 | 0.5 | <0.0001 | 0.0022 | <0.0004 | <0.0006 | 0.498 | 0.222 | 0.007 | 0.0052 | 0.0001 | <0.0004 | <0.0004 | 0.519 | 0.0005 | 0.00008 | 0.002 | <0.0001 | 0.094 |
| **STP07-159-SS** | **STP07159-GW47** | **June 21, 2009** | 0.0013 | <0.010 | 0.23 | 0.134 | NA | <0.00010 | 0.0013 | <0.00040 | <0.00060 | 0.374 | 0.229 | 0.002 | 0.0039 | 0.0009 | <0.00040 | 0.00088 | 0.261 | <0.00030 | <0.000050 | 0.0009 | <0.00010 | 0.222 |
| **STP07-159-SS** | **STP07159-GW47D** | **June 21, 2009** | 0.0013 | <0.010 | 0.23 | 0.133 | NA | <0.00010 | 0.0012 | <0.00040 | <0.00060 | 0.321 | 0.204 | 0.0016 | 0.004 | 0.00043 | <0.00040 | 0.00041 | 0.255 | <0.00030 | <0.000050 | 0.0009 | <0.00010 | 0.221 |

Notes:

Only those parameters detected above laboratory detection limits at least once are listed

< - Not Detected Above Numeric Value that Follows

NA - Not Analyzed

*All Concentrations in mg/L

**Table 4-26: Post PA Water Injection Dissolved Organics Concentrations at STP-07-159-SS**

| | | | VOCs | | | | | Trimethylbenzene | | | PAHs | | | | | |
|---|---|---|---|---|---|---|---|---|---|---|---|---|---|---|---|---|
| | | | Benzene | Toluene | EthylBenzene | p+m-Xylene | o-Xylene | 1,3,5-trimethylbenzene | 1,2,4-trimethylbenzene | 1,2,3-trimethylbenzene | Naphthalene | Indole+2-methyl naphthalene | 1-methyl naphthalene | Acenaphthylene | DOC | Naphthenic Acids |
| **Alberta Tier 1 Groundwater Remediation Guidelines for Natural Area with Coarse Soil Type** | | | 5 | 24 | 2.4 | 300 | | Not Listed | Not Listed | Not Listed | 1.1 | Not Listed | Not Listed | 46 | Not Listed | Not Listed |
| **Sample Location** | **Sample ID** | **Sample Date** | | | | | | | | | | | | | | |
| **STP07-159-SS** | **STP07159-GW35** | **August 8, 2008** | 1.8 | 4.4 | 2.1 | 13.3 | 6.6 | 1.6 | 3.0 | 5.1 | <2.2 | 3.2 | 2.0 | <1.4 | 57 | 32.4 |
| **STP07-159-SS** | **STP07159-GW36** | **August 21, 2008** | 2.3 | 3.8 | 1.4 | 9.3 | 4.4 | 0.8 | 3.5 | 4.2 | 1.7 | 2.4 | 2.5 | <1.4 | 40 | 31.5 |
| **STP07-159-SS** | **STP07159-GW37** | **August 27, 2008** | 1.9 | 4.3 | 1.1 | 8.0 | 3.3 | 1.2 | 2.5 | 4.5 | <2.2 | 1.6 | 1.7 | <1.4 | 15 | 10.1 |
| **STP07-159-SS** | **STP07159-GW38** | **September 3, 2008** | 1.7 | 3.4 | 1.7 | 7.8 | 3.3 | 1.2 | 3.1 | 5.1 | 1.8 | 2.3 | 2.0 | <1.4 | 10 | 6.6 |
| **STP07-159-SS** | **STP07159-GW39** | **September 12, 2008** | 1.7 | 3.5 | <1.5 | 6.6 | 3.3 | <1.0 | 3.7 | 6.3 | 1.4 | <2.8 | <1.4 | 4.5 | 9 | 5.3 |
| **STP07-159-SS** | **STP07159-GW40** | **September 17, 2008** | 2.8 | 3.6 | <1.5 | 6.5 | 2.9 | <1.0 | 3.6 | 7.1 | 4.6 | 2.5 | <1.4 | <1.4 | 7 | 2.8 |
| **STP07-159-SS** | **STP07159-GW41** | **September 25, 2008** | 1.2 | 4.0 | <1.5 | 6.0 | 2.3 | <1.0 | 2.5 | 11.4 | 2.2 | 1.5 | 2.2 | 6.8 | 7 | 1.2 |
| **STP07-159-SS** | **STP07159-GW42** | **September 30, 2008** | <1.3 | 2.9 | <1.5 | 4.6 | 1.5 | <1.0 | 2.0 | 9.0 | 2.2 | <2.8 | 2.1 | 5.2 | 4 | 1.5 |
| **STP07-159-SS** | **STP07159-GW43** | **October 8, 2008** | 1.4 | 2.0 | <1.5 | 4.4 | 1.7 | <1.0 | 2.6 | 7.1 | 1.9 | 2.4 | 2.7 | 3.0 | 5 | 1.1 |
| **STP07-159-SS** | **STP07159-GW44** | **October 16, 2008** | 1.4 | 2.5 | <1.5 | 3.7 | 1.4 | <1.0 | 2.3 | 10.1 | 2.5 | <2.8 | <1.4 | 4.5 | 4 | <1.0 |
| **STP07-159-SS** | **STP07159-GW45** | **October 23, 2008** | <1.3 | 1.7 | <1.5 | 3.1 | 1.4 | <1.0 | 2 | 6 | 2.4 | 2.2 | <1.4 | 3.1 | 4 | <1.0 |
| **STP07-159-SS** | **STP07159-GW46** | **November 1, 2008** | 1.1 | 1.2 | <1.5 | 2.5 | 1.1 | 0 | 2 | 4 | 2.9 | 1.6 | <1.4 | 2.1 | 4 | <1.0 |
| **STP07-159-SS** | **STP07159-GW47** | **June 21, 2009** | NA | NA | NA | NA | NA | NA | NA | NA | NA | NA | NA | NA | 3.6 | <0.5 |
| **STP07-159-SS** | **STP07159-GW47D** | **June 21, 2009** | NA | NA | NA | NA | NA | NA | NA | NA | NA | NA | NA | NA | 3.5 | <0.5 |

Notes:

Only those parameters detected above laboratory detection limits at least once are listed

< - Not Detected Above Numeric Value that Follows

NA - Not Analyzed

*All Concentrations in mg/L unless otherwise noted

1) VOC, TMB, and PAH concentrations in µg/L including remediation guidelines

## Table 4-27: Post PA Water Injection Major Ions and Miscellaneous Groundwater Data at STP-07-159-SS

| | | | Chloride (Cl) | Calcium (Ca) | Potassium (K) | Magnesium (Mg) | Sodium (Na) | Sulfate ($SO_4$) | Nitrate+Nitrite-N | Nitrate-N | Ammonia | Ion Balance[1] | TDS (Calculated) | Hardness (as $CaCO_3$) | Conductivity (EC)[2] | Bicarbonate ($HCO_3$) | Carbonate ($CO_3$) | Hydroxide (OH) | Alkalinity, Total (as $CaCO_3$) |
|---|---|---|---|---|---|---|---|---|---|---|---|---|---|---|---|---|---|---|---|
| **Alberta Tier 1 Groundwater Remediation Guidelines for Natural Area with Coarse Soil Type (mg/L)** | | | 230 | Not Listed | Not Listed | Not Listed | 200 | 500 | - | 13 | 1.37 | Not Listed | 500 | Not Listed | Not Listed | Not Listed | Not Listed | Not Listed | Not Listed |
| **Sample Location** | **Sample ID** | **Sample Date** | | | | | | | | | | | | | | | | | |
| **STP07-159-SS** | **STP07159-GW35** | **August 8, 2008** | 692 | 10.8 | 9 | 5.2 | 721 | 186 | <0.1 | <0.1 | 1.39 | 95.1 | 1950 | 48 | 3310 | 638 | 12 | <5 | 544 |
| **STP07-159-SS** | **STP07159-GW36** | **August 21, 2008** | 433 | 9.5 | 5.1 | 4.5 | 544 | 127 | <0.1 | <0.1 | 0.54 | 97.6 | 1440 | 42 | 2490 | 634 | <5 | <5 | 520 |
| **STP07-159-SS** | **STP07159-GW37** | **August 27, 2008** | 125 | 5.3 | 3.4 | 2.3 | 299 | 45.2 | <0.1 | <0.1 | 0.31 | 99.2 | 761 | 23 | 1360 | 561 | <5 | <5 | 468 |
| **STP07-159-SS** | **STP07159-GW38** | **September 3, 2008** | 73 | 10.8 | 3.5 | 4.4 | 228 | 26.9 | <0.1 | <0.1 | 0.49 | 98.5 | 629 | 46 | 1090 | 527 | 11 | <5 | 450 |
| **STP07-159-SS** | **STP07159-GW39** | **September 12, 2008** | 70 | 23.4 | 6.1 | 10.1 | 209 | 28.1 | <0.1 | <0.1 | 0.73 | 99.2 | 610 | 100 | 1050 | 519 | 8 | <5 | 438 |
| **STP07-159-SS** | **STP07159-GW40** | **September 17, 2008** | 64 | 31.9 | 6.8 | 14.3 | 162 | 26.7 | <0.1 | <0.1 | 0.77 | 91.4 | 563 | 139 | 971 | 523 | <5 | <5 | 429 |
| **STP07-159-SS** | **STP07159-GW41** | **September 25, 2008** | 49 | 48.4 | 6.3 | 20.1 | 133 | 16.5 | 0.4 | 0.4 | 0.43 | 98.4 | 528 | 204 | 905 | 514 | <5 | <5 | 421 |
| **STP07-159-SS** | **STP07159-GW42** | **September 30, 2008** | 48 | 52.6 | 6.5 | 21.6 | 128 | 16.6 | 0.2 | 0.2 | 0.49 | 101 | 525 | 220 | 887 | 510 | <5 | <5 | 418 |
| **STP07-159-SS** | **STP07159-GW43** | **October 8, 2008** | 42 | 55.4 | 5.7 | 21.7 | 99 | 14.2 | 0.1 | 0.1 | 0.31 | 93.1 | 484 | 228 | 863 | 499 | <5 | <5 | 409 |
| **STP07-159-SS** | **STP07159-GW44** | **October 16, 2008** | 42 | 57.1 | 4.9 | 22.2 | 94 | 13.1 | <0.1 | <0.1 | 0.37 | 92.1 | 479 | 234 | 863 | 500 | <5 | <5 | 410 |
| **STP07-159-SS** | **STP07159-GW45** | **October 23, 2008** | 39 | 67.3 | 6.1 | 25 | 89 | 13.5 | <0.1 | <0.1 | 0.49 | 99.5 | 484 | 271 | 840 | 495 | <5 | <5 | 406 |
| **STP07-159-SS** | **STP07159-GW46** | **November 1, 2008** | 40 | 72.8 | 4.7 | 24.9 | 77 | 14.5 | <0.1 | <0.1 | 0.36 | 98.1 | 471 | 284 | 850 | 482 | <5 | <5 | 395 |
| **STP07-159-SS** | **STP07159-GW47** | **June 21, 2009** | 36.9 | 77.6 | 22.7 | 2.32 | 81.3 | 12.6 | <0.050 | <0.071 | 0.077 | 105 | 461 | 287 | 813 | 463 | <5 | <5 | 380 |
| **STP07-159-SS** | **STP07159-GW47D** | **June 21, 2009** | 36.9 | 68.1 | 20.1 | 2.13 | 71.1 | 12.6 | <0.050 | <0.071 | <0.050 | 92.2 | 438 | 253 | 815 | 463 | <5 | <5 | 379 |

Notes:

Only those parameters detected above laboratory detection limits at least once are listed

< - Not Detected Above Numeric Value that Follows

NA - Not Analyzed

*All Concentrations in mg/L unless otherwise noted

1) Values of ion balance are percentages

2) Units of conductivity: µS/cm

## Table 4-28: Post PA Water Injection Dissolved Metals Concentrations at STP-08-159A2

| | | | Arsenic (As) | Aluminum (Al) | Boron (B) | Barium (Ba) | Bromide (Br) | Cadmium (Cd) | Cobalt (Co) | Chromium (Cr) | Copper (Cu) | Iron (Fe) | Manganese (Mn) | Molybdenum (Mo) | Nickel (Ni) | Lead (Pb) | Antimony (Sb) | Selenium (Se) | Tin (Sn) | Strontium (Sr) | Titanium (Ti) | Thallium (Tl) | Uranium (U) | Vanadium (V) | Zinc (Zn) |
|---|---|---|---|---|---|---|---|---|---|---|---|---|---|---|---|---|---|---|---|---|---|---|---|---|---|
| **Alberta Tier 1 Groundwater Remediation Guidelines for Natural Area with Coarse Soil Type (mg/L)** | | | 0.005 | 0.1 | 5 | 1 | Not Listed | 0.005 | Not Listed | 0.001 | 0.004 | 0.3 | 0.05 | Not Listed | 0.15 | 0.007 | 0.006 | 0.001 | Not Listed | Not Listed | Not Listed | Not Listed | 0.02 | Not Listed | 0.03 |
| **Sample Location** | **Sample ID** | **Sample Date** | | | | | | | | | | | | | | | | | | | | | | | |
| **STP08-159A2** | **STP08159A2-GW01** | **September 12, 2008** | 0.004 | 0.02 | 0.326 | 0.076 | 0.9 | 0.0002 | 0.0042 | 0.0008 | <0.0006 | 0.656 | 0.225 | 0.0944 | 0.0097 | <0.0001 | 0.001 | <0.0004 | <0.0002 | 0.202 | <0.0003 | <0.00005 | 0.0004 | 0.0003 | 0.002 |
| **STP08-159A2** | **STP08159A2-GW02** | **September 17, 2008** | 0.0028 | <0.01 | 0.295 | 0.0743 | 1.6 | 0.0001 | 0.0037 | 0.0007 | <0.0006 | 0.661 | 0.19 | 0.0752 | 0.0075 | 0.0001 | 0.001 | 0.0004 | <0.0002 | 0.207 | <0.0003 | <0.00005 | 0.0002 | 0.0004 | 0.01 |
| **STP08-159A2** | **STP08159A2-GW03** | **September 25, 2008** | 0.0039 | <0.01 | 0.357 | 0.0788 | 0.8 | <0.0001 | 0.0096 | 0.0005 | <0.0006 | 0.881 | 0.225 | 0.0629 | 0.0152 | <0.0001 | 0.0008 | <0.0004 | <0.0002 | 0.242 | <0.0003 | <0.00005 | 0.0002 | 0.0006 | <0.002 |
| **STP08-159A2** | **STP08159A2-GW04** | **October 8, 2008** | 0.0025 | <0.01 | 0.356 | 0.0913 | 1.0 | <0.0001 | 0.0045 | <0.0004 | <0.0006 | 3.97 | 0.31 | 0.0476 | 0.0079 | <0.0001 | 0.0006 | <0.0004 | <0.0002 | 0.261 | 0.0004 | <0.00005 | <0.0001 | 0.0003 | 0.002 |
| **STP08-159A2** | **STP08159A2-GW05** | **October 16, 2008** | 0.0030 | <0.01 | 0.383 | 0.084 | 0.8 | <0.0001 | 0.0052 | <0.0004 | <0.0006 | 2.66 | 0.327 | 0.0608 | 0.0108 | <0.0001 | 0.0011 | 0.0007 | <0.0002 | 0.261 | <0.0003 | <0.00005 | 0.0004 | <0.001 | 0.002 |
| **STP08-159A2** | **STP08159A2-GW06** | **October 23, 2008** | 0.0027 | <0.01 | 0.348 | 0.102 | 0.9 | <0.0001 | 0.0042 | 0.0005 | <0.0006 | 4.58 | 0.353 | 0.0397 | 0.0068 | <0.0001 | 0.0004 | 0.0007 | 0.0002 | 0.281 | <0.0003 | <0.00005 | 0.0002 | <0.001 | 0.002 |
| **STP08-159A2** | **STP08159A2-GW07** | **November 1, 2008** | 0.0037 | <0.01 | 0.371 | 0.108 | 0.9 | <0.0001 | 0.0072 | <0.0004 | <0.0006 | 6.58 | 0.372 | 0.0386 | 0.0118 | <0.0001 | 0.0005 | <0.0004 | <0.0002 | 0.265 | 0.0008 | 0.00011 | 0.0002 | <0.0001 | <0.001 |
| **STP08-159A2** | **STP08159A2-GW08** | **November 8, 2008** | 0.0040 | <0.01 | 0.37 | 0.110 | 0.7 | <0.0001 | 0.0079 | <0.0004 | <0.0006 | 5.96 | 0.337 | 0.0517 | 0.0154 | <0.0001 | 0.0005 | <0.0004 | 0.0004 | 0.275 | <0.0003 | 0.00012 | 0.0003 | <0.0001 | 0.002 |
| **STP08-159A2** | **STP08159A2-GW09** | **November 16, 2008** | 0.0037 | <0.01 | 0.34 | 0.112 | 0.9 | <0.0001 | 0.0068 | <0.0004 | 0.0007 | 8.9 | 0.389 | 0.0318 | 0.0112 | 0.0001 | 0.001 | <0.0004 | 0.0003 | 0.256 | 0.0003 | 0.00015 | 0.0002 | 0.0001 | 0.005 |
| **STP08-159A2** | **STP08159A2-GW10** | **November 22, 2008** | 0.0034 | <0.01 | 0.358 | 0.112 | 1.1 | <0.0001 | 0.0061 | 0.0006 | 0.0011 | 8.88 | 0.33 | 0.0289 | 0.0109 | <0.0001 | 0.0009 | <0.0004 | 0.0003 | 0.243 | 0.0007 | 0.00009 | 0.0002 | 0.0005 | 0.003 |
| **STP08-159A2** | **STP08159A2-GW11** | **January 17, 2009** | 0.0021 | 0.07 | 0.387 | 0.160 | <0.5 | <0.0001 | 0.0029 | 0.0008 | 0.0439 | 9.64 | 0.211 | 0.0155 | 0.0064 | <0.0001 | 0.0004 | <0.0004 | <0.0002 | 0.237 | 0.0024 | 0.00027 | <0.0001 | 0.0002 | 0.004 |
| **STP08-159A2** | **STP08159A2-GW12** | **June 21, 2009** | 0.0007 | <0.010 | 0.353 | 0.138 | NA | <0.00010 | 0.0004 | <0.00040 | 0.00242 | 9.9 | 0.197 | 0.0047 | 0.0013 | <0.00010 | <0.00040 | 0.00072 | <0.00020 | 0.256 | <0.00030 | <0.000050 | 0.0001 | <0.00010 | 0.0123 |

Notes:

Only those parameters detected above laboratory detection limits at least once are listed

< - Not Detected Above Numeric Value that Follows

NA - Not Analyzed

*All Concentrations in mg/L

**Table 4-29: Post PA Water Injection Dissolved Organics Concentrations at STP-08-159A2**

| | | | VOCs | | | | | PAHs | | |
|---|---|---|---|---|---|---|---|---|---|---|
| | | | Benzene | Toluene | p+m-Xylene | o-Xylene | 1,2,3-trimethylbenzene | Indole+2-methyl naphthalene | DOC | Naphthenic Acids |
| **Alberta Tier 1 Groundwater Remediation Guidelines for Natural Area with Coarse Soil Type** | | | 5 | 24 | 300 | | Not Listed | Not Listed | Not Listed | Not Listed |
| **Sample Location** | **Sample ID** | **Sample Date** | | | | | | | | |
| **STP08-159A2** | **STP08159A2-GW01** | **September 12, 2008** | 9.2 | 38.0 | 1.4 | 1.5 | 11.3 | 3.2 | 26 | <1.0 |
| **STP08-159A2** | **STP08159A2-GW02** | **September 17, 2008** | 8.2 | 37.2 | 1.3 | <1.8 | 6.5 | 1.9 | 23 | <1.0 |
| **STP08-159A2** | **STP08159A2-GW03** | **September 25, 2008** | <1.3 | 12.4 | <2.6 | <1.8 | 1.9 | 1.6 | 16 | <1.0 |
| **STP08-159A2** | **STP08159A2-GW04** | **October 8, 2008** | <1.3 | 14.4 | <2.6 | <1.8 | 1.3 | 1.8 | 12 | <1.0 |
| **STP08-159A2** | **STP08159A2-GW05** | **October 16, 2008** | <1.3 | 7.7 | <2.6 | <1.8 | 5.0 | <2.8 | 9 | <1.0 |
| **STP08-159A2** | **STP08159A2-GW06** | **October 23, 2008** | <1.3 | 6.7 | <2.6 | <1.8 | <1.2 | 2.8 | 8 | <1.0 |
| **STP08-159A2** | **STP08159A2-GW07** | **November 1, 2008** | <1.3 | 3.5 | 0.9 | <1.8 | <1.2 | <2.8 | 6 | <1.0 |
| **STP08-159A2** | **STP08159A2-GW08** | **November 8, 2008** | Sample Bottles Broke During Shipment | | | | Bottles Broke | Bottles Broke | 5 | Bottle Broke |
| **STP08-159A2** | **STP08159A2-GW09** | **November 16, 2008** | | | | | | | 5 | <1.0 |
| **STP08-159A2** | **STP08159A2-GW10** | **November 22, 2008** | 1.9 | 5.4 | <2.6 | <1.8 | 1.8 | 0.9 | 5 | <1.0 |
| **STP08-159A2** | **STP08159A2-GW11** | **January 17, 2009** | <1.3 | 3.6 | <2.6 | <1.8 | <1.2 | <2.8 | 6 | <1.0 |
| **STP08-159A2** | **STP08159A2-GW12** | **June 21, 2009** | 2.3 | <1.1 | <2.6 | <1.8 | <1.2 | <2.8 | 3.6 | <0.5 |

Notes:

Only those parameters detected above laboratory detection limits at least once are listed

< - Not Detected Above Numeric Value that Follows

NA - Not Analyzed

*All Concentrations in mg/L unless otherwise noted

1) VOC, TMB, and PAH concentrations in µg/L including remediation guidelines

**Table 4-30: Post PA Water Injection Major Ions and Miscellaneous Groundwater Data at STP-08-159A2**

| | | | Chloride (Cl) | Calcium (Ca) | Potassium (K) | Magnesium (Mg) | Sodium (Na) | Sulfate ($SO_4$) | Nitrate+Nitrite-N | Nitrate-N | Ion Balance[1] | TDS (Calculated) | Hardness (as $CaCO_3$) | Conductivity (EC)[2] | Bicarbonate ($HCO_3$) | Carbonate ($CO_3$) | Alkalinity, Total (as $CaCO_3$) |
|---|---|---|---|---|---|---|---|---|---|---|---|---|---|---|---|---|---|
| **Alberta Tier 1 Groundwater Remediation Guidelines for Natural Area with Coarse Soil Type (mg/L)** | | | 230 | Not Listed | Not Listed | Not Listed | 200 | 500 | - | 13 | Not Listed | 500 | Not Listed | Not Listed | Not Listed | Not Listed | Not Listed |
| **Sample Location** | **Sample ID** | **Sample Date** | | | | | | | | | | | | | | | |
| **STP08-159A2** | **STP08159A2-GW01** | **September 12, 2008** | 52 | 43.1 | 4.3 | 22.9 | 99 | 12.1 | <0.1 | <0.1 | 99.1 | 437 | 202 | 798 | 399 | 8 | 340 |
| **STP08-159A2** | **STP08159A2-GW02** | **September 17, 2008** | 50 | 41.4 | 4.4 | 22.9 | 100 | 13.2 | <0.1 | <0.1 | 102 | 433 | 198 | 756 | 400 | <5 | 335 |
| **STP08-159A2** | **STP08159A2-GW03** | **September 25, 2008** | 52 | 51 | 4.7 | 25.6 | 110 | 12.3 | <0.1 | <0.1 | 105 | 478 | 233 | 820 | 451 | <5 | 370 |
| **STP08-159A2** | **STP08159A2-GW04** | **October 8, 2008** | 51 | 46.8 | 3.8 | 21.6 | 98 | 11.8 | <0.1 | <0.1 | 91.2 | 461 | 206 | 845 | 452 | 6 | 380 |
| **STP08-159A2** | **STP08159A2-GW05** | **October 16, 2008** | 47 | 42.8 | 4.3 | 23.3 | 96 | 15.2 | 0.1 | 0.1 | 96.1 | 440 | 203 | 796 | 429 | <5 | 351 |
| **STP08-159A2** | **STP08159A2-GW06** | **October 23, 2008** | 50 | 52.2 | 4.1 | 22.2 | 105 | 12.3 | <0.1 | <0.1 | 95 | 483 | 222 | 853 | 483 | <5 | 396 |
| **STP08-159A2** | **STP08159A2-GW07** | **November 1, 2008** | 52 | 65.5 | 3.6 | 27 | 107 | 42 | <0.1 | <0.1 | 100 | 534 | 275 | 881 | 481 | <5 | 394 |
| **STP08-159A2** | **STP08159A2-GW08** | **November 8, 2008** | 52 | 56.2 | 3.9 | 22.9 | 110 | 13.5 | <0.1 | <0.1 | 98.6 | 497 | 235 | 881 | 486 | <5 | 398 |
| **STP08-159A2** | **STP08159A2-GW09** | **November 16, 2008** | 52 | 58.3 | 3.6 | 20.6 | 109 | 17.5 | 0.1 | 0.1 | 98.2 | 494 | 230 | 877 | 474 | <5 | 388 |
| **STP08-159A2** | **STP08159A2-GW10** | **November 22, 2008** | 49 | 52.8 | 3.9 | 18.4 | 102 | 13.5 | <0.1 | <0.1 | 92.4 | 472 | 208 | 866 | 472 | <5 | 387 |
| **STP08-159A2** | **STP08159A2-GW11** | **January 17, 2009** | 51 | 57.7 | 3.3 | 17.7 | 112 | 13 | <0.1 | <0.1 | 97.9 | 488 | 217 | 851 | 475 | <5 | 389 |
| **STP08-159A2** | **STP08159A2-GW12** | **June 21, 2009** | 50.6 | 62.2 | 18.6 | 2.7 | 114 | 12.4 | <0.050 | <0.071 | 103 | 492 | 232 | 870 | 471 | <5.0 | 386 |

Notes:

Only those parameters detected above laboratory detection limits at least once are listed

< - Not Detected Above Numeric Value that Follows

NA - Not Analyzed

*All Concentrations in mg/L unless otherwise noted

1) Values of ion balance are percentages

2) Units of conductivity: µS/cm

## Table 4-31: Post PA Water Injection Dissolved Metals Concentrations at STP-08-159A3

| | | | Arsenic (As) | Aluminum (Al) | Boron (B) | Barium (Ba) | Bromide (Br) | Cadmium (Cd) | Cobalt (Co) | Chromium (Cr) | Copper (Cu) | Iron (Fe) | Manganese (Mn) | Molybdenum (Mo) | Nickel (Ni) | Lead (Pb) | Antimony (Sb) | Selenium (Se) | Tin (Sn) | Strontium (Sr) | Titanium (Ti) | Thallium (Tl) | Uranium (U) | Vanadium (V) | Zinc (Zn) |
|---|---|---|---|---|---|---|---|---|---|---|---|---|---|---|---|---|---|---|---|---|---|---|---|---|---|
| **Alberta Tier 1 Groundwater Remediation Guidelines for Natural Area with Coarse Soil Type (mg/L)** | | | 0.005 | 0.1 | 5 | 1 | Not Listed | 0.005 | Not Listed | 0.001 | 0.004 | 0.3 | 0.05 | Not Listed | 0.15 | 0.007 | 0.006 | 0.001 | Not Listed | Not Listed | Not Listed | Not Listed | 0.02 | Not Listed | 0.03 |
| **Sample Location** | **Sample ID** | **Sample Date** | | | | | | | | | | | | | | | | | | | | | | | |
| **STP08-159A3** | **STP08159A3-GW01** | **August 21, 2008** | 0.004 | 0.1 | 0.284 | 0.076 | 0.4 | 0.0001 | 0.0048 | 0.004 | 0.0025 | 2.89 | 0.683 | 0.0423 | 0.0094 | 0.0003 | 0.0006 | <0.0004 | 0.0004 | 0.257 | 0.0053 | 0.00023 | 0.0018 | 0.0012 | 0.014 |
| **STP08-159A3** | **STP08159A3-GW02** | **August 27, 2008** | 0.0037 | 0.01 | 0.330 | 0.08 | 0.6 | <0.001 | 0.002 | <0.005 | <0.001 | 2.7 | 0.664 | 0.038 | 0.004 | <0.005 | NA | <0.0004 | <0.05 | 0.248 | <0.001 | <0.05 | NA | <0.001 | 0.003 |
| **STP08-159A3** | **STP08159A3-GW03** | **September 3, 2008** | 0.003 | <0.01 | 0.418 | 0.0775 | 1.1 | <0.0001 | 0.0015 | 0.0004 | 0.0013 | 2.74 | 0.62 | 0.0346 | 0.0026 | <0.0001 | <0.0004 | 0.0005 | <0.0002 | 0.260 | 0.0009 | <0.00005 | 0.0011 | 0.0018 | 0.01 |
| **STP08-159A3** | **STP08159A3-GW04** | **September 12, 2008** | 0.0037 | <0.01 | 0.440 | 0.0782 | 0.7 | <0.0001 | 0.0016 | 0.0009 | <0.0006 | 2.45 | 0.585 | 0.0318 | 0.0033 | <0.0001 | <0.0004 | <0.0004 | 0.0002 | 0.252 | 0.0006 | <0.00005 | 0.0013 | 0.0008 | 0.015 |
| **STP08-159A3** | **STP08159A3-GW05** | **September 17, 2008** | 0.0031 | 0.01 | 0.405 | 0.0791 | 0.7 | <0.0001 | 0.0024 | 0.0011 | <0.0006 | 2.95 | 0.575 | 0.0292 | 0.0046 | <0.0001 | <0.0004 | <0.0004 | 0.0004 | 0.271 | 0.001 | 0.00005 | 0.0008 | 0.0009 | 0.007 |
| **STP08-159A3** | **STP08159A3-GW06** | **September 25, 2008** | 0.0037 | <0.01 | 0.421 | 0.0813 | 1.0 | <0.0001 | 0.0043 | 0.0004 | <0.0006 | 2.53 | 0.483 | 0.0271 | 0.0076 | <0.0001 | <0.0004 | 0.0004 | <0.0002 | 0.284 | 0.0005 | <0.00005 | 0.0009 | 0.0008 | <0.002 |
| **STP08-159A3** | **STP08159A3-GW07** | **September 30, 2008** | 0.0032 | <0.01 | 0.403 | 0.0855 | 1.3 | <0.0001 | 0.0021 | <0.0004 | <0.0006 | 3.38 | 0.519 | 0.0224 | 0.004 | <0.0001 | <0.0004 | <0.0004 | 0.0002 | 0.292 | 0.0006 | <0.00005 | 0.0008 | 0.0008 | 0.006 |
| **STP08-159A3** | **STP08159A3-GW08** | **October 8, 2008** | 0.0022 | <0.01 | 0.415 | 0.0904 | 1.2 | <0.0001 | 0.0012 | 0.0011 | <0.0006 | 5.12 | 0.468 | 0.0164 | 0.0021 | <0.0001 | <0.0004 | 0.0004 | <0.0002 | 0.296 | 0.0007 | <0.00005 | 0.0005 | 0.0006 | <0.001 |
| **STP08-159A3** | **STP08159A3-GW09** | **October 16, 2008** | 0.0024 | <0.01 | 0.438 | 0.0802 | 0.8 | <0.0001 | 0.0023 | <0.0004 | <0.0006 | 2.47 | 0.496 | 0.0241 | 0.0046 | 0.0002 | 0.0008 | 0.0005 | 0.0005 | 0.284 | <0.0003 | <0.00005 | 0.0008 | <0.001 | 0.004 |
| **STP08-159A3** | **STP08159A3-GW10** | **October 23, 2008** | 0.0026 | <0.01 | 0.397 | 0.0928 | 0.8 | <0.0001 | 0.0014 | 0.0004 | <0.0006 | 5.14 | 0.487 | 0.0133 | 0.0022 | <0.0001 | <0.0004 | 0.0009 | <0.0002 | 0.308 | <0.0003 | <0.00005 | 0.0006 | <0.001 | 0.003 |
| **STP08-159A3** | **STP08159A3-GW11** | **November 1, 2008** | 0.0033 | <0.01 | 0.418 | 0.0909 | 0.8 | <0.0001 | 0.0035 | <0.0004 | <0.0006 | 5.19 | 0.48 | 0.0138 | 0.0064 | <0.0001 | <0.0004 | <0.0004 | 0.0003 | 0.291 | 0.001 | 0.00011 | 0.0006 | <0.0001 | <0.001 |
| **STP08-159A3** | **STP08159A3-GW12** | **November 8, 2008** | 0.0073 | <0.01 | 0.434 | 0.0916 | 0.7 | <0.0001 | 0.0127 | 0.0005 | <0.0006 | 4.5 | 0.38 | 0.0156 | 0.0262 | <0.0001 | 0.0005 | <0.0004 | 0.0005 | 0.301 | 0.0005 | 0.0001 | 0.0008 | 0.0003 | 0.002 |
| **STP08-159A3** | **STP08159A3-GW13** | **November 16, 2008** | 0.004 | <0.01 | 0.425 | 0.1 | 0.5 | <0.0001 | 0.005 | NA | <0.0006 | 6.78 | 0.349 | 0.0098 | 0.0086 | <0.0001 | 0.0008 | <0.0004 | 0.0002 | 0.309 | 0.0005 | 0.00013 | 0.0005 | <0.0001 | 0.003 |
| **STP08-159A3** | **STP08159A3-GW14** | **November 22, 2008** | 0.0028 | <0.01 | 0.444 | 0.0949 | 0.9 | <0.0001 | 0.0023 | 0.0004 | 0.0007 | 7.47 | 0.306 | 0.0066 | 0.0033 | <0.0001 | 0.0006 | <0.0004 | 0.0003 | 0.289 | 0.0011 | 0.00007 | 0.0003 | 0.0006 | 0.003 |
| **STP08-159A3** | **STP08159A3-GW15** | **January 17, 2009** | 0.0017 | <0.01 | 0.472 | 0.1040 | <0.5 | <0.0001 | 0.0015 | 0.0007 | <0.0006 | 6.71 | 0.249 | 0.0048 | 0.0017 | <0.0001 | <0.0004 | <0.0004 | <0.0002 | 0.275 | 0.001 | 0.00029 | 0.0003 | 0.0002 | 0.003 |
| **STP08-159A3** | **STP08159A3-GW16** | **June 21, 2009** | 0.0013 | <0.010 | 0.438 | 0.1020 | NA | <0.00010 | 0.00089 | <0.0004 | <0.0006 | 6.08 | 0.183 | 0.0032 | 0.0015 | <0.0001 | <0.0004 | <0.0004 | <0.0002 | 0.290 | <0.0003 | <0.00005 | 0.0001 | <0.0001 | 0.0012 |
| **STP08-159A3** | **STP08159A3-GW16D** | **June 21, 2009** | 0.0013 | <0.010 | 0.433 | 0.103 | NA | <0.00010 | 0.00087 | <0.0004 | <0.0006 | 5.93 | 0.181 | 0.0032 | 0.0015 | <0.0001 | <0.0004 | 0.00087 | <0.0002 | 0.288 | <0.0003 | <0.00005 | 0.0001 | <0.0001 | 0.0016 |

Notes:

Only those parameters detected above laboratory detection limits at least once are listed

< - Not Detected Above Numeric Value that Follows

NA - Not Analyzed

*All Concentrations in mg/L

## Table 4-32: Post PA Water Injection Dissolved Organics Concentrations at STP-08-159A3

| | | | VOCs | | | | PAHs | | | | |
|---|---|---|---|---|---|---|---|---|---|---|---|
| | | | Benzene | Toluene | p+m-Xylene | 1,2,3-trimethylbenzene | Naphthalene | Indole+2-methyl naphthalene | Acenaphthylene | DOC | Naphthenic Acids |
| **Alberta Tier 1 Groundwater Remediation Guidelines for Natural Area with Coarse Soil Type** | | | 5 | 24 | 300 | Not Listed | 1.1 | Not Listed | 46 | Not Listed | Not Listed |
| **Sample Location** | **Sample ID** | **Sample Date** | | | | | | | | | |
| **STP08-159A3** | **STP08159A3-GW01** | **August 21, 2008** | 3.2 | 2.0 | 1.1 | 2.9 | <2.2 | 2.8 | <1.4 | 18 | 1.2 |
| **STP08-159A3** | **STP08159A3-GW02** | **August 27, 2008** | <1.3 | 8.6 | 1.1 | <1.2 | <2.2 | <2.8 | <1.4 | 14 | <1.0 |
| **STP08-159A3** | **STP08159A3-GW03** | **September 3, 2008** | <1.3 | 9.6 | 1.0 | 2.1 | <2.2 | 5.6 | <1.4 | 12 | <1.0 |
| **STP08-159A3** | **STP08159A3-GW04** | **September 12, 2008** | 3.2 | 8.5 | 1.1 | 3.2 | <2.2 | 2.4 | <1.4 | 21 | <1.0 |
| **STP08-159A3** | **STP08159A3-GW05** | **September 17, 2008** | 20.5 | 13.6 | 1.1 | 14.0 | <2.2 | 1.5 | <1.4 | 9 | <1.0 |
| **STP08-159A3** | **STP08159A3-GW06** | **September 25, 2008** | <1.3 | 14.1 | 1.0 | 1.7 | <2.2 | 2.9 | <1.4 | 8 | <1.0 |
| **STP08-159A3** | **STP08159A3-GW07** | **September 30, 2008** | 11.8 | 6.9 | 1.0 | 1.3 | <2.2 | 2.6 | <1.4 | 6 | <1.0 |
| **STP08-159A3** | **STP08159A3-GW08** | **October 8, 2008** | <1.3 | 9.8 | 0.9 | <1.2 | <2.2 | 0.0 | <1.4 | 6 | <1.0 |
| **STP08-159A3** | **STP08159A3-GW09** | **October 16, 2008** | <1.3 | 6.8 | 1.0 | <1.2 | <2.2 | 1.6 | <1.4 | 7 | <1.0 |
| **STP08-159A3** | **STP08159A3-GW10** | **October 23, 2008** | <1.3 | 3.6 | <2.6 | <1.2 | <2.2 | 2.2 | <1.4 | 5 | <1.0 |
| **STP08-159A3** | **STP08159A3-GW11** | **November 1, 2008** | <1.3 | 6.6 | 0.9 | <1.2 | <2.2 | 0.0 | <1.4 | 6 | <1.0 |
| **STP08-159A3** | **STP08159A3-GW12** | **November 8, 2008** | Bottles Broke | | | Bottle Broke | Bottles Broke During Shipment | | | 5 | Sample Lost Shipping |
| **STP08-159A3** | **STP08159A3-GW13** | **November 16, 2008** | <1.3 | 2.6 | 1.1 | <1.2 | <2.2 | 1.4 | 1.1 | 5 | <1.0 |
| **STP08-159A3** | **STP08159A3-GW14** | **November 22, 2008** | 1.0 | 3.8 | 0.9 | 3.6 | 1.6 | <2.8 | <1.4 | 8 | <1.0 |
| **STP08-159A3** | **STP08159A3-GW15** | **January 17, 2009** | <1.3 | 1.5 | <2.6 | <1.2 | <2.2 | <2.8 | <1.4 | 5 | <1.0 |
| **STP08-159A3** | **STP08159A3-GW16** | **June 21, 2009** | 2.2 | <1.1 | <2.6 | <1.2 | <2.2 | <2.8 | <1.4 | 3.8 | <0.5 |
| **STP08-159A3** | **STP08159A3-GW16D** | **June 21, 2009** | 0.9 | <1.1 | <2.6 | <1.2 | <2.2 | <2.8 | <1.4 | 4 | <0.5 |

Notes:

Only those parameters detected above laboratory detection limits at least once are listed

< - Not Detected Above Numeric Value that Follows

NA - Not Analyzed

*All Concentrations in mg/L unless otherwise noted

1) VOC, TMB, and PAH concentrations in µg/L including remediation guidelines

## Table 4-33: Post PA Water Injection Major Ions and Miscellaneous Groundwater Data at STP-08-159A3

| | | | Chloride (Cl) | Calcium (Ca) | Potassium (K) | Magnesium (Mg) | Sodium (Na) | Sulfate ($SO_4$) | Nitrate+Nitrite-N | Nitrate-N | Nitrite-N | Ammonia | Ion Balance[1] | TDS (Calculated) | Hardness (as $CaCO_3$) | Conductivity (EC)[2] | Bicarbonate ($HCO_3$) | Alkalinity, Total (as $CaCO_3$) |
|---|---|---|---|---|---|---|---|---|---|---|---|---|---|---|---|---|---|---|
| **Alberta Tier 1 Groundwater Remediation Guidelines for Natural Area with Coarse Soil Type (mg/L)** | | | 230 | Not Listed | Not Listed | Not Listed | 200 | 500 | - | 13 | 0.06 | 1.37 | Not Listed | 500 | Not Listed | Not Listed | Not Listed | Not Listed |
| **Sample Location** | **Sample ID** | **Sample Date** | | | | | | | | | | | | | | | | |
| **STP08-159A3** | **STP08159A3-GW01** | **August 21, 2008** | 10 | 46.7 | 2.2 | 23 | 21 | 20.2 | <0.1 | <0.1 | <0.05 | 0.1 | 98.4 | 261 | 211 | 494 | 279 | 229 |
| **STP08-159A3** | **STP08159A3-GW02** | **August 27, 2008** | 35 | 51.1 | 2.5 | 25.3 | 60 | 20.4 | <0.1 | <0.1 | <0.05 | 0.11 | 98.6 | 374 | 232 | 671 | 366 | 300 |
| **STP08-159A3** | **STP08159A3-GW03** | **September 3, 2008** | 60 | 53.6 | 2.8 | 26.1 | 115 | 13.7 | <0.1 | <0.1 | <0.05 | 0.11 | 103 | 516 | 241 | 927 | 484 | 397 |
| **STP08-159A3** | **STP08159A3-GW04** | **September 12, 2008** | 64 | 55.7 | 3.3 | 25.9 | 113 | 15.6 | <0.1 | <0.1 | <0.05 | 0.11 | 101 | 507 | 246 | 895 | 467 | 383 |
| **STP08-159A3** | **STP08159A3-GW05** | **September 17, 2008** | 66 | 52.2 | 2.7 | 24.9 | 112 | 14.2 | <0.1 | <0.1 | <0.05 | 0.07 | 95.4 | 509 | 233 | 892 | 482 | 395 |
| **STP08-159A3** | **STP08159A3-GW06** | **September 25, 2008** | 66 | 55.9 | 2.9 | 25.4 | 116 | 13.1 | 0.6 | 0.6 | <0.05 | 0.06 | 98 | 523 | 244 | 915 | 490 | 402 |
| **STP08-159A3** | **STP08159A3-GW07** | **September 30, 2008** | 66 | 58.5 | 3.1 | 25.1 | 117 | 13.6 | 1 | 1 | <0.05 | 0.06 | 98 | 532 | 249 | 920 | 497 | 407 |
| **STP08-159A3** | **STP08159A3-GW08** | **October 8, 2008** | 65 | 55 | 3.3 | 22.2 | 118 | 13.4 | <0.1 | <0.1 | <0.05 | 0.09 | 94.7 | 524 | 229 | 942 | 502 | 412 |
| **STP08-159A3** | **STP08159A3-GW09** | **October 16, 2008** | 64 | 54 | 3.5 | 24.3 | 114 | 15.3 | <0.1 | <0.1 | <0.05 | <0.05 | 94.4 | 521 | 235 | 940 | 500 | 409 |
| **STP08-159A3** | **STP08159A3-GW10** | **October 23, 2008** | 65 | 59.1 | 3.2 | 22.3 | 124 | 13.7 | <0.1 | <0.1 | <0.05 | 0.1 | 98.7 | 536 | 239 | 938 | 505 | 414 |
| **STP08-159A3** | **STP08159A3-GW11** | **November 1, 2008** | 67 | 57.4 | 2.8 | 20.8 | 115 | 13.1 | <0.1 | <0.1 | <0.05 | 0.1 | 93.2 | 522 | 229 | 956 | 500 | 410 |
| **STP08-159A3** | **STP08159A3-GW12** | **November 8, 2008** | 68 | 59.5 | 3.1 | 20.6 | 124 | 15 | <0.1 | <0.1 | <0.05 | 0.1 | 97.1 | 537 | 233 | 962 | 501 | 411 |
| **STP08-159A3** | **STP08159A3-GW13** | **November 16, 2008** | 68 | 63.3 | 3.2 | 20.5 | 129 | 16.3 | <0.1 | <0.1 | <0.05 | 0.07 | 101 | 546 | 242 | 964 | 500 | 410 |
| **STP08-159A3** | **STP08159A3-GW14** | **November 22, 2008** | 66 | 54.9 | 3.1 | 17.8 | 117 | 14 | <0.1 | <0.1 | <0.05 | 0.09 | 91.2 | 516 | 210 | 951 | 496 | 406 |
| **STP08-159A3** | **STP08159A3-GW15** | **January 17, 2009** | 67 | 58.8 | 3.3 | 17.5 | 134 | 15.4 | <0.1 | <0.1 | <0.05 | 0.08 | 101 | 536 | 219 | 926 | 488 | 400 |
| **STP08-159A3** | **STP08159A3-GW16** | **June 21, 2009** | 58.7 | 57.5 | 17.5 | 2.84 | 134 | 13 | <0.050 | <0.071 | <0.050 | 0.09 | 105 | 518 | 216 | 908 | 476 | 390 |
| **STP08-159A3** | **STP08159A3-GW16D** | **June 21, 2009** | 58.5 | 57.4 | 17.2 | 2.79 | 134 | 12.9 | <0.050 | <0.071 | <0.050 | 0.088 | 105 | 517 | 214 | 911 | 477 | 391 |

Notes:

Only those parameters detected above laboratory detection limits at least once are listed

< - Not Detected Above Numeric Value that Follows

NA - Not Analyzed

*All Concentrations in mg/L unless otherwise noted

1) Values of ion balance are percentages

2) Units of conductivity: µS/cm

**Table 4-34: Post PA Water Injection Dissolved Metals Concentrations at STP-08-159A1**

| | | | Arsenic (As) | Boron (B) | Barium (Ba) | Bromide (Br) | Cobalt (Co) | Iron (Fe) | Manganese (Mn) | Molybdenum (Mo) | Nickel (Ni) | Strontium (Sr) | Titanium (Ti) | Uranium (U) | Zinc (Zn) |
|---|---|---|---|---|---|---|---|---|---|---|---|---|---|---|---|
| **Alberta Tier 1 Groundwater Remediation Guidelines for Natural Area with Coarse Soil Type (mg/L)** | | | 0.005 | 5 | 1 | Not Listed | Not Listed | 0.3 | 0.05 | Not Listed | 0.15 | Not Listed | Not Listed | 0.02 | 0.03 |
| **Sample Location** | **Sample ID** | **Sample Date** | | | | | | | | | | | | | |
| **STP08-159A1** | **STP08159A1-GW01** | **June 21, 2009** | 0.00393 | 0.177 | 0.177 | NA | 0.00413 | 9.69 | 0.281 | 0.0156 | 0.00901 | 0.186 | 0.00065 | 0.00026 | 0.0015 |

Notes:

Only those parameters detected above laboratory detection limits at least once are listed

< - Not Detected Above Numeric Value that Follows

NA - Not Analyzed

*All Concentrations in mg/L

**Table 4-35: Post PA Water Injection Dissolved Organics Concentrations at STP-08-159A1**

| | | | DOC | Naphthenic Acids |
|---|---|---|---|---|
| **Alberta Tier 1 Groundwater Remediation Guidelines for Natural Area with Coarse Soil Type (mg/L)** | | | Not Listed | Not Listed |
| **Sample Location** | **Sample ID** | **Sample Date** | | |
| **STP08-158A1** | **STP08158A1-GW01** | **June 20, 2009** | 4.1 | <0.5 |
| Notes: | | | | |
| Only those parameters detected above laboratory | | | | |
| detection limits at least once are listed | | | | |
| < - Not Detected Above Numeric Value that Follows | | | | |
| NA - Not Analyzed | | | | |
| *All Concentrations in mg/L | | | | |

**Table 4-36: Post PA Water Injection Major Ions and Miscellaneous Groundwater Data at STP-08-159A1**

| | | | Chloride (Cl) | Calcium (Ca) | Potassium (K) | Magnesium (Mg) | Sodium (Na) | Sulfate ($SO_4$) | Ion Balance[1] | TDS (Calculated) | Hardness (as $CaCO_3$) | Conductivity (EC)[2] | Bicarbonate ($HCO_3$) | Alkalinity, Total (as $CaCO_3$) |
|---|---|---|---|---|---|---|---|---|---|---|---|---|---|---|
| **Alberta Tier 1 Groundwater Remediation Guidelines for Natural Area with Coarse Soil Type (mg/L)** | | | 230 | Not Listed | Not Listed | Not Listed | 200 | 500 | Not Listed | 500 | Not Listed | Not Listed | Not Listed | Not Listed |
| **Sample Location** | **Sample ID** | **Sample Date** | | | | | | | | | | | | |
| **STP08-159A1** | **STP08159A1-GW01** | **June 21, 2009** | 30.8 | 69.6 | 20.9 | 2.36 | 82.2 | 11.8 | 102 | 443 | 260 | 791 | 459 | 376 |

Notes:

Only those parameters detected above laboratory detection limits at least once are listed

< - Not Detected Above Numeric Value that Follows

NA - Not Analyzed

*All Concentrations in mg/L unless otherwise noted

1) Values of ion balance are percentages

2) Units of conductivity: µS/cm

**Table 4-37: Post PA Water Injection Dissolved Metals Concentrations at STP-08-158A1**

| | | | Arsenic (As) | Boron (B) | Barium (Ba) | Cobalt (Co) | Copper (Cu) | Iron (Fe) | Manganese (Mn) | Molybdenum (Mo) | Nickel (Ni) | Strontium (Sr) | Titanium (Ti) | Uranium (U) | Vanadium (V) | Zinc (Zn) |
|---|---|---|---|---|---|---|---|---|---|---|---|---|---|---|---|---|
| **Alberta Tier 1 Groundwater Remediation Guidelines for Natural Area with Coarse Soil Type (mg/L)** | | | 0.005 | 5 | 1 | Not Listed | 0.004 | 0.3 | 0.05 | Not Listed | 0.15 | Not Listed | Not Listed | 0.02 | Not Listed | 0.03 |
| **Sample Location** | **Sample ID** | **Sample Date** | | | | | | | | | | | | | | |
| **STP08-158A1** | **STP08158A1-GW01** | **June 20, 2009** | 0.004 | 0.212 | 0.319 | 0.00152 | 0.0023 | 3.77 | 0.176 | 0.0036 | 0.0044 | 1.170 | 0.00122 | 0.00013 | 0.0001 | 0.0103 |

Notes:

Only those parameters detected above laboratory detection limits at least once are listed

< - Not Detected Above Numeric Value that Follows

NA - Not Analyzed

*All Concentrations in mg/L

**Table 4-38: Post PA Water Injection Dissolved Organics Concentrations at STP-08-158A1**

| | | | DOC | Naphthenic Acids |
|---|---|---|---|---|
| **Alberta Tier 1 Groundwater Remediation Guidelines for Natural Area with Coarse Soil Type (mg/L)** | | | Not Listed | Not Listed |
| **Sample Location** | **Sample ID** | **Sample Date** | | |
| **STP08-158A1** | **STP08158A1-GW01** | **June 20, 2009** | 5.8 | 1.2 |
| Notes: | | | | |
| Only those parameters detected above laboratory | | | | |
| detection limits at least once are listed | | | | |
| < - Not Detected Above Numeric Value that Follows | | | | |
| NA - Not Analyzed | | | | |
| *All Concentrations in mg/L | | | | |

**Table 4-39: Post PA Water Injection Major Ions and Miscellaneous Groundwater Data at STP-08-158A1**

| | | | Chloride (Cl) | Calcium (Ca) | Potassium (K) | Magnesium (Mg) | Sodium (Na) | Sulfate ($SO_4$) | Ammonia | Ion Balance[1] | TDS (Calculated) | Hardness (as $CaCO_3$) | Conductivity (EC)[2] | Bicarbonate ($HCO_3$) | Alkalinity, Total (as $CaCO_3$) |
|---|---|---|---|---|---|---|---|---|---|---|---|---|---|---|---|
| **Alberta Tier 1 Groundwater Remediation Guidelines for Natural Area with Coarse Soil Type (mg/L)** | | | 230 | Not Listed | Not Listed | Not Listed | 200 | 500 | 1.37 | Not Listed | 500 | Not Listed | Not Listed | Not Listed | Not Listed |
| **Sample Location** | **Sample ID** | **Sample Date** | | | | | | | | | | | | | |
| **STP08-158A1** | **STP08158A1-GW01** | **June 20, 2009** | 2.27 | 91.5 | 29.1 | 5.17 | 15.2 | 26.8 | 0.11 | 90.7 | 408 | 348 | 748 | 484 | 397 |

Notes:

Only those parameters detected above laboratory detection limits at least once are listed

< - Not Detected Above Numeric Value that Follows

NA - Not Analyzed

*All Concentrations in mg/L unless otherwise noted

1) Values of ion balance are percentages

2) Units of conductivity: µS/cm

**Table 4-40: Post PA Water Injection Dissolved Metals Concentrations at STP-08-158A2**

| | | | Arsenic (As) | Boron (B) | Barium (Ba) | Cobalt (Co) | Copper (Cu) | Iron (Fe) | Manganese (Mn) | Molybdenum (Mo) | Nickel (Ni) | Strontium (Sr) | Titanium (Ti) | Uranium (U) | Zinc (Zn) |
|---|---|---|---|---|---|---|---|---|---|---|---|---|---|---|---|
| **Alberta Tier 1 Groundwater Remediation Guidelines for Natural Area with Coarse Soil Type (mg/L)** | | | 0.005 | 5 | 1 | Not Listed | 0.004 | 0.3 | 0.05 | Not Listed | 0.15 | Not Listed | Not Listed | 0.02 | 0.03 |
| **Sample Location** | **Sample ID** | **Sample Date** | | | | | | | | | | | | | |
| **STP08-158A2** | **STP08158A2-GW01** | **June 20, 2009** | 0.001 | 0.127 | 0.278 | 0.00203 | 0.0022 | 9.14 | 1.8 | 0.0057 | 0.0046 | 0.814 | 0.00108 | 0.0013 | 0.011 |

Notes:

Only those parameters detected above laboratory detection limits at least once are listed

< - Not Detected Above Numeric Value that Follows

NA - Not Analyzed

*All Concentrations in mg/L

**Table 4-41: Post PA Water Injection Dissolved Organics Concentrations at STP-08-158A2**

| | | | DOC | Naphthenic Acids |
|---|---|---|---|---|
| **Alberta Tier 1 Groundwater Remediation Guidelines for Natural Area with Coarse Soil Type (mg/L)** | | | Not Listed | Not Listed |
| **Sample Location** | **Sample ID** | **Sample Date** | | |
| **STP08-158A2** | **STP08158A2-GW01** | **June 20, 2009** | 4.1 | 0.7 |
| Notes: | | | | |
| Only those parameters detected above laboratory | | | | |
| detection limits at least once are listed | | | | |
| < - Not Detected Above Numeric Value that Follows | | | | |
| NA - Not Analyzed | | | | |
| *All Concentrations in mg/L | | | | |

**Table 4-42: Post PA Water Injection Major Ions and Miscellaneous Groundwater Data at STP-08-158A2**

| | | | Chloride (Cl) | Calcium (Ca) | Potassium (K) | Magnesium (Mg) | Sodium (Na) | Sulfate ($SO_4$) | Ammonia | Ion Balance[1] | TDS (Calculated) | Hardness (as $CaCO_3$) | Conductivity (EC)[2] | Bicarbonate ($HCO_3$) | Alkalinity, Total (as $CaCO_3$) |
|---|---|---|---|---|---|---|---|---|---|---|---|---|---|---|---|
| **Alberta Tier 1 Groundwater Remediation Guidelines for Natural Area with Coarse Soil Type (mg/L)** | | | 230 | Not Listed | Not Listed | Not Listed | 200 | 500 | 1.37 | Not Listed | 500 | Not Listed | Not Listed | Not Listed | Not Listed |
| **Sample Location** | **Sample ID** | **Sample Date** | | | | | | | | | | | | | |
| **STP08-158A2** | **STP08158A2-GW01** | **June 20, 2009** | 1.78 | 111 | 34.2 | 4.33 | 11.5 | 22.2 | 0.174 | 105 | 426 | 418 | 749 | 489 | 401 |

Notes:

Only those parameters detected above laboratory detection limits at least once are listed

< - Not Detected Above Numeric Value that Follows

NA - Not Analyzed

*All Concentrations in mg/L unless otherwise noted

1) Values of ion balance are percentages

2) Units of conductivity: µS/cm

**Table 4-43: Trace Element Concentrations from Sequential Extractions and Percent FOC and TIC in WCSC Sediments**

| | Depth (Ft BGS) | Sr | Ag | Al | As | Ba | Cd | Co | Cr | Cu | Fe | Mn | Ni | Pb | Sb | V | Zn | FOC | TIC |
|---|---|---|---|---|---|---|---|---|---|---|---|---|---|---|---|---|---|---|---|
| | | mg/kg | mg/kg | mg/kg | mg/kg | mg/kg | mg/kg | mg/kg | mg/kg | mg/kg | mg/kg | mg/kg | mg/kg | mg/kg | mg/kg | mg/kg | mg/kg | % | % |
| F1: WCSC | 51-53 | 0.33 | 0.06 | 0.62 | 0.51 | 0.32 | 0.45 | 0.16 | 0.10 | 0.71 | 0.67 | 0.29 | 0.13 | 0.16 | 0.42 | 0.37 | 4.51 | | |
| F2: WCSC | 51-53 | 2.10 | 0.07 | 26.7 | 0.55 | 0.86 | 0.64 | 0.25 | 0.33 | 0.94 | 101 | 0.15 | 0.29 | 0.21 | 0.54 | 0.47 | 5.99 | | |
| F3: WCSC | 51-53 | 0.12 | ND | 1.47 | 1.57 | 0.18 | 0.66 | 0.26 | 0.25 | 1.13 | 2.03 | 0.10 | 0.19 | 0.46 | 0.79 | 0.58 | 1.76 | 0.111 | 0.100 |
| F4: WCSC | 51-53 | ND | ND | 0.92 | 0.60 | 0.19 | 0.23 | 0.18 | 0.16 | 0.71 | 1.22 | 0.06 | 0.12 | 0.18 | 0.54 | 0.36 | 3.05 | | |
| F5: WCSC | 51-53 | 0.58 | ND | 15.2 | 1.88 | 0.73 | 0.76 | 0.56 | 0.56 | 2.25 | 14.5 | 0.22 | 0.41 | 0.65 | 1.69 | 1.20 | 18.8 | | |
| | | | | | | | | | | | | | | | | | | | |
| F1: WCSC | 78-80 | 0.26 | 0.06 | 0.52 | 0.51 | 0.15 | 0.50 | 0.17 | 0.11 | 0.71 | 0.68 | 0.13 | 0.12 | 0.16 | 0.42 | 0.38 | 1.60 | | |
| F2: WCSC | 78-80 | 1.87 | 0.06 | 14.7 | 0.76 | 0.52 | 0.47 | 0.27 | 0.24 | 0.92 | 47.9 | 2.39 | 0.28 | 0.12 | 0.47 | 0.25 | 1.99 | | |
| F3: WCSC | 78-80 | 0.34 | 0.08 | 2.03 | 1.37 | 0.19 | 0.73 | 0.26 | 0.16 | 1.11 | 3.44 | 0.16 | 0.17 | 0.41 | 0.74 | 0.31 | 1.73 | 0.064 | 0.130 |
| F4: WCSC | 78-80 | 0.04 | ND | 0.81 | 0.59 | 0.19 | 0.23 | 0.17 | 0.17 | 0.71 | 0.44 | 0.06 | 0.12 | 0.21 | 0.53 | 0.37 | 3.06 | | |
| F5: WCSC | 78-80 | 0.35 | 0.19 | 9.41 | 1.87 | 0.41 | 1.43 | 0.54 | 0.76 | 2.25 | 6.68 | 0.22 | 0.48 | 0.60 | 1.27 | 0.63 | 9.63 | | |
| | | | | | | | | | | | | | | | | | | | |
| F1: WCSC | 102-104 | 0.46 | 0.06 | 1.57 | 0.48 | 0.19 | 0.44 | 0.17 | 0.12 | 0.71 | 4.32 | 0.36 | 0.13 | 0.15 | 0.41 | 0.38 | 1.60 | | |
| F2: WCSC | 102-104 | 2.03 | 0.06 | 12.8 | 0.78 | 0.58 | 0.47 | 0.23 | 0.19 | 0.91 | 48.5 | 2.13 | 0.24 | 0.16 | 0.51 | 0.25 | 1.98 | | |
| F3: WCSC | 102-104 | 0.12 | 0.08 | 1.46 | 1.51 | 0.16 | 0.66 | 0.25 | 0.15 | 1.07 | 3.43 | 0.09 | 0.17 | 0.48 | 0.75 | 0.29 | 1.69 | 0.065 | 0.103 |
| F4: WCSC | 102-104 | 0.11 | ND | 0.80 | 0.57 | 0.19 | 0.23 | 0.16 | 0.16 | 0.72 | 0.05 | 0.05 | 0.12 | 0.19 | 0.56 | 0.36 | 3.05 | | |
| F5: WCSC | 102-104 | 1.74 | ND | 76.9 | 1.84 | 0.63 | 0.73 | 0.54 | 0.73 | 2.34 | 38.7 | 0.48 | 0.60 | 0.60 | 1.71 | 1.27 | 18.9 | | |

Notes:

F1: Easily exchangeable trace elements extracted with $MgCl_2$

F2: Trace elements associated with poorly crystalline Fe oxides extracted with $NH_2OH{\bullet}HCl$ and HCl

F3: Trace elements associated with well crystallized Fe oxides extracted with $NH_2OH{\bullet}HCl$ and $CH_3COOH$

F4: Trace elements associated with the organic fraction and sulfide minerals extracted with $H_2O_2$, $HNO_3$, and $CH_3COONH_4$

F5: Trace elements associated with silicates and other primary minerals extracted with $HNO_3$ and HCl

Depths: 51-53 feet bgs corresponds to the shallow injection interval, 102-104 feet bgs corresponds to the deep injection interval and 78-80 was collected from an intermediate depth

**Table 4-44: Inputs for MODFLOW Model of STP-07-158-SS Injection**

| Parameter | Value | Justification |
|---|---|---|
| WCSC Longitudinal Dispersivity | 0.06 m | Value adjusted until modelled concentration profile matched observed concentration profile |
| WCSC Transverse Horizontal Dispersivity | 0.006 m | Set Transverse Horizontal Dispersivity an order of magnitude less than longitudinal dispersivity, consistent with observations of Sudicky, et al. (1983) |
| WCSC Transverse Vertical Dispersivity | 0.0006 m | Set Transverse Vertical Dispersivity two orders of magnitude less than longitudinal dispersivity, consistent with observations of Sudicky, et al. (1983) |
| WCSC Hydraulic Conductivity in X, Y, and Z Direction | $2.25 \times 10^{-3}$ m/s | Near Hydraulic Conductivities determined by KCB via Slug Tests for the Shallow Aquifer Depth – Adjusted value until modelled concentration profile matched observed concentration profile |
| WCSC Porosity | 0.3 | Typical porosity of sand aquifer from Freeze and Cherry (1979) |
| WCSC Specific Storage | $1.075 \times 10^{-5}$ $m^{-1}$ | From Klohn Crippen Consultants Ltd. (2004) |
| WCSC Specific Yield | $2 \times 10^{-2}$ | From Klohn Crippen Consultants Ltd. (2004) |
| WCSC Recharge | 88.39 mm/yr | Twenty percent of the site's mean annual precipitation. Precipitation data from Klohn Crippen (2004). |
| Glacial Till Hydraulic Conductivity | $2.25 \times 10^{-7}$ m/s | Till was unsaturated for all model runs. Set hydraulic conductivity several orders of magnitude higher than WCSC to prevent flow through the unit. |
| Up-gradient Constant Head Boundary Condition | 355.2813 m amsl | Set Up-gradient Constant Head Boundary to create hydraulic gradient to drive groundwater flow at velocity of 5 cm/day |
| Down-gradient Constant Head Boundary Condition | 355.2787 m amsl | Set Down-gradient Constant Head Boundary to create hydraulic gradient to drive groundwater flow at velocity of 5 cm/day |
| Initial Head Condition (Set in the middle of the domain where the injection well was positioned | 355.280 m amsl | Groundwater Elevation at STP-07-158-SS immediately before PA water injection |
| Chloride Concentration of Injectate | 537 mg/L | Maximum concentration of chloride detected in PA water injectate (Table 4-18) |
| Background Chloride Concentration | 10 mg/L | Average chloride concentration in background samples (Table 4-12) |
| Injection Rate | 19.90 $m^3$/day | Calculated from the volume of PA water injected divided by the time to complete the injection |
| Effective Molecular Diffusion in Water | $6.0 \times 10^{-5}$ $m^2$/day | From Lobo and Quaresma (1989) |

**Table 4-45: Inputs for MODFLOW Model of STP-07-159-SS Injection without Vertical Flow Component**

| Parameter | Value | Justification |
|---|---|---|
| WCSC Longitudinal Dispersivity | 0.51 m | Value adjusted until modelled concentration profile matched observed concentration profile |
| WCSC Transverse Horizontal Dispersivity | 0.051 m | Set Transverse Horizontal Dispersivity an order of magnitude less than longitudinal dispersivity, consistent with observations of Sudicky, et al. (1983) |
| WCSC Transverse Vertical Dispersivity | 0.0051 m | Set Transverse Vertical Dispersivity two orders of magnitude less than longitudinal dispersivity, consistent with observations of Sudicky, et al. (1983) |
| WCSC Hydraulic Conductivity in X, Y, and Z Direction | $2.5x10^{-3}$ m/s | Near Hydraulic Conductivities determined by KCB via Slug Tests for the Shallow Aquifer Depth – Adjusted value until modelled concentration profile matched observed concentration profile |
| WCSC Porosity | 0.3 | Typical porosity of sand aquifer from Freeze and Cherry (1979) |
| WCSC Specific Storage | $1.075x10^{-5}$ $m^{-1}$ | From Klohn Crippen Consultants Ltd. (2004) |
| WCSC Specific Yield | $2 \times 10^{-2}$ | From Klohn Crippen Consultants Ltd. (2004) |
| WCSC Recharge | 88.39 mm/yr | Twenty percent of the site's mean annual precipitation. Precipitation data from Klohn Crippen (2004). |
| Glacial Till Hydraulic Conductivity | $2.5x10^{-7}$ m/s | Till was unsaturated for all model runs. Set hydraulic conductivity several orders of magnitude higher than WCSC to prevent flow through the unit. |
| Up-gradient Constant Head Boundary Condition | 355.36264 m amsl | Set Up-gradient Constant Head Boundary to create hydraulic gradient to drive groundwater flow at velocity of 10 cm/day |
| Down-gradient Constant Head Boundary Condition | 355.35936 m amsl | Set Down-gradient Constant Head Boundary to create hydraulic gradient to drive groundwater flow at velocity of 10 cm/day |
| Initial Head Condition (Set in the middle of the domain where the injection well was positioned | 355.361 m amsl | Groundwater Elevation at STP-07-159-SS immediately before PA water injection |
| Chloride Concentration of Injectate | 583 mg/L | Maximum concentration of chloride detected in PA water injectate (Table 4-21) |
| Background Chloride Concentration | 35.5 mg/L | Average chloride concentration in background samples (Table 4-15) |
| Injection Rate | 30.09 $m^3$/day | Calculated from the volume of PA water injected divided by the time to complete the injection |
| Effective Molecular Diffusion in Water | $6.0x10^{-5}$ $m^2$/day | From Lobo and Quaresma (1989) |

# Figures

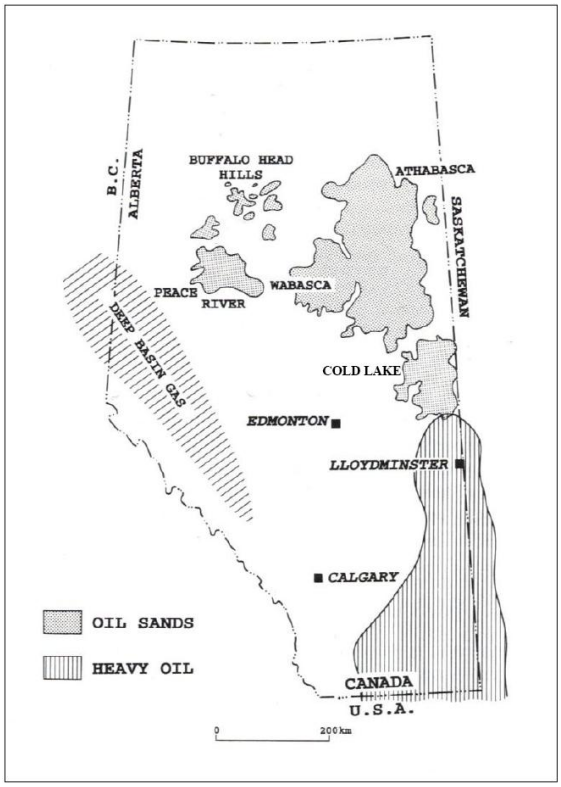


**Figure 1-1: Oil Sands Regions of Alberta. Source: Greiner and Chi (1995).**

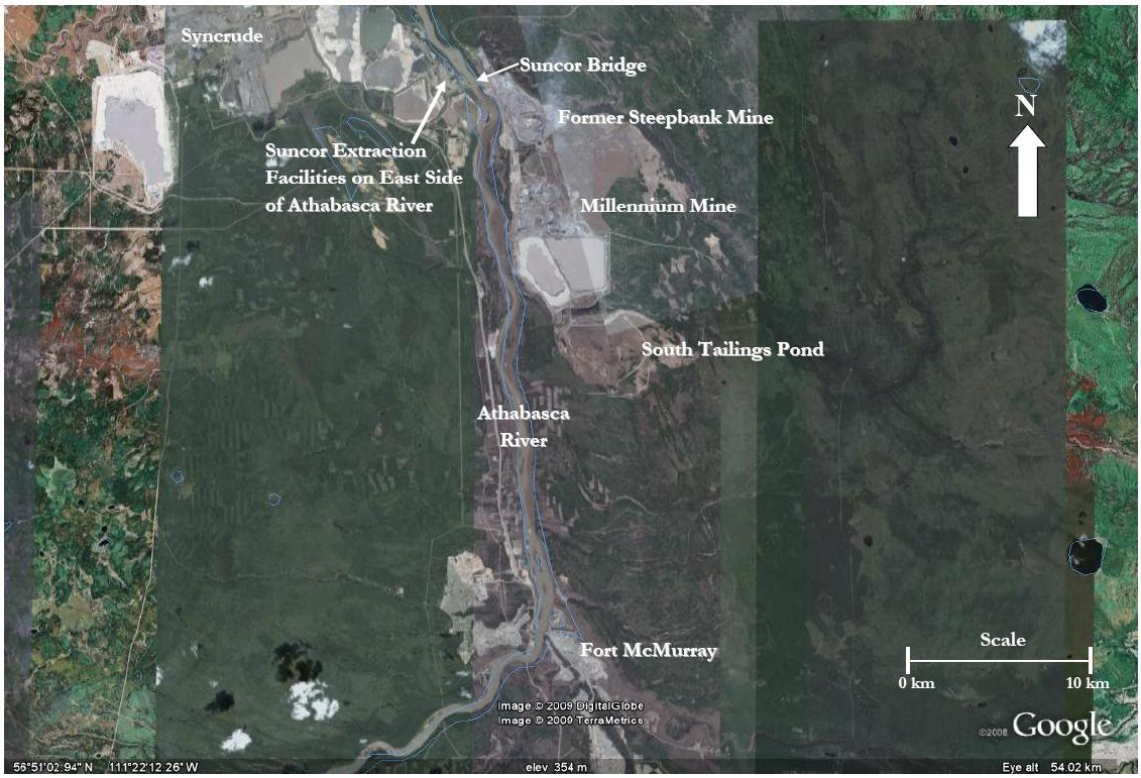


**Figure 1-2: Location of Suncor Energy Inc. Oil Sands Mining Facility. From: ©2008 Google, Image ©2009 DigitalGlobe, Image ©2009 TerraMetrics.**


**Figure 1-3: Suncor Energy Inc. Mining Facilities on the East Side of the Athabasca River.**

**Figure 1-4: View of South Tailings Pond from Siphon Line off North Dike (Photographed June 24, 2009). View is to the southeast.**


**Figure 1-5: Location of In Situ Aquifer Test Facility.**

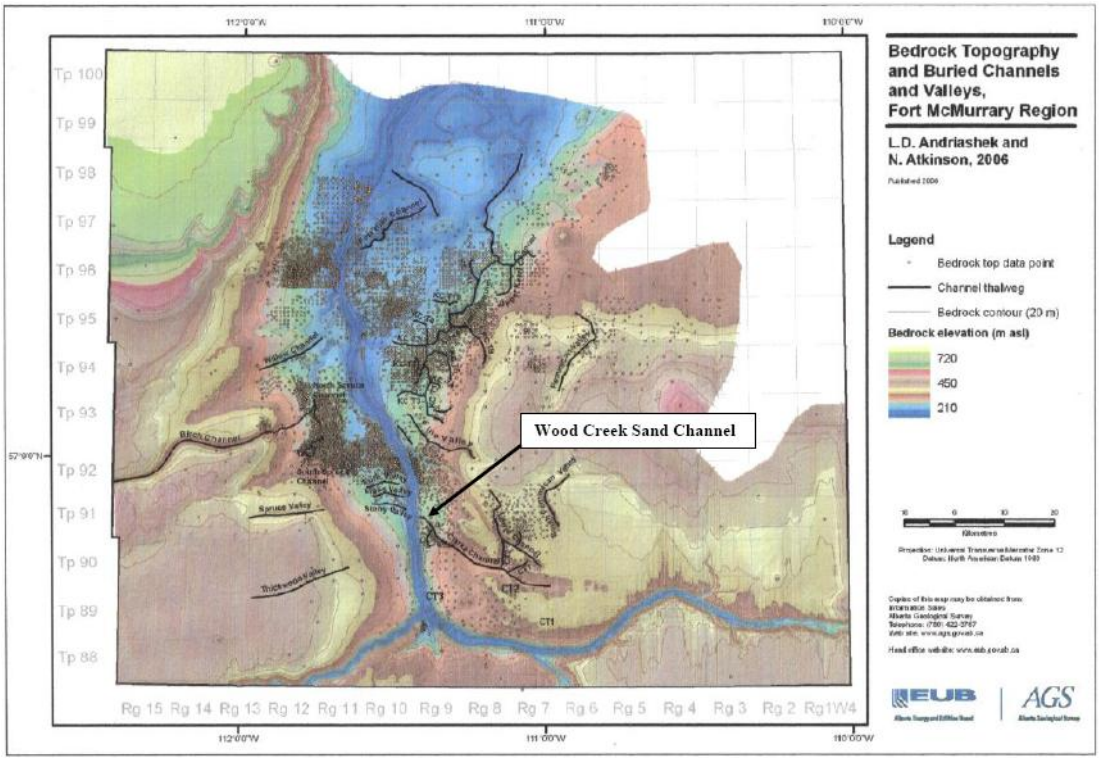


**Figure 1-6: Location of Buried Channels near Fort McMurray, Alberta. Source: Andriashek and Atkinson (2007).**

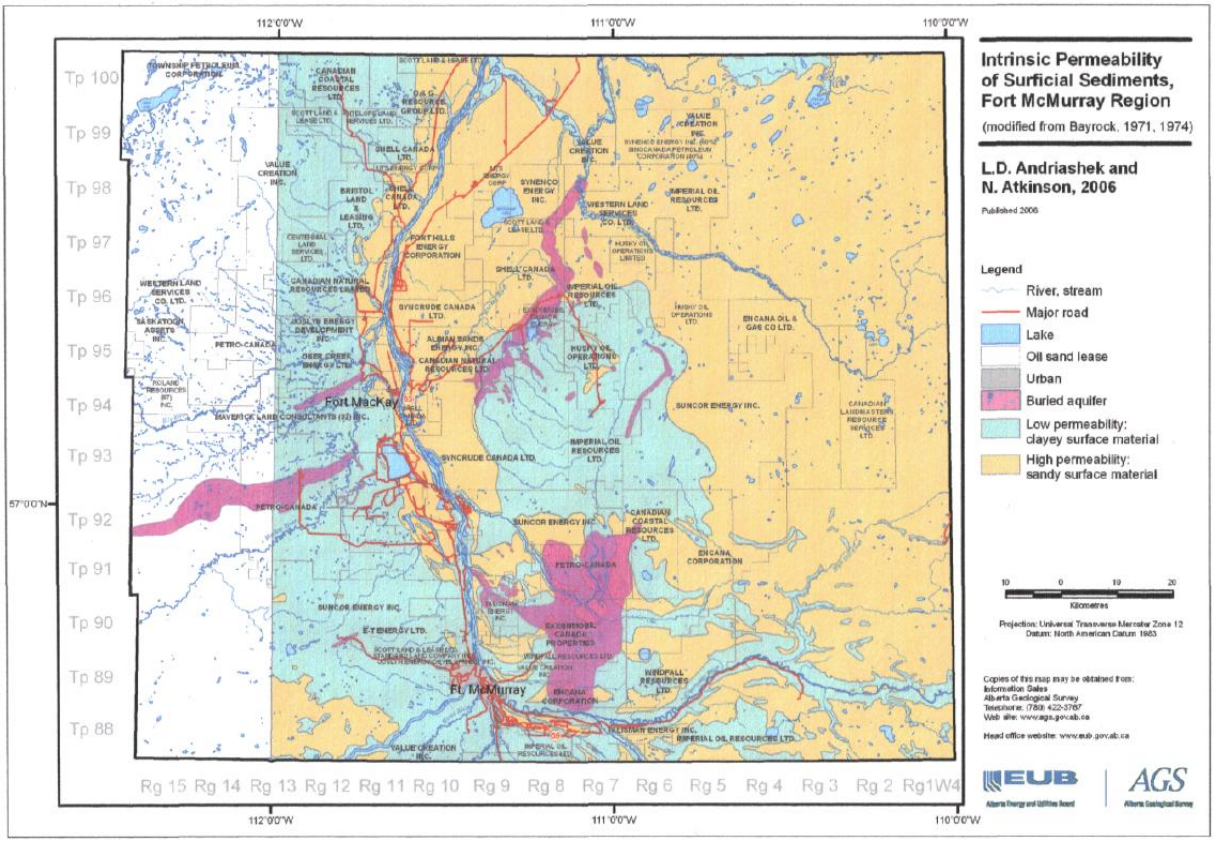


**Figure 1-7: Distribution of Low and High Permeability Surficial Sediments near Fort McMurray, Alberta. Source: Andriashek and Atkinson (2007).**

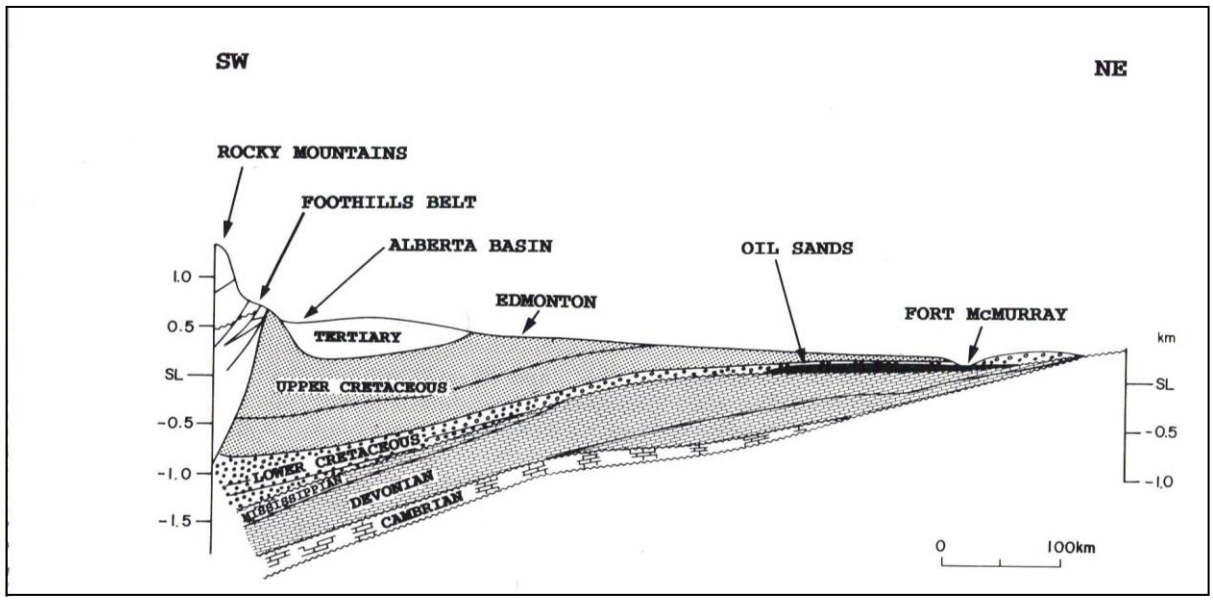


**Figure 2-1: Migration of oil in the Manville Group to its current position near Fort McMurray, Alberta. Source: Greiner and Chi (1995).**

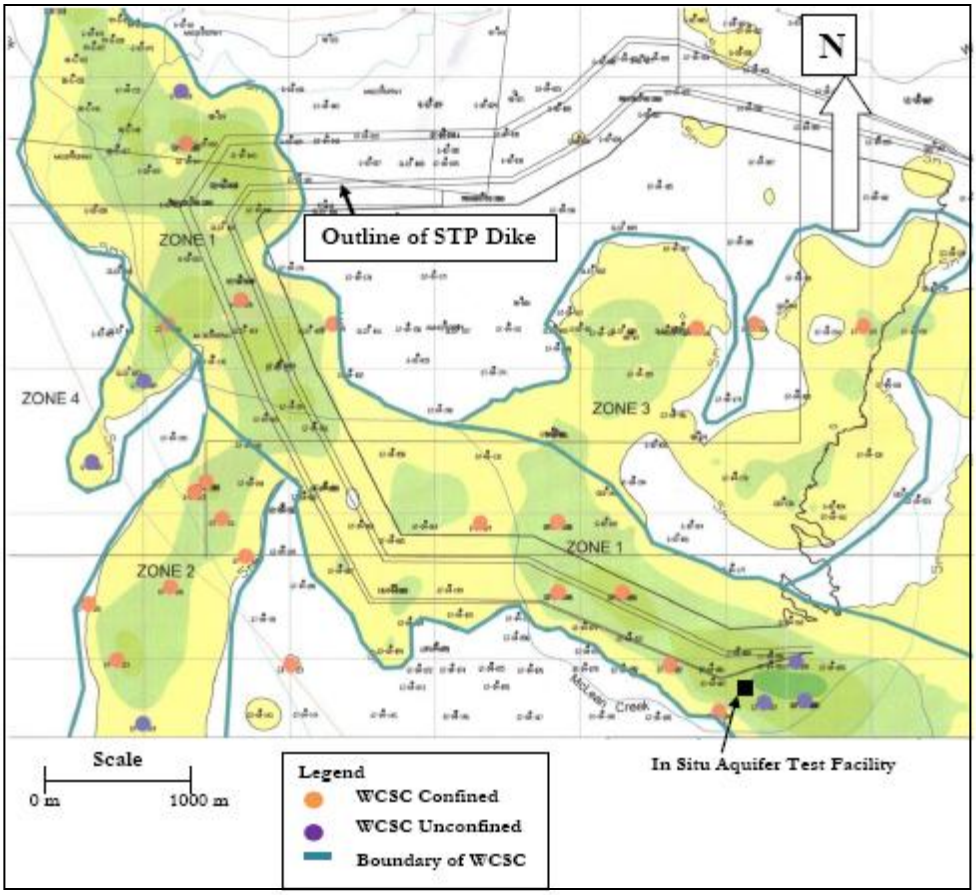


**Figure 2-2: Position of Wood Creek Sand Channel Beneath the South Tailings Pond. Source: Klohn Crippen Consultants Ltd. (2004).**

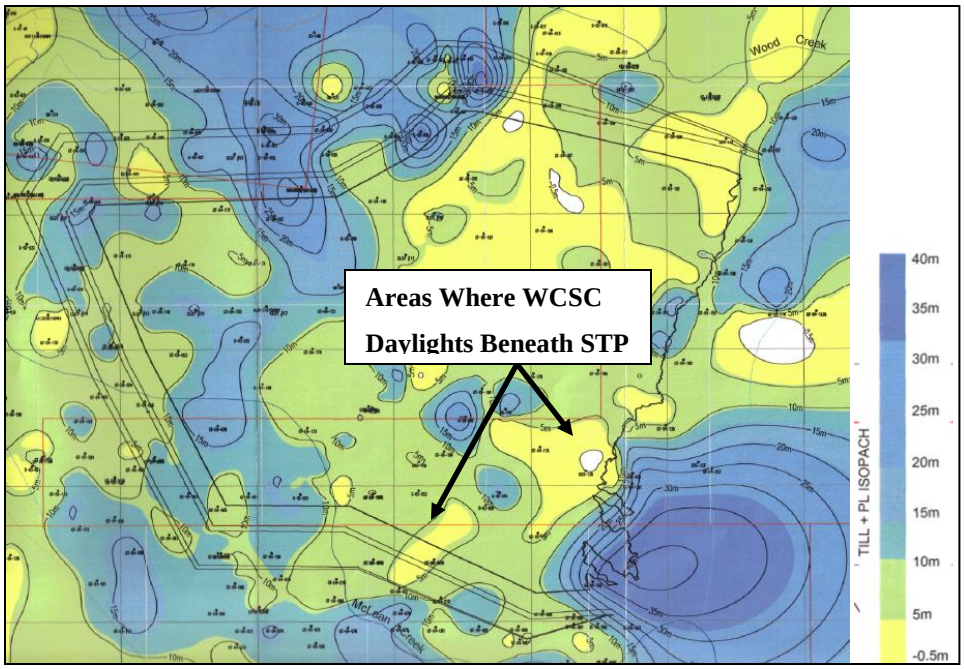


**Figure 2-3: Thickness of till and Pleistocene lacustrine sediments in the vicinity of the South Tailings Pond. Source: Klohn Crippen Consultants Ltd. (2004).**

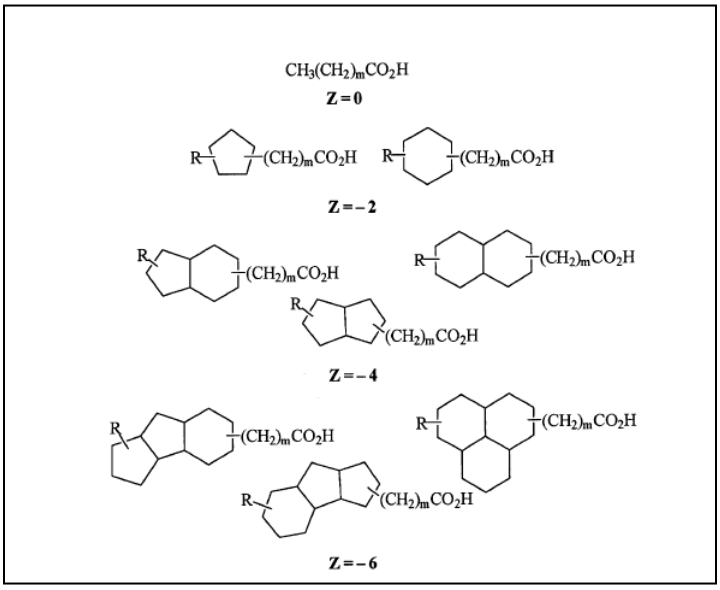


**Figure 2-4: Structure of naphthenic acids for different Z families (Z = 0, -2, -4 or -6) with 5 or 6 carbons in the cycloalkanes. Source: Holowenko et al. (2002).**


**Figure 2-5: Arrangements of *n, iso, sec,* and *tert*-butyl alkyl substituents. Source: Smith, et al. (2008).**

**a)**

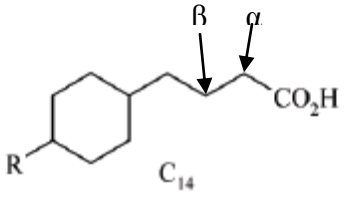


**b)**

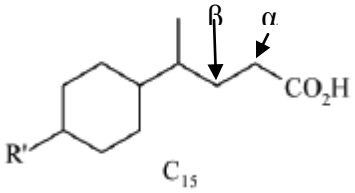


**Figure 2-6: Arrangement of: a) Butylcyclohexylbutanoic Acid (BCHBA); and b) Butylcyclohexylpentanoic Acid (BCHPA) illustrating the difference in arrangement of the alkanoate substituents and highlighting the alpha (α) and beta (β) positions on the side-chain connecting the carboxyl group to the cycloalkane. Source: Smith, et al. (2008).**

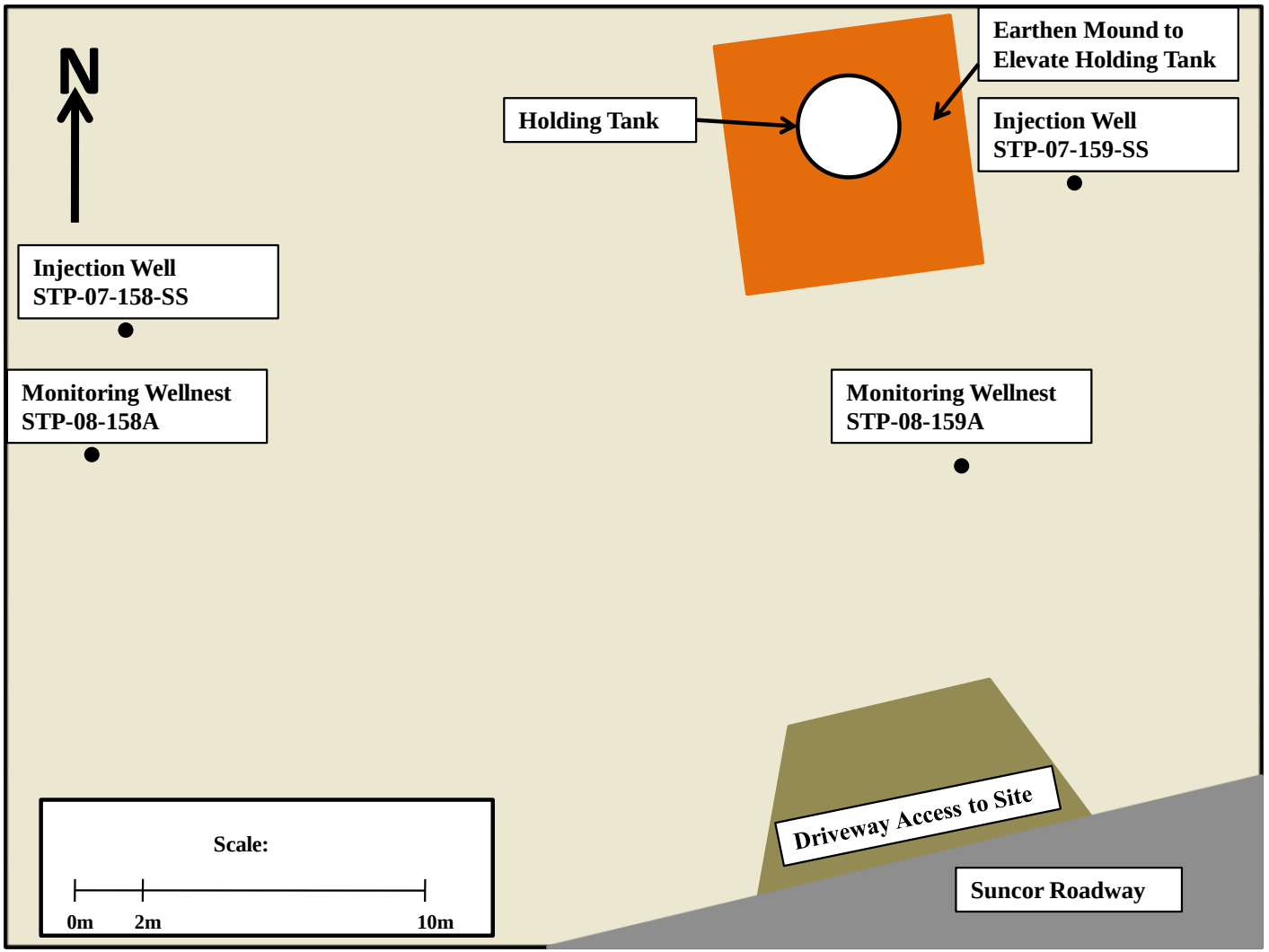


**Figure 3-1: Site layout of the In Situ Aquifer Test Facility (ISATF)**


**Figure 3-2: In Situ Aquifer Test Facility – View to the Northwest.**

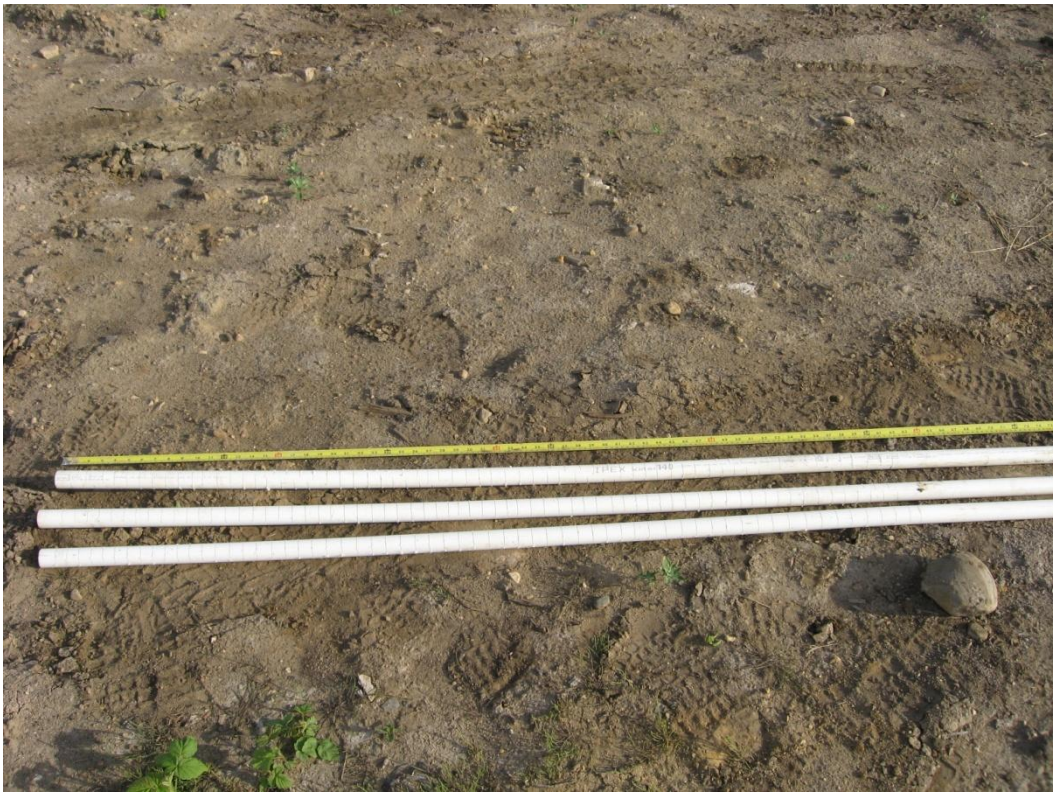

**Figure 3-3: Hand-slotted 1-Inch PVC well screens used at monitoring well nest STP-08-159A.**

**Figure 3-4: Hand-slotted 1-Inch PVC well screen wrapped with filter fabric.**

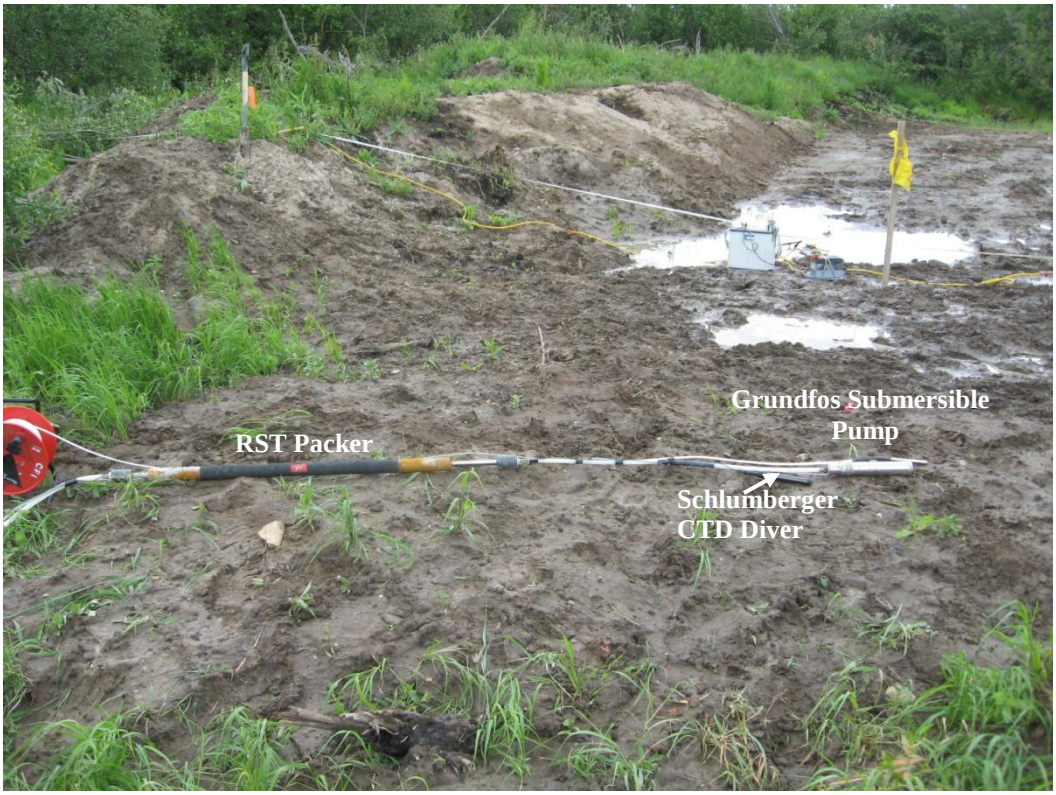


**Figure 3-5: Packer/Probe/Pump System installed in the ISATF Injection Wells.**

**Figure 3-6: RST Packer used in ISATF Injection Wells.**

**Figure 3-7: Schlumberger CTD Diver connected to direct read cable used in ISATF Injection Wells.**

**Figure 3-8: Grundfos Redi-flo 2 Submersible Pump used in ISATF Injection Wells.**

**Figure 3-9: Injection System.**

**Figure 3-10: Injection System – Garden hose running from injection tank to STP-07-159-SS.**

**Figure 3-11: Withdrawal of process-affected water from the South Tailings Pond via vacuum truck.**

**Figure 3-12: Transfer of PA water from vacuum truck to holding tank at the ISATF.**

**a) Groundwater Conductivity and Temperature**

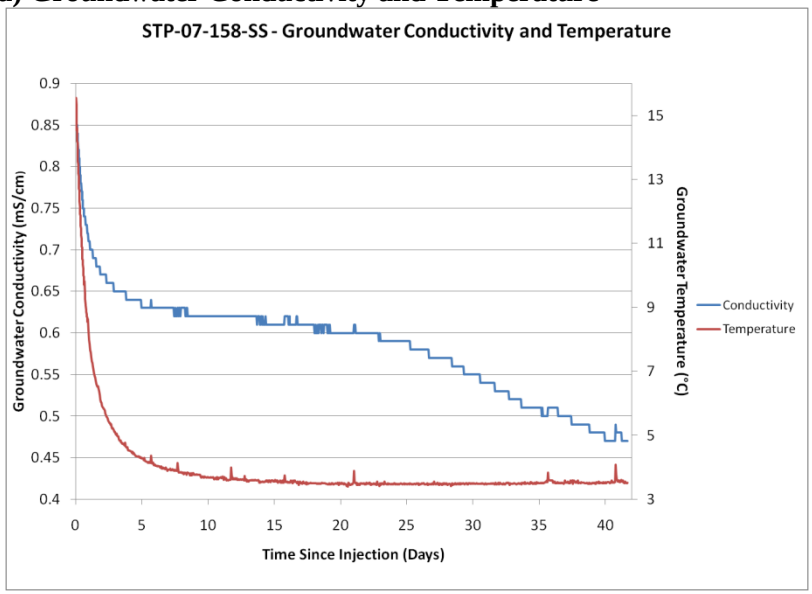


**b) Groundwater Elevation**

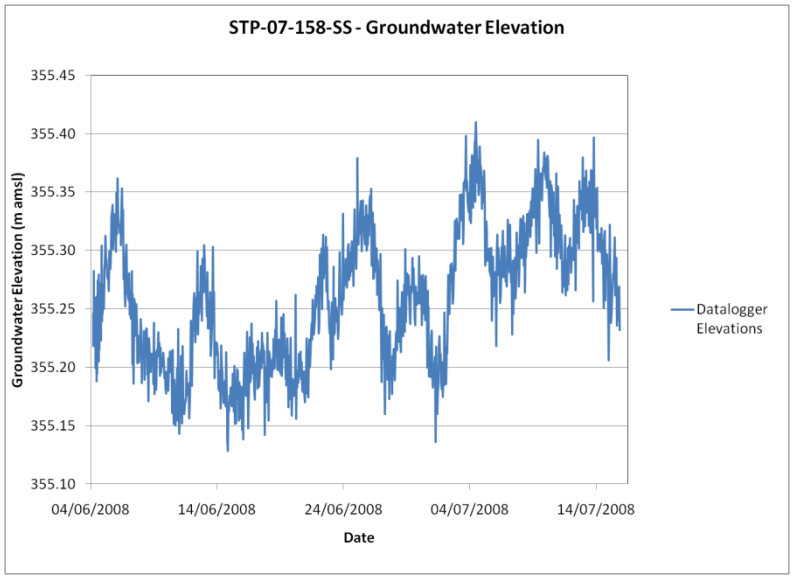


**Figure 4-1: Data from CTD Diver deployed at STP-07-158-SS following preliminary injection (June 4-July 16, 2008) including: (a) groundwater conductivity and temperature; and (b) groundwater elevation.**

**Groundwater Conductivity and Temperature**

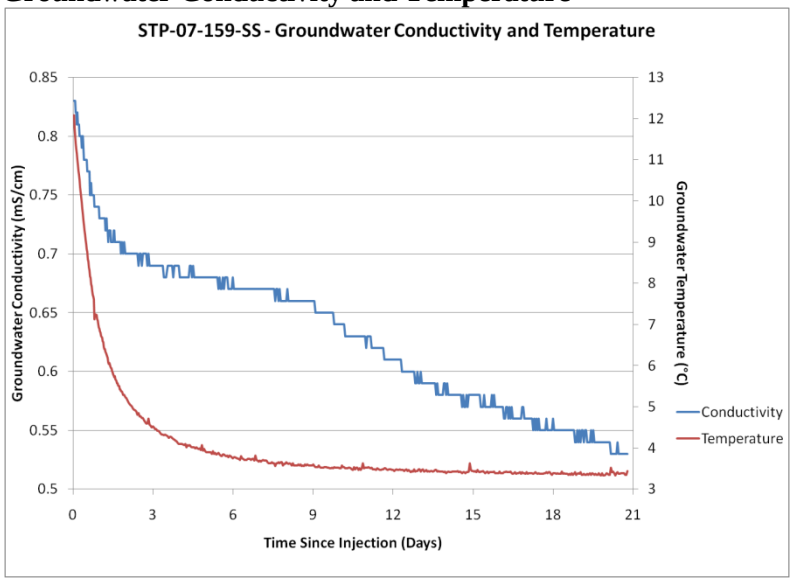


**Figure 4-2: Data from CTD Diver deployed at STP-07-159-SS following preliminary injection (June 4-26, 2008).**

**a) June 4-July 16, 2008**

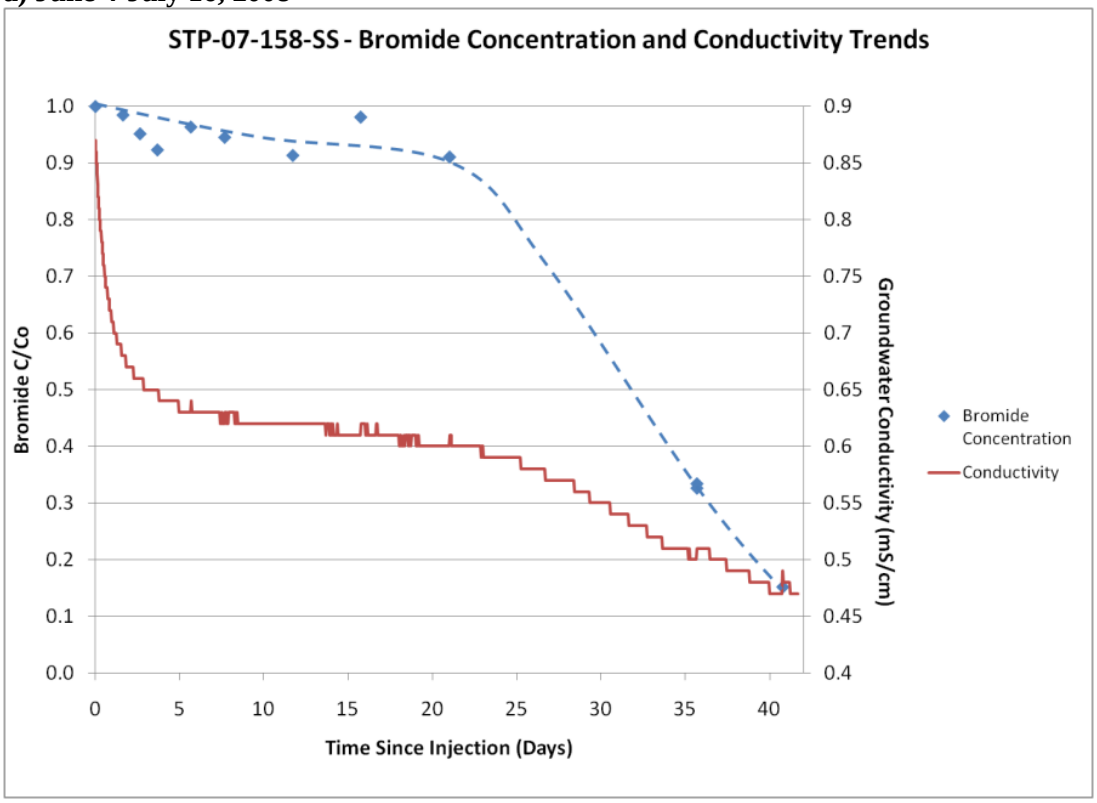


**b) June 13-July 16, 2008**

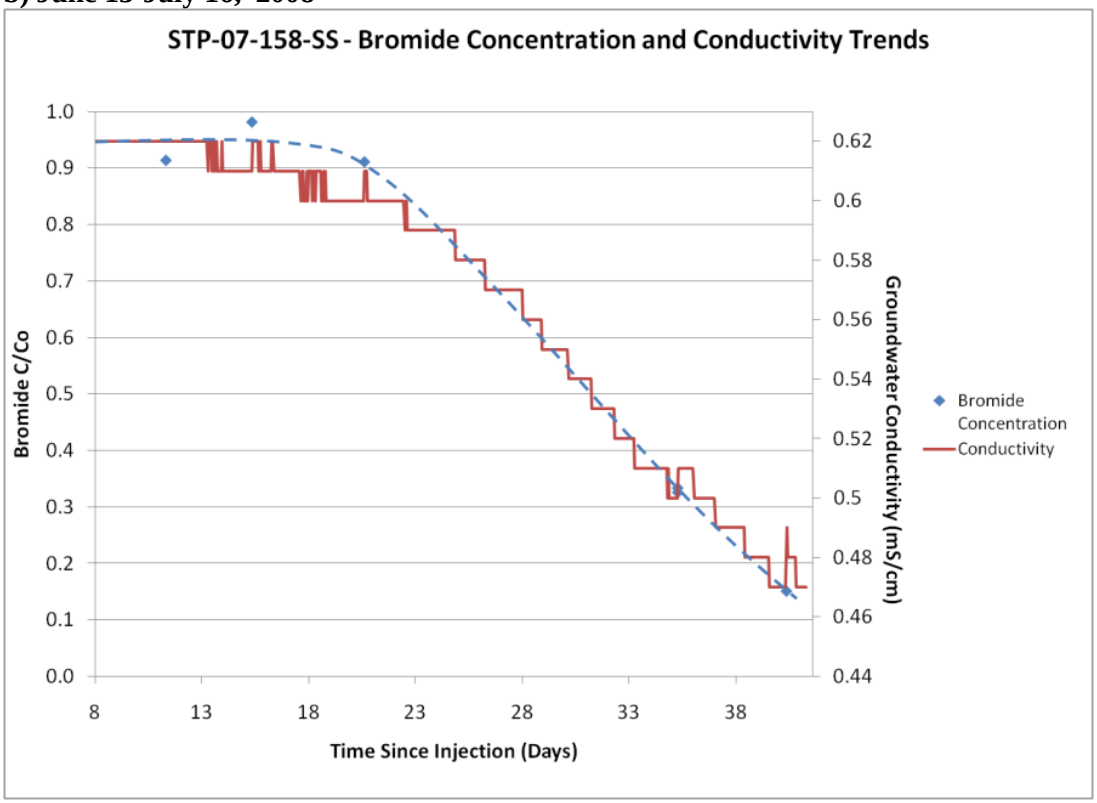


**Figure 4-3: Comparison of groundwater conductivity trends to bromide concentrations at STP-07-158-SS following preliminary injection including: (a) data from June 4-July 16, 2008 showing dissimilarity of overall conductivity and bromide trends; (b) data from June 13-July 16, 2008 showing similarity of conductivity and bromide trends from later time data.**

**a) June 4-June 26, 2008**

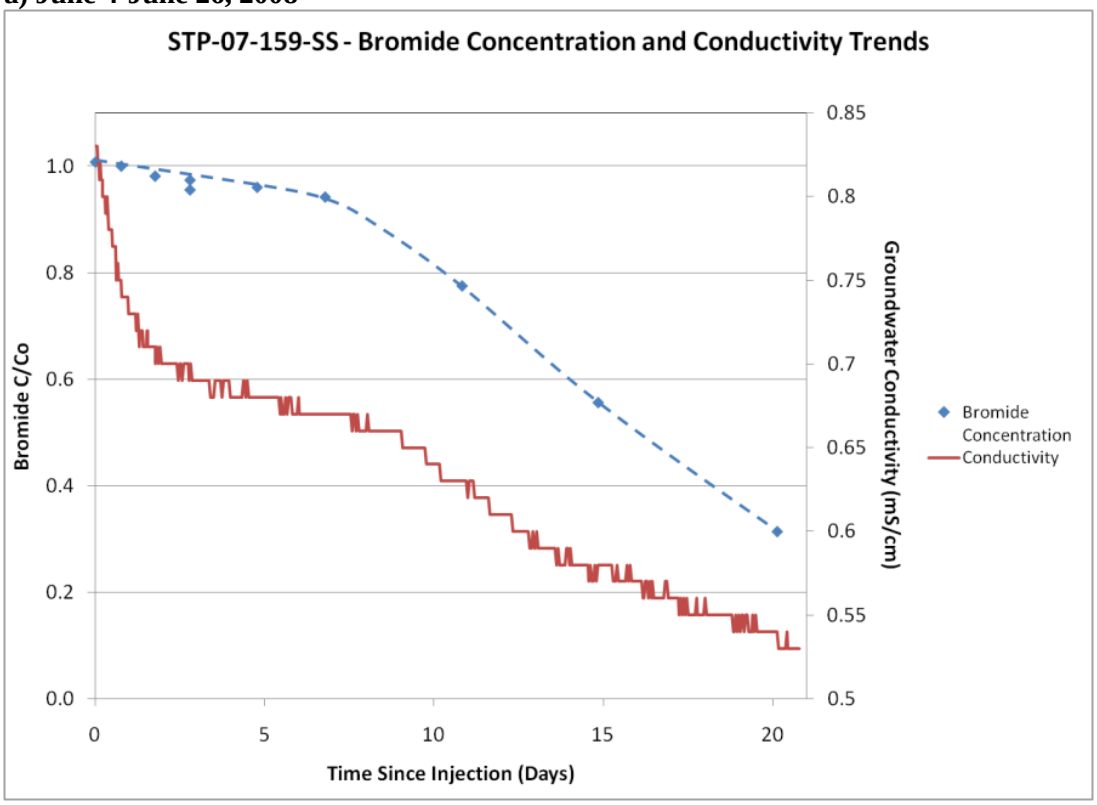


**b) June 11-June 26, 2008**

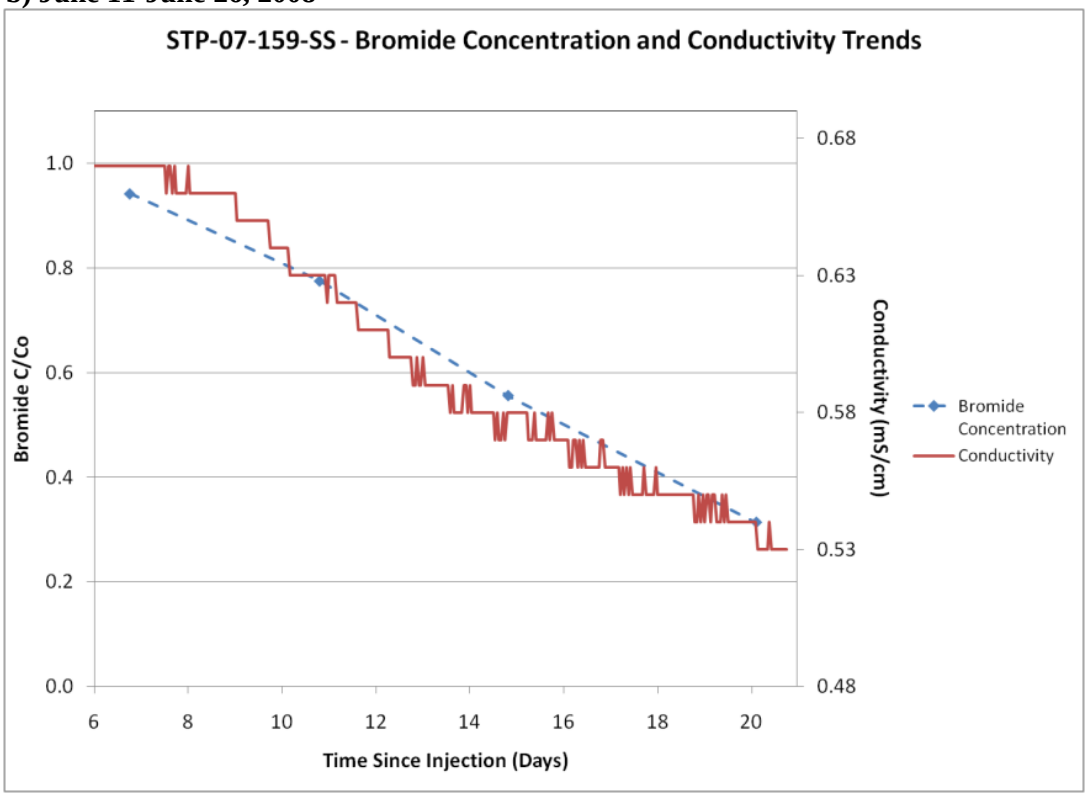


**Figure 4-4: Comparison of groundwater conductivity trends to bromide concentrations at STP-07-159-SS following preliminary injection including: (a) data from June 4-June 26, 2008 showing dissimilarity of overall conductivity and bromide trends; (b) data from June 11-June 26, 2008 showing similarity of conductivity and bromide trends from later time data.**

**a) Relative concentrations (C/Co)**

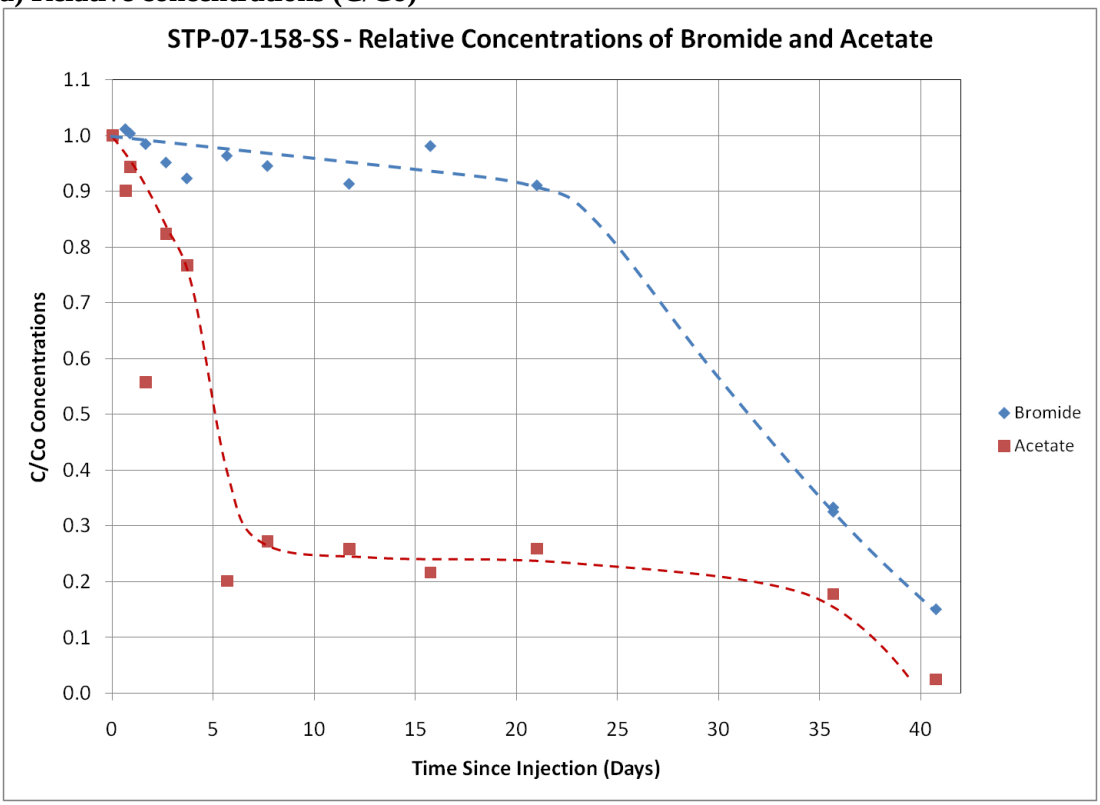


**b) Normalized acetate concentrations (C/Co)/(Br/Br$_o$) and relative bromide concentrations**

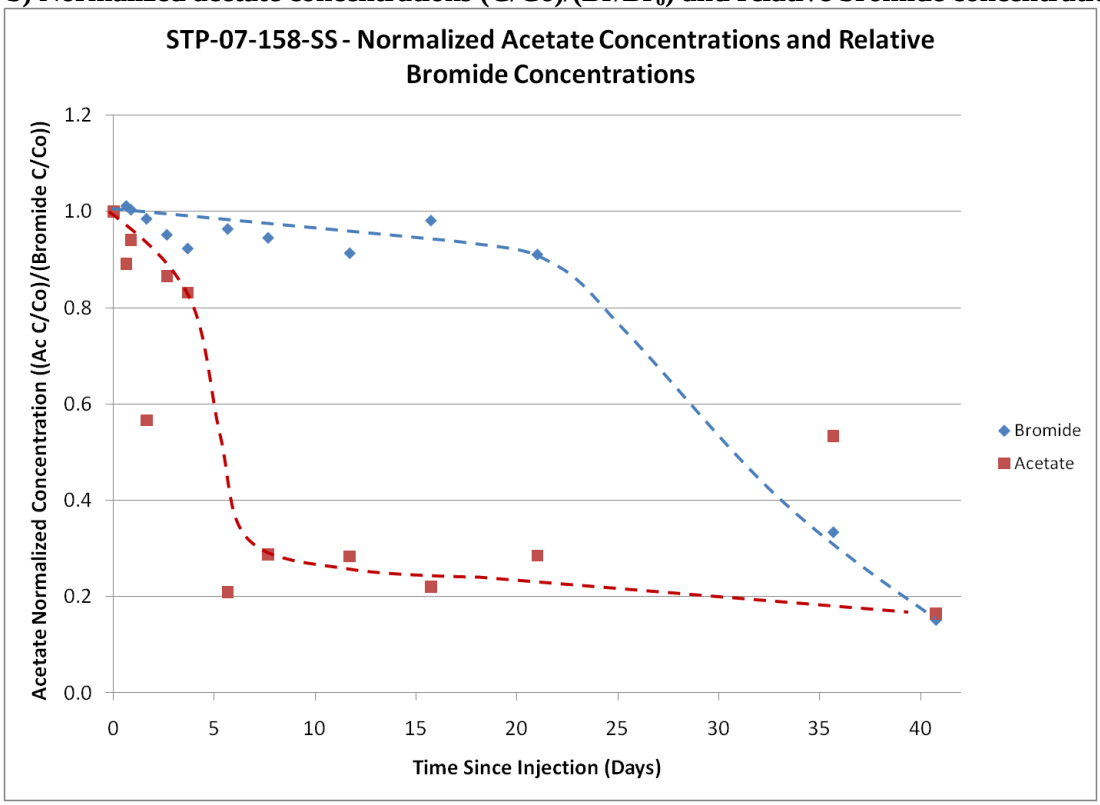


**Figure 4-5: Acetate and bromide concentration trends observed at STP-07-158-SS following preliminary injection showing: (a) relative concentrations (C/Co) of acetate and bromide; and (b) normalized acetate concentration (C/Co)/(Br/Br$_o$) and relative concentrations of bromide (Br/Br$_o$).**

**a) Relative concentrations (C/Co)**

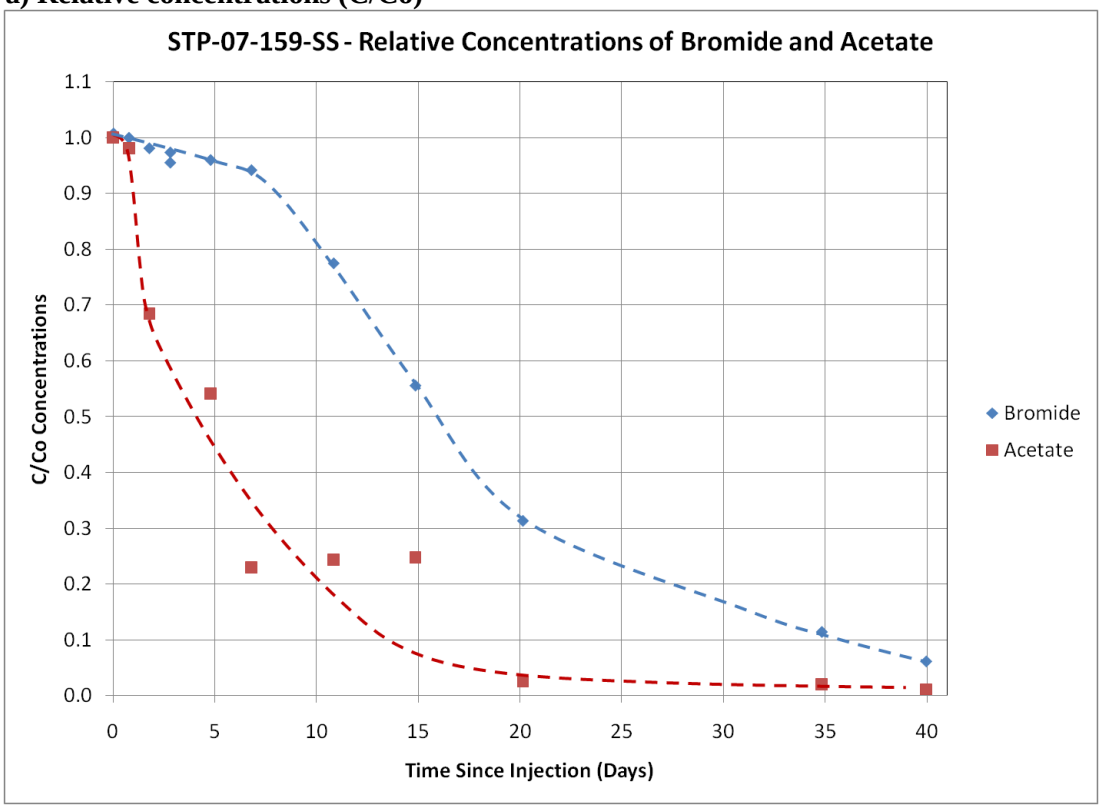


**b) Normalized acetate concentrations (C/Co)/(Br/Br$_o$) and relative bromide concentrations**

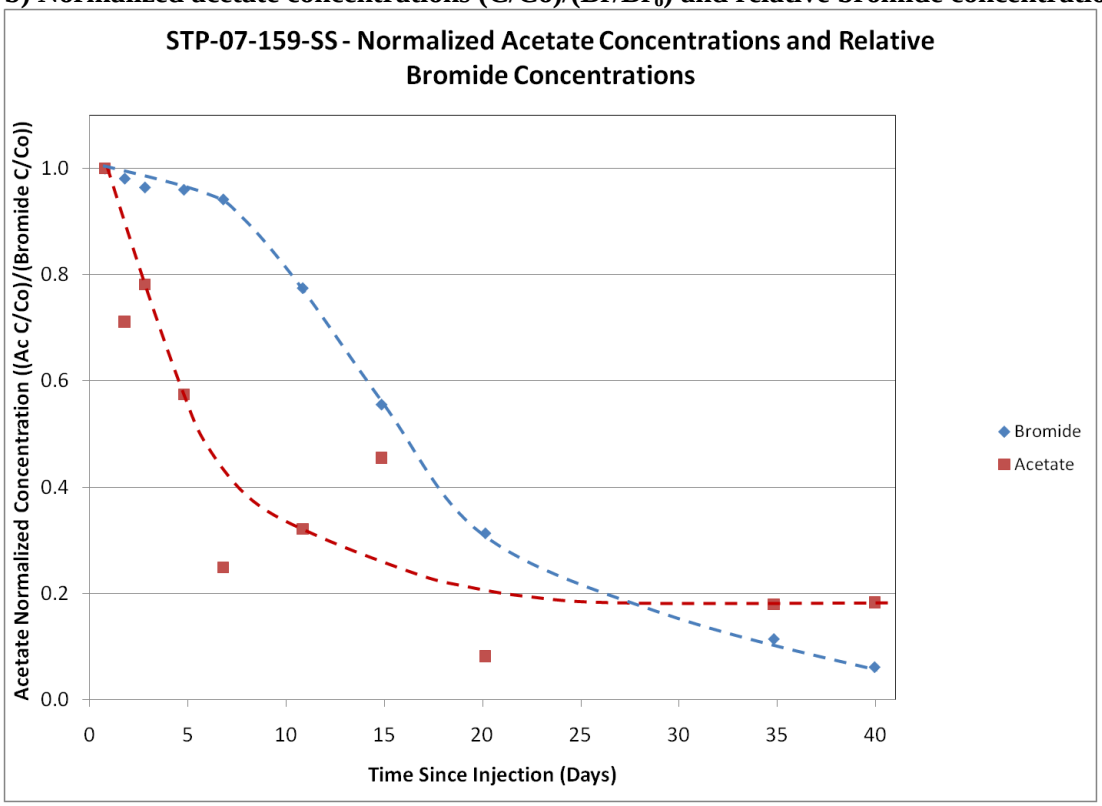


**Figure 4-6: Acetate and bromide concentration trends observed at STP-07-159-SS following preliminary injection showing: (a) Relative concentrations (C/Co) of acetate and bromide; and (b) normalized acetate concentrations (C/Co)/(Br/Br$_o$) and relative concentrations of bromide (Br/Br$_o$).**

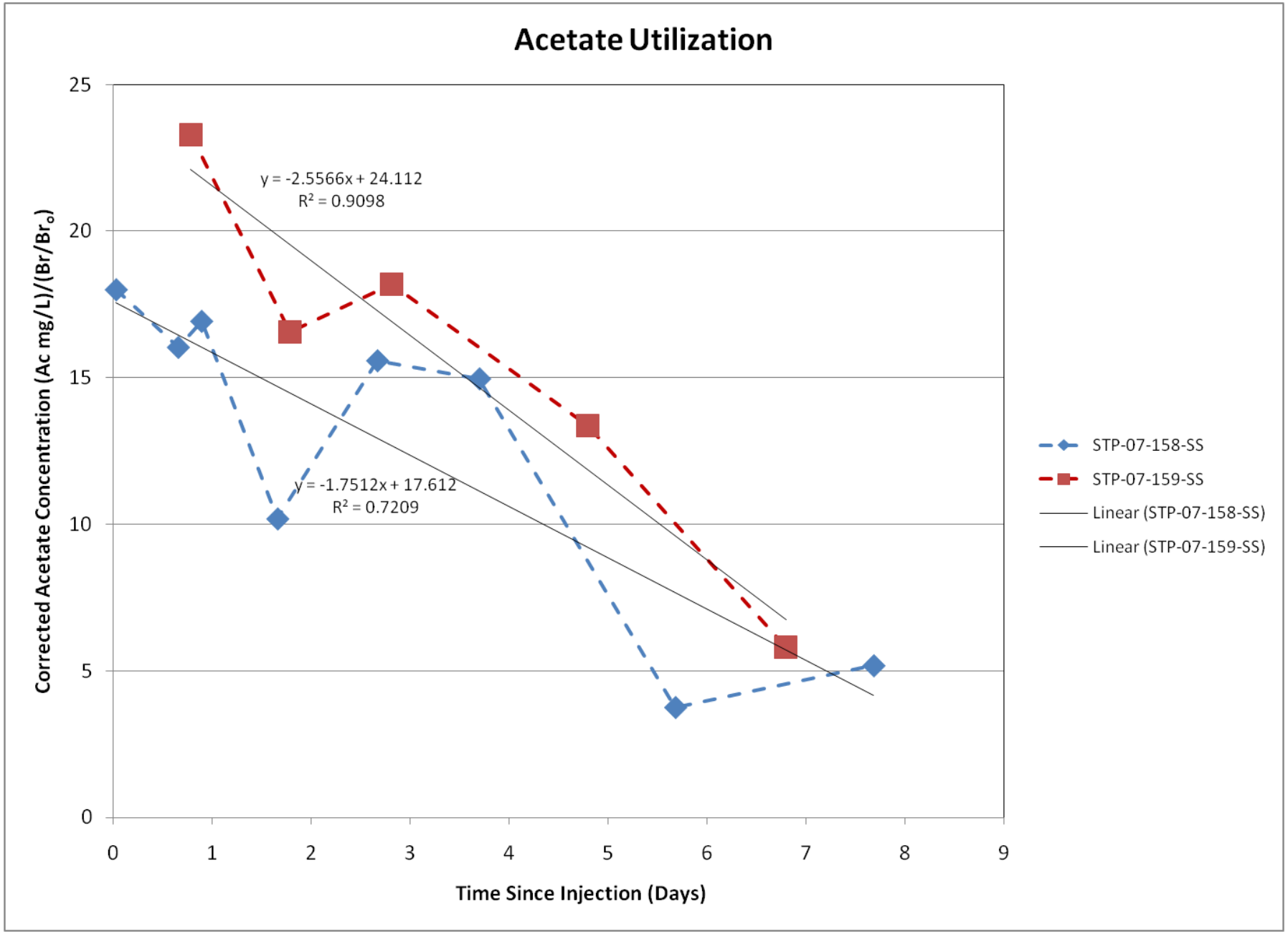


**Figure 4-7: Corrected acetate concentrations {(acetate mg/L)/(Br/Br$_o$)} at STP-07-158-SS and STP-07-159-SS over the 7-8 days immediately following the preliminary injections.**

**a) Groundwater Conductivity and Temperature**

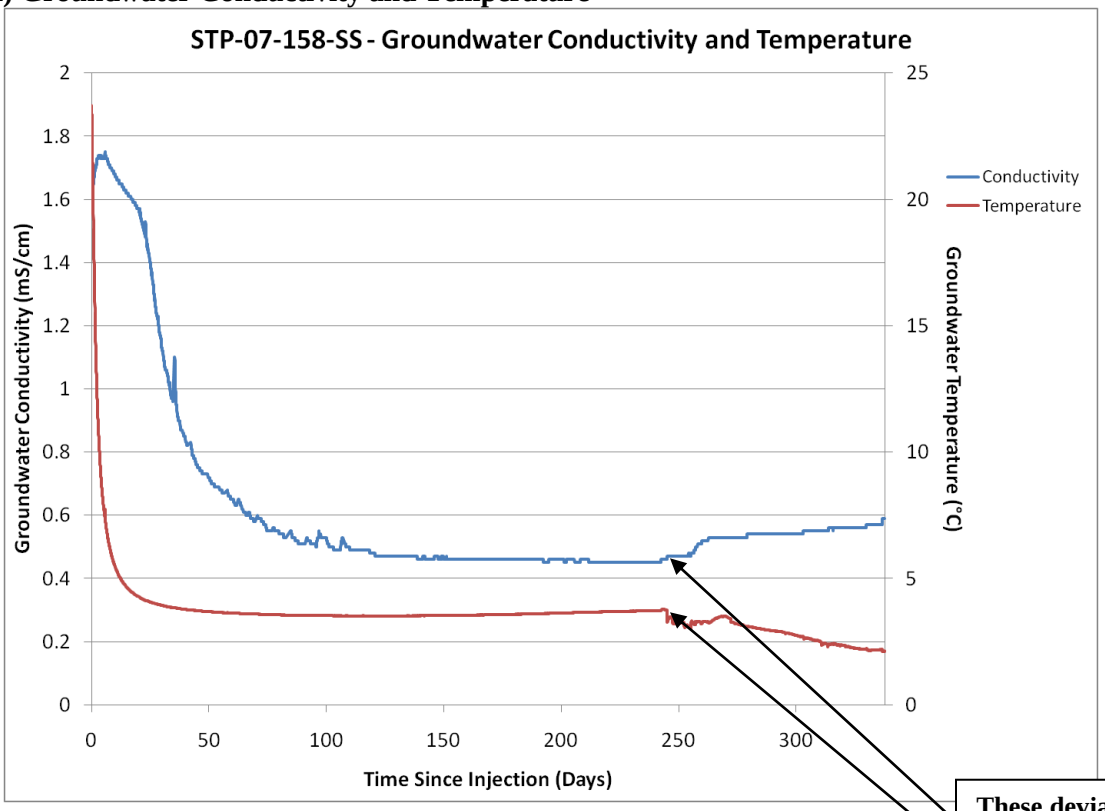


**b) Groundwater elevation**

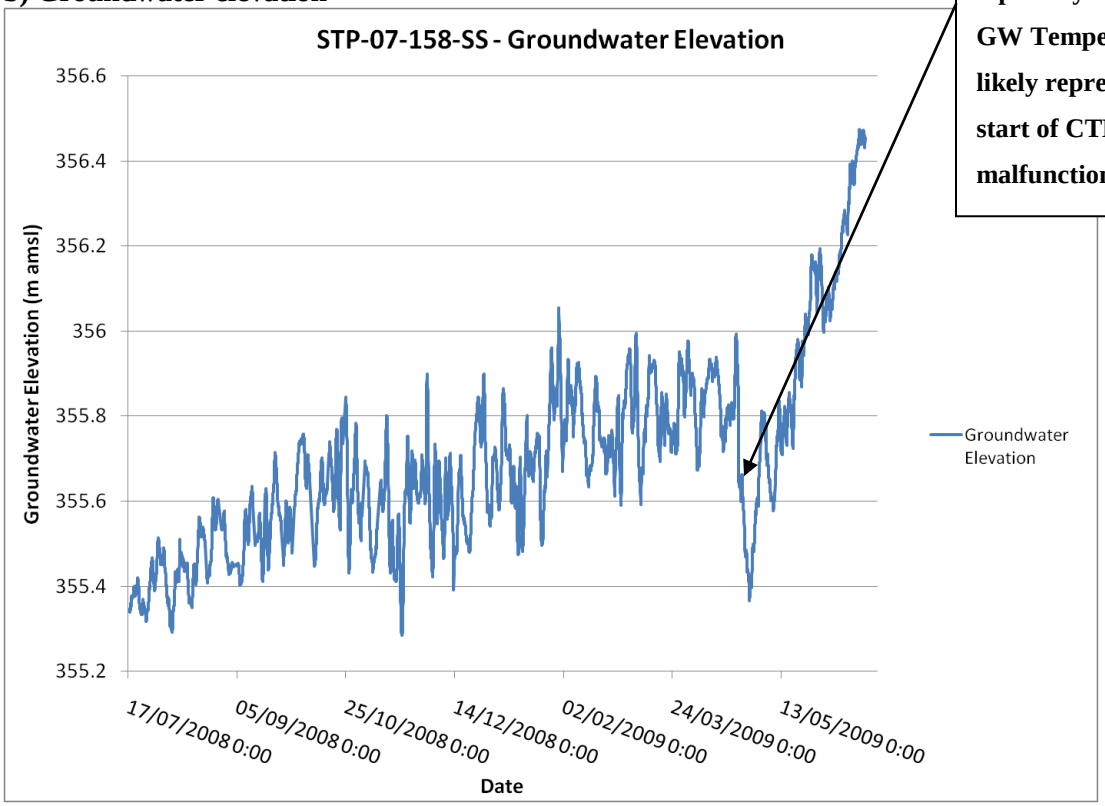


**These deviations, especially drop in GW Temperature likely represent the start of CTD Diver malfunction.**

**Figure 4-8: Data from CTD Diver at STP-07-158-SS following PA-water injection (July 17, 2008 – June 20, 2009) including: (a) Groundwater conductivity and temperature; and (b) groundwater elevation.**

**a) Groundwater Conductivity and Temperature**

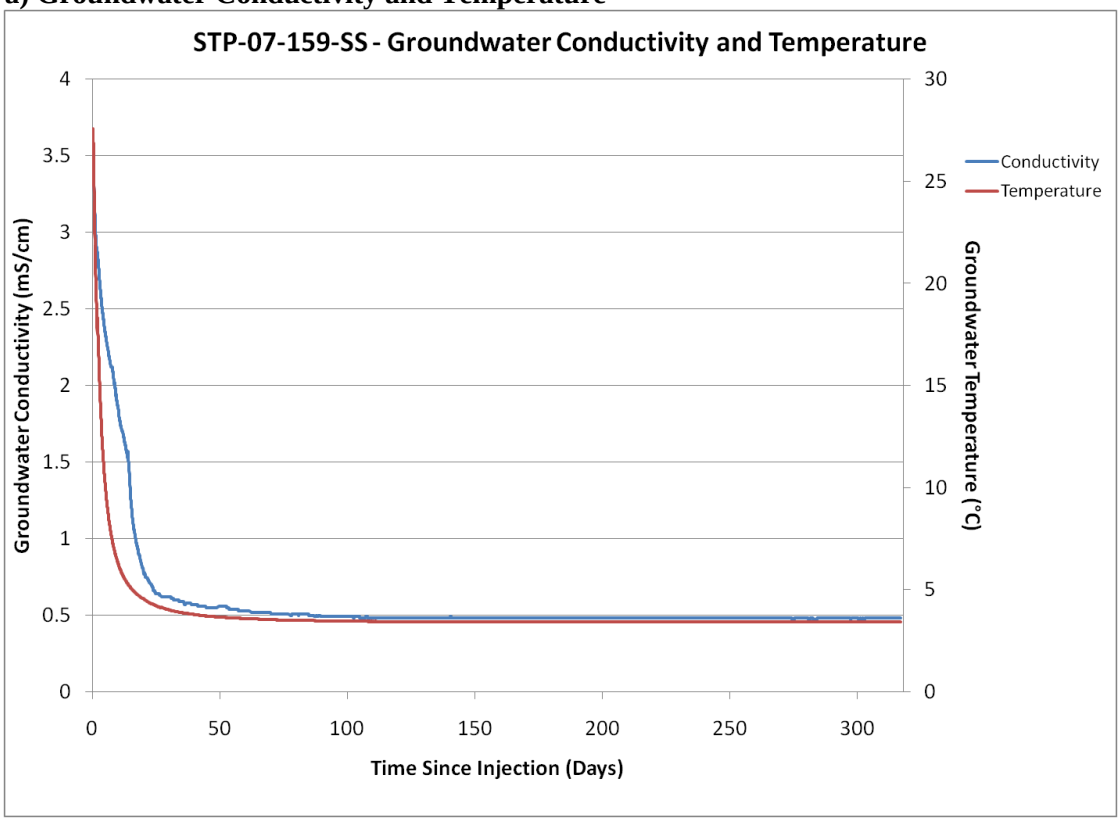


**b) Groundwater Elevation**

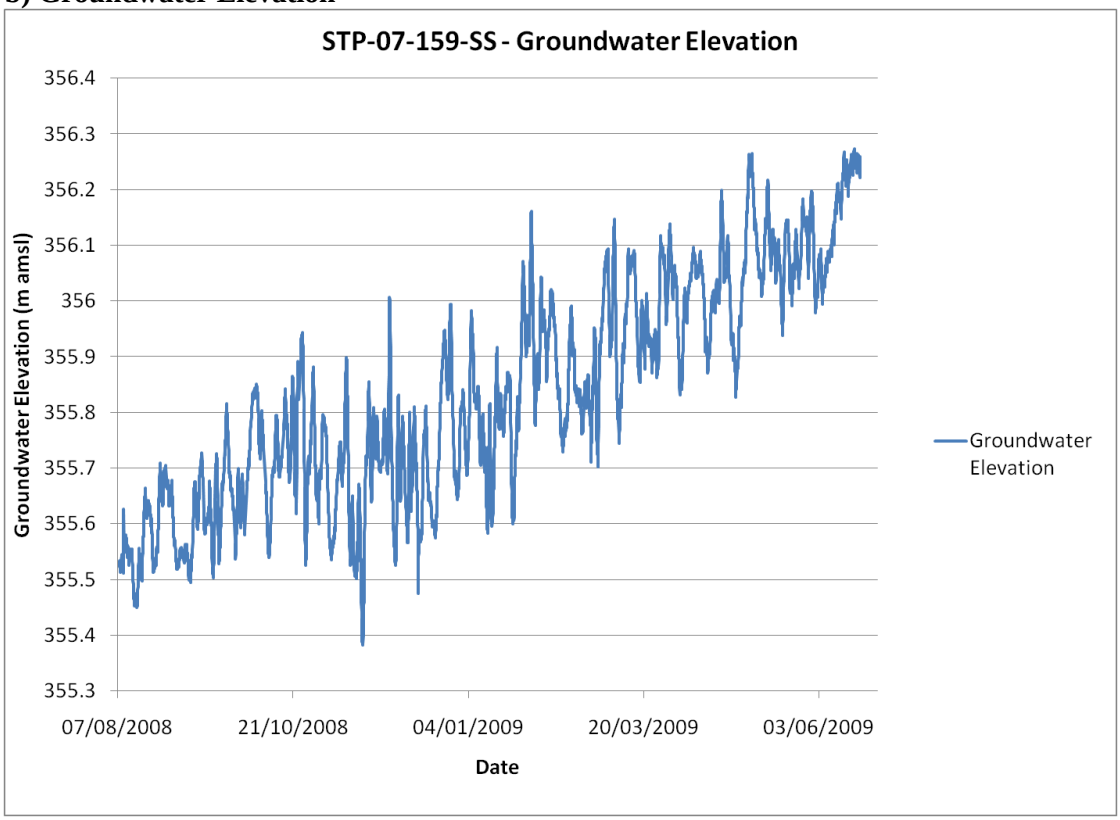


**Figure 4-9: Data from CTD Diver at STP-07-159-SS following PA-water injection (August 7, 2008-June 20, 2009) including: (a) Groundwater conductivity and temperature; and (b) groundwater elevation.**

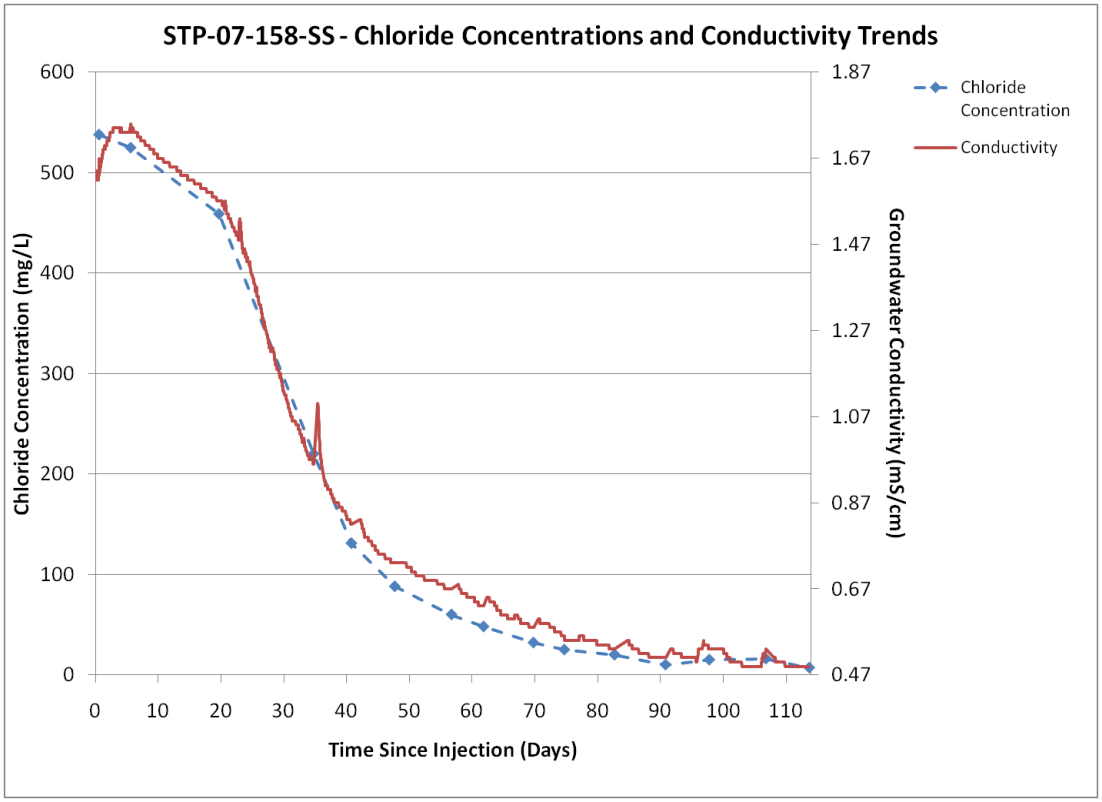


**Figure 4-10: Chloride concentration and groundwater conductivity trends at STP-07-158-SS following PA water injection ( July 17-November 8, 2008) illustrating the overall similarity of conductivity and chloride trends.**

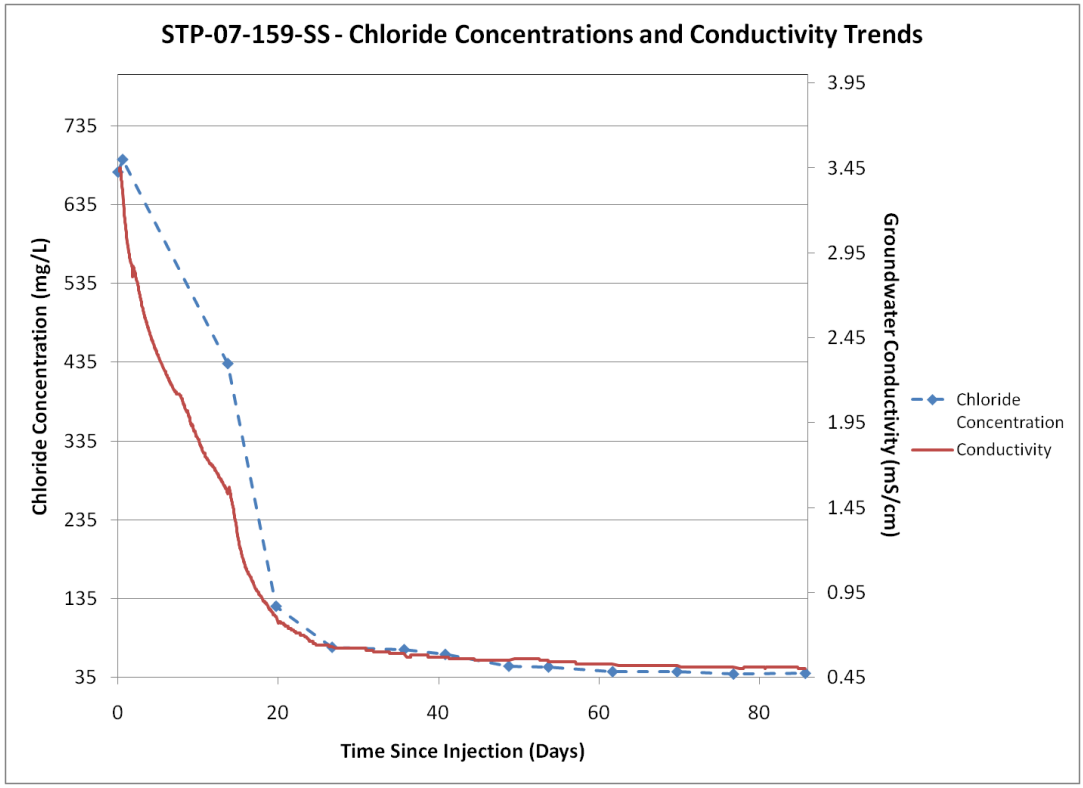


**Figure 4-11: Chloride concentration and groundwater conductivity trends at STP-07-159-SS following PA water injection (August 7-November 1, 2008) illustrating the overall similarity of conductivity and chloride trends.**

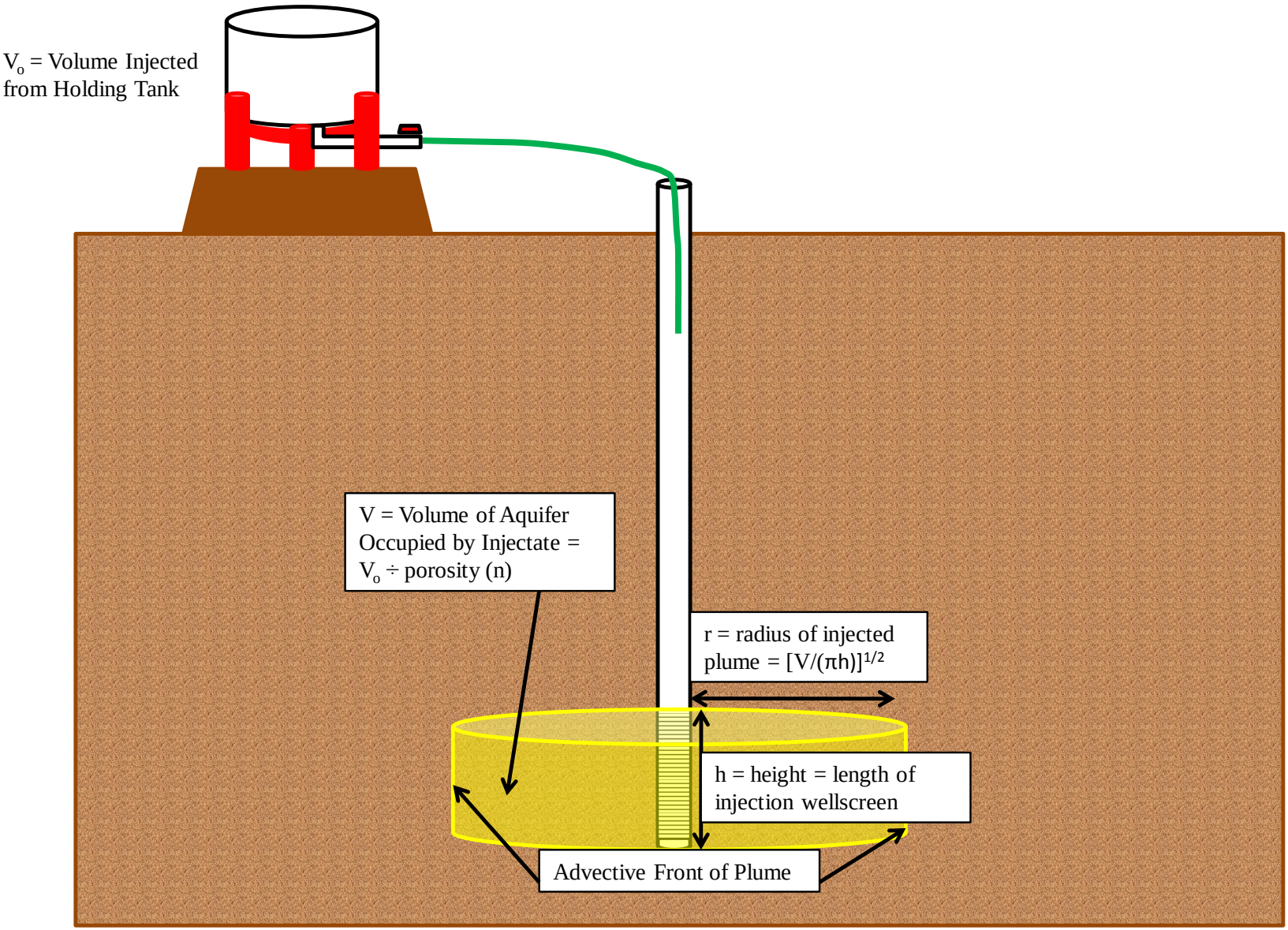


**Figure 4-12: Conceptual model of injectate distribution immediately following an injection.**

**a) Bromide C/Co following Preliminary Injections - Advective Front Arrival Times Highlighted**

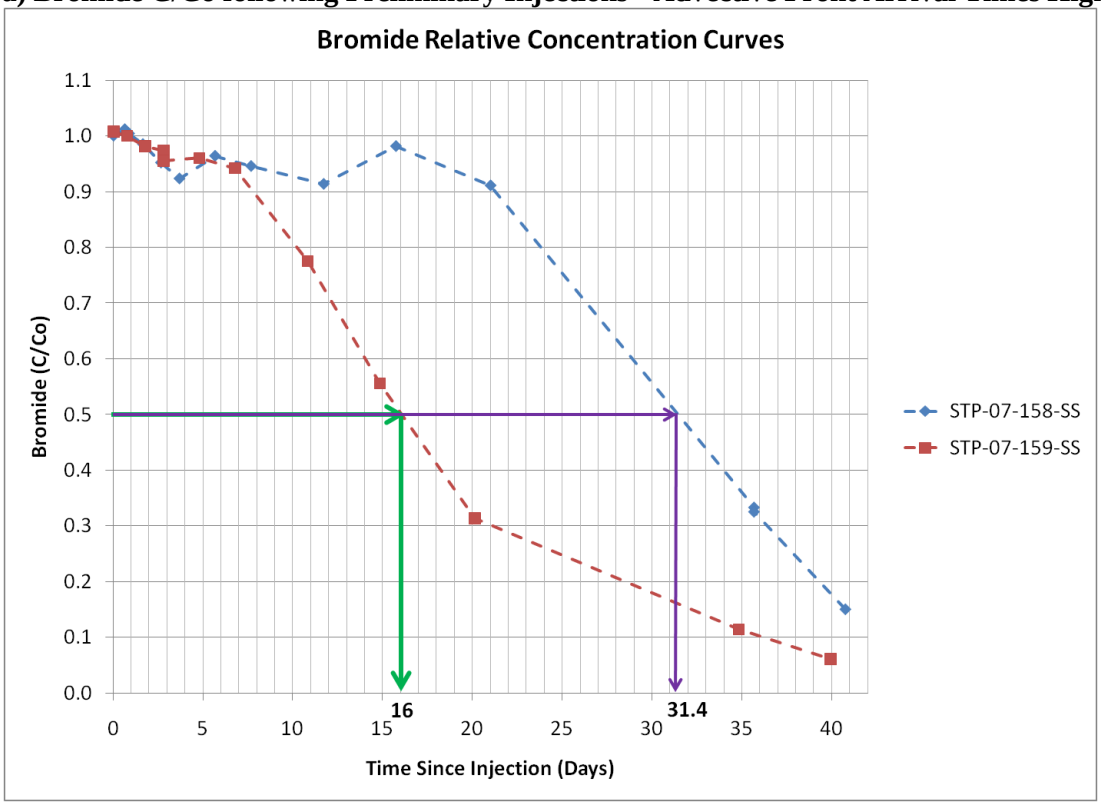


**b) Chloride C/Co following PA Water Injections – Advective Front Arrival Times Highlighted**

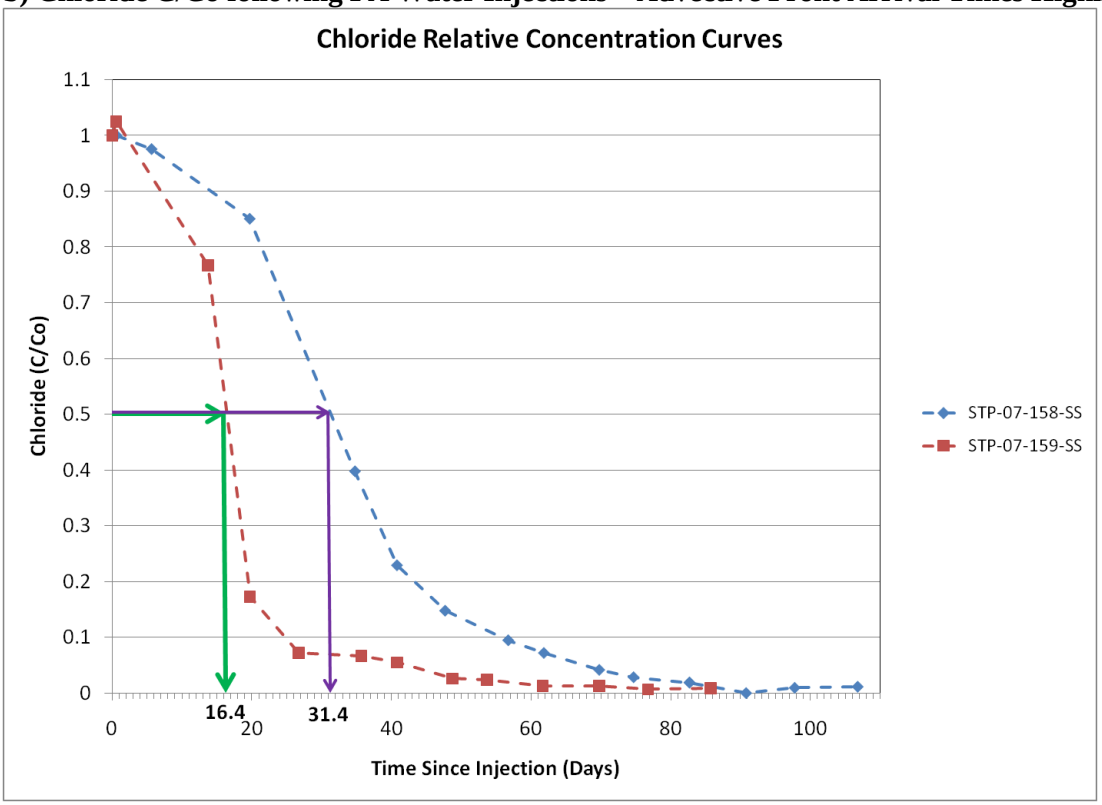


**Figure 4-13: Relative concentrations (C/Co) of tracers at STP-07-158-SS and STP-07-159-SS including: (a) bromide concentrations following preliminary injections; and (b) chloride concentrations following PA water injections. A relative concentration of 0.5 was assumed to represent the arrival of the plume's advective front at the well. These times were used to calculate groundwater velocities.**

**a) STP-07-158-SS Relative Bromide Concentrations**

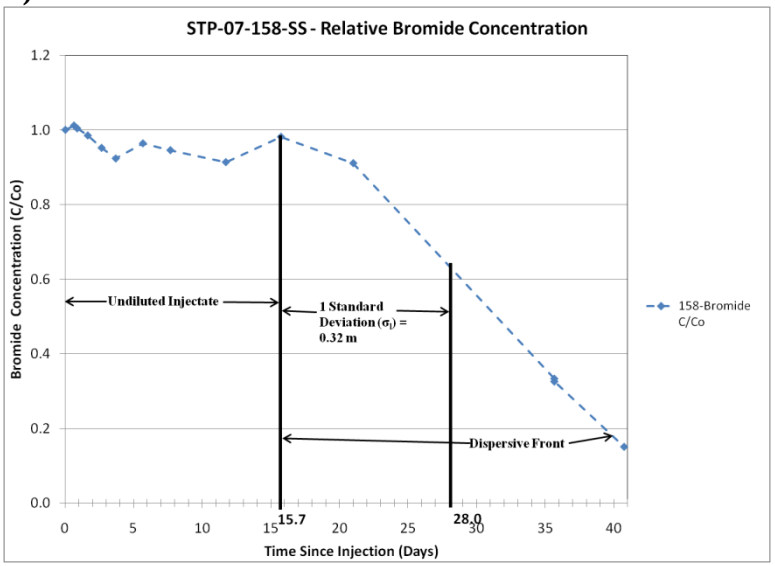


**b) STP-07-159-SS Relative Bromide Concentrations**

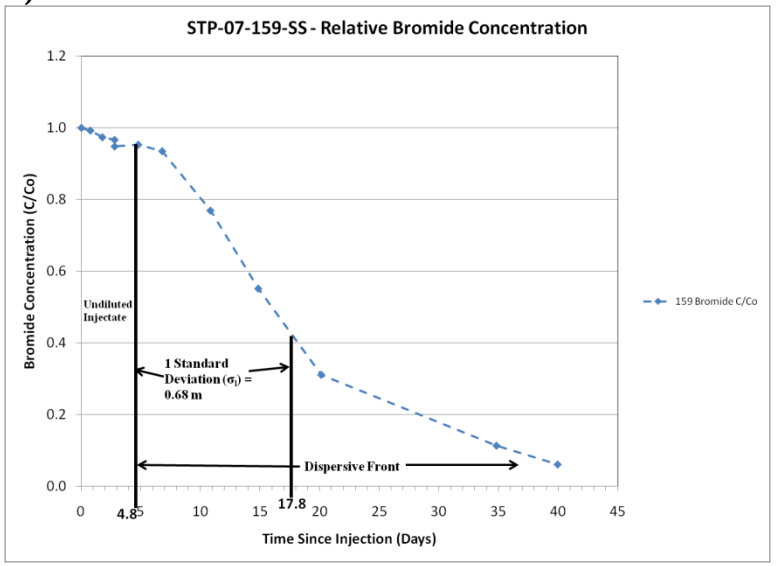


**c) STP-07-158-SS Relative Chloride Concentrations**

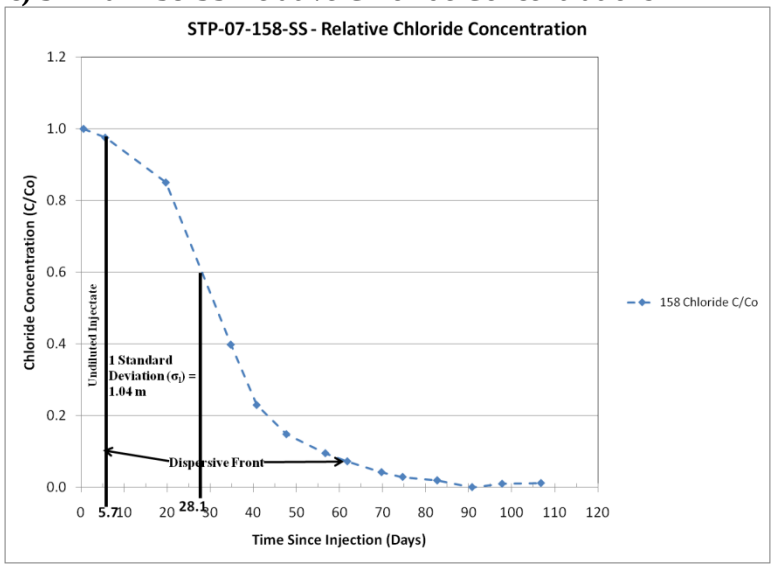


**d) STP-07-159-SS Relative Chloride Concentrations**

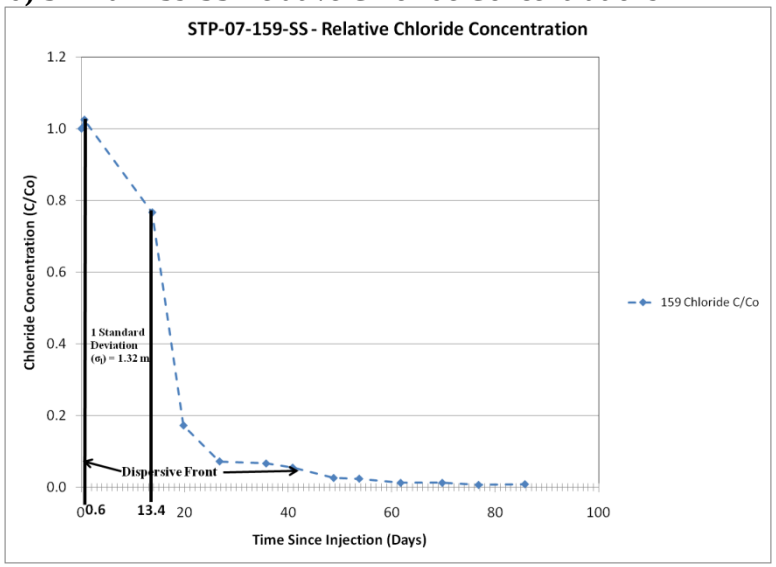


**Figure 4-14: Relative concentrations (C/Co) of conservative tracers following injections at the ISATF with distribution of undiluted injectate, 1 standard deviation, and the dispersive front highlighted. These values were used in calculating hydrodynamic dispersion coefficients and longitudinal dispersivities using: (a) bromide concentrations at STP-07-158-SS following the preliminary injection; (b) bromide concentrations at STP-07-159-SS following the preliminary injection; (c) chloride concentrations at STP-07-158-SS following the PA water injection; and (d) chloride concentrations at STP-07-159-SS following the PA water injection.**

**a) STP-07-158-SS - Preliminary Injection**

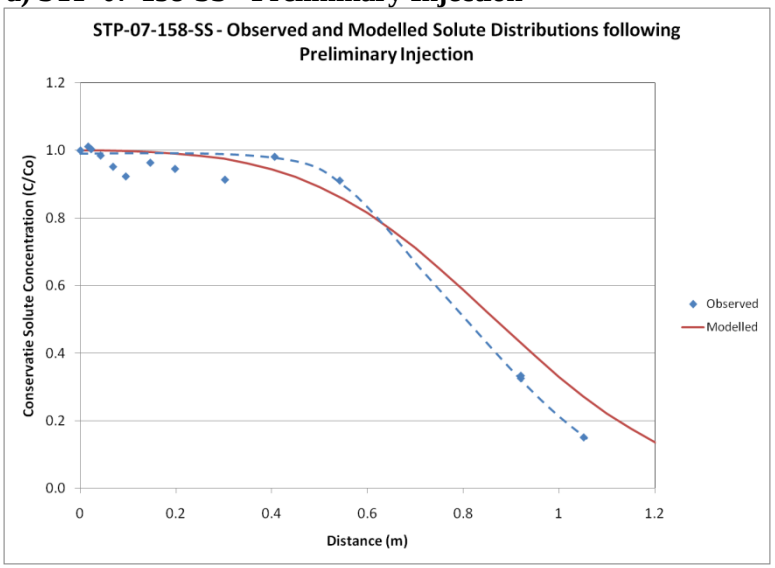


**b) STP-07-159-SS – Preliminary Injection**

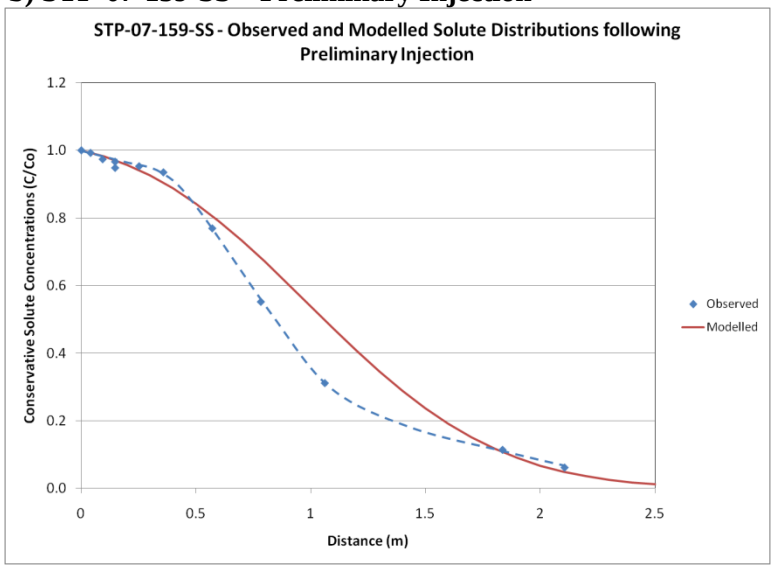


**c) STP-07-158-SS – PA Water Injection**

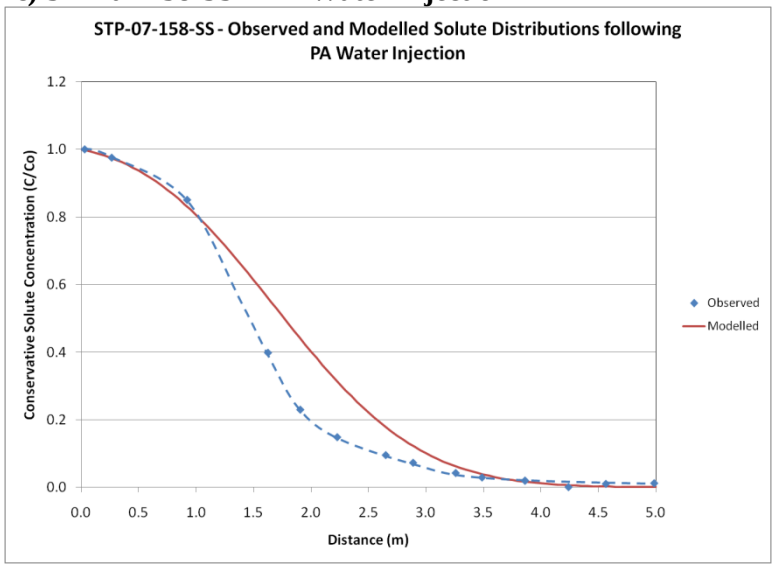


**d) STP-07-159-SS – PA Water Injection**

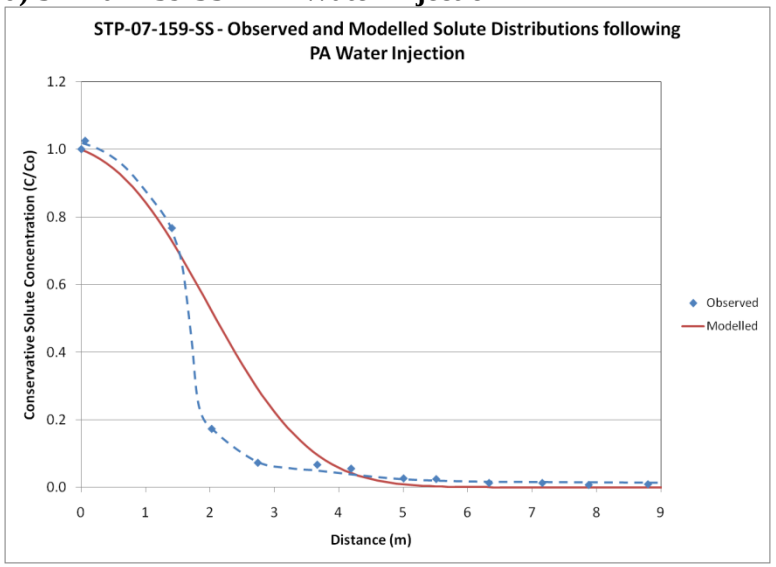


**Figure 4-15: Comparison of observed and modelled conservative solute breakthrough curves following injections showing: (a) STP-07-158-SS breakthrough curves following the preliminary injection; (b) STP-07-159-SS breakthrough curves following the preliminary injection; (c) STP-07-158-SS breakthrough curves following the PA water injection; and (d) STP-07-159-SS breakthrough curves following the PA water injection.**

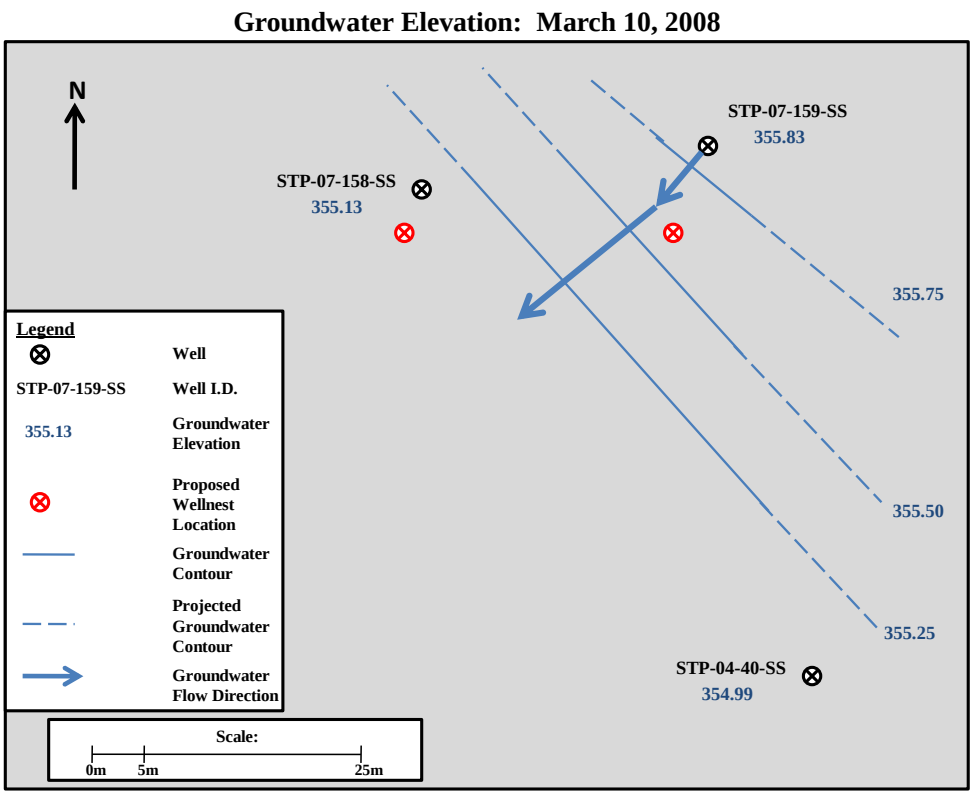


**Figure 4-16: Potentiometric surface map plotted from groundwater elevations measured March 10, 2008.**

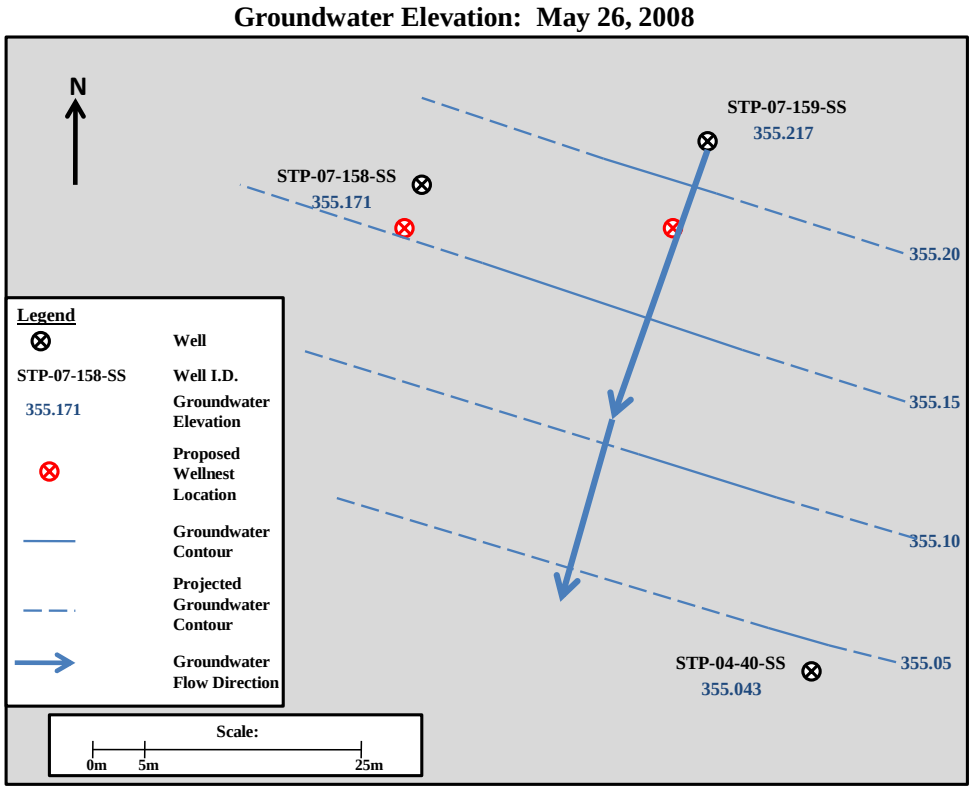


**Figure 4-17: Potentiometric surface map plotted from groundwater elevations measured May 26, 2008.**

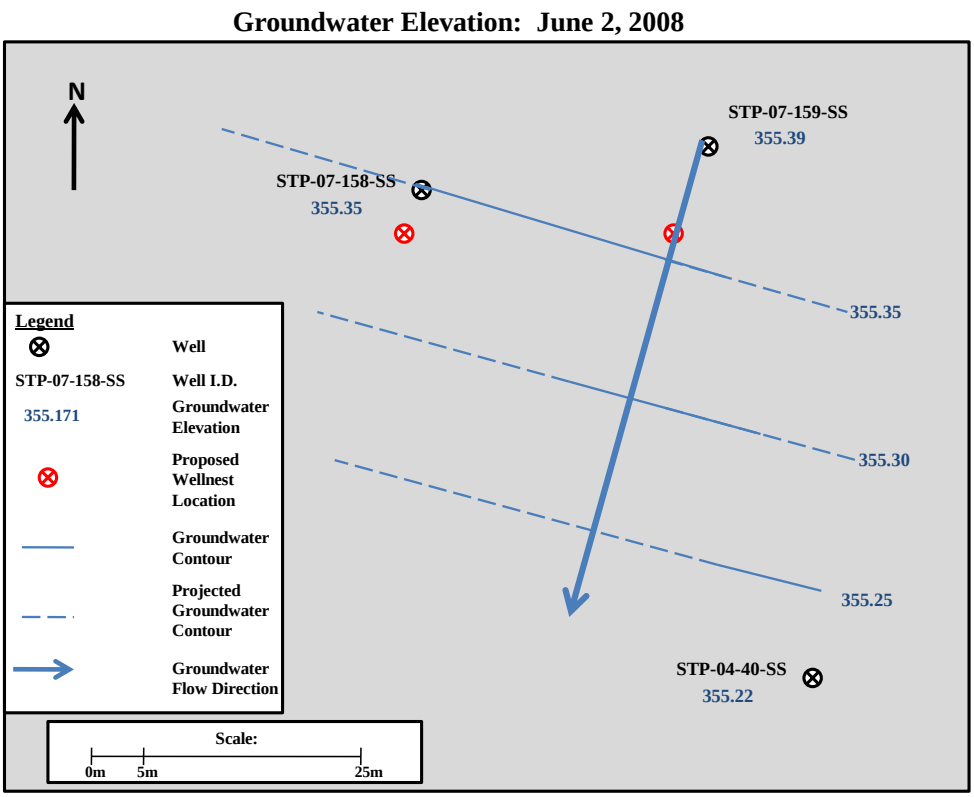


**Figure 4-18: Potentiometric surface map plotted from groundwater elevations measured June 2, 2008.**

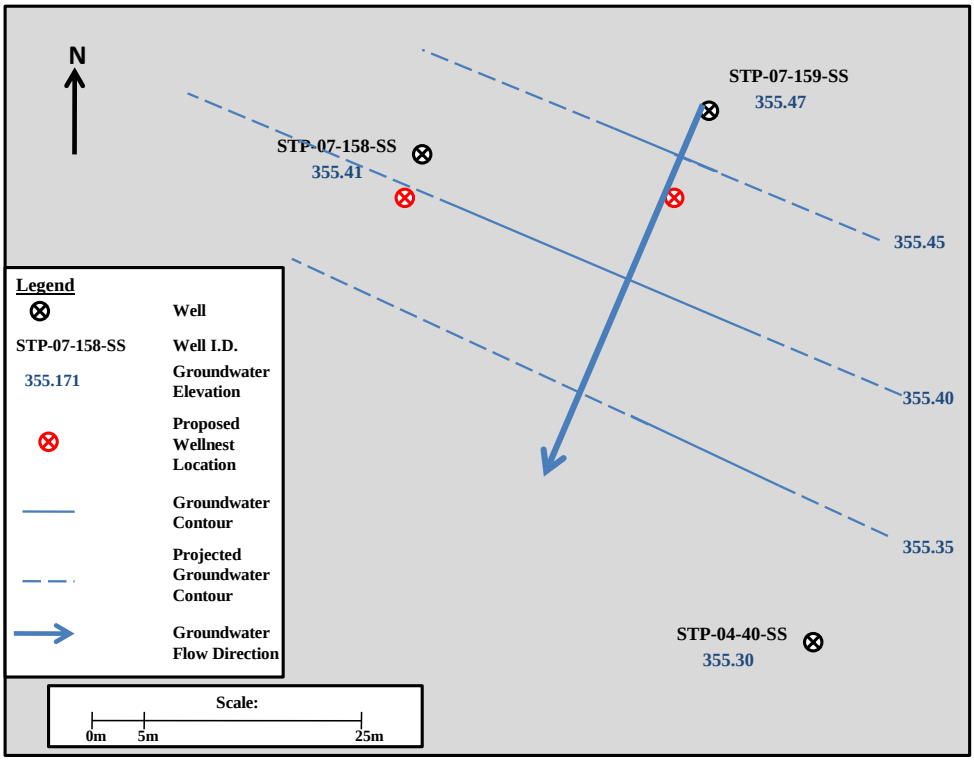


**Figure 4-19: Potentiometric surface map plotted from groundwater elevations measured June 3, 2008.**

**Groundwater Elevation: July 15, 2008**

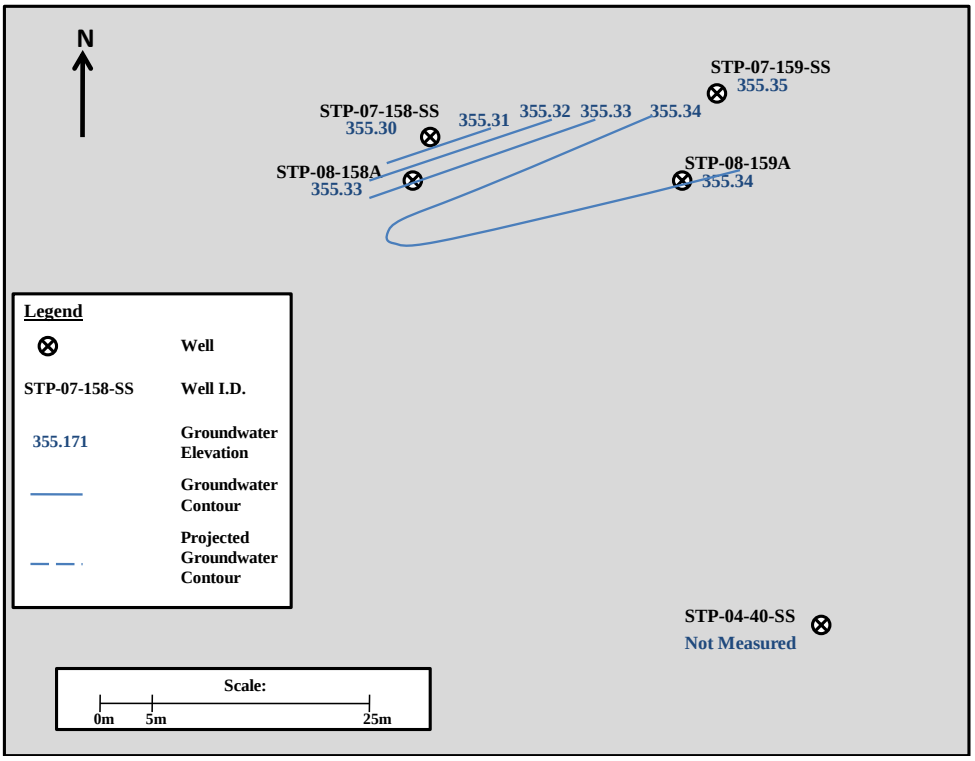


**Figure 4-20: Potentiometric surface map plotted from groundwater elevations measured July 15, 2008.**

**Groundwater Elevation: August 21, 2008**

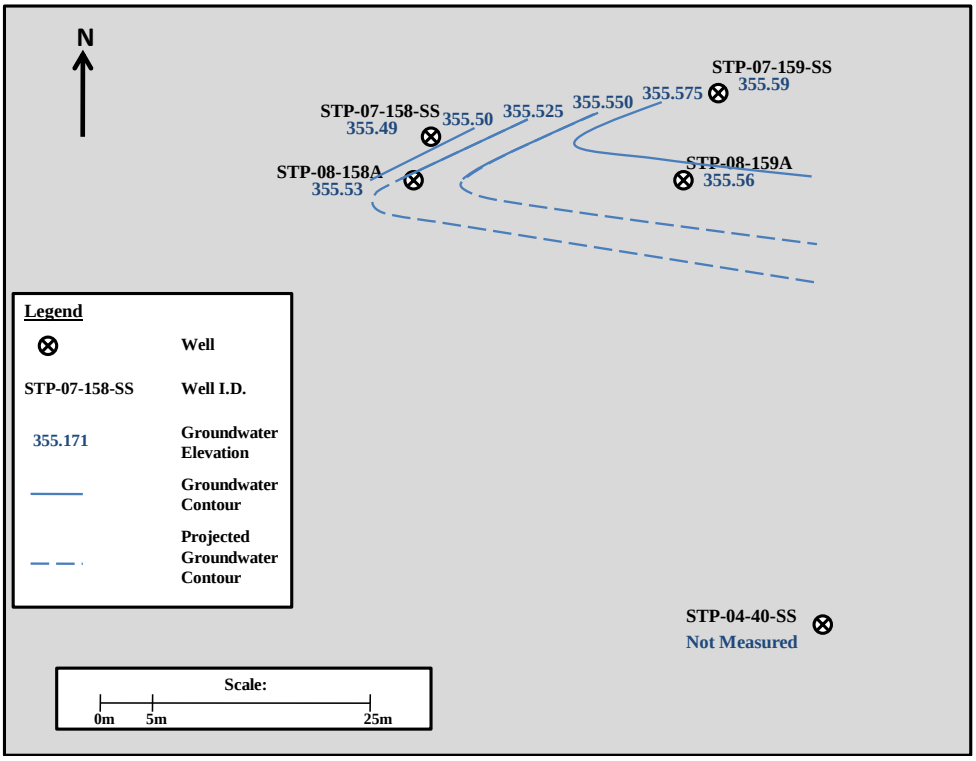


**Figure 4-21: Potentiometric surface map plotted from groundwater elevations measured August 21, 2008.**

**Groundwater Elevation: September 17, 2008**

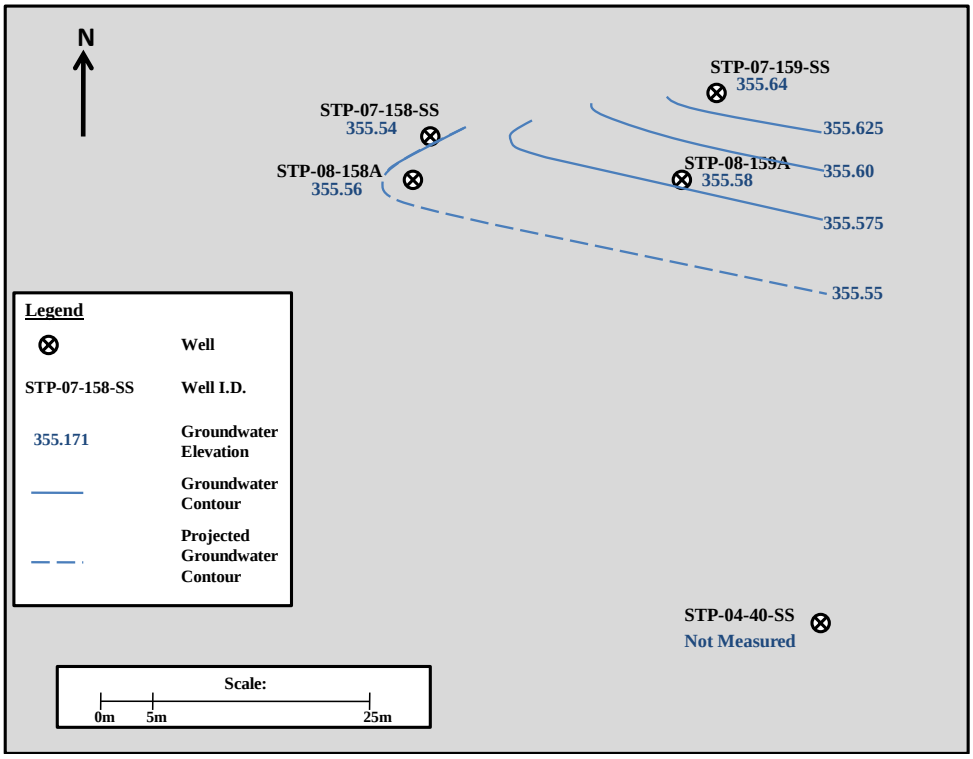


**Figure 4-22: Potentiometric surface map plotted from groundwater elevations measured September 17, 2008.**

**Groundwater Elevation: October 16, 2008**

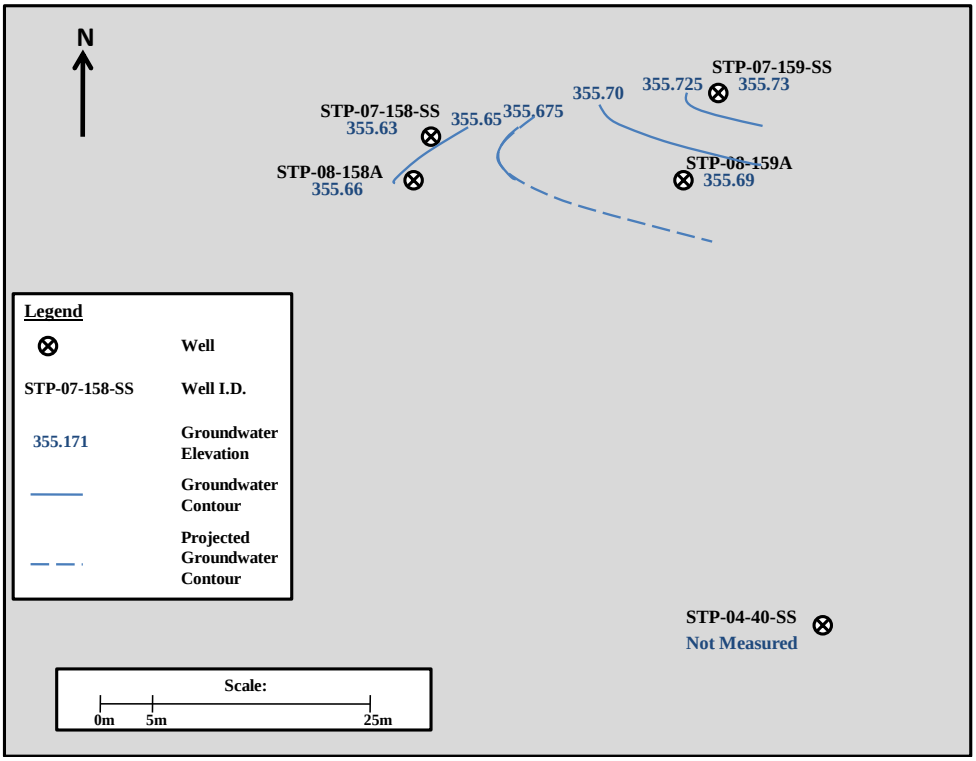


**Figure 4-23: Potentiometric surface map plotted from groundwater elevations measured October 16, 2008.**

**Groundwater Elevation: November 15, 2008**

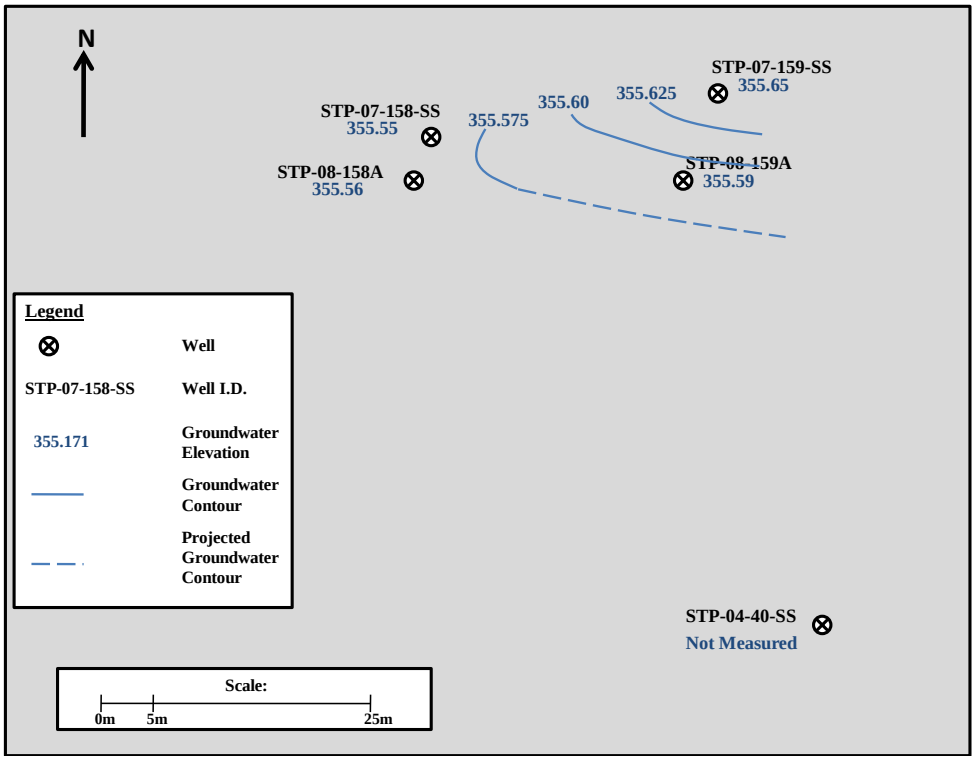


**Figure 4-24: Potentiometric surface map plotted from groundwater elevations measured November 15, 2008.**

**Groundwater Elevation: January 17, 2009**

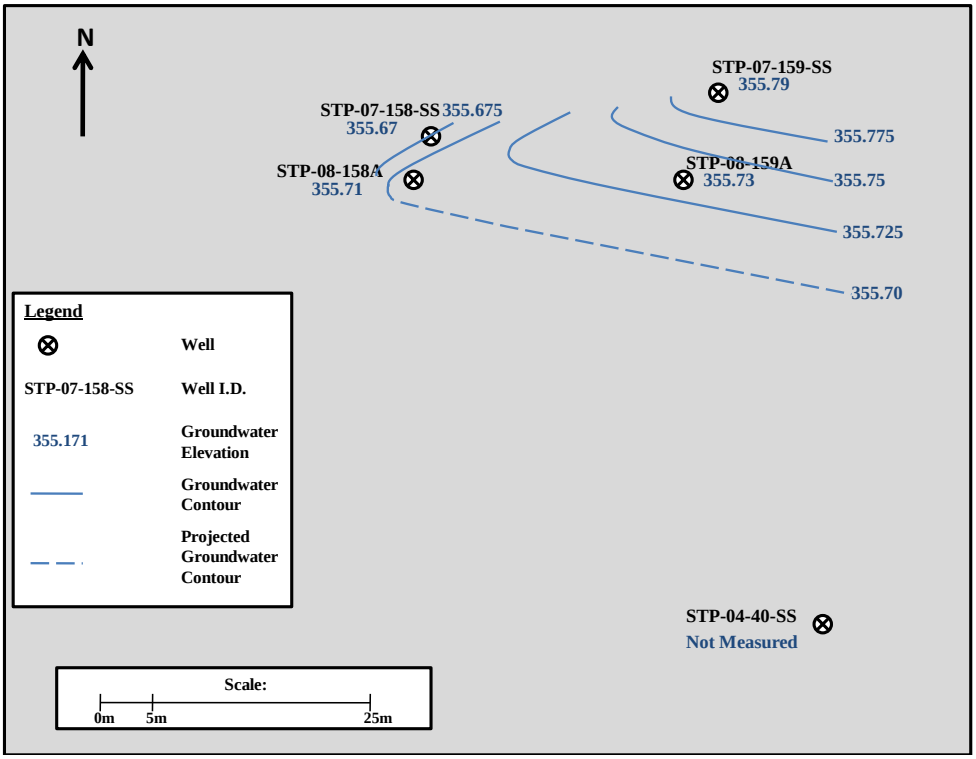


**Figure 4-25: Potentiometric surface map plotted from groundwater elevations measured January 17, 2009.**

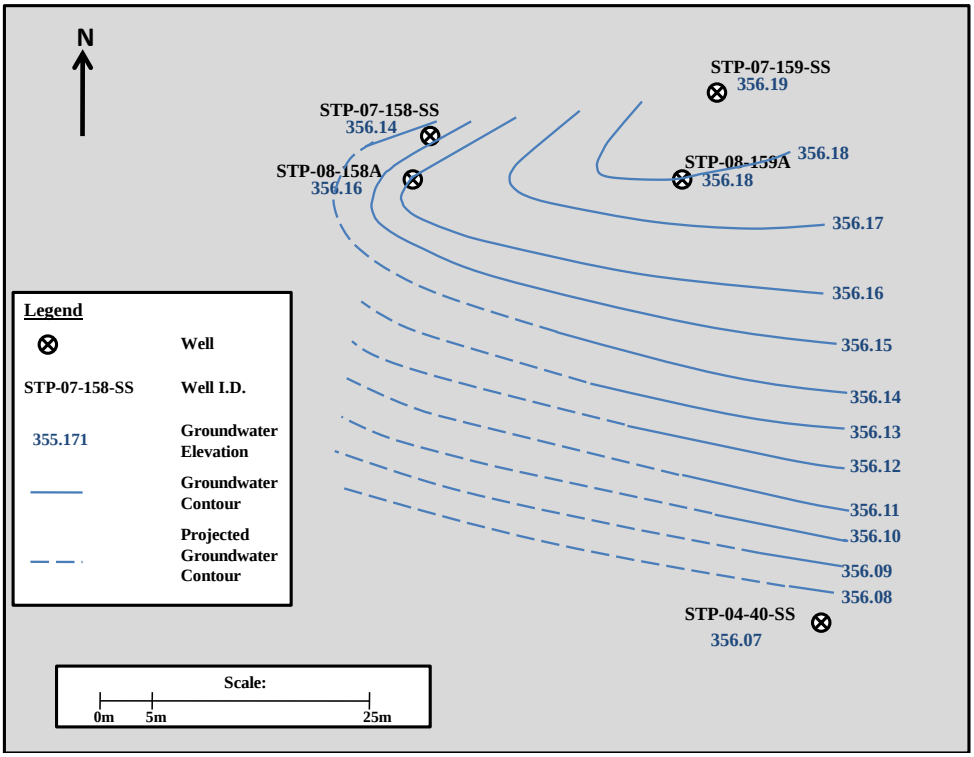


**Figure 4-26: Potentiometric surface map plotted from groundwater elevations measured June 24, 2009.**

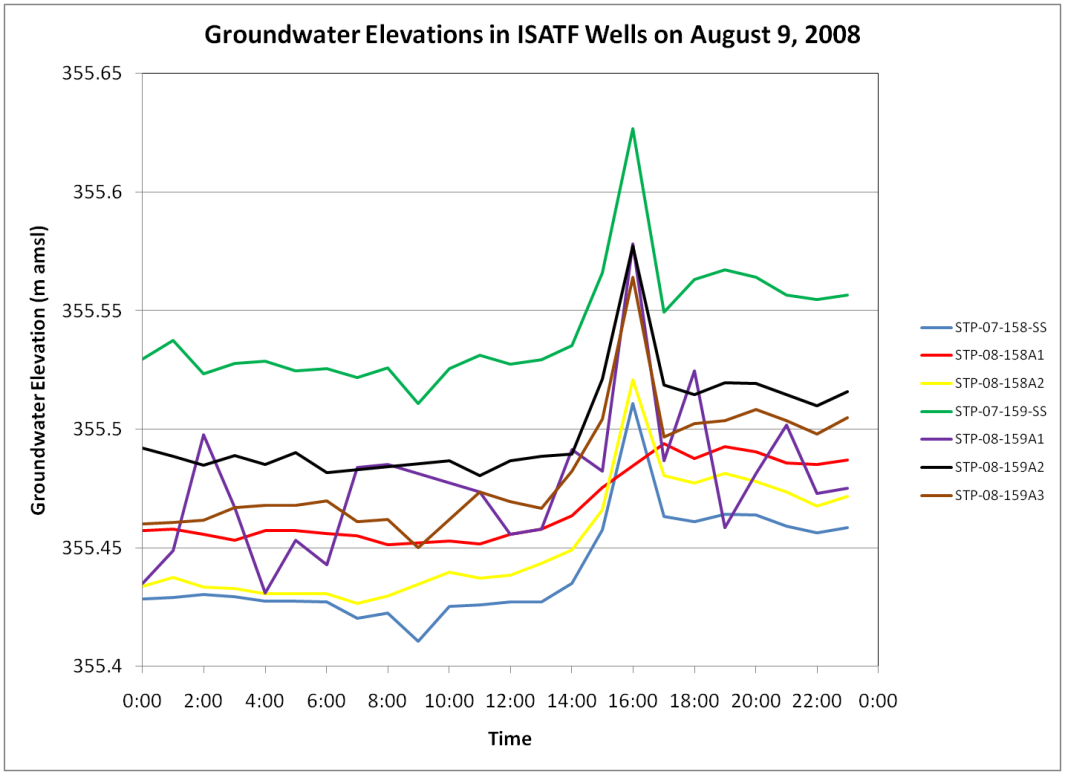


**Figure 4-27: Groundwater elevation in ISATF wells on August 9, 2008 showing a sharp increase in elevation at 16:00 in response to an injection stressor approximately 100 m northeast of the site.**

**a) STP-08-158A Well Cluster**

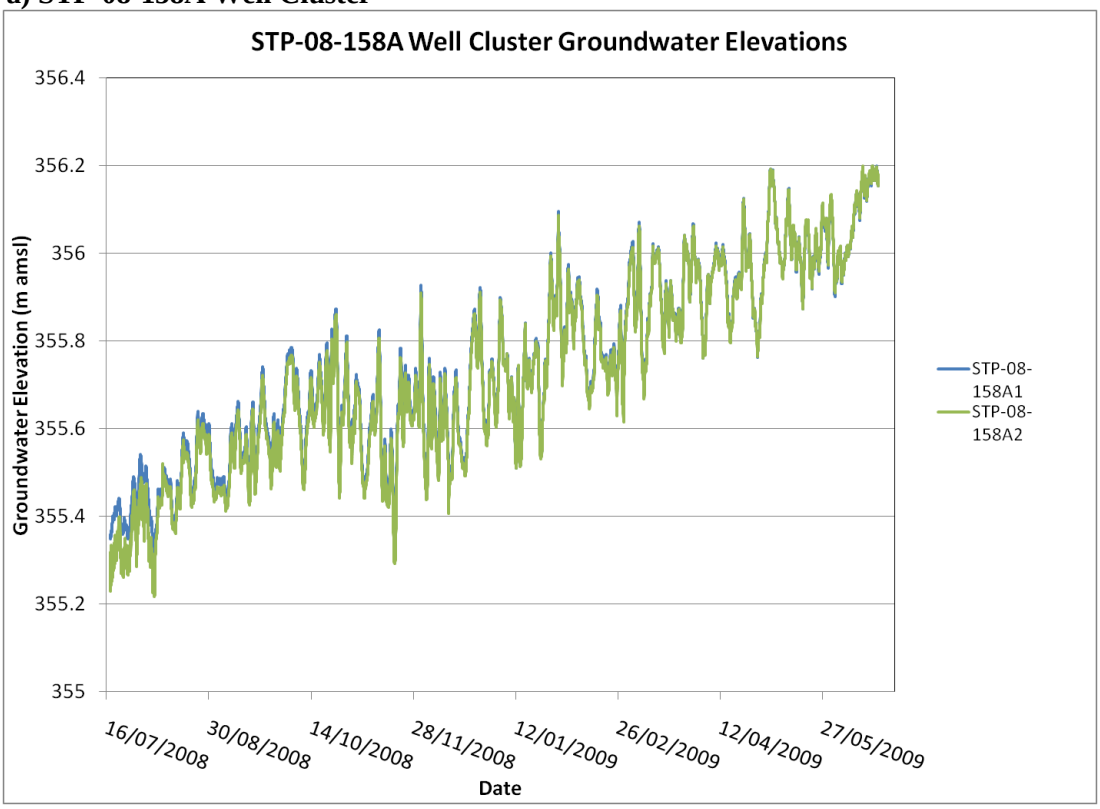


**b) STP-08-159A Well Cluster**

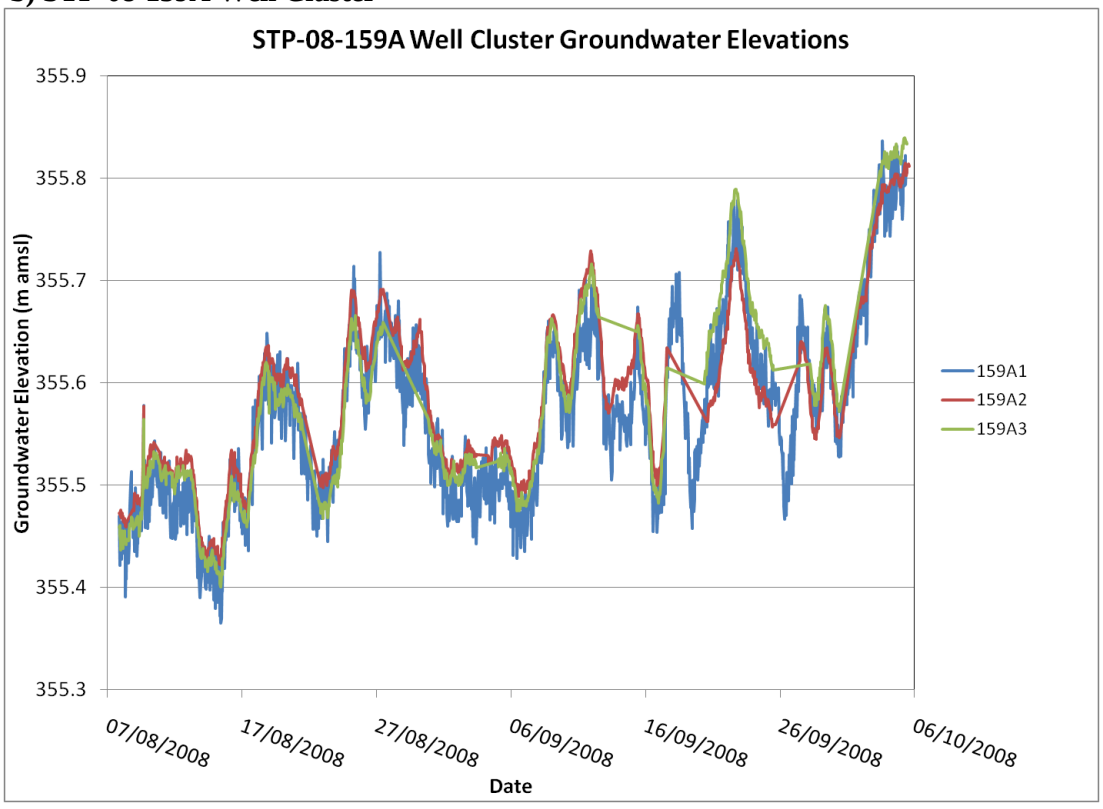


**Figure 4-28: Groundwater elevation trends as recorded by CTD Divers at: (a) STP-08-158A well cluster from July 17, 2008-June 20, 2009 and; (b) STP-08-159A well cluster from August 7-October 5, 2008.**

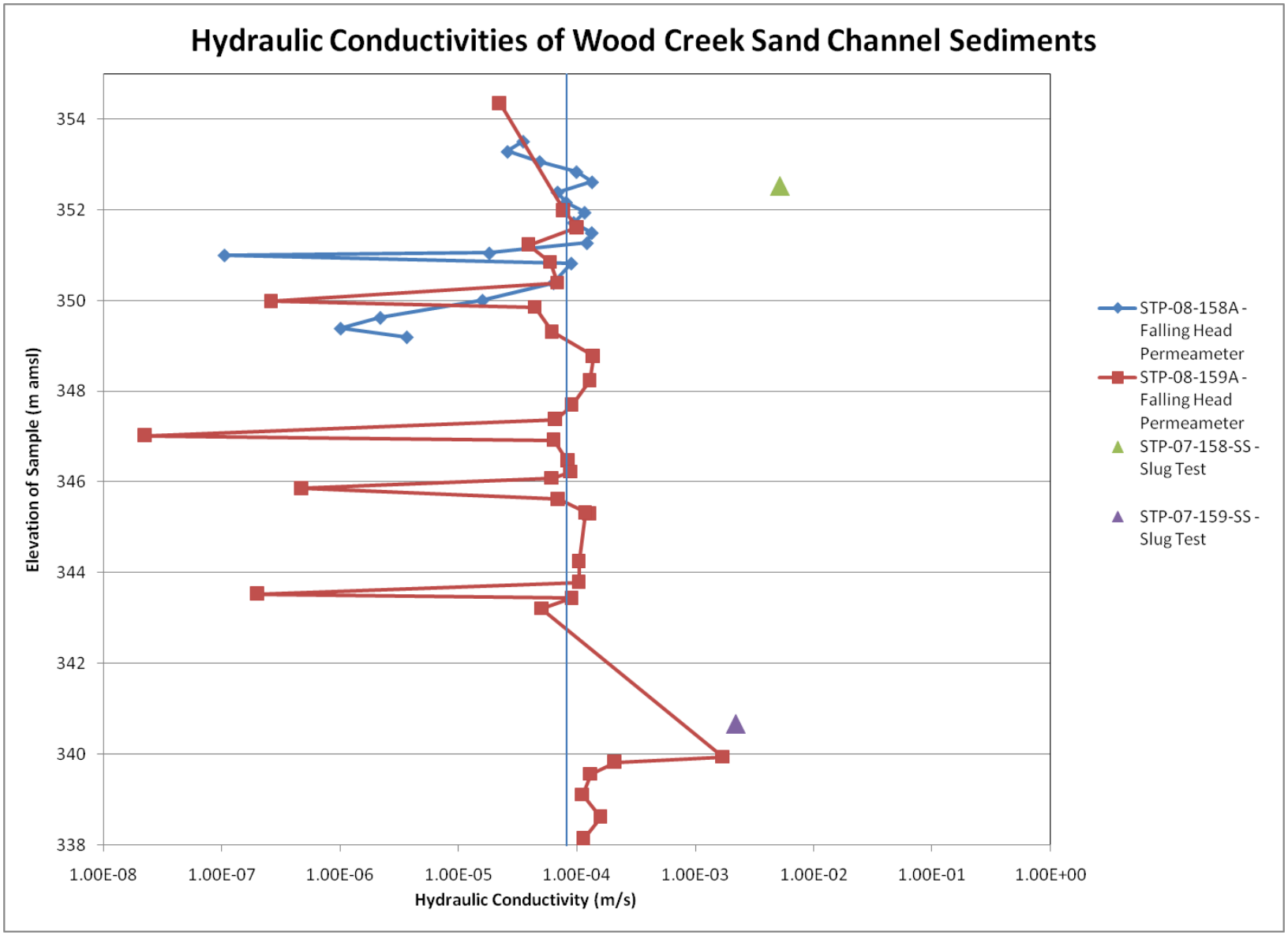


**Figure 4-29: Hydraulic conductivity profile for sediments from the Wood Creek Sand Channel as tested with a falling head permeameter (Soil Borings STP-08-158A and STP-08-159A) and via slug tests (Wells STP-07-158-SS and STP-07-159-SS).**

**a) STP-07-158-SS**

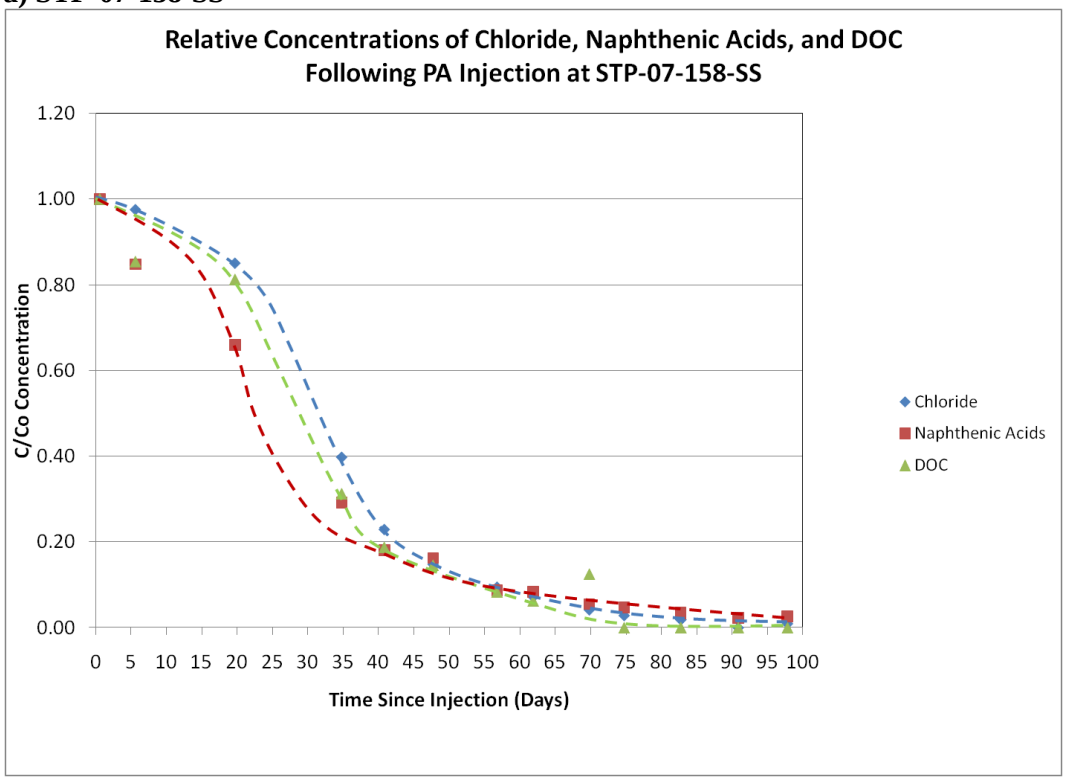


**b) STP-07-159-SS**

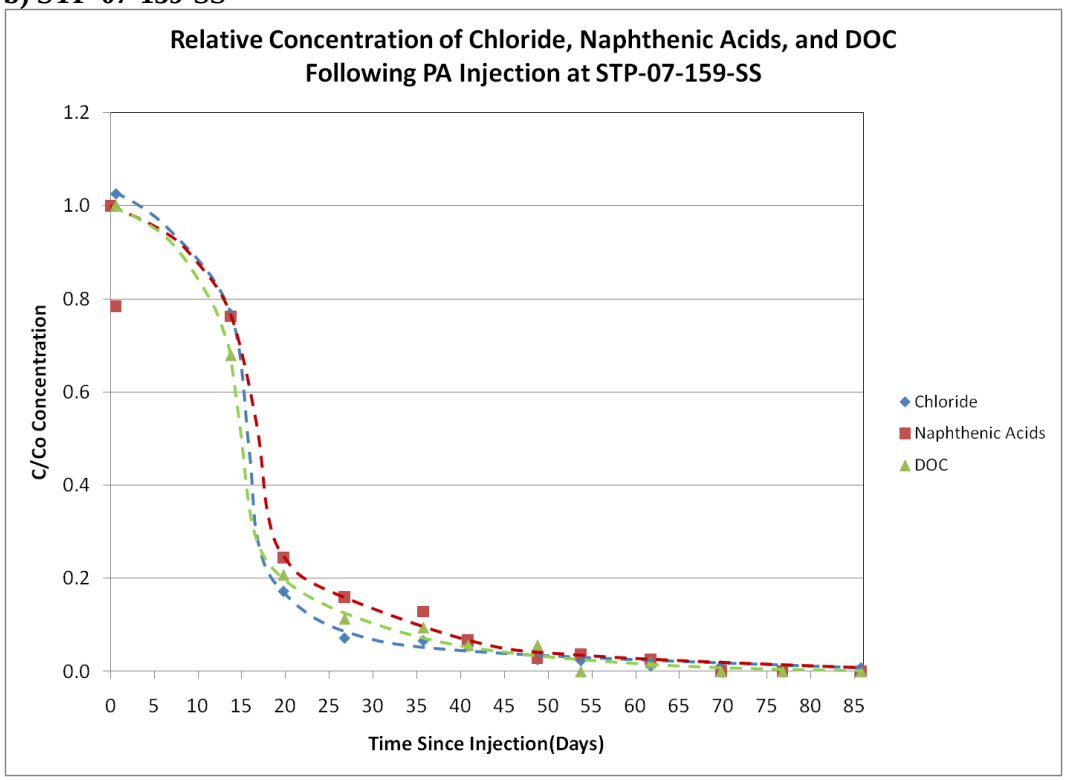


**Figure 4-30: Relative concentrations of chloride, naphthenic acids and DOC following PA water injections at: (a) STP-07-158-SS and; (b) STP-07-159-SS.**

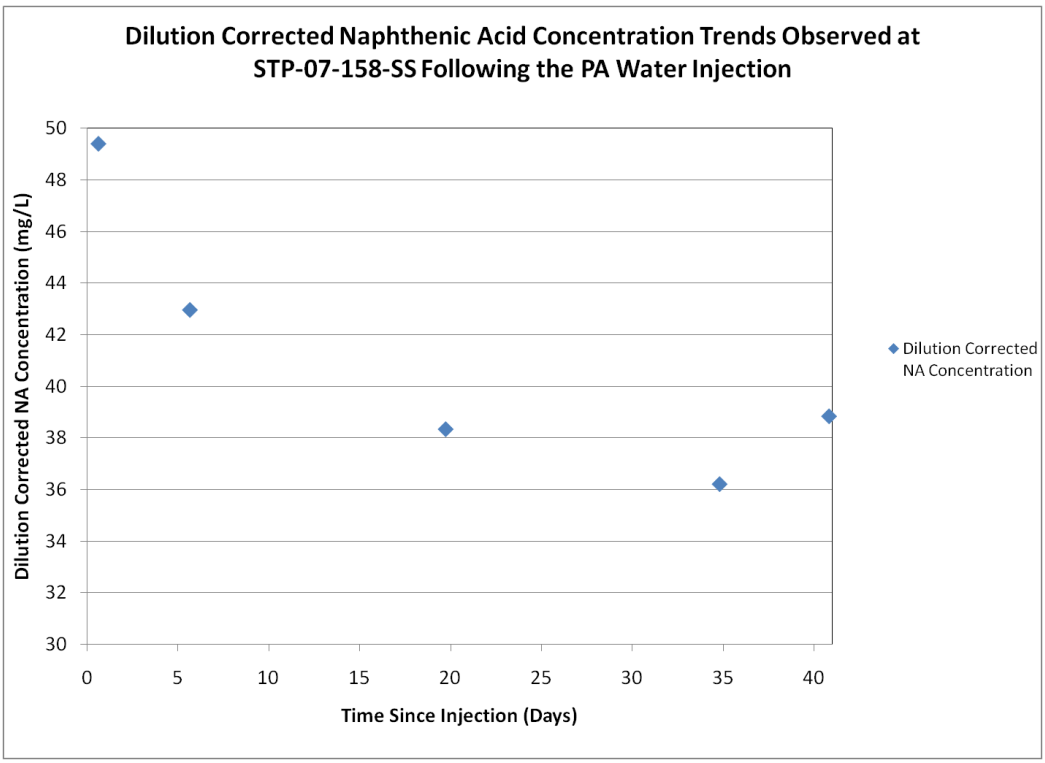


**Figure 4-31: Dilution corrected naphthenic acid concentrations {(naphthenic acids mg/L)/(Cl/Cl$_0$)} at STP-07-158-SS from July 18 – August 27, 2008.**

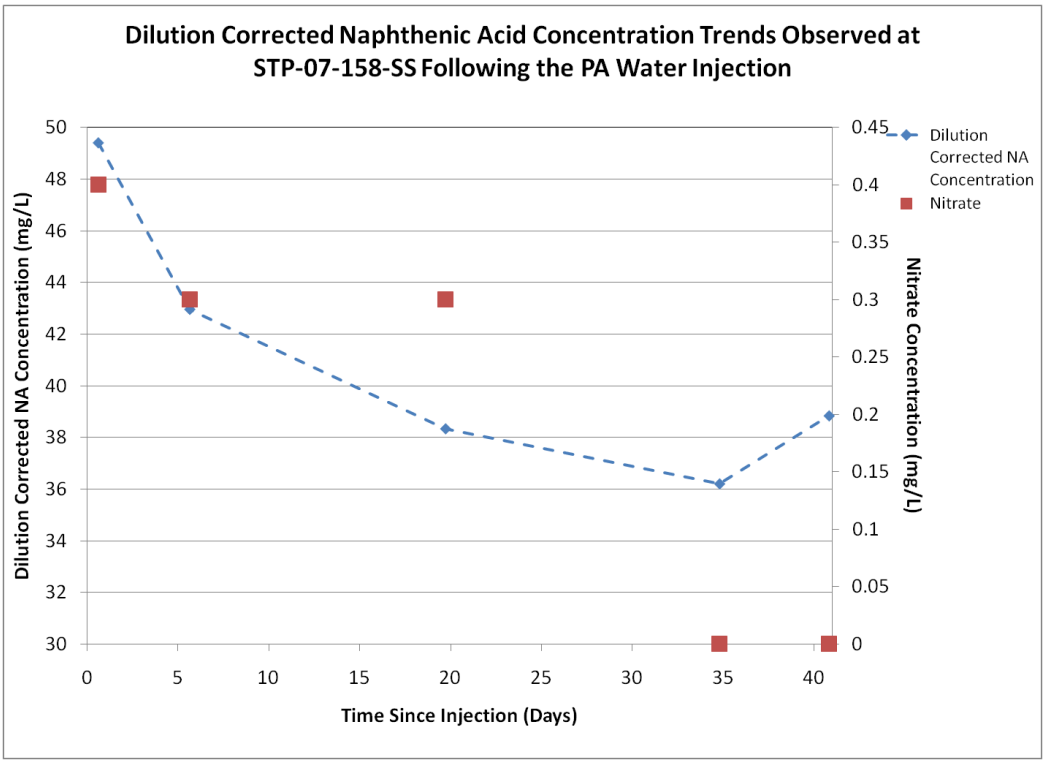


**Figure 4-32: Dilution corrected naphthenic acid concentrations and nitrate concentrations observed at STP-07-158-SS following the PA water injections. Figure illustrates the potential dependence of reaction of NAs on the availability of nitrate.**

**a) Matrix Presentation of GC-MS Data**

| STP07158-GW16 41.9mg/L NA July 23, 2008 | | | | | | | | |
|---|---|---|---|---|---|---|---|---|
| C number | z number | | | | | | | |
| | 0 | 2 | 4 | 6 | 8 | 10 | 12 | % carbon no |
| 5 | 2 | 0 | 0 | 0 | 0 | 0 | 0 | 2 |
| 6 | 2 | 0 | 0 | 0 | 0 | 0 | 0 | 2 |
| 7 | 1 | 1 | 0 | 0 | 0 | 0 | 0 | 3 |
| 8 | 1 | 1 | 0 | 0 | 0 | 0 | 0 | 2 |
| 9 | 1 | 2 | 0 | 0 | 0 | 0 | 0 | 3 |
| 10 | 1 | 1 | 1 | 0 | 0 | 0 | 0 | 3 |
| 11 | 1 | 1 | 1 | 0 | 0 | 0 | 0 | 2 |
| 12 | 1 | 1 | 2 | 1 | 0 | 0 | 0 | 5 |
| 13 | 0 | 1 | 3 | 3 | 0 | 0 | 0 | 8 |
| 14 | 1 | 1 | 3 | 4 | 1 | 0 | 0 | 10 |
| 15 | 1 | 1 | 2 | 3 | 2 | 0 | 0 | 8 |
| 16 | 1 | 1 | 1 | 2 | 1 | 1 | 0 | 7 |
| 17 | 1 | 1 | 1 | 1 | 1 | 1 | 0 | 6 |
| 18 | 1 | 1 | 1 | 1 | 1 | 1 | 1 | 6 |
| 19 | 1 | 0 | 1 | 1 | 1 | 1 | 1 | 4 |
| 20 | 1 | 1 | 0 | 0 | 0 | 0 | 1 | 3 |
| 21 | 1 | 1 | 0 | 0 | 0 | 0 | 0 | 3 |
| 22 | 1 | 0 | 0 | 0 | 0 | 0 | 0 | 3 |
| 23 | 1 | 0 | 0 | 0 | 0 | 0 | 0 | 3 |
| 24 | 0 | 1 | 0 | 0 | 0 | 0 | 1 | 3 |
| 25 | 1 | 1 | 0 | 0 | 0 | 0 | 1 | 4 |
| 26 | 1 | 0 | 0 | 0 | 0 | 0 | 0 | 2 |
| 27 | 0 | 0 | 0 | 0 | 0 | 0 | 0 | 2 |
| 28 | 0 | 0 | 0 | 0 | 0 | 0 | 0 | 2 |
| 29 | 0 | 0 | 0 | 0 | 0 | 0 | 0 | 1 |
| 30 | 0 | 0 | 0 | 0 | 0 | 0 | 0 | 1 |
| 31 | 0 | 0 | 0 | 0 | 0 | 0 | 0 | 1 |
| 32 | 0 | 0 | 0 | 0 | 0 | 0 | 0 | 1 |
| 33 | 0 | 0 | 0 | 0 | 0 | 0 | 0 | 1 |
| % by z No | 21 | 16 | 20 | 20 | 9 | 7 | 7 | 100 |

**b) Three-Dimensional Plot of STP07158-GW16 GC-MS Data**

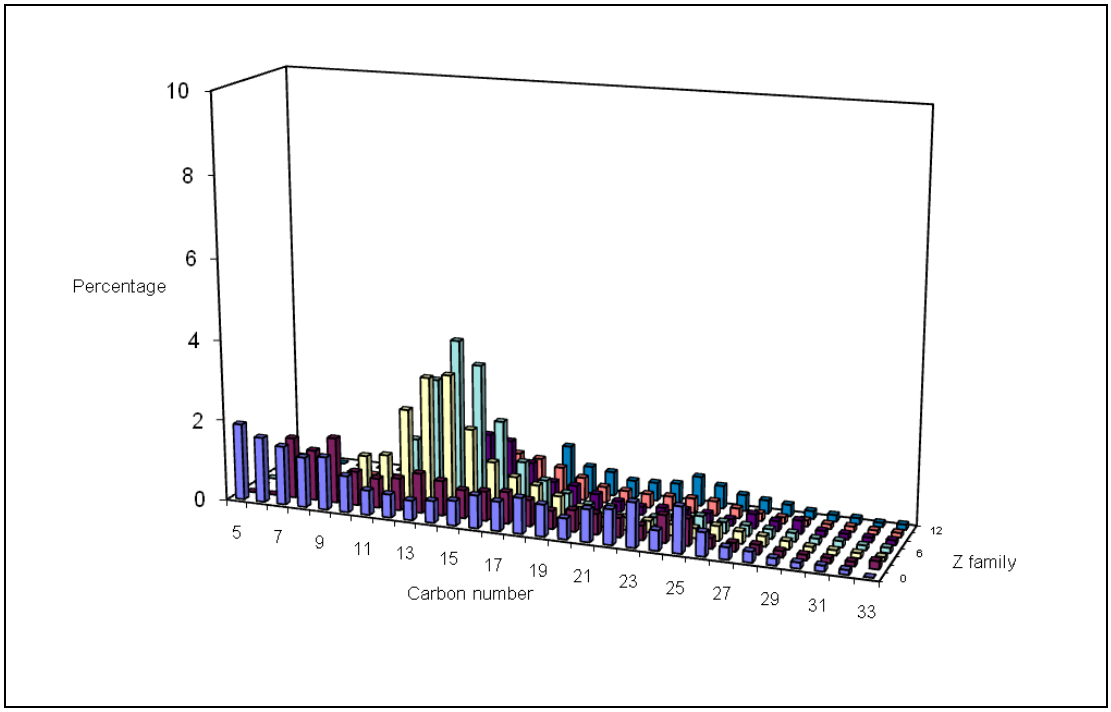


**Figure 4-33: Common methods used to present naphthenic acid data derived from gas chromatography – electron impact mass spectrometry analysis including: (a) matrix listing the relative proportion of a sample's isomer classes and; (b) three-dimensional bar graph showing the relative proportion of each isomer class.**

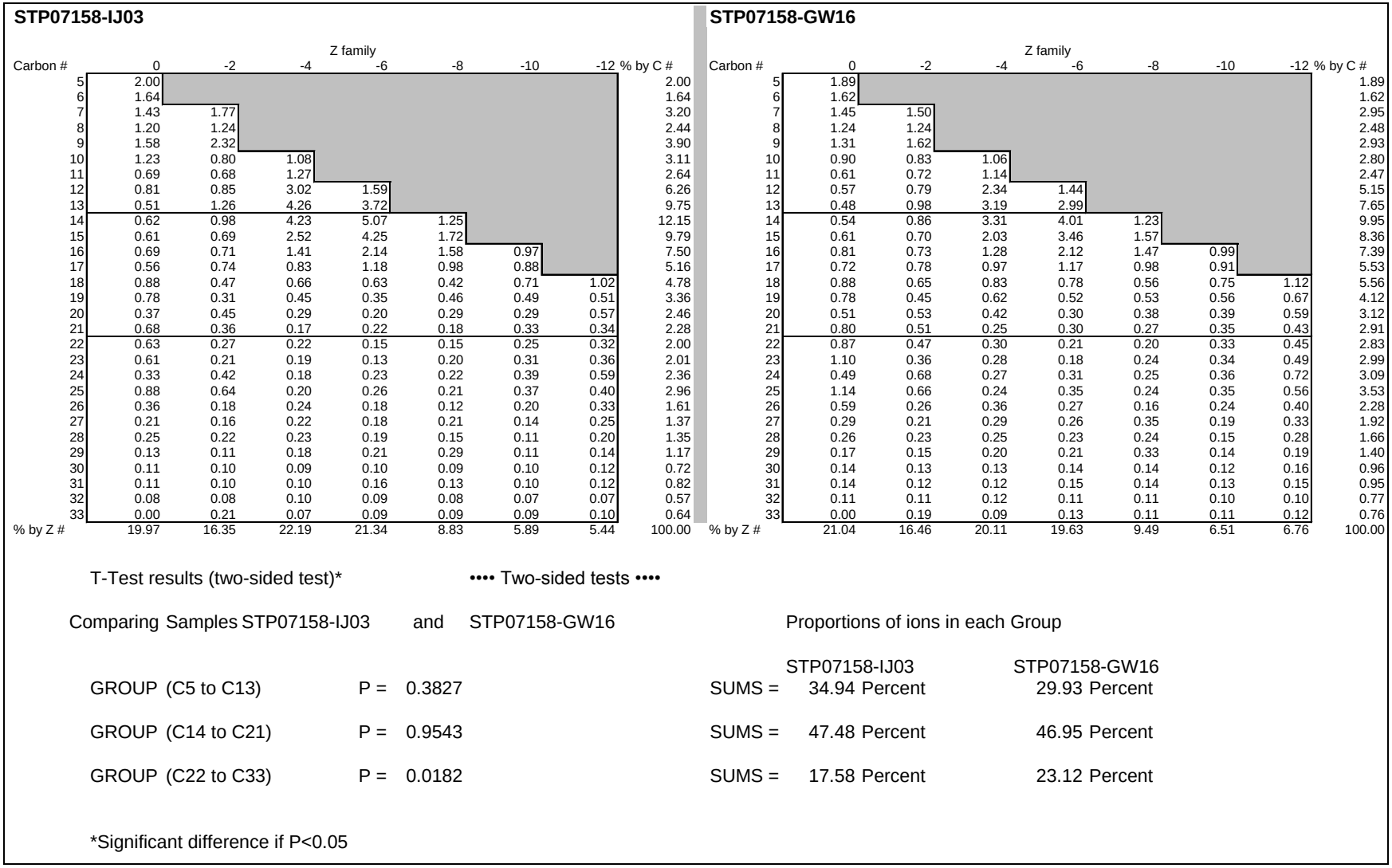

**STP07158-IJ03**

| Carbon # | Z family 0 | -2 | -4 | -6 | -8 | -10 | -12 | % by C # |
|---|---|---|---|---|---|---|---|---|
| 5 | 2.00 | | | | | | | 2.00 |
| 6 | 1.64 | | | | | | | 1.64 |
| 7 | 1.43 | 1.77 | | | | | | 3.20 |
| 8 | 1.20 | 1.24 | | | | | | 2.44 |
| 9 | 1.58 | 2.32 | | | | | | 3.90 |
| 10 | 1.23 | 0.80 | 1.08 | | | | | 3.11 |
| 11 | 0.69 | 0.68 | 1.27 | | | | | 2.64 |
| 12 | 0.81 | 0.85 | 3.02 | 1.59 | | | | 6.26 |
| 13 | 0.51 | 1.26 | 4.26 | 3.72 | | | | 9.75 |
| 14 | 0.62 | 0.98 | 4.23 | 5.07 | 1.25 | | | 12.15 |
| 15 | 0.61 | 0.69 | 2.52 | 4.25 | 1.72 | | | 9.79 |
| 16 | 0.69 | 0.71 | 1.41 | 2.14 | 1.58 | 0.97 | | 7.50 |
| 17 | 0.56 | 0.74 | 0.83 | 1.18 | 0.98 | 0.88 | | 5.16 |
| 18 | 0.88 | 0.47 | 0.66 | 0.63 | 0.42 | 0.71 | 1.02 | 4.78 |
| 19 | 0.78 | 0.31 | 0.45 | 0.35 | 0.46 | 0.49 | 0.51 | 3.36 |
| 20 | 0.37 | 0.45 | 0.29 | 0.20 | 0.29 | 0.29 | 0.57 | 2.46 |
| 21 | 0.68 | 0.36 | 0.17 | 0.22 | 0.18 | 0.33 | 0.34 | 2.28 |
| 22 | 0.63 | 0.27 | 0.22 | 0.15 | 0.15 | 0.25 | 0.32 | 2.00 |
| 23 | 0.61 | 0.21 | 0.19 | 0.13 | 0.20 | 0.31 | 0.36 | 2.01 |
| 24 | 0.33 | 0.42 | 0.18 | 0.23 | 0.22 | 0.39 | 0.59 | 2.36 |
| 25 | 0.88 | 0.64 | 0.20 | 0.26 | 0.21 | 0.37 | 0.40 | 2.96 |
| 26 | 0.36 | 0.18 | 0.24 | 0.18 | 0.12 | 0.20 | 0.33 | 1.61 |
| 27 | 0.21 | 0.16 | 0.22 | 0.18 | 0.21 | 0.14 | 0.25 | 1.37 |
| 28 | 0.25 | 0.22 | 0.23 | 0.19 | 0.15 | 0.11 | 0.20 | 1.35 |
| 29 | 0.13 | 0.11 | 0.18 | 0.21 | 0.29 | 0.11 | 0.14 | 1.17 |
| 30 | 0.11 | 0.10 | 0.09 | 0.10 | 0.09 | 0.10 | 0.12 | 0.72 |
| 31 | 0.11 | 0.10 | 0.10 | 0.16 | 0.13 | 0.10 | 0.12 | 0.82 |
| 32 | 0.08 | 0.08 | 0.10 | 0.09 | 0.08 | 0.07 | 0.07 | 0.57 |
| 33 | 0.00 | 0.21 | 0.07 | 0.09 | 0.09 | 0.09 | 0.10 | 0.64 |
| % by Z # | 19.97 | 16.35 | 22.19 | 21.34 | 8.83 | 5.89 | 5.44 | 100.00 |

**STP07158-GW16**

| Carbon # | Z family 0 | -2 | -4 | -6 | -8 | -10 | -12 | % by C # |
|---|---|---|---|---|---|---|---|---|
| 5 | 1.89 | | | | | | | 1.89 |
| 6 | 1.62 | | | | | | | 1.62 |
| 7 | 1.45 | 1.50 | | | | | | 2.95 |
| 8 | 1.24 | 1.24 | | | | | | 2.48 |
| 9 | 1.31 | 1.62 | | | | | | 2.93 |
| 10 | 0.90 | 0.83 | 1.06 | | | | | 2.80 |
| 11 | 0.61 | 0.72 | 1.14 | | | | | 2.47 |
| 12 | 0.57 | 0.79 | 2.34 | 1.44 | | | | 5.15 |
| 13 | 0.48 | 0.98 | 3.19 | 2.99 | | | | 7.65 |
| 14 | 0.54 | 0.86 | 3.31 | 4.01 | 1.23 | | | 9.95 |
| 15 | 0.61 | 0.70 | 2.03 | 3.46 | 1.57 | | | 8.36 |
| 16 | 0.81 | 0.73 | 1.28 | 2.12 | 1.47 | 0.99 | | 7.39 |
| 17 | 0.72 | 0.78 | 0.97 | 1.17 | 0.98 | 0.91 | | 5.53 |
| 18 | 0.88 | 0.65 | 0.83 | 0.78 | 0.56 | 0.75 | 1.12 | 5.56 |
| 19 | 0.78 | 0.45 | 0.62 | 0.52 | 0.53 | 0.56 | 0.67 | 4.12 |
| 20 | 0.51 | 0.53 | 0.42 | 0.30 | 0.38 | 0.39 | 0.59 | 3.12 |
| 21 | 0.80 | 0.51 | 0.25 | 0.30 | 0.27 | 0.35 | 0.43 | 2.91 |
| 22 | 0.87 | 0.47 | 0.30 | 0.21 | 0.20 | 0.33 | 0.45 | 2.83 |
| 23 | 1.10 | 0.36 | 0.28 | 0.18 | 0.24 | 0.34 | 0.49 | 2.99 |
| 24 | 0.49 | 0.68 | 0.27 | 0.31 | 0.25 | 0.36 | 0.72 | 3.09 |
| 25 | 1.14 | 0.66 | 0.24 | 0.35 | 0.24 | 0.35 | 0.56 | 3.53 |
| 26 | 0.59 | 0.26 | 0.36 | 0.27 | 0.16 | 0.24 | 0.40 | 2.28 |
| 27 | 0.29 | 0.21 | 0.29 | 0.26 | 0.35 | 0.19 | 0.33 | 1.92 |
| 28 | 0.26 | 0.23 | 0.25 | 0.23 | 0.24 | 0.15 | 0.28 | 1.66 |
| 29 | 0.17 | 0.15 | 0.20 | 0.21 | 0.33 | 0.14 | 0.19 | 1.40 |
| 30 | 0.14 | 0.13 | 0.13 | 0.14 | 0.14 | 0.12 | 0.16 | 0.96 |
| 31 | 0.14 | 0.12 | 0.12 | 0.15 | 0.14 | 0.13 | 0.15 | 0.95 |
| 32 | 0.11 | 0.11 | 0.12 | 0.11 | 0.11 | 0.10 | 0.10 | 0.77 |
| 33 | 0.00 | 0.19 | 0.09 | 0.13 | 0.11 | 0.11 | 0.12 | 0.76 |
| % by Z # | 21.04 | 16.46 | 20.11 | 19.63 | 9.49 | 6.51 | 6.76 | 100.00 |

T-Test results (two-sided test)* •••• Two-sided tests ••••

Comparing Samples STP07158-IJ03 and STP07158-GW16

| | | | STP07158-IJ03 | STP07158-GW16 |
|---|---|---|---|---|
| | | Proportions of ions in each Group | | |
| GROUP (C5 to C13) | P = 0.3827 | SUMS = | 34.94 Percent | 29.93 Percent |
| GROUP (C14 to C21) | P = 0.9543 | SUMS = | 47.48 Percent | 46.95 Percent |
| GROUP (C22 to C33) | P = 0.0182 | SUMS = | 17.58 Percent | 23.12 Percent |

*Significant difference if P<0.05

**Figure 4-34: T-test plot comparing samples STP07158-IJ03 and STP07158-GW16. The C22 to C33 group shows a significant difference between samples suggesting degradation of the NAs in sample STP07158-GW16.**

**STP07159-IJ11**

| | Z family | | | | | | | |
|---|---|---|---|---|---|---|---|---|
| Carbon # | 0 | -2 | -4 | -6 | -8 | -10 | -12 | % by C # |
| 5 | 2.04 | | | | | | | 2.04 |
| 6 | 1.69 | | | | | | | 1.69 |
| 7 | 1.47 | 1.59 | | | | | | 3.06 |
| 8 | 1.24 | 1.29 | | | | | | 2.53 |
| 9 | 1.03 | 2.54 | | | | | | 3.57 |
| 10 | 0.71 | 0.85 | 1.14 | | | | | 2.70 |
| 11 | 0.56 | 0.71 | 1.41 | | | | | 2.68 |
| 12 | 0.50 | 0.94 | 3.54 | 1.71 | | | | 6.70 |
| 13 | 0.46 | 1.47 | 4.71 | 4.02 | | | | 10.65 |
| 14 | 0.52 | 1.05 | 4.60 | 5.18 | 1.26 | | | 12.61 |
| 15 | 0.56 | 0.67 | 2.51 | 4.14 | 1.68 | | | 9.57 |
| 16 | 0.67 | 0.68 | 1.38 | 2.05 | 1.52 | 0.92 | | 7.22 |
| 17 | 0.53 | 0.79 | 0.76 | 1.12 | 0.92 | 0.71 | | 4.83 |
| 18 | 1.12 | 0.44 | 0.64 | 0.60 | 0.39 | 0.68 | 1.00 | 4.88 |
| 19 | 1.01 | 0.28 | 0.45 | 0.30 | 0.42 | 0.47 | 0.48 | 3.39 |
| 20 | 0.34 | 0.49 | 0.28 | 0.19 | 0.26 | 0.26 | 0.63 | 2.45 |
| 21 | 0.76 | 0.33 | 0.17 | 0.24 | 0.17 | 0.27 | 0.33 | 2.27 |
| 22 | 0.53 | 0.22 | 0.22 | 0.15 | 0.15 | 0.28 | 0.31 | 1.86 |
| 23 | 0.43 | 0.18 | 0.17 | 0.12 | 0.23 | 0.36 | 0.30 | 1.79 |
| 24 | 0.28 | 0.34 | 0.17 | 0.25 | 0.26 | 0.50 | 0.51 | 2.31 |
| 25 | 0.81 | 0.74 | 0.19 | 0.26 | 0.21 | 0.45 | 0.33 | 3.00 |
| 26 | 0.36 | 0.18 | 0.24 | 0.18 | 0.12 | 0.19 | 0.35 | 1.62 |
| 27 | 0.25 | 0.19 | 0.25 | 0.21 | 0.18 | 0.14 | 0.29 | 1.50 |
| 28 | 0.19 | 0.25 | 0.30 | 0.23 | 0.14 | 0.10 | 0.21 | 1.44 |
| 29 | 0.13 | 0.13 | 0.25 | 0.20 | 0.14 | 0.11 | 0.15 | 1.10 |
| 30 | 0.12 | 0.11 | 0.10 | 0.11 | 0.10 | 0.10 | 0.13 | 0.78 |
| 31 | 0.11 | 0.11 | 0.10 | 0.09 | 0.06 | 0.08 | 0.11 | 0.66 |
| 32 | 0.09 | 0.08 | 0.09 | 0.09 | 0.08 | 0.05 | 0.06 | 0.52 |
| 33 | 0.00 | 0.23 | 0.05 | 0.07 | 0.08 | 0.08 | 0.09 | 0.59 |
| % by Z # | 18.52 | 16.88 | 23.72 | 21.52 | 8.35 | 5.74 | 5.28 | 100.00 |

**STP07159-GW36**

| | Z family | | | | | | | |
|---|---|---|---|---|---|---|---|---|
| Carbon # | 0 | -2 | -4 | -6 | -8 | -10 | -12 | % by C # |
| 5 | 1.94 | | | | | | | 1.94 |
| 6 | 1.63 | | | | | | | 1.63 |
| 7 | 1.45 | 1.48 | | | | | | 2.93 |
| 8 | 1.20 | 1.21 | | | | | | 2.41 |
| 9 | 0.89 | 1.04 | | | | | | 1.93 |
| 10 | 0.66 | 0.81 | 1.11 | | | | | 2.58 |
| 11 | 0.54 | 0.74 | 1.27 | | | | | 2.55 |
| 12 | 0.50 | 0.85 | 2.76 | 1.62 | | | | 5.72 |
| 13 | 0.45 | 0.98 | 3.96 | 3.55 | | | | 8.95 |
| 14 | 0.48 | 0.96 | 4.07 | 4.65 | 1.31 | | | 11.48 |
| 15 | 0.57 | 0.74 | 2.34 | 3.92 | 1.66 | | | 9.22 |
| 16 | 0.75 | 0.67 | 1.36 | 2.30 | 1.52 | 0.99 | | 7.58 |
| 17 | 0.73 | 0.65 | 0.92 | 1.15 | 0.97 | 0.88 | | 5.30 |
| 18 | 0.88 | 0.58 | 0.72 | 0.70 | 0.54 | 0.70 | 1.08 | 5.20 |
| 19 | 0.81 | 0.42 | 0.53 | 0.45 | 0.44 | 0.51 | 0.68 | 3.84 |
| 20 | 0.49 | 0.48 | 0.37 | 0.27 | 0.32 | 0.34 | 0.57 | 2.85 |
| 21 | 0.64 | 0.47 | 0.24 | 0.27 | 0.24 | 0.31 | 0.40 | 2.57 |
| 22 | 0.75 | 0.42 | 0.29 | 0.21 | 0.18 | 0.30 | 0.39 | 2.54 |
| 23 | 0.96 | 0.31 | 0.28 | 0.18 | 0.23 | 0.34 | 0.42 | 2.73 |
| 24 | 0.42 | 0.61 | 0.26 | 0.30 | 0.32 | 0.41 | 0.62 | 2.95 |
| 25 | 0.94 | 0.43 | 0.20 | 0.32 | 0.23 | 0.34 | 0.49 | 2.95 |
| 26 | 0.57 | 0.25 | 0.35 | 0.26 | 0.16 | 0.23 | 0.34 | 2.16 |
| 27 | 0.28 | 0.21 | 0.30 | 0.26 | 0.34 | 0.18 | 0.30 | 1.85 |
| 28 | 0.20 | 0.18 | 0.27 | 0.25 | 0.23 | 0.15 | 0.26 | 1.53 |
| 29 | 0.17 | 0.15 | 0.22 | 0.21 | 0.18 | 0.14 | 0.18 | 1.23 |
| 30 | 0.14 | 0.14 | 0.13 | 0.14 | 0.13 | 0.12 | 0.15 | 0.95 |
| 31 | 0.13 | 0.12 | 0.12 | 0.14 | 0.10 | 0.10 | 0.14 | 0.85 |
| 32 | 0.11 | 0.12 | 0.12 | 0.11 | 0.11 | 0.10 | 0.10 | 0.78 |
| 33 | 0.00 | 0.25 | 0.09 | 0.12 | 0.11 | 0.11 | 0.13 | 0.81 |
| % by Z # | 19.29 | 15.23 | 22.28 | 21.37 | 9.35 | 6.24 | 6.24 | 100.00 |

T-Test results (two-sided test)* •••• Two-sided tests ••••

Comparing Samples STP07159-IJ11 and STP07159-GW36

Proportions of ions in each Group

| | | STP07159-IJ11 | | STP07159-GW36 | |
|---|---|---|---|---|---|
| GROUP (C5 to C13) P = 0.4742 | SUMS = | 35.62 | Percent | 30.63 | Percent |
| GROUP (C14 to C21) P = 0.9344 | SUMS = | 47.21 | Percent | 48.05 | Percent |
| GROUP (C22 to C33) P = 0.0452 | SUMS = | 17.16 | Percent | 21.32 | Percent |

*Significant difference if P<0.05

**Figure 4-35: T-test plot comparing samples STP07159-IJ11 and STP07159-GW36. The C22 to C33 group shows a significant difference between samples suggesting degradation of the NAs in sample STP07159-GW36.**

**a) STP-07-158-SS**

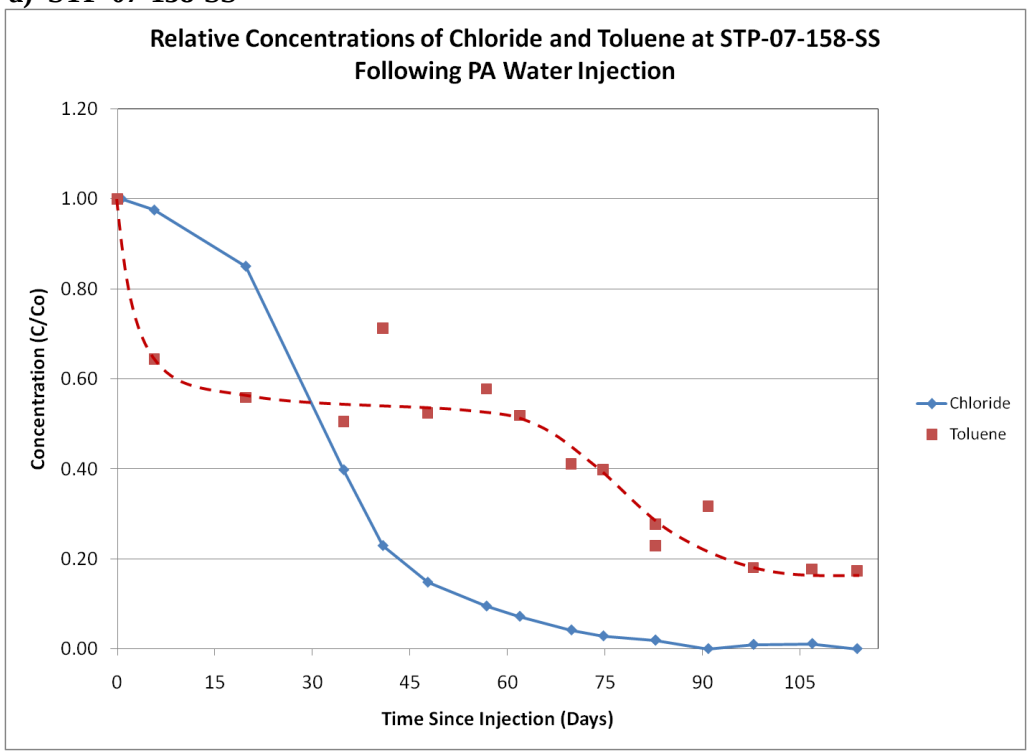


**b) STP-07-159-SS**

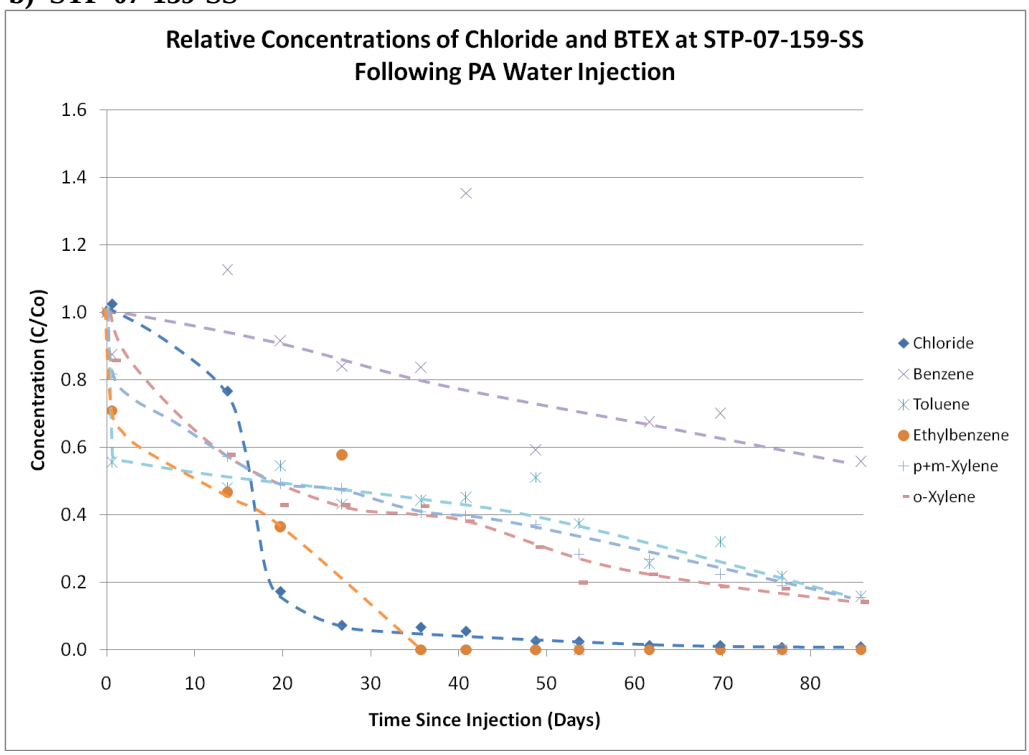


**Figure 4-36: Relative concentrations of chloride and aromatic hydrocarbons following PA water injections at: (a) STP-07-158-SS showing chloride and toluene concentrations and; (b) STP-07-159-SS showing chloride and BTEX concentrations.**

**a) STP-07-158-SS**

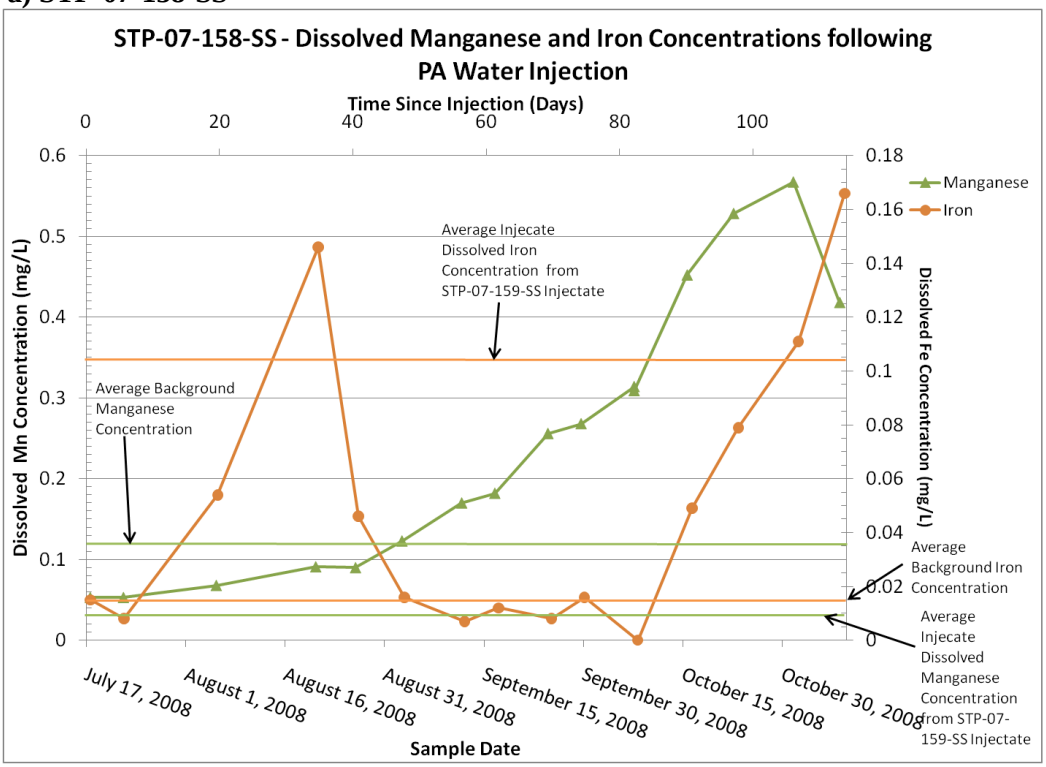


**b) STP-07-159-SS**

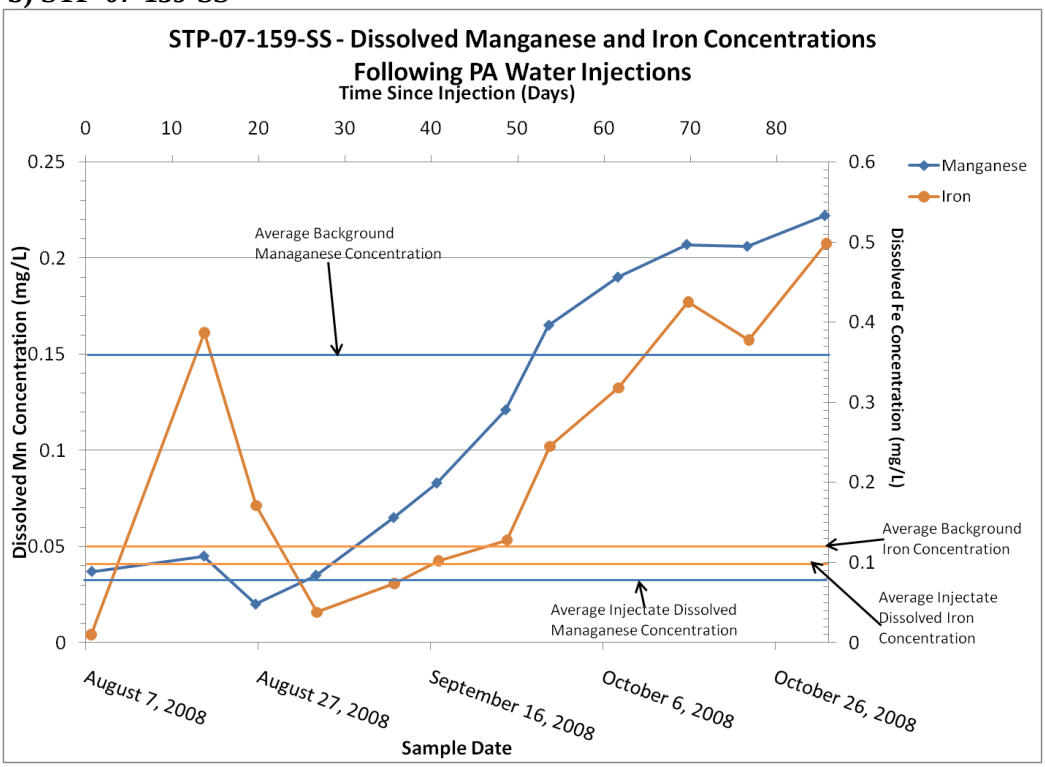


**Figure 4-37: Dissolved manganese and iron concentrations observed following the PA water injections at: (a) STP-07-158-SS and; (b) STP-07-159-SS.**

**a) STP-07-158-SS**

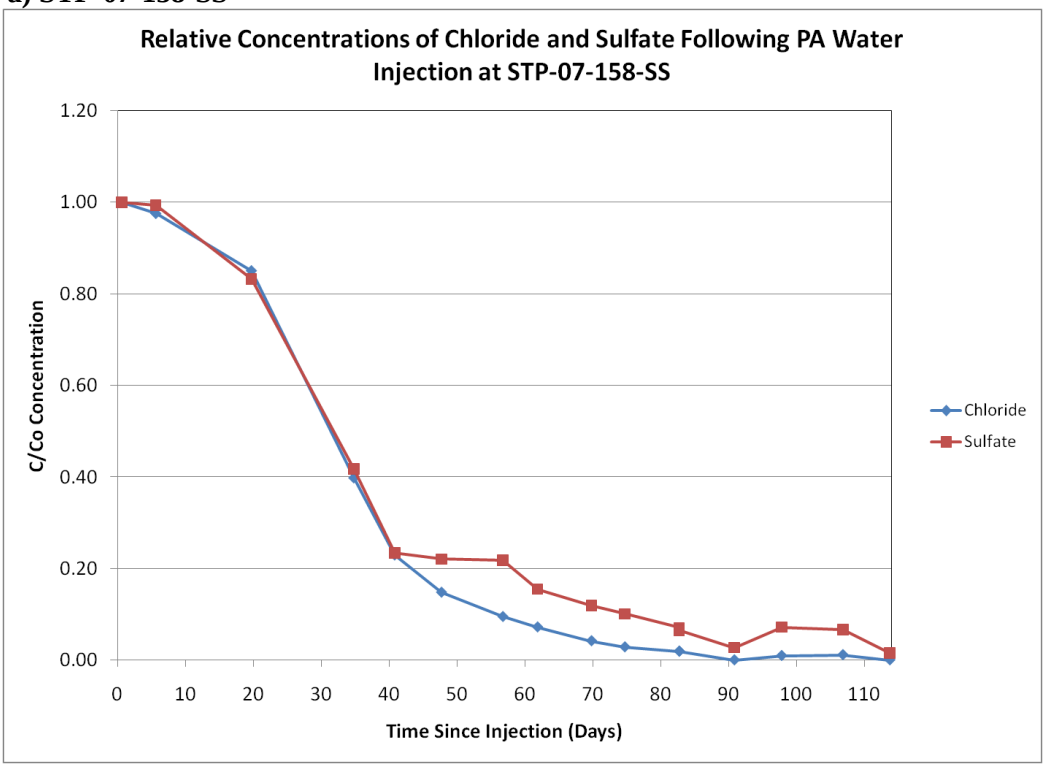


**b) STP-07-159-SS**

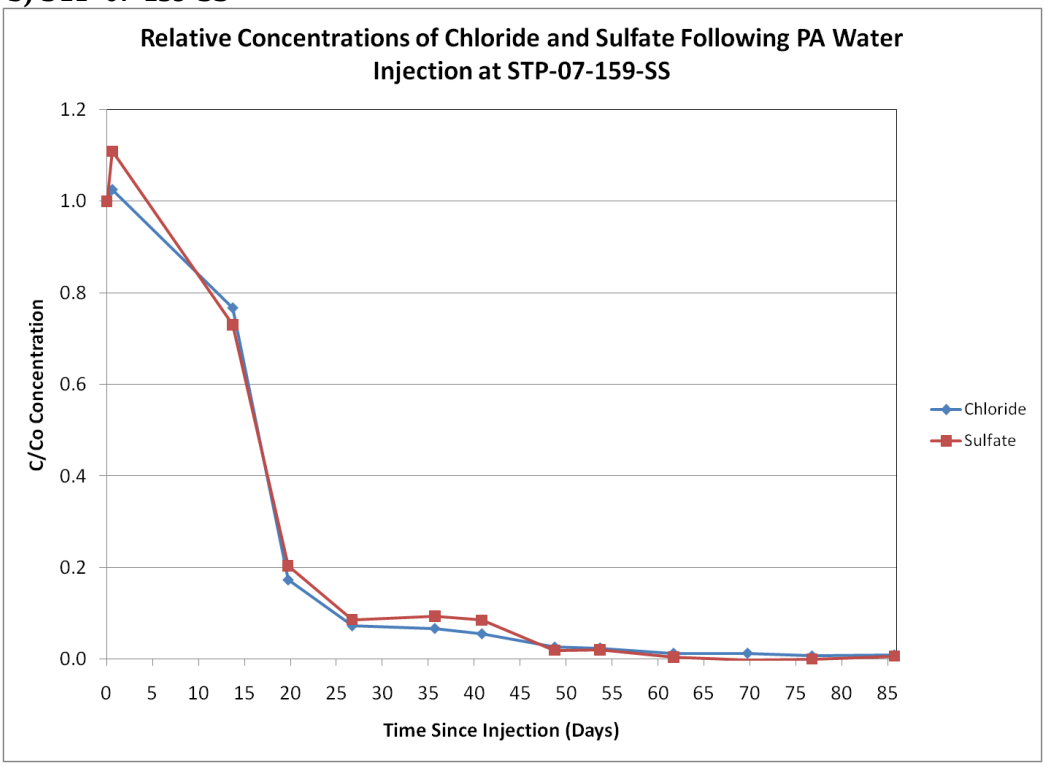


**Figure 4-38: Relative concentrations of chloride and sulfate observed following the PA water injections at: (a) STP-07-158-SS and; (b) STP-07-159-SS.**

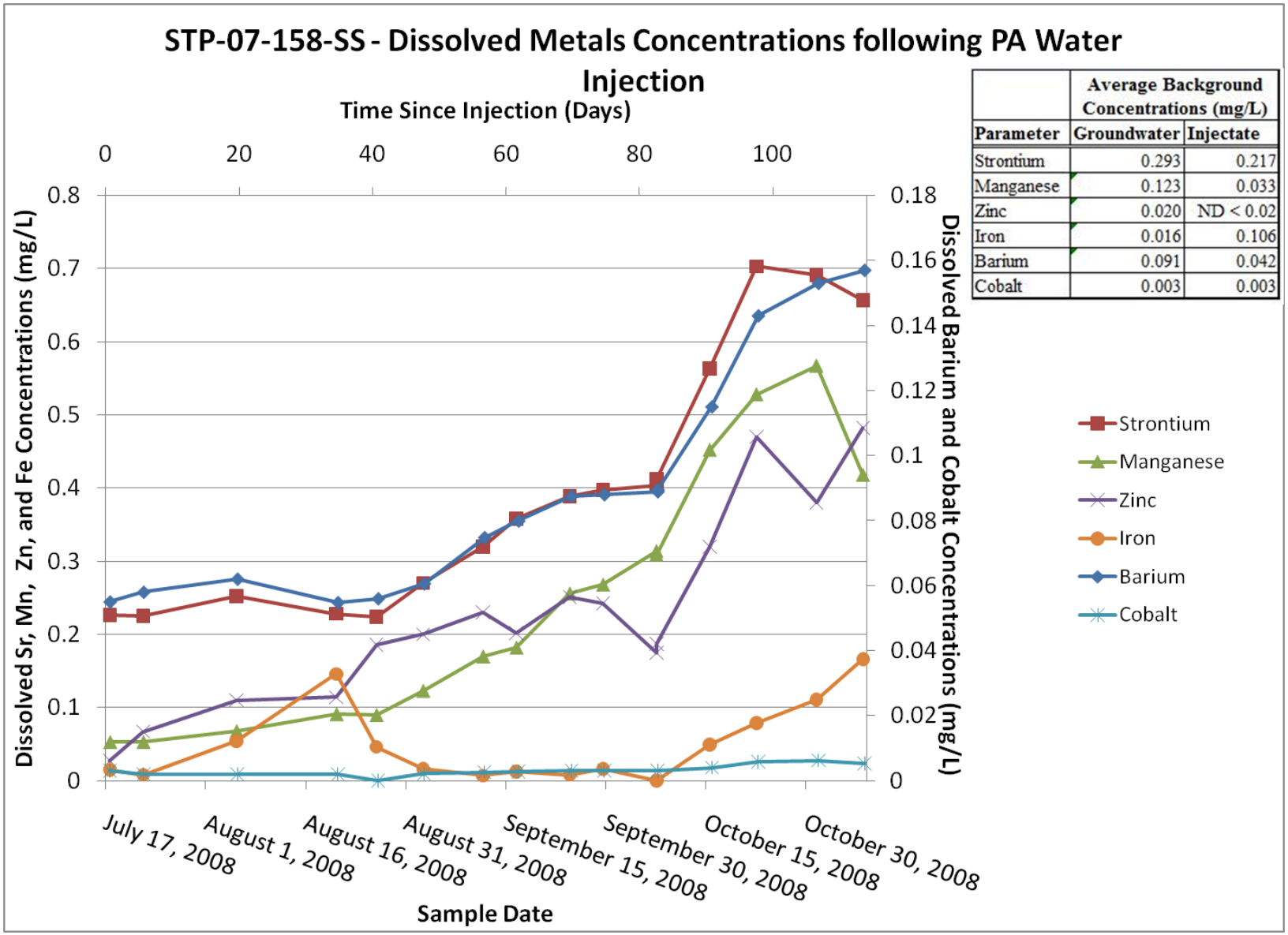


| Parameter | Average Background Concentrations (mg/L) Groundwater | Injectate |
|---|---|---|
| Strontium | 0.293 | 0.217 |
| Manganese | 0.123 | 0.033 |
| Zinc | 0.020 | ND < 0.02 |
| Iron | 0.016 | 0.106 |
| Barium | 0.091 | 0.042 |
| Cobalt | 0.003 | 0.003 |

**Figure 4-39: Dissolved metals concentrations observed at STP-07-158-SS following the PA water injection. Only metals that showed increasing concentration trends not attributable to elevated injectate levels or a return to background conditions are shown.**

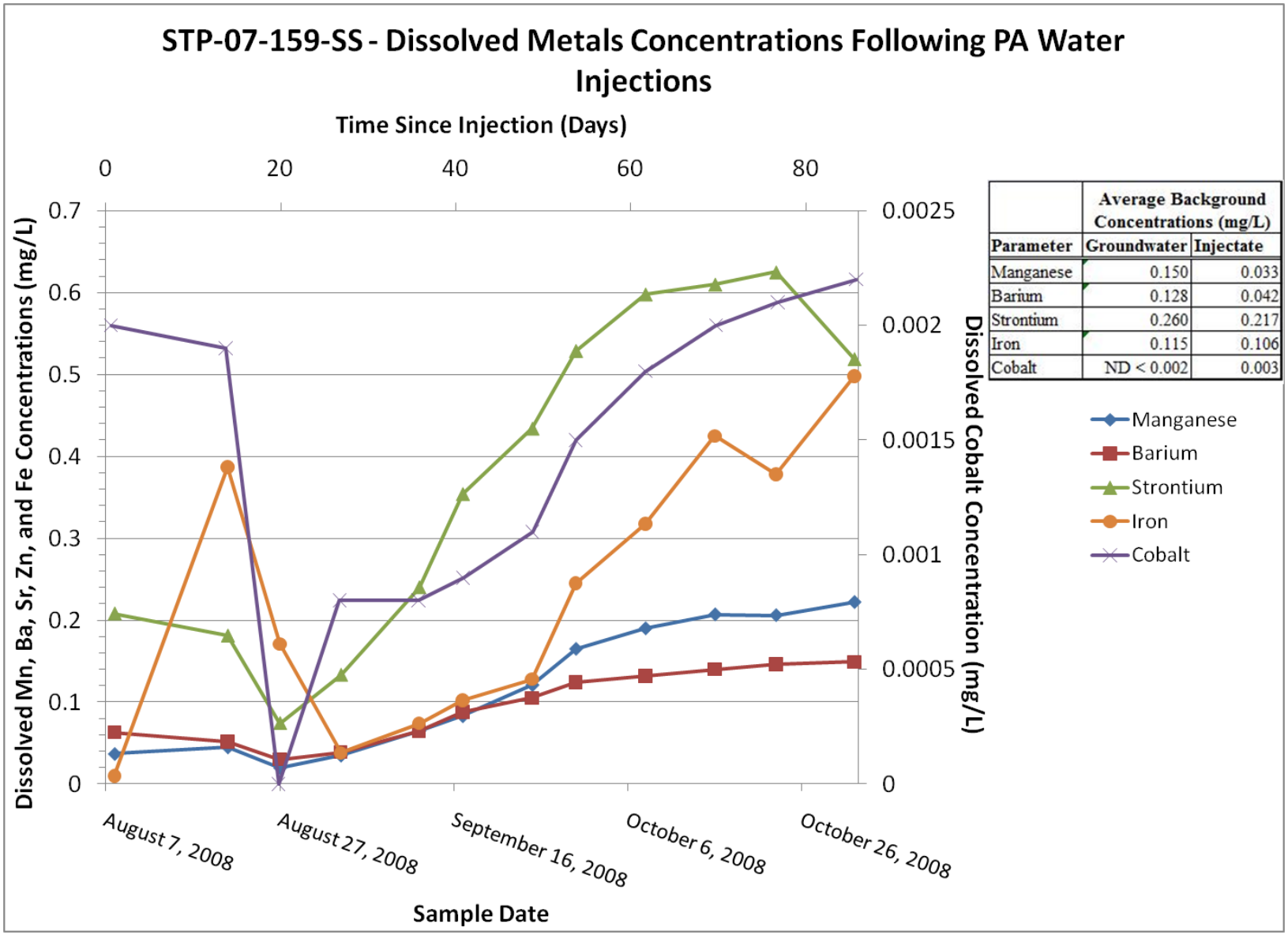


| Parameter | Average Background Concentrations (mg/L) Groundwater | Injectate |
|---|---|---|
| Manganese | 0.150 | 0.033 |
| Barium | 0.128 | 0.042 |
| Strontium | 0.260 | 0.217 |
| Iron | 0.115 | 0.106 |
| Cobalt | ND < 0.002 | 0.003 |

**Figure 4-40: Dissolved metals concentrations observed at STP-07-159-SS following the PA water injection. Only metals that showed increasing concentration trends not attributable to elevated injectate levels or a return to background conditions are shown.**

**a) STP-08-158A1: July 17, 2008 – June 20, 2009**

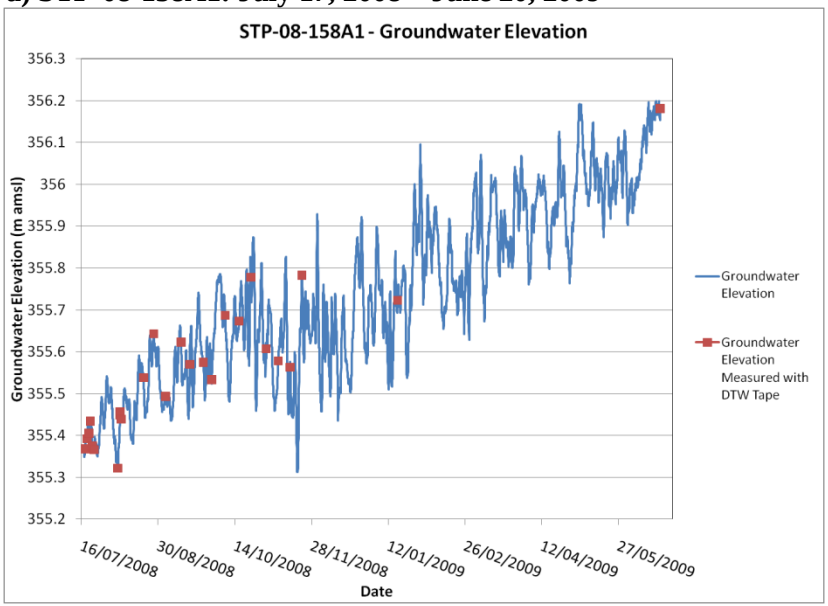


**b) STP-08-158A2: July 17, 2008 – June 20, 2009**

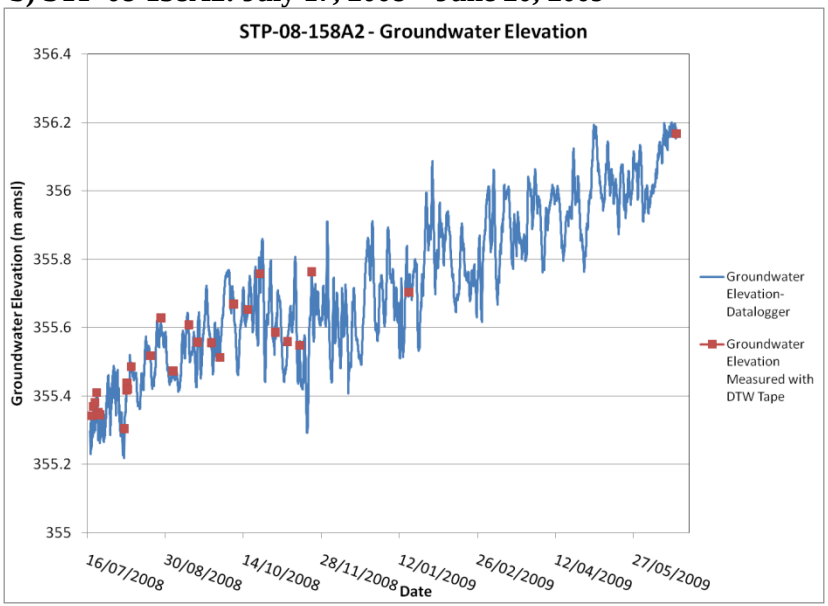


**c) STP-08-158A3: August 8, 2008 – June 20, 2009**

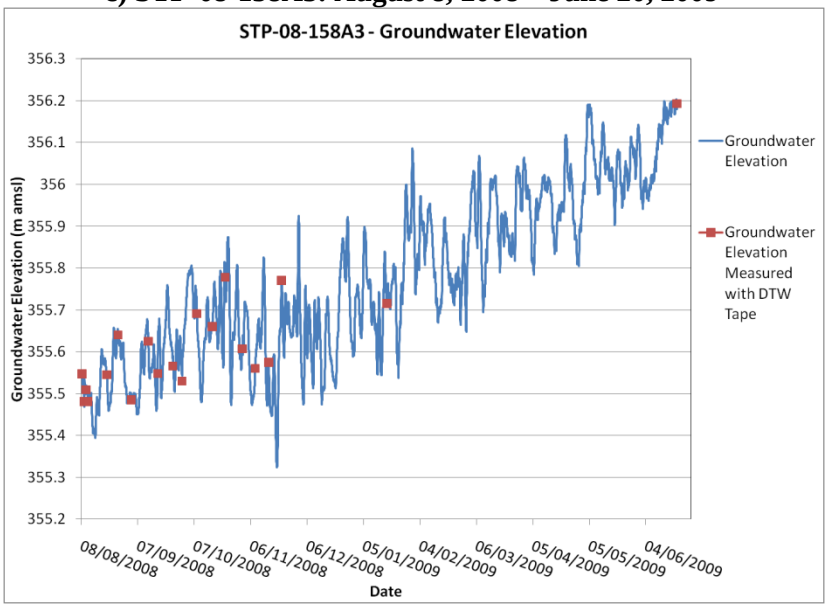


**Figure 4-41: Groundwater elevation data from the STP-08-158A well cluster measured by DTW tape and CTD divers following the PA-water injection at STP-07-158-SS including wells: (a) STP-08-158A1 (July 17, 2008-June 20, 2009); (b) STP-08-158A2 (July 17, 2008-June 20, 2009) and; (c) STP-08-158A3 (August 8, 2008-June 20, 2009).**

**a) STP-08-158A1: July 17, 2008 – June 20, 2009**

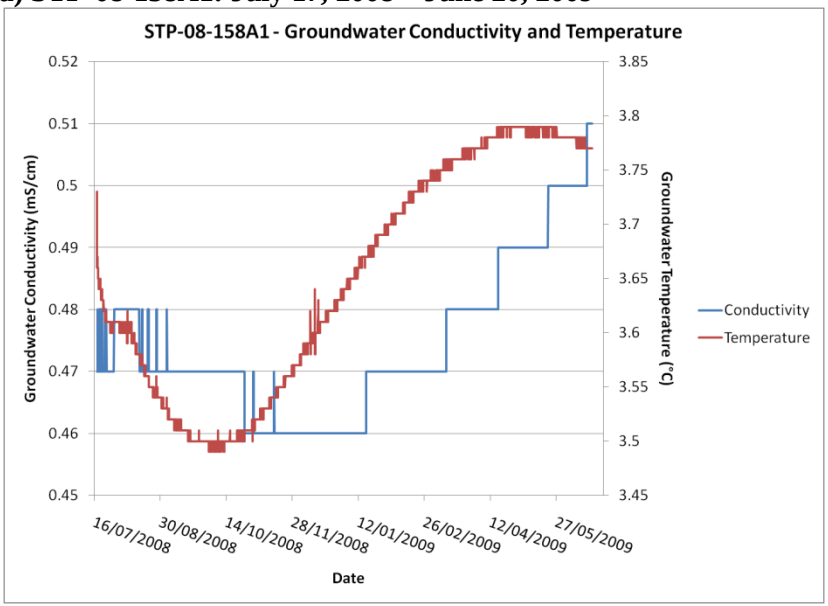


**b) STP-08-158A2: July 17, 2008 – June 20, 2009**

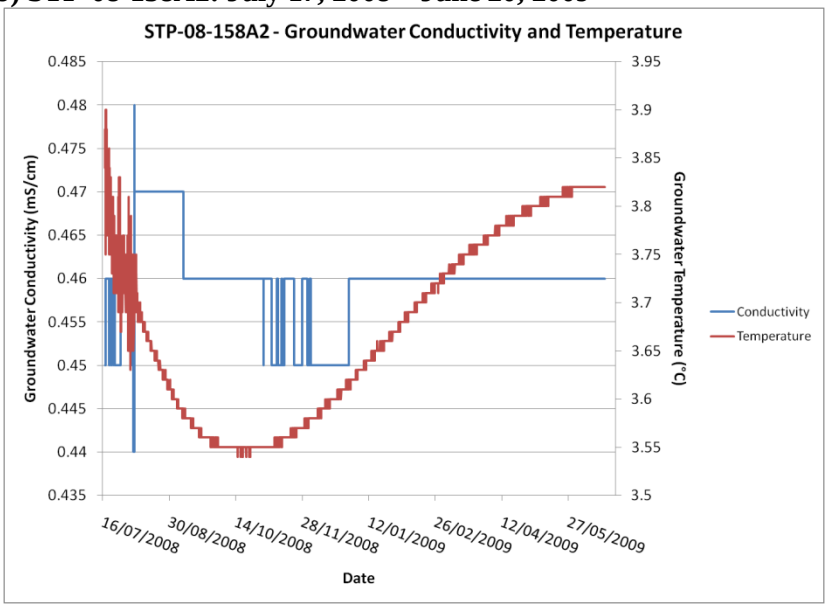


**c) STP-08-158A3: August 8, 2008 – June 20, 2009**

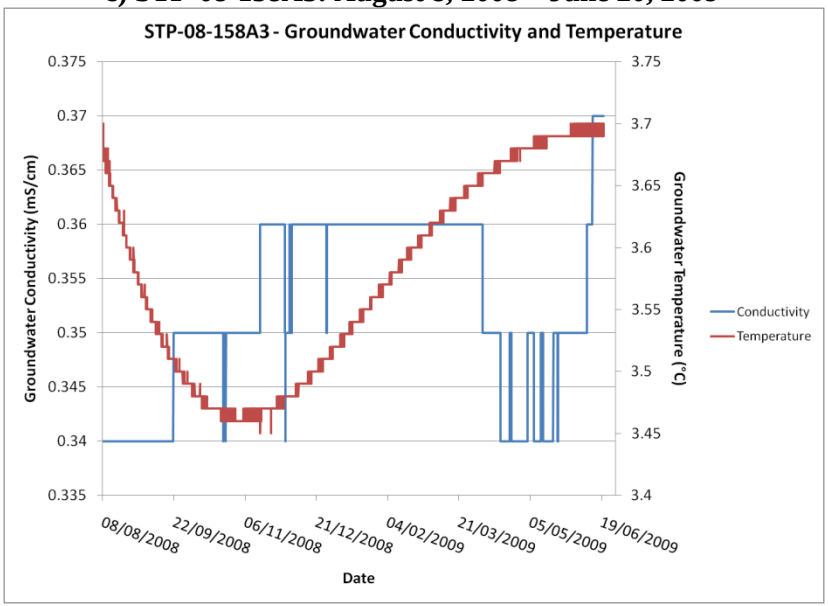


**Figure 4-42: Groundwater conductivity and temperature data from the STP-08-158A well cluster measured by CTD divers after the PA-water injection at STP-07-158-SS including wells: (a) STP-08-158A1 (July 17, 2008-June 20, 2009); (b) STP-08-158A2 (July 17, 2008-June 20, 2009) and; (c) STP-08-158A3 (August 8, 2008-June 20, 2009).**

**a) STP-08-159A1: August 7, 2008 – June 20, 2009**

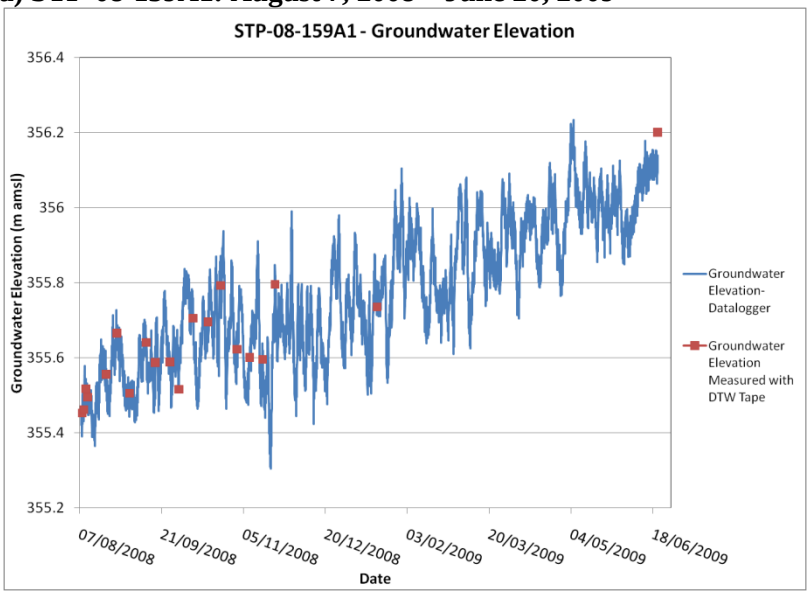


**b) STP-08-159A2: August 7, 2008 – October 5, 2008**

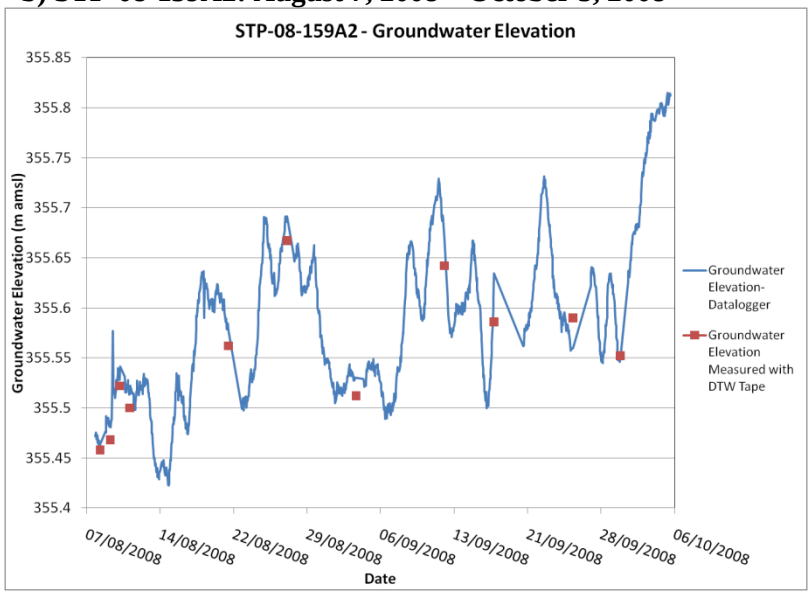


**c) STP-08-159A3: August 7, 2008 – November 22, 2008**

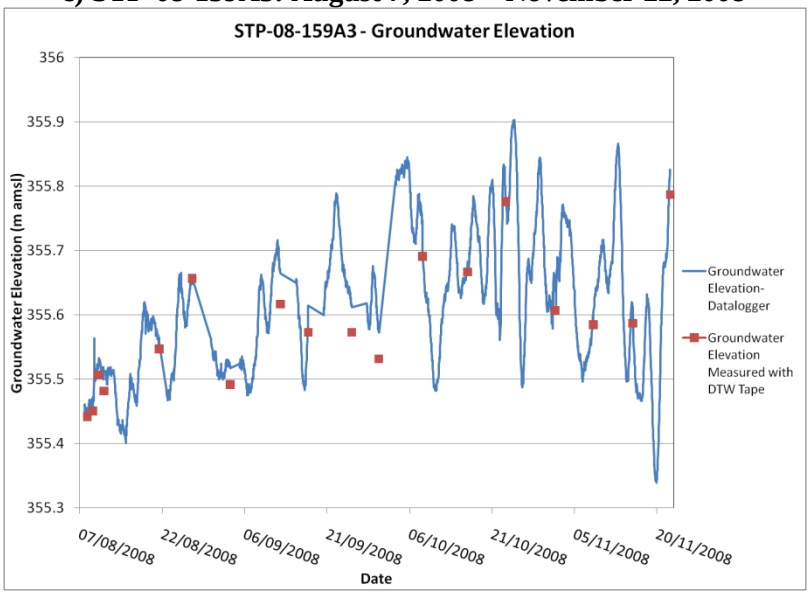


**Figure 4-43: Groundwater elevation data from the STP-08-159A well cluster measured by DTW tape and CTD divers following the PA-water injection at STP-07-159-SS including wells: (a) STP-08-159A1 (August 7, 2008-June 20, 2009); (b) STP-08-159A2 (August 7, 2008-October 5, 2008) and; (c) STP-08-159A3 (August 7, 2008-November 22, 2009). CTD Divers deployed at STP-08-159A2 and STP-08-159A3 stopped operating correctly on October 5 and November 22, 2008, respectively.**

**a) STP-08-159A1: August 7, 2008 – June 20, 2009**

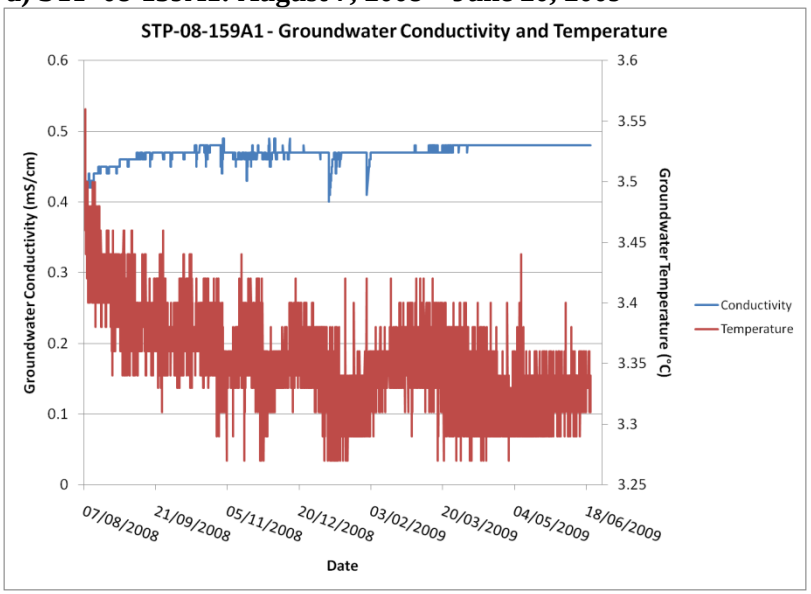


**b) STP-08-159A2: August 7, 2008 – October 5, 2008**

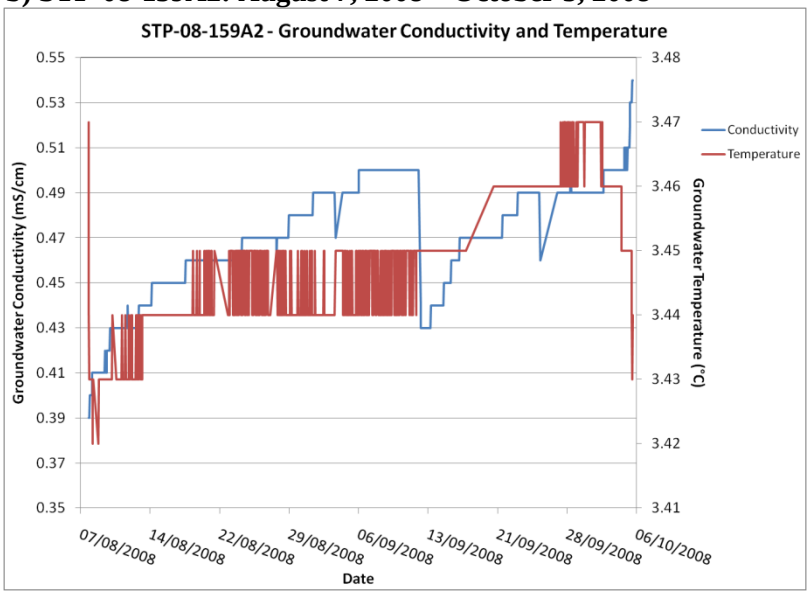


**c) STP-08-159A3: August 7, 2008 – November 22, 2008**

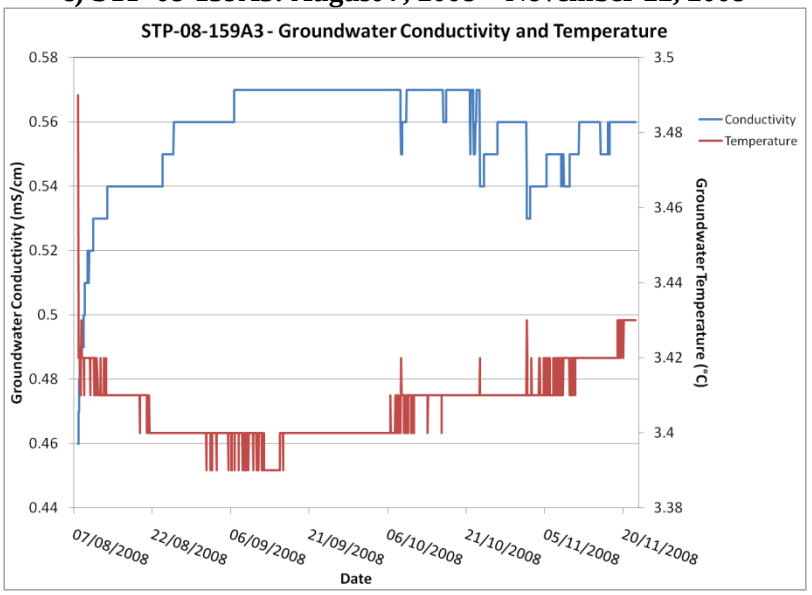


**Figure 4-44: Groundwater conductivity and temperature data from the STP-08-159A well cluster measured by CTD divers following the PA-water injection at STP-07-159-SS including wells: (a) STP-08-159A1 (August 7, 2008-June 20, 2009); (b) STP-08-159A2 (August 7, 2008-October 5, 2008) and; (c) STP-08-159A3 (August 7, 2008-November 22, 2009). CTD Divers deployed at STP-08-159A2 and STP-08-159A3 stopped operating correctly on October 5 and November 22, 2008, respectively.**

**a) STP-08-159A2**

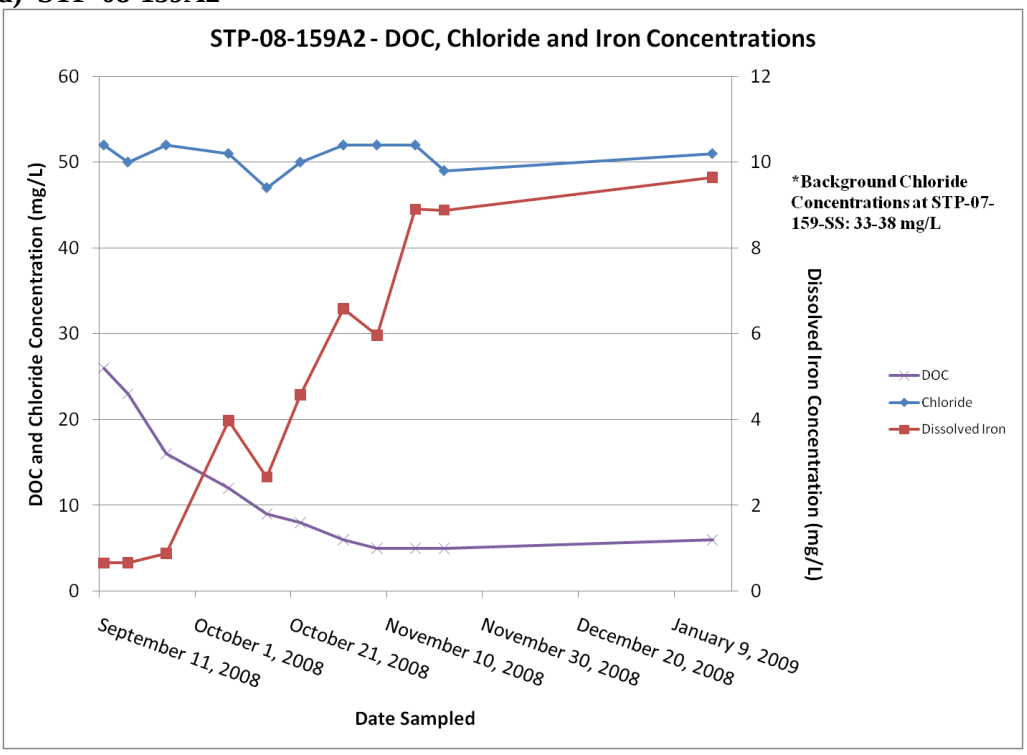


**b) STP-08-159A3**

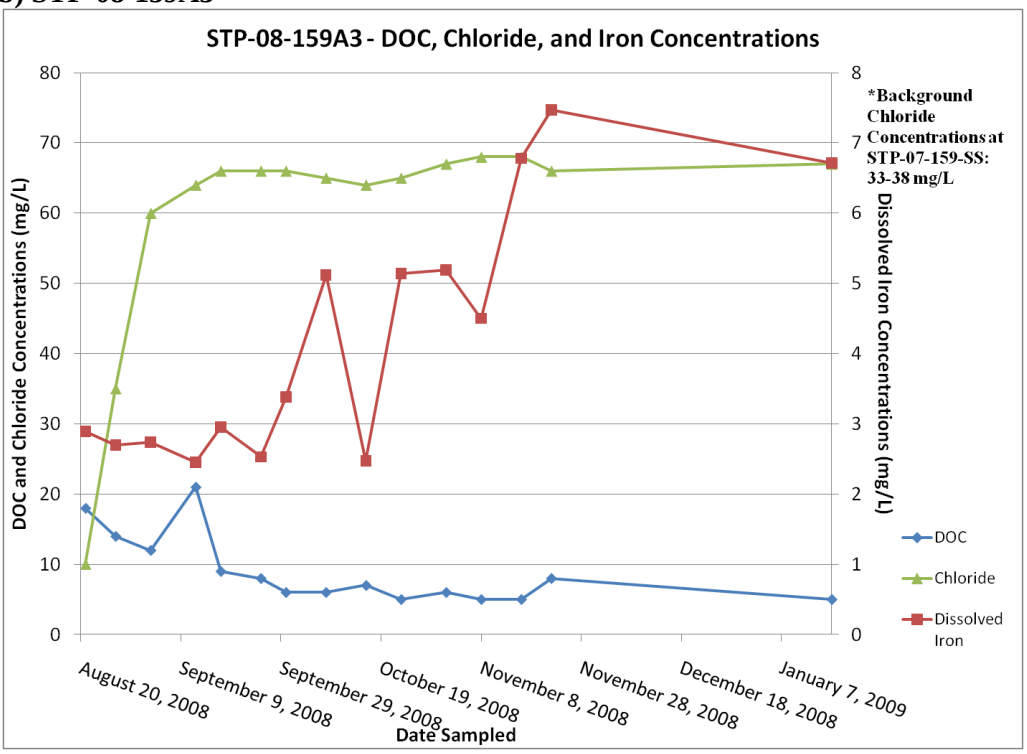


**Figure 4-45: DOC, chloride and iron concentrations following the STP-07-159-SS PA water injections observed at: (a) STP-08-159A2 and; (b) STP-08-159A3.**

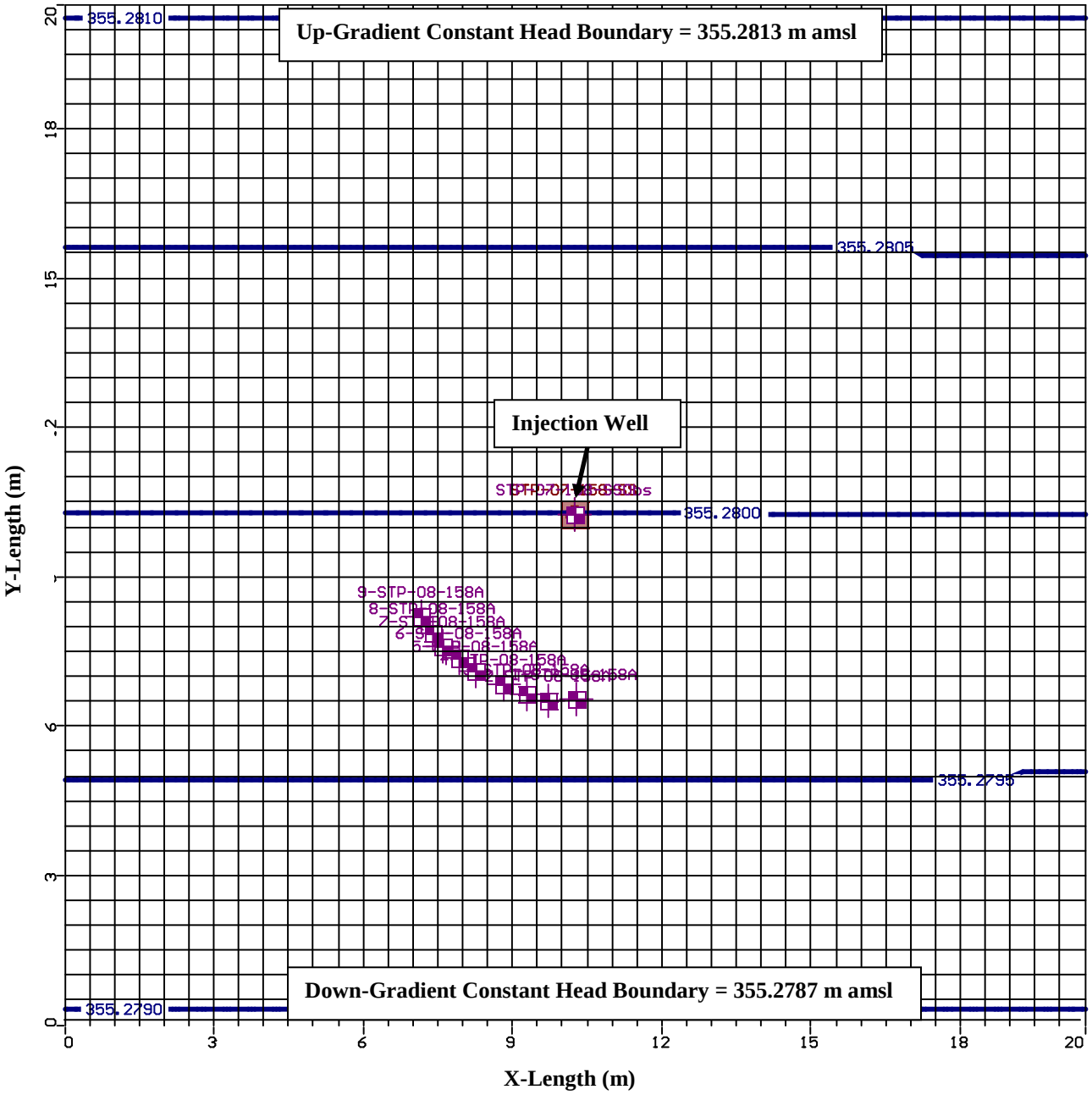


**Figure 4-46: Plan view of grid discretization showing the position of the injection and down-gradient monitoring wells and the head levels prior to injection for the model of the STP-07-158-SS injection. This view is of the layer from 352.5 to 353.0 m amsl which is the depth at which the injection well was screened.**

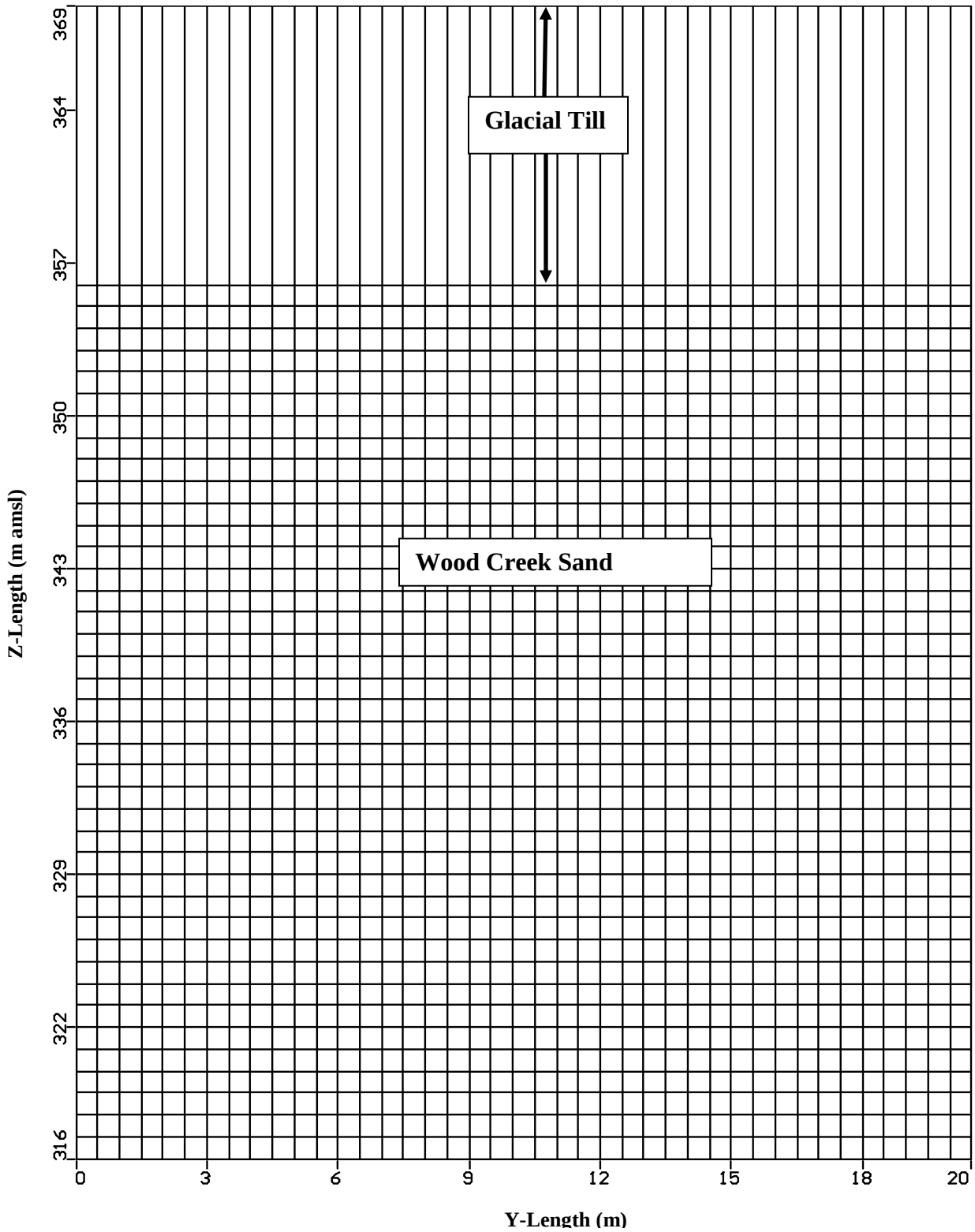


**Figure 4-47: Cross-section of grid for model of STP-07-158-SS injection.**

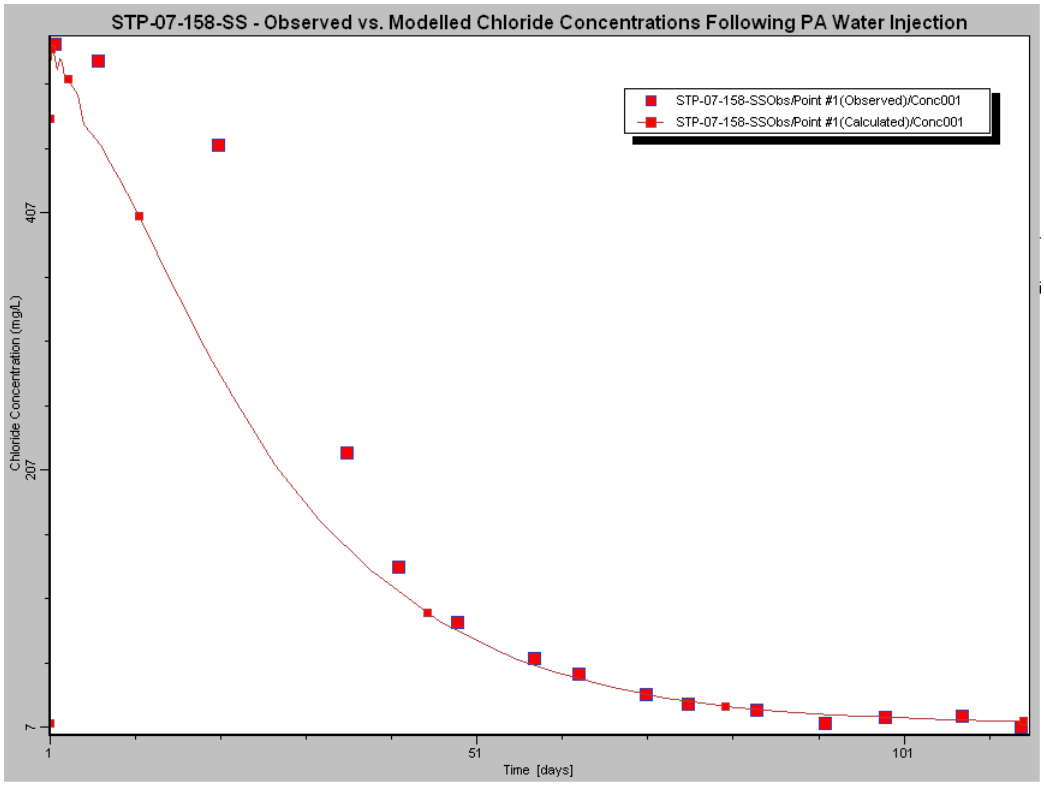


**Figure 4-48: Observed vs. modelled chloride concentrations following the PA water injection at STP-07-158-SS.**

**a) Chloride Concentrations Immediately After Injection**

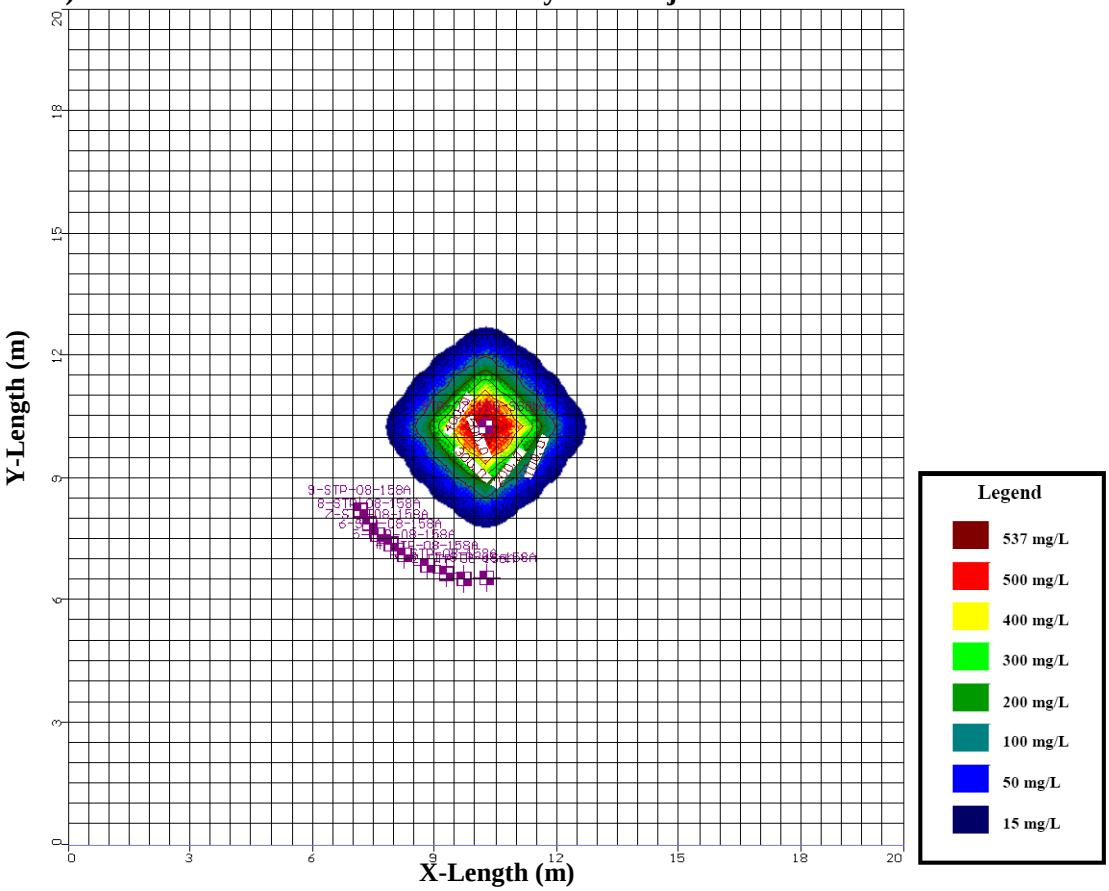


**b) Chloride Concentration 20 Days after Injection**

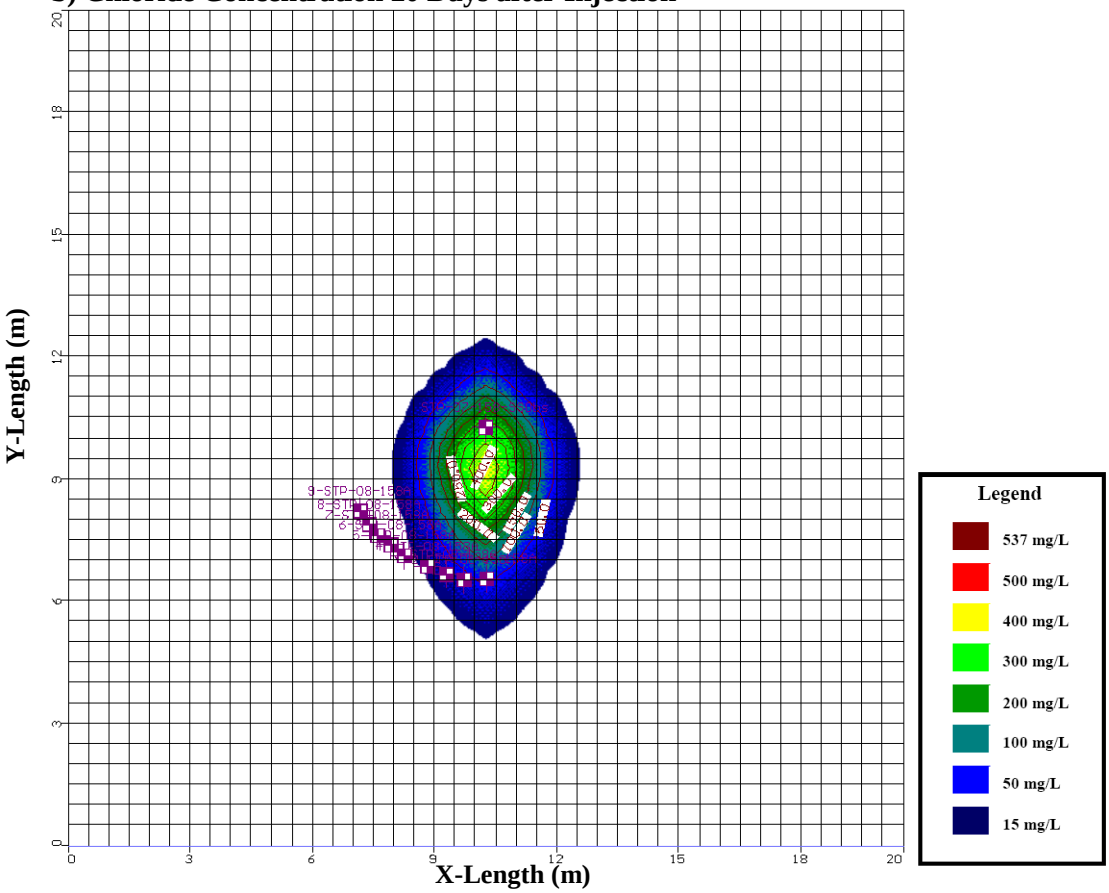

c) Chloride Concentration 60 Days After Injection

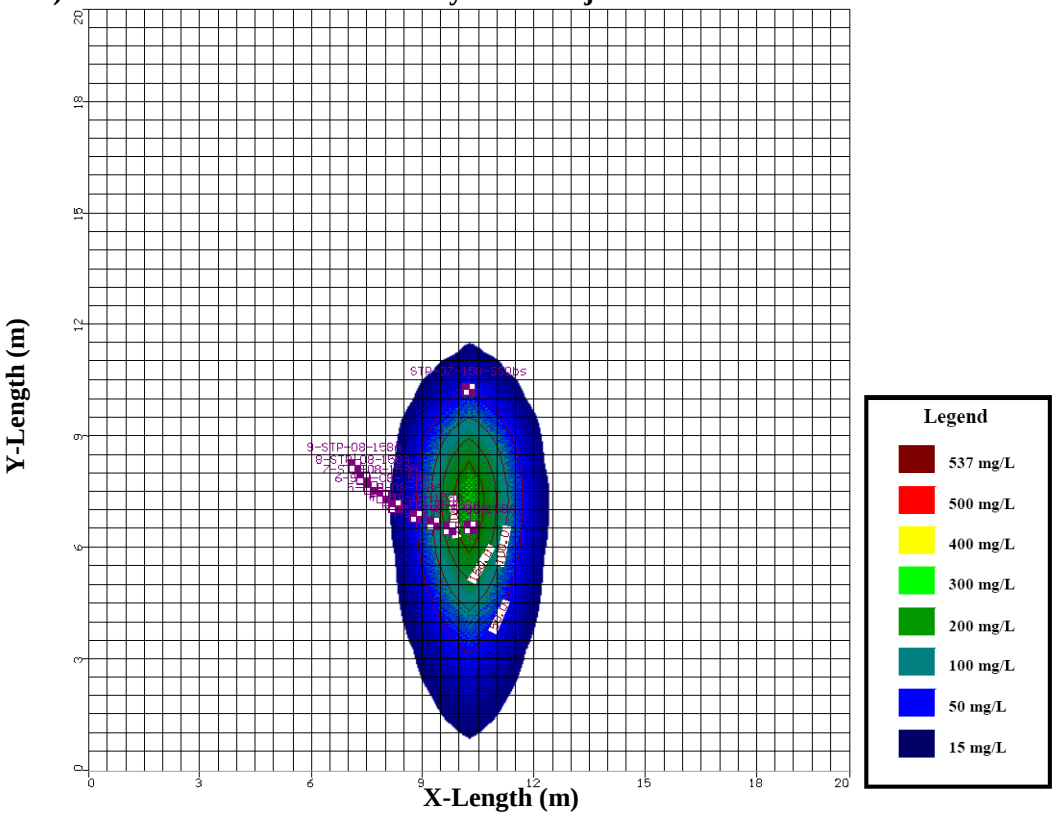


d) Chloride Concentration 115 Days After Injection

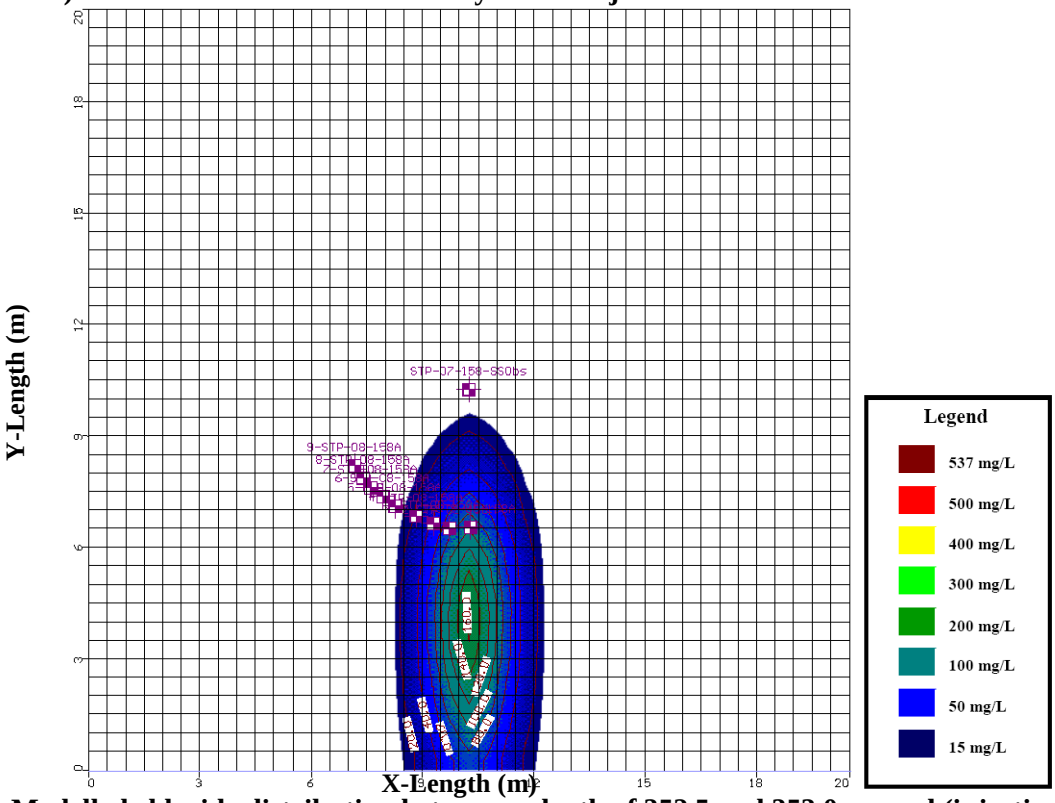


**Figure 4-49: Modelled chloride distribution between a depth of 352.5 and 353.0 m amsl (injection depth) following the PA water injection at STP-07-158-SS. Figures show chloride distribution: (a) immediately after injection; (b) 20 days after injection; (c) 60 days after injection and; (d) 115 days after injection.**

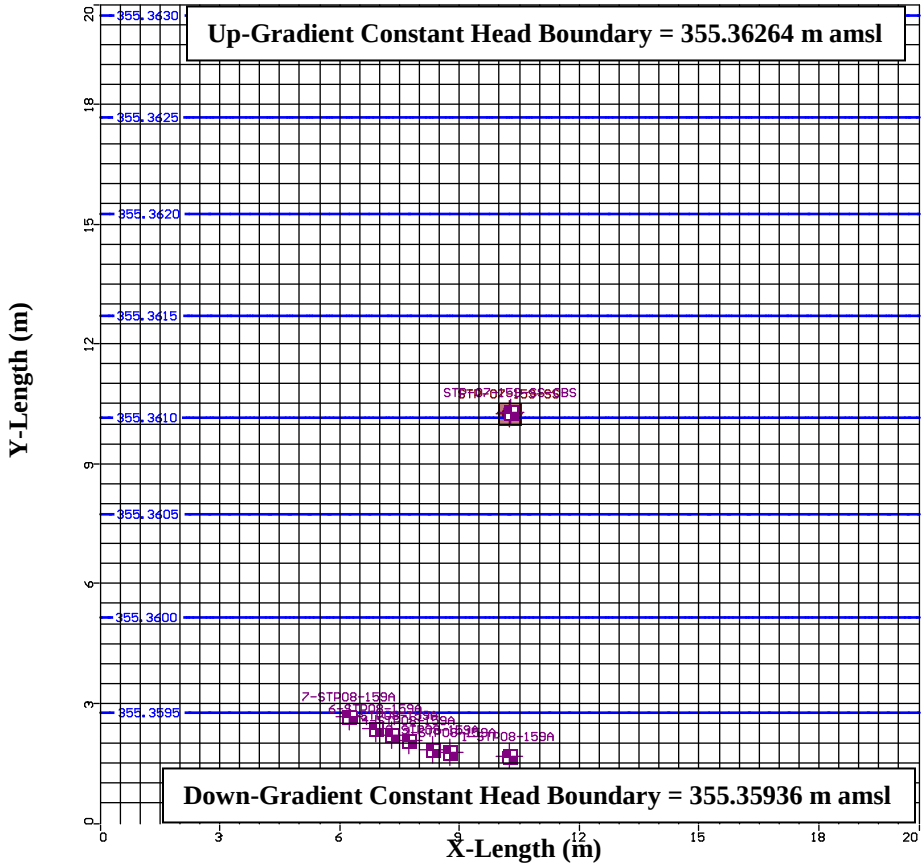


**Figure 4-50: Plan view of grid discretization showing the position of the injection and down-gradient monitoring wells and the head levels prior to injection for the model of the STP-07-159-SS injection. This view is of the layer from 340.5 to 341.0 m amsl, the depth at which the injection well was screened.**

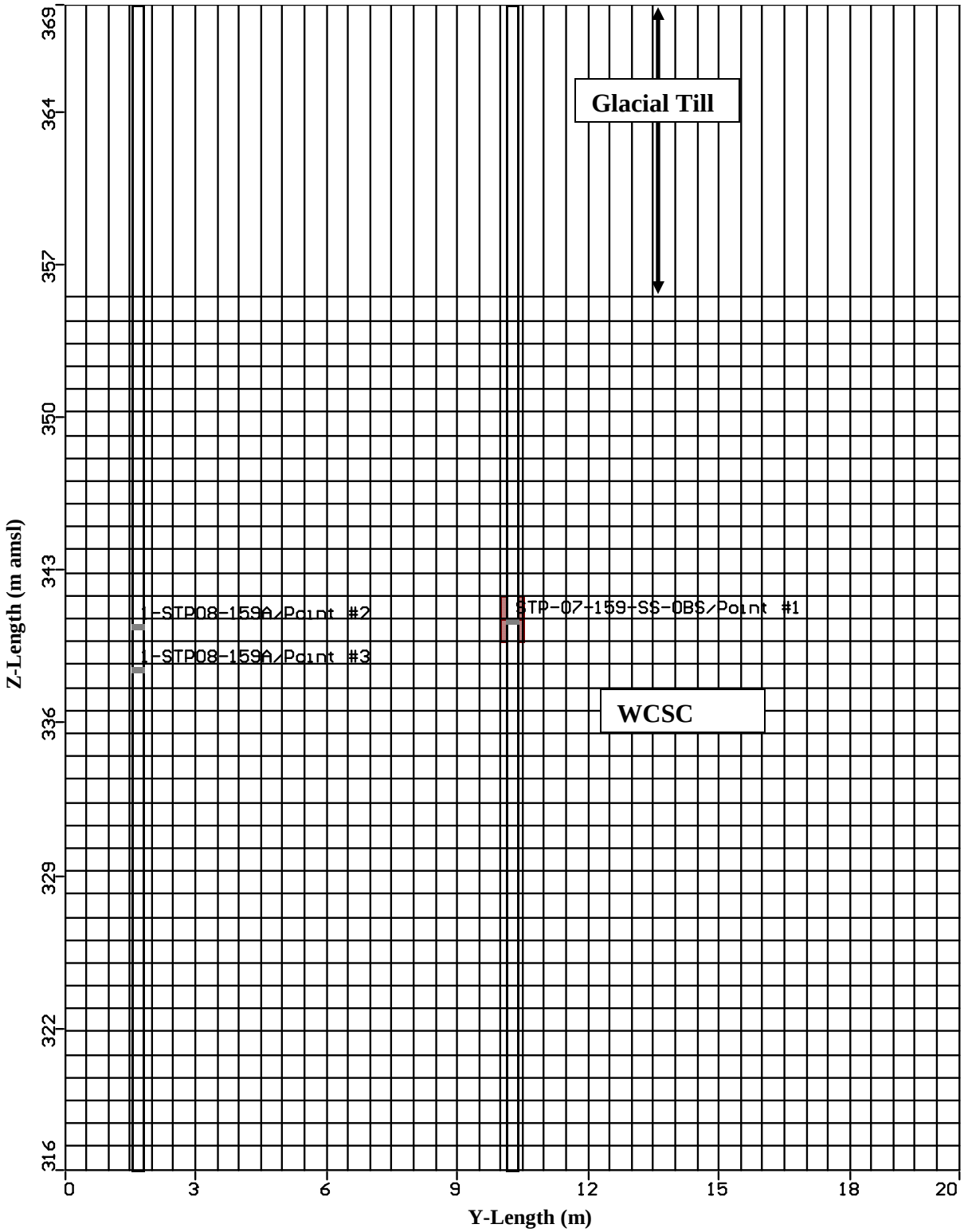


**Figure 4-51: Cross-section of grid for model of STP-07-159-SS injection.**

**a) Chloride Concentration Immediately after Injection**

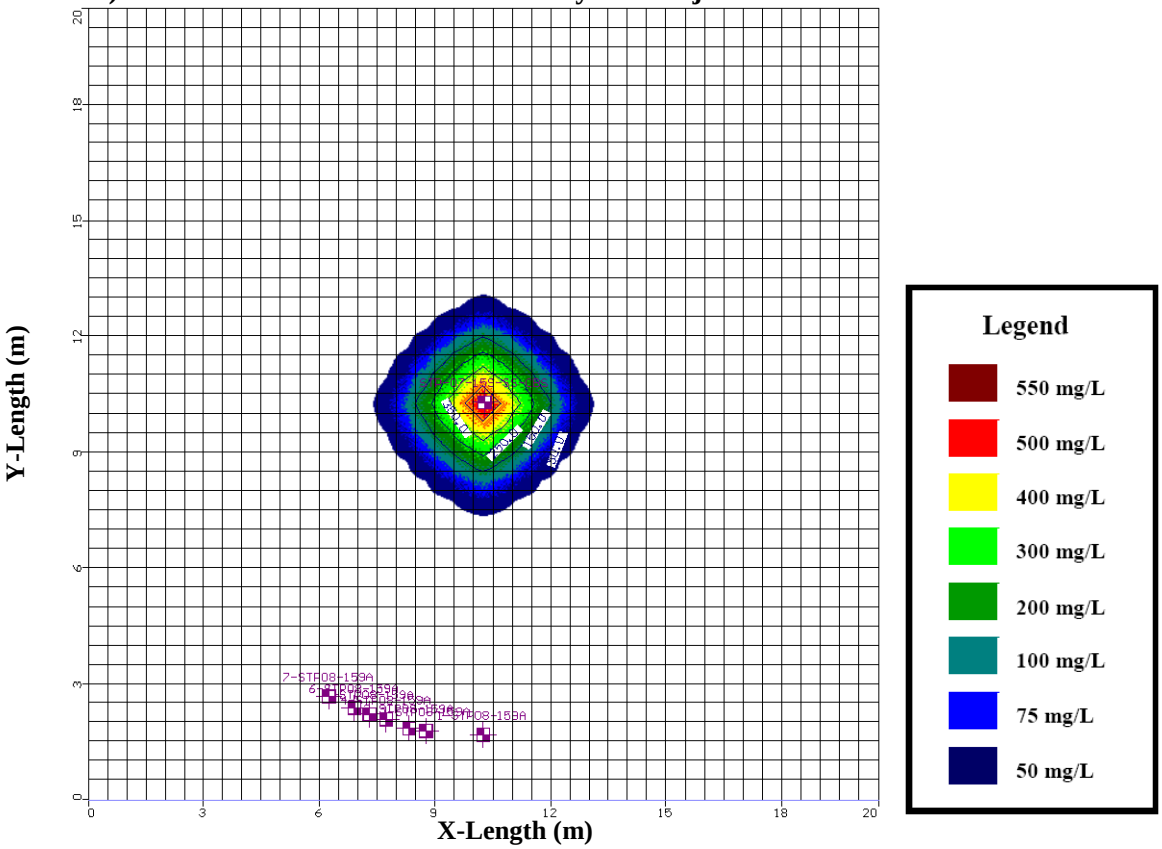


**b) Chloride Concentration 20 Days after Injection**

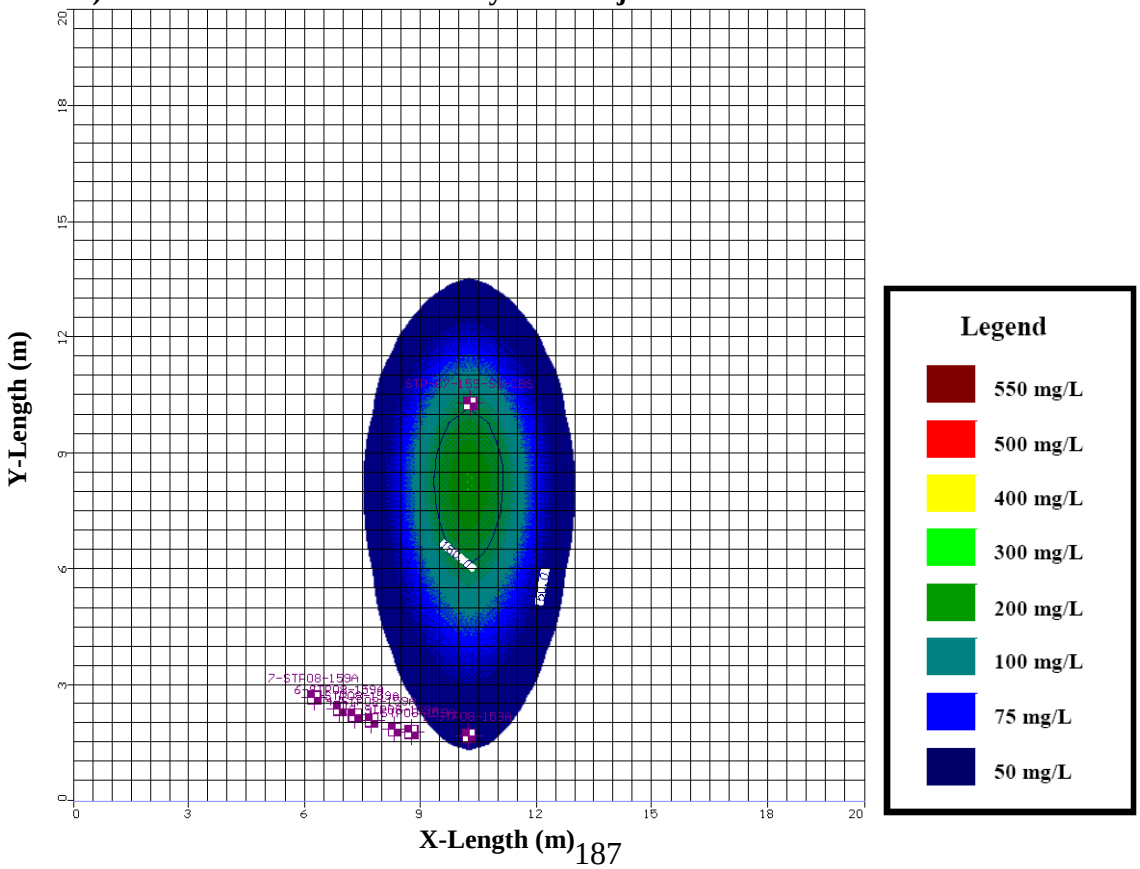

c) Chloride Concentration 80 Days after Injection

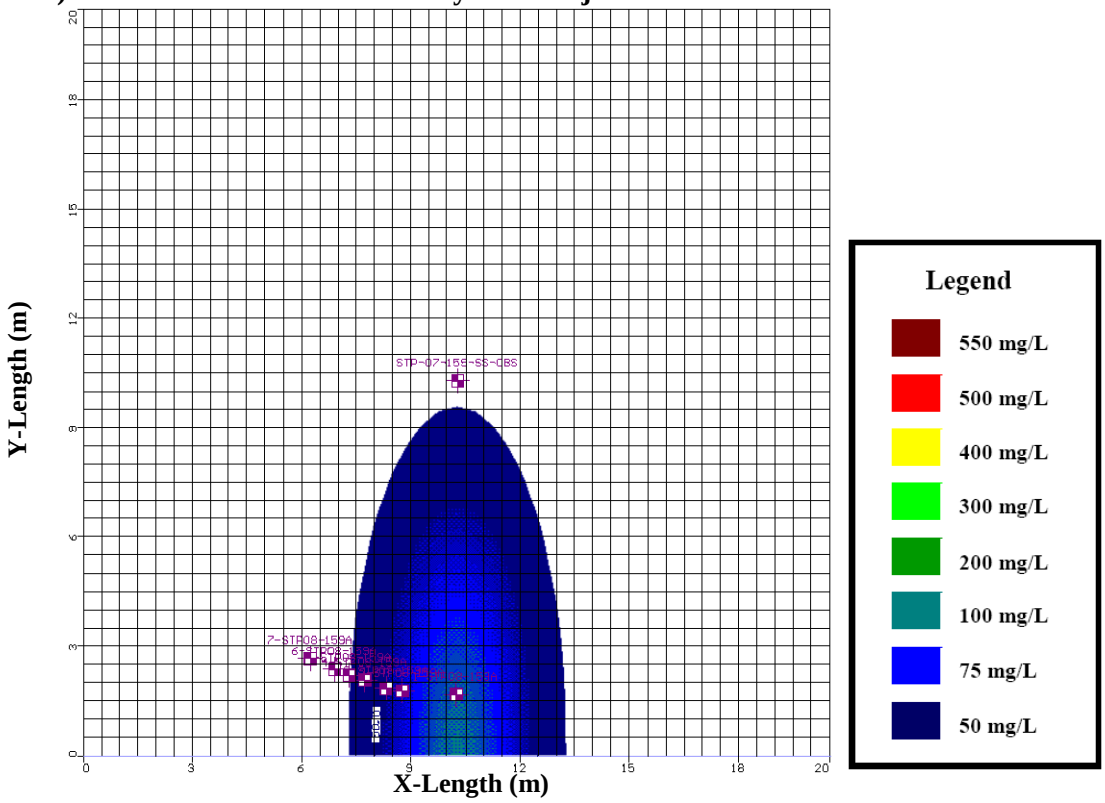


d) Chloride Concentration 150 Days after Injection

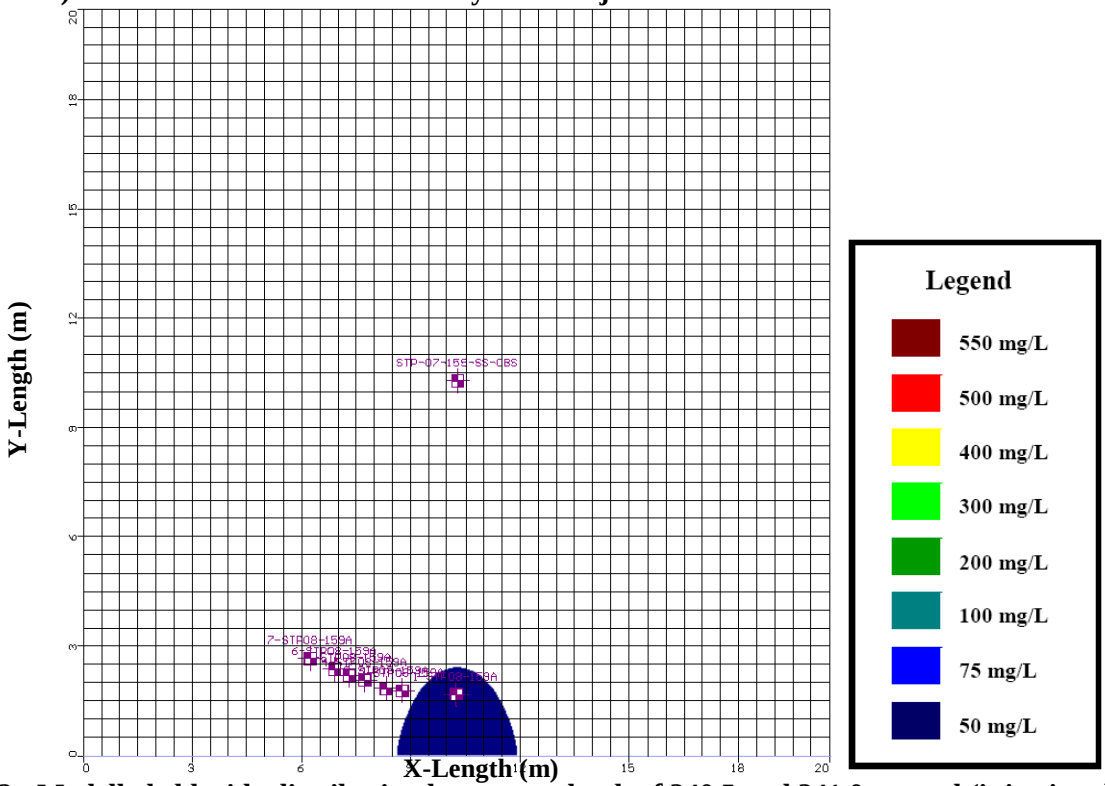


**Figure 4-52: Modelled chloride distribution between a depth of 340.5 and 341.0 m amsl (injection depth) following the PA water injection at STP-07-159-SS. Figures show chloride distribution: (a) immediately after injection; (b) 20 days after injection; (c) 80 days after injection and; (d) 150 days after injection. Model was run without vertical flow component or variability in hydraulic conductivity within the WCSC.**

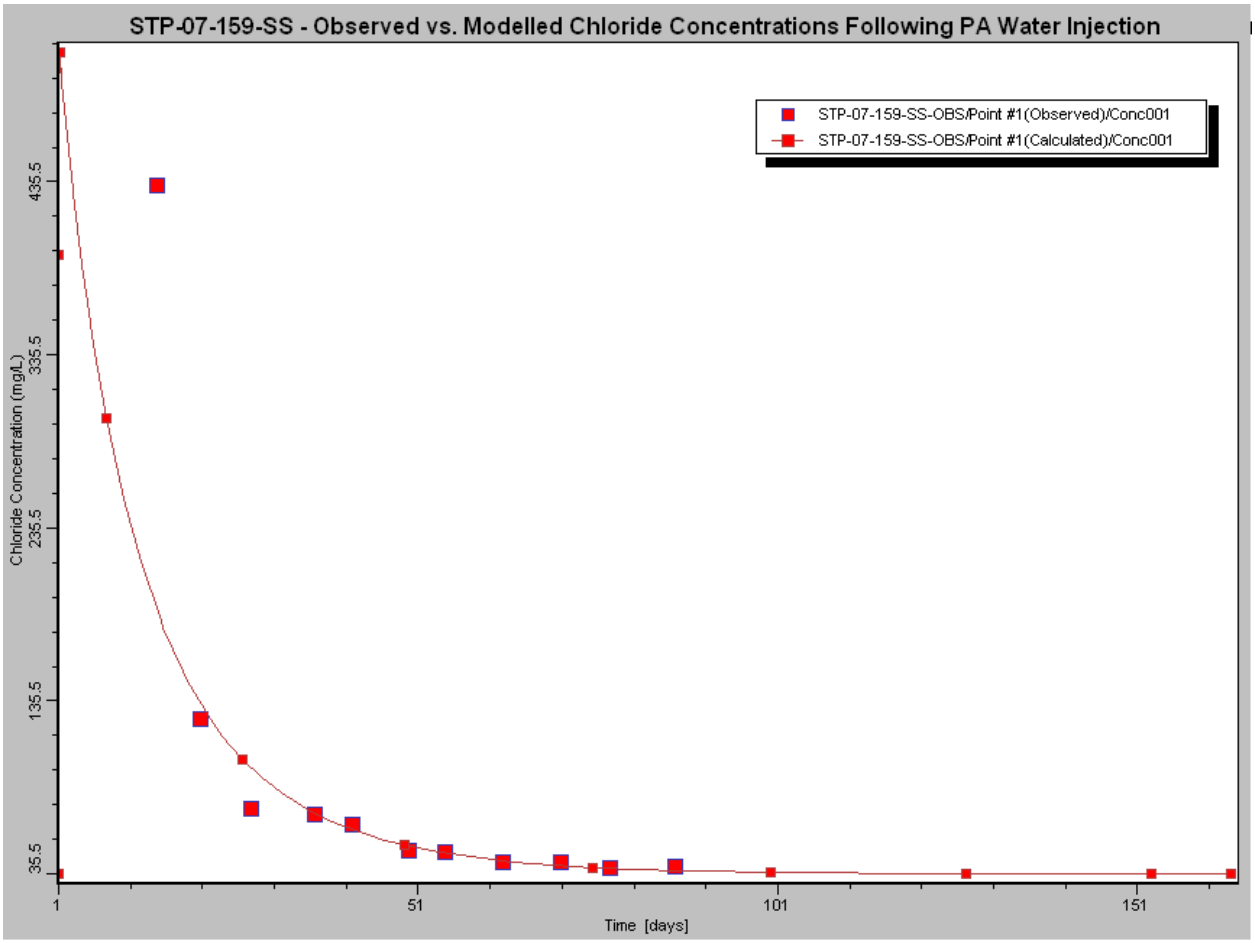


**Figure 4-53: Observed vs. Modelled chloride concentrations following the PA water injection at STP-07-159-SS.**

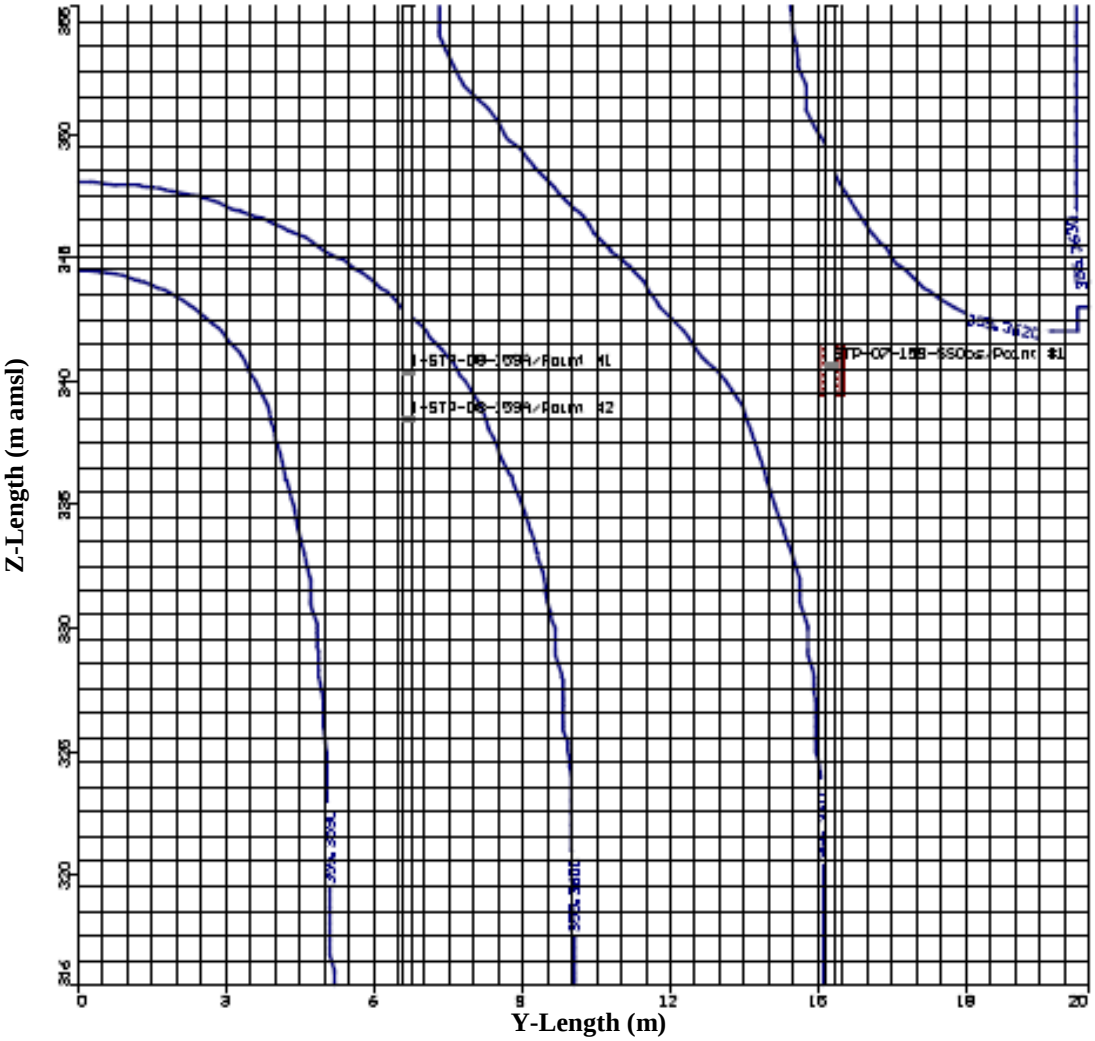


**Figure 4-54: Cross-section of WCSC showing the initial head equipotentials created in Modflow by varying the up-gradient and down-gradient constant head boundary conditions to drive vertical components of flow through the aquifer.**

**a) STP-07-159-SS**

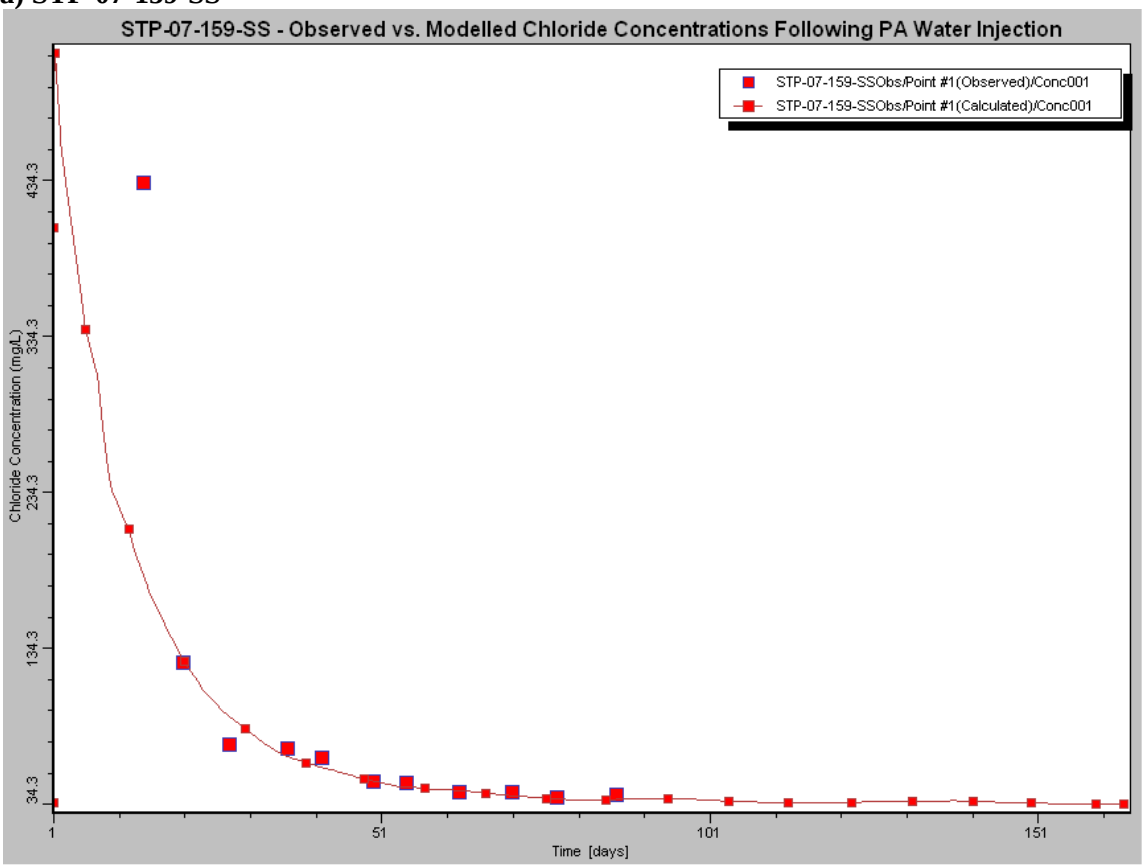


**b) STP-08-159A2**

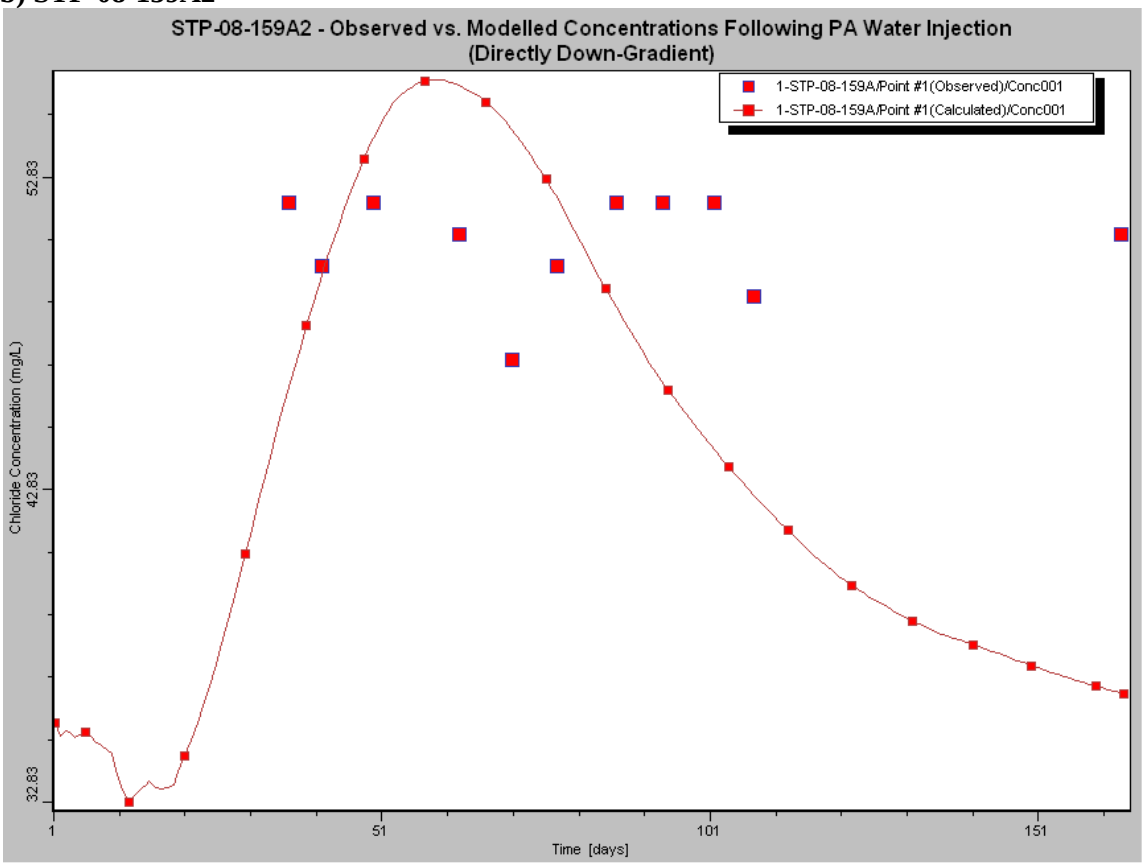

**c) STP-08-159A3**

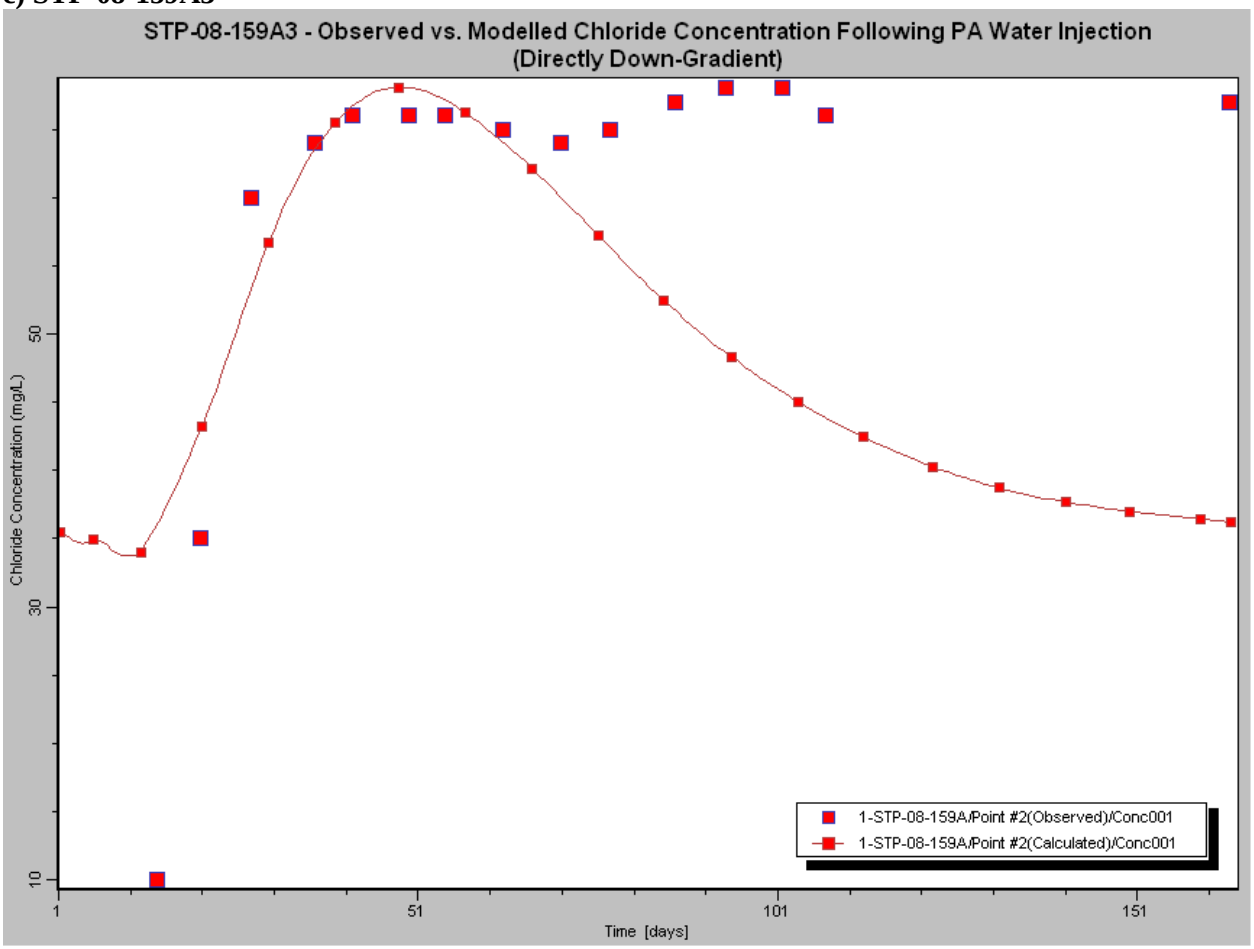


**Figure 4-55: Observed vs. Modelled chloride concentrations following the STP-07-159-SS PA water injection at: (a) STP-07-159-SS; (b) STP-08-159A2 and; (c) STP-08-159A3.**

**a) Chloride Concentration Immediately After Injection**

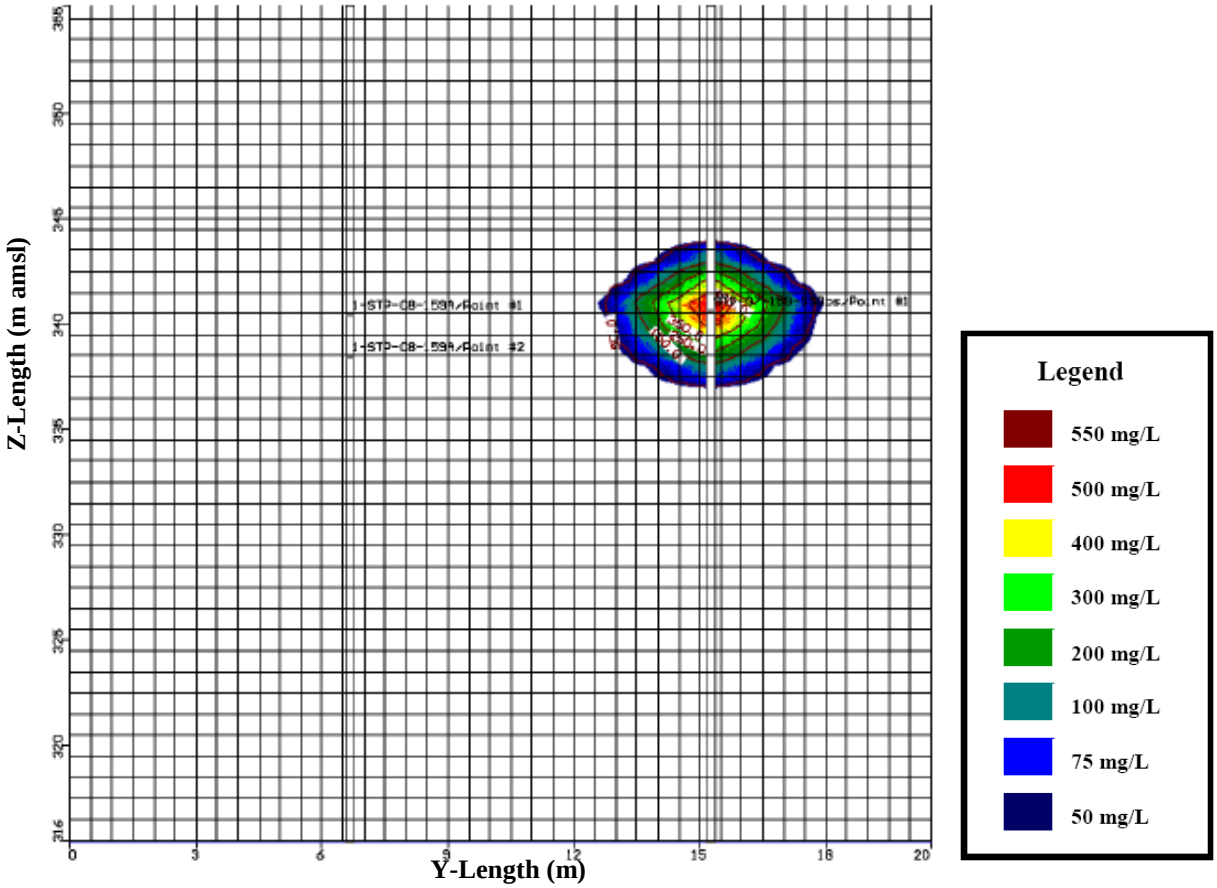


**b) Chloride Concentration 20 Days after Injection**

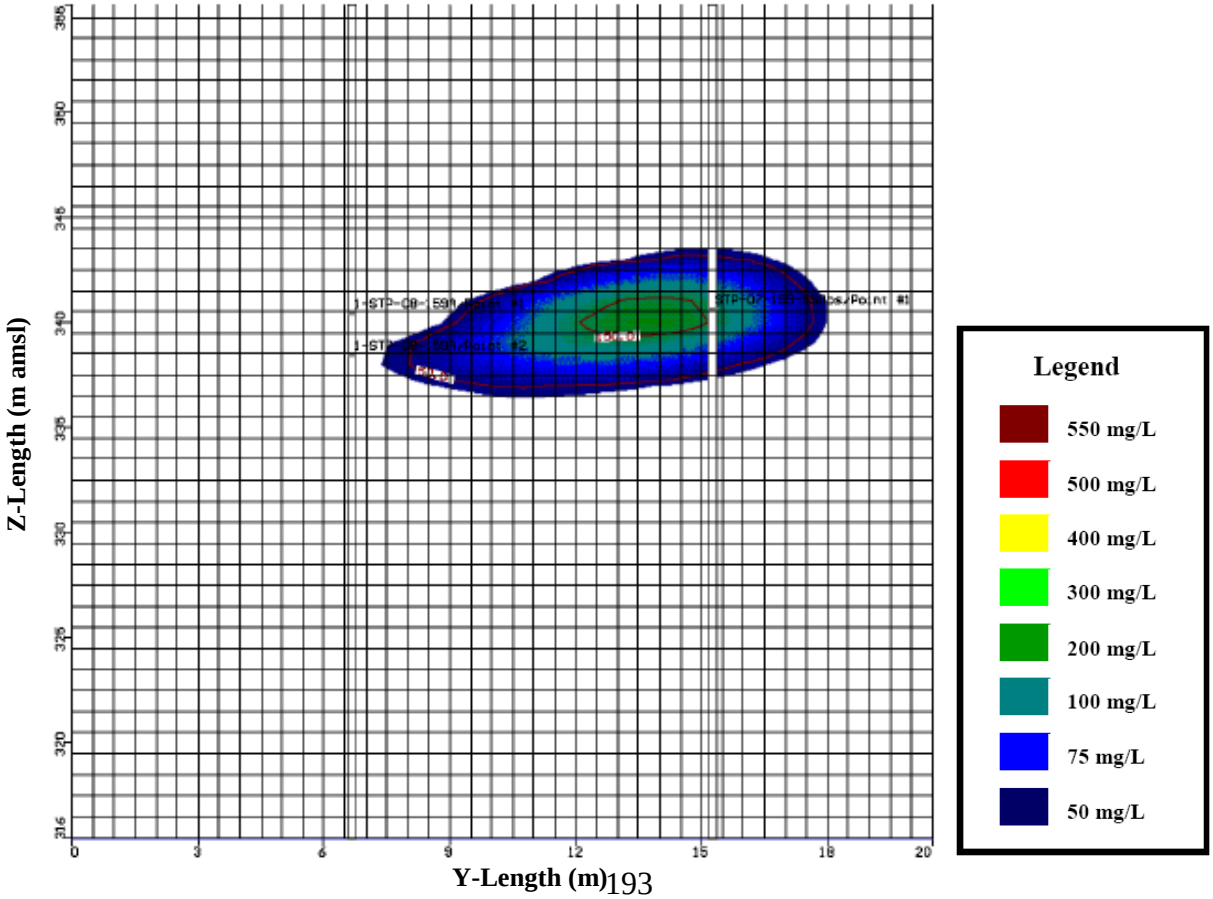

c) Chloride Concentration 75 Days after Injection

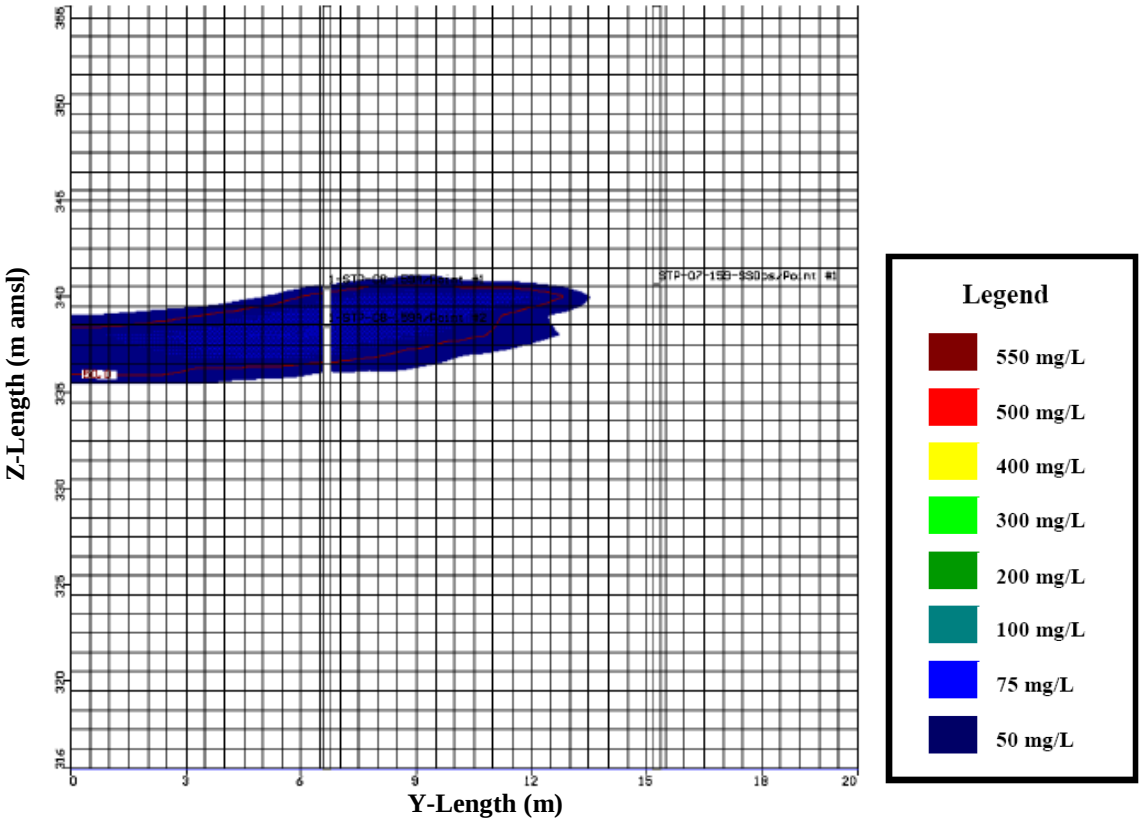


d) Chloride Concentration 100 Days after Injection

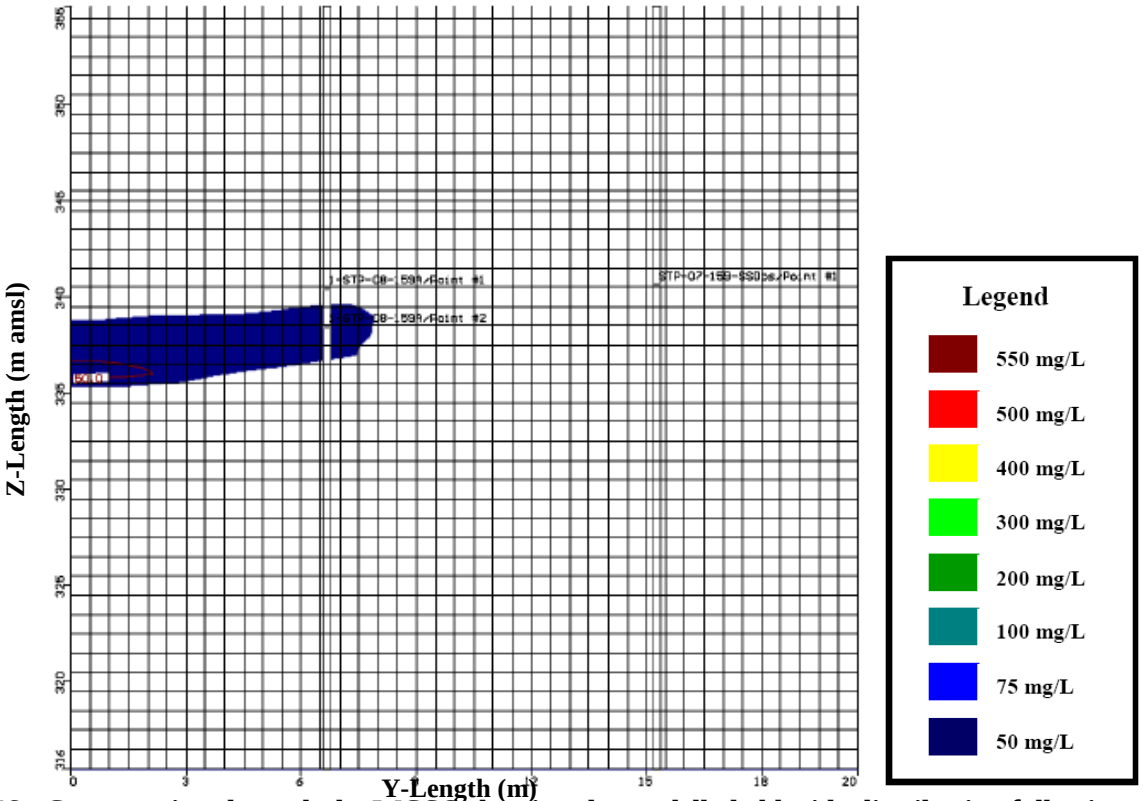


**Figure 4-56: Cross section through the WCSC showing the modelled chloride distribution following the PA water injection at STP-07-159-SS: (a) Immediately after injection; (b) 20 days after injection; (c) 75 days after injection and; (d) 100 days after injection. Model was run with a vertical flow component and variability in hydraulic conductivity in the WCSC.**

**a) STP-07-159-SS**

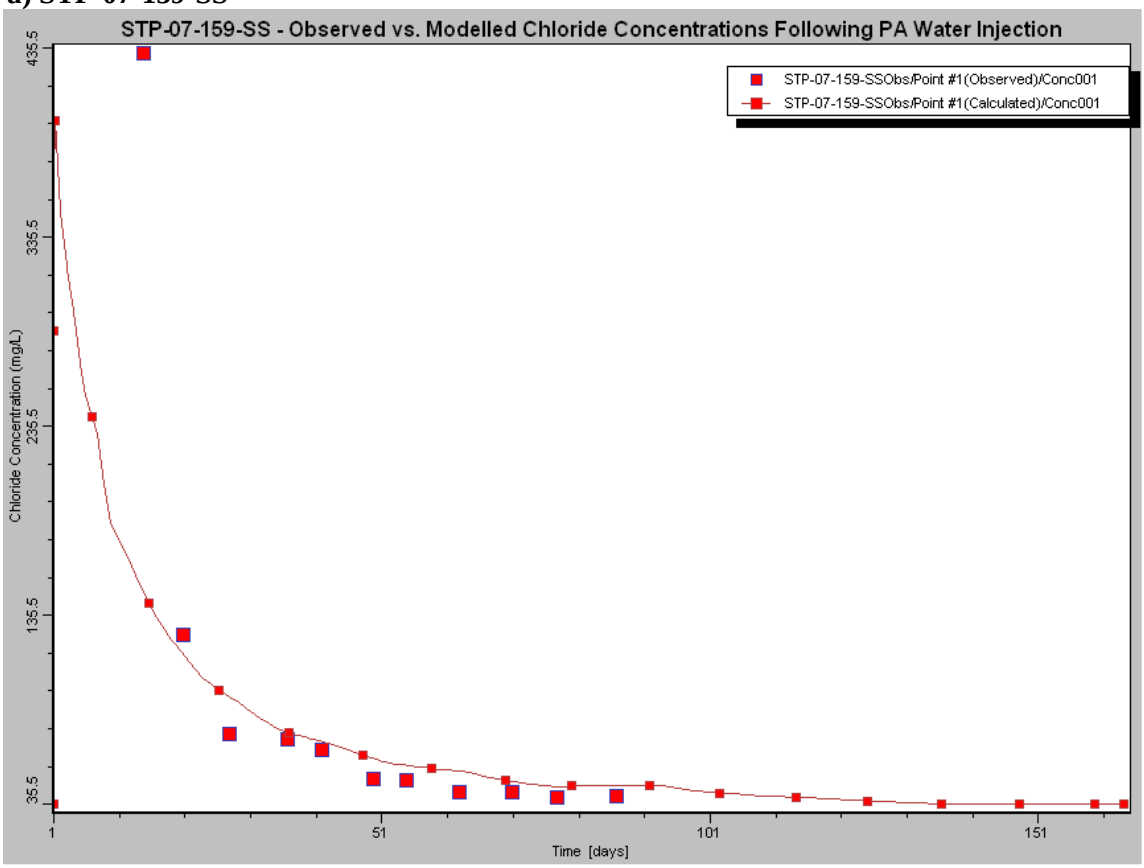


**b) STP-08-159A2**

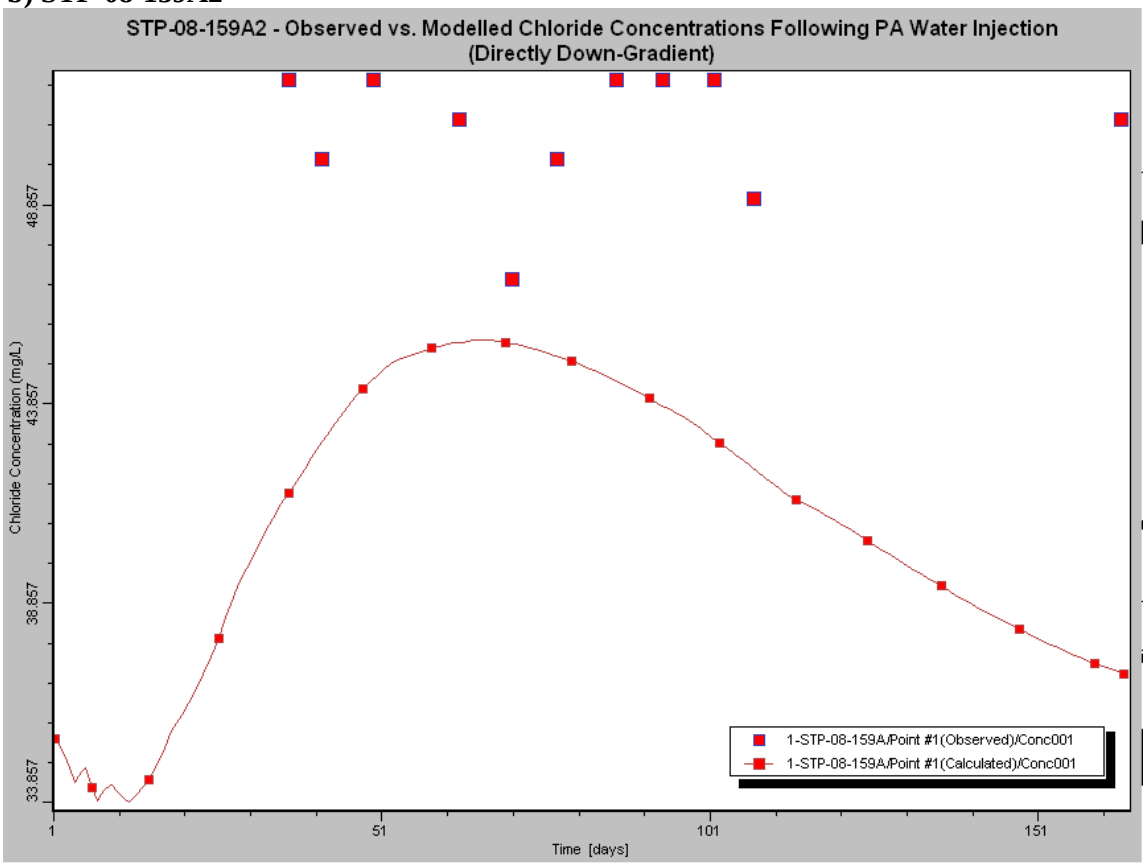

**c) STP-08-159A3**

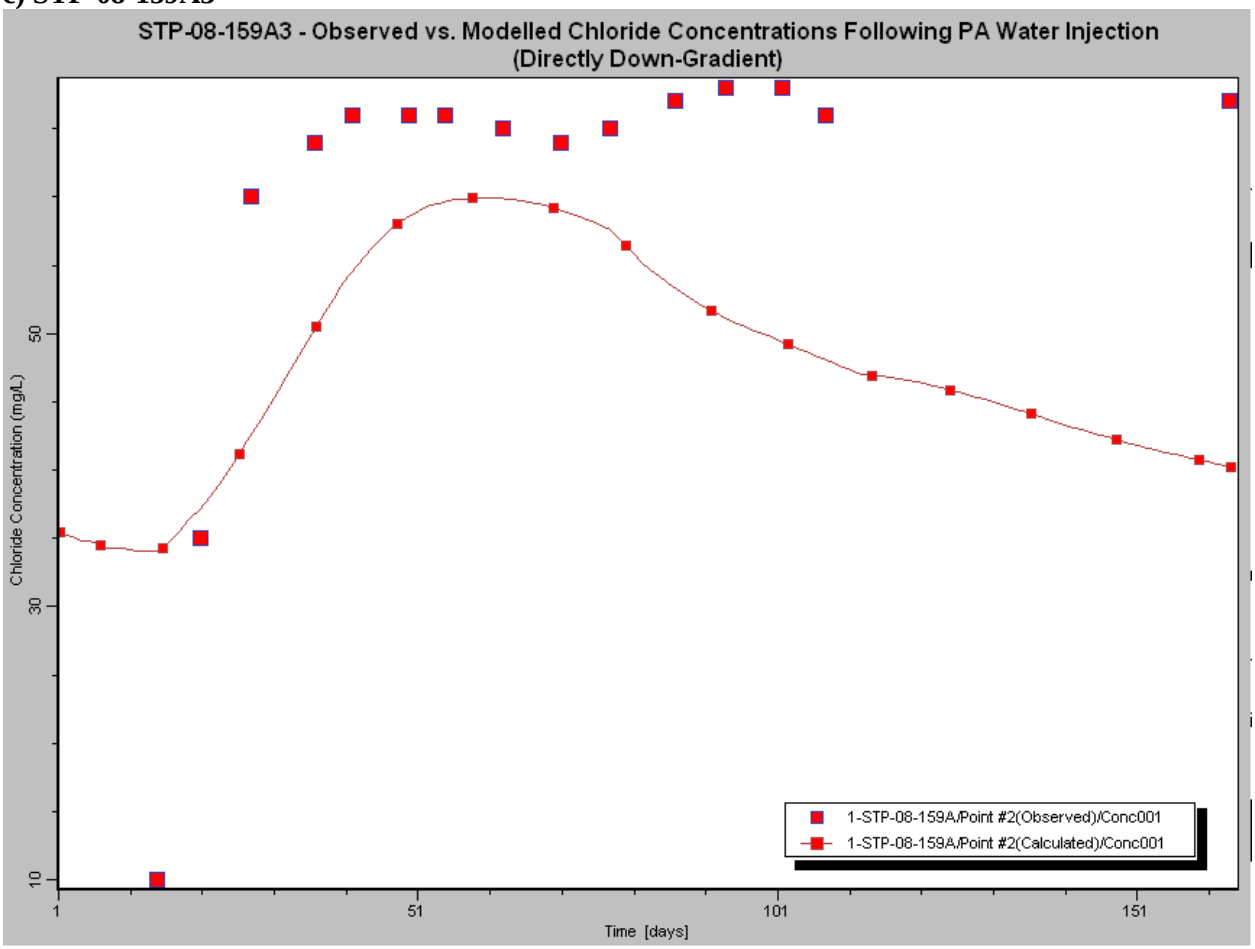


**Figure 4-57: Observed vs. Modelled chloride concentrations following STP-07-159-SS PA water injection at: (a) STP-07-159-SS; (b) STP-08-159A2 and; (c) STP-08-159A3. Model was run with large value of dispersivity.**

## REFERENCES


Acton, D.W. and Barker, J.F. (1992). In situ biodegradation potential of aromatic hydrocarbons in anaerobic groundwaters. Journal of Contaminant Hydrology, 9: 325-352.

Albrechtsen, H-J., and Christensen, T.H. (1994). Evidence for Microbial Iron Reduction in a Landfill Leachate-Polluted Aquifer (Vejen, Denmark). Applied and Environmental Microbiology, 60 (11): 3920-3925.

Allen, E.W. (2008). Process water treatment in Canada's oil sands industry: I. Target pollutants and treatment objectives. J. Environ. Eng. Sci., 7: 123-138.

Anderson, M. (1979). Modelling of groundwater flow systems as they relate to the movement of contaminants. C.R.C. Critical Reviews in Environmental Control, 9: 97-156.

Andriashek, L.D. and Atkinson, N. (2007). Buried Channels and Glacial Drift Aquifers in the Fort McMurray Region, Northeast Alberta. Alberta Energy and Utilities Board, EUB/AGS Earth Sciences Report 2007-01, 169 p.

Appelo, C.A.J. and Postma, D. (2005). Geochemistry, Groundwater and Pollution (2nd Edition). A.A. Balkema Publishers, Leiden, Netherlands.

Axe, L. and Trivedi, P. (2002). Intraparticle Surface Diffusion of Metal Contaminants and their Attenuation in Microporous Amorphous Al, Fe, and Mn Oxides. Journal of Colloid and Interface Science, 247: 259-265.

Baedecker, M.J., Cozzarelli, I.M., Eganhouse, R.P., Siegel, D.I., and Bennett, P.C. (1993). Crude oil in a shallow sand and gravel aquifer---III. Biogeochemical reactions and mass balance modeling in anoxic groundwater. Applied Geochemistry, 8: 569-586.

Barker, J.F. and Chatten, S. (1982). A Technique for Determining Low Concentrations of Total Carbonate in Geologic Materials. Chemical Geology, 36: 317-323.

Barker, J.F., Tessman, J.S., Plotz, P.E. and Reinhard, M. (1986). The Organic Geochemistry of a Sanitary Landfill Leachate Plume. Journal of Contaminant Hydrology, 1: 171-189.

Bataineh, M., Scott, A.C., Fedorak, P.M., and Martin, J.W. (2006). Capillary HPLC/QTOF-MS for Characterizing Naphthenic Acid Mixtures and Their Microbial Transformation. Analytical Chemistry, 78: 8354-8361.

Bevington, P. R. and Robinson D. K. (1992). Data reduction and error analysis for the physical sciences. McGraw-Hill, Inc., New York.

Bradl, H.B. (2004). Adsorption of heavy metal ions on soils and soils constituents. Journal of Colloid and Interface Science, 277: 1-18.

Brient, J.A., Wessner, P.J., and Doyle, M.N. (1995). Naphthenic acids, fourth ed.. In: Kroschwitz, J.I. (Ed.), Encyclopedia of Chemical Technology, vol. 16 John Wiley, New York, 1019-1029.

Bruno, J., Duro, L., de Pablo, J., Casas, I., Ayora, C., Delgado, J., Gimeno, M.J., Peña, J., Linklater, C., Pérez del Villar, L., and Gómez, P. (1998). Estimation of the concentrations of trace metals in natural systems: The application of codissolution and coprecipitation approaches to El Berrocal (Spain) and Poços de Caldas (Brazil). Chemical Geology, 151: 277-291.

Carrera, J. (1993). An overview of uncertainties in modelling groundwater solute transport. Journal of Contaminant Hydrology, 13: 23-48.

Chapelle, F.H. and Lovley, D.R. (1992). Competitive Exclusion of Sulfate Reduction by Fe(III)-Reducing Bacteria: A Mechanism for Producing Discrete Zones of High-Iron Ground Water. Ground Water, 30: 29-36.

Churcher, P.L. and Dickhout, R.D. (1987). Analysis of Ancient Sediments for Total Organic Carbon – Some New Ideas. Journal of Geochemical Exploration, 29: 235-246.

Clemente, J.S., Prasad, N.G.N., MacKinnon, M.D., and Fedorak, P.M. (2003). A statistical comparison of naphthenic acids characterized by gas chromatography-mass spectrometry. Chemosphere, 50: 1265-1274.

Clemente, J.S. and Fedorak, P.M. (2005). A review of the occurrence, analyses, toxicity, and biodegradation of napthenic acids. Chemosphere, 60: 585-600.

Deng, Y. And Stumm, W. (1993). Kinetics of redox cycling of iron coupled with fulvic acid. Aquatic Sciences, 55(2): 103-111.

Drayton, E. (2007). Design of a Field Experiment to Increase the Understanding of Contaminant Transport in the Wood Creek Sand Channel. BSc Thesis, University of Waterloo, Waterloo, Ontario, Canada.

Fetter, C.W. (2001). Applied Hydrogeology (Fourth Edition). Prentice Hall, Upper Saddle River, New Jersey, U.S.A.

Freeze, R.A. and Cherry, J.A. (1979). Groundwater. Prentice Hall, Englewood Cliffs, New Jersey, U.S.A.

Freyberg, D.L. (1986). A natural gradient experiment in solute transport in a sand aquifer:
2. Spatial moments and the advection and dispersion of nonreactive tracers. Water Resources Research, 22: 2031-2046.

Gervais, F.J.M. (2004). Fate and Transport of Napthenic Acids in a Glacial Aquifer. MSc Thesis, University of Waterloo, Waterloo, Ontario, Canada.

Gervais, F. and Barker, J. (2004). Fate and transport of napthenic acids in groundwater. In: Thomson, N.R. (Ed), Bringing Groundwater Quality Research to the Watershed Scale, Proceedings of GQ2004, the 4th International Groundwater Quality Conference, Waterloo, Ontario, Canada, July 2004, International Association of Hydrological Sciences Publ. 297, 305-310.

Government of Alberta (2008). Fact Sheets. Oil Sands Discovery Centre.

Government of Alberta: Energy (2009). Oil Sands: http://www.energy.gov.ab.ca/News/oilsands.asp.

Grantham, M.C., Dove, P.M. and DiChristina, T.J. (1997). Microbially catalyzed dissolution of iron and aluminum oxyhydroxide mineral surface coatings. Geochimica et Cosmochimica Acta, 61(21): 4467-4477.

Greiner, G. and Chi, B. (1995). Canada/Kanada. In: Kulke, H. (Ed), Regional Petroleum Geology of the World: Part II: Africa, America, Australia and Antarctica. Gebrüder Borntraeger, Berlin, Germany, 279-334.

Grove, D.W. and Wood, W.W. (1979). Prediction and Field Verification of Subsurface-Water Quality Changes During Artificial Recharge, Lubbock, Texas. Groundwater, 17: 250-257.

Guo, H., Wand, Y., Shpeizer, G.M., and Yan, S. (2003). Natural Occurrence of Arsenic in Shallow Groundwater, Shanyin, Datong Basin, China. J. of Environ. Sci. And Health (Part A Toxic/Hazardous Substances & Environmental Engineering), A38(11): 2565-2580.

Hall, S.H., Luttrell, S.P. and Cronin, W.E. (1991). A Method for Estimating Effective Porosity and Ground-Water Velocity. Ground Water, 29 (2): 171-174.

Han, X.M., Scott, A.C., Fedorak, P.M., Bataineh, M. and Martin, J.W. (2008). Influence of Molecular Structure on the Biodegradability of Naphthenic Acids. Environ. Sci. Technol, 42 (4): 1290-1295.

Haque, S., Ji, J. and Johannesson, K.H. (2008). Evaluating mobilization and transport of arsenic in sediments and groundwaters of Aquia aquifer, Maryland, USA. Journal of Contaminant Hydrology, 99: 68-84.

Headley, J.V. and McMartin, D.W. (2004). A Review of the Occurrence and Fate of Napthenic Acids in Aquatic Environments. J. of Environ. Sci. And Health (Part A Toxic/Hazardous Substances & Environmental Engineering), A39(8): 1989-2010.

Henderson, J.E., Peyton, G.R. and Glaze, W.H. (1976). A Convenient Liquid-Liquid Extraction Method for Determination of Halomethanes in Water at the Parts-Per-Billion Level. In: Keith, L.H. (Ed.), Identification and Analysis of Organic Pollutants in Water. Ann Arbor Science Publishers Inc., Ann Arbor, Michigan, USA.

Herbert, R.B. Jr. (1997). Partitioning of Heavy Metals in Podzol Soils Contaminated by Mine Drainage Waters, Dalarna, Sweden. Water, Air, and Soil Pollution, 96: 39-59.

Herbert, R.B. Jr. (2006). Seasonal variations in the composition of mine drainage-contaminated groundwater in Dalarna, Sweden. Journal of Geochemical Exploration, 90: 197-214.

Herman, D.C., Fedorak, P.M., MacKinnon, M.D. and Costerton, J.W. (1994). Biodegradation of naphthenic acids by microbial populations indigenous to oil sands tailings. Can. J. Microbiol, 40: 467-477.

Heron, G. and Christensen, T.H. (1995). Impact of Sediment-Bound Iron on Redox Buffering in a Landfill Leachate Polluted Aquifer (Vejen, Denmark). Environmental Science and Technology, 29: 187-192.

Heron, G., Crouzet, C., Bourg, A.C.M., and Christensen, T.H. (1994). Speciation of Fe (II) and Fe (III) in Contaminated Aquifer Sediments Using Chemical Extraction Techniques. Environmental Science and Technology, 28: 1698-1705.

Holmström, H., and Öhlander, B. (2001). Layers rich in Fe- and Mn-oxyhydroxides formed at the tailings-pond water interface, a possible trap for trace metals in flooded mine tailings. Journal of Geochemical Exploration, 74: 189-203.

Holowenko, F.W., MacKinnon, M.D., and Fedoark, P.M. (2000). Methanogens and sulphate-reducing bacteria in oil sands fine tailings waste. Can. J. Microbiol, 46: 927-937.

Holowenko, F.M., MacKinnon, M.D., and Fedorak, P.M. (2001). Napthenic Acids and Surrogate Napthenic Acids in Methanogenic Microcosms. Water Res, 35(11): 2595-2606.

Holowenko, F.M., MacKinnon, M.D. and Fedorak, P.M. (2002). Characterization of naphthenic acids in oil sands wastewaters by gas chromatography-mass spectrometry. Water Res, 36: 2843-2855.

Huisman, D.J., Vermeulen, F.J.H., Baker, J., Veldkamp, A., Kroonenberg, S.B., Klaver, G.Th. (1997). A geological interpretation of heavy metal concentrations in soils and sediments in the southern Netherlands. Journal of Geochemical Exploration, 59: 163-174.

Hunter, K.S., Wang, Y., Van Cappellen, P. (1998). Kinetic modeling of microbially-driven redox chemistry of subsurface environments: coupling transport, microbial metabolism and geochemistry. Journal of Hydrology, 209: 53-80.

Istok, J.D., Humphrey, M.D., Scroth, M.H., Hyman, M.R., O'Reilly, K.T. (1997). Single-Well, "Push-Pull" Test for In Situ Determination of Microbial Activities. Groundwater, 35(4): 619-631.

Janfada, A., Headley, J.V., Peru, K.M., and Barbour, S.L. (2006). A Laboratory Evaluation of the Sorption of Oil Sands Naphthenic Acids on Organic Rich Soils. J. of Environ. Sci. And Health (Part A Toxic/Hazardous Substances & Environmental Engineering), A41(6): 985-997

Jivraj, M.N., MacKinnon, M.D. and Fung, B. (1995). Naphthenic Acids Extraction and Quantitative Analyses with FT-IR Spectroscopy. Syncrude Analytical Methods Manual. 4th ed. Syncrude Canada Ltd. Research Department, Edmonton, Alberta, Canada.

Kaplan, P.G. and Leap, D.I. (1985). Predicting The Advective Flow Velocity In A Confined Aquifer Using A Single Well Tracer Test. Technical Report No. 171. United States Geological Survey.

Kasperski, K.L. (1992). A Review of Properties and Treatment of Oil Sands Tailings. AOSTRA Journal of Research, 8:11-53.

Klohn Crippen Consultants Ltd. (2004). Millenium Mine Design of the South Tailings Pond – Final Report. Report submitted to Suncor Energy, Inc., November 2004.

Lai, J.W.S., Pinto, L.J., Kiehlmann, E., Bendell-Young, L.I. and Moore, M.M. (1996). Factors that Affect the Degradation of Napthenic Acids in Oil Sands Wastewater by Indigenous Microbial Communities. Environ. Toxicol.Chem, 15(9): 1482-1491.

Lo, C.C., Brownlee, B.G., and Bunce, N.J. (2006). Mass spectrometric and toxicological assays of Athabasca oil sands naphthenic acids. Water Research, 40: 655-664.

Lobo, V.M.M. and Quaresma, J.L. (1989). Handbook of Electrolyte Solutions – Part B. Elsevier: Amsterdam: 1611.

Lovley, D.R. and Goodwin, S. (1988). Hydrogen concentrations as an indicator of the predominant terminal electron-accepting reactions in aquatic sediments. Geochimica et Cosmochimica Acta, 52: 2993-3003.

Lovley, D.R. and Lonergan, D.J. (1988). Novel Mode of Microbial Energy Metabolism: Organic Carbon Oxidation Coupled to Dissimilatory Reduction of Iron or Manganese. Applied and Environmental Microbiology, 54: 1472-1480.

Lovely, D.R., Phillips, E.J.P., and Lonergan, D.J. (1991). Enzymatic versus Nonenzymatic Mechanisms for Fe(III) Reduction in Aquatic Sediments. Environmental Science and Technology, 25: 1062-1067.

Lyngkilde, J. and Christensen, T.H. (1992). Fate of organic contaminants in the redox zones of a landfill leachate pollution plume (Vejen, Denmark). Journal of Contaminant Hydrology, 10: 291-307.

Lyngkilde, J. and Christensen, T.H. (1992). Redox zones of a landfill leachate pollution plume (Vejen, Denmark). Journal of Contaminant Hydrology, 10: 273-289.

MacKinnon, M.D. (1981). A Study of the Chemical and Physical Properties of Syncrude's Tailings Pond, Mildred Lake, 1980. Syncrude Canada, Ltd., Environmental Research Report 1981.

MacKinnon, M.D. and Boerger, H. (1986). Description of Two Treatment Methods for Detoxifying Oil Sands Tailings Pond Water. Water Poll. Res. J. Canada, 21(4): 496-512.

MacKinnon, M.D. (1989). Development of the Tailings Pond at Syncrude's Oil Sands Plant; 1978-1987. AOSTRA Journal of Research, 5: 109-133.

MacKinnon, M., Kampala, G., Marsh, B., Fedorak, P., and Guigard, S. (2004). Indicators for assessing transport of oil sands process-affected waters. In: Thomson, N.R. (Ed), Bringing Groundwater Quality Research to the Watershed Scale, Proceedings of GQ2004, the 4th International Groundwater Quality Conference, Waterloo, Ontario, Canada, July 2004, International Association of Hydrological Sciences Publ. 297, 71-80.

Marsden, W. (2007). Stupid To The Last Drop: How Alberta is Bringing Environmental Armageddon To Canada (And Doesn't Seem To Care). Alfred A. Knopf Canada, Toronto, 248 pp.

Michelson, A.R., Jacobson, M.E., Scranton, M.I., and Mackin, J.E. (1989). Modeling the distribution of acetate in anoxic estuarine sediments. Limnology and Oceanography, 34(4): 747-757.

Molz, F.J., Melville, J.G., Güven, O., Crocker, R.D., and Matteson, K.T. (1985). Design and Performance of Single-Well Tracer Tests at the Mobile Site. Water Resources Research, 21(10): 1497-1502.

National Energy Board. (2004). Canada's Oil Sands: Opportunities and Challenges to 2015 – An Energy Market Assessment – May 2004. National Energy Board, Calgary, 138 pp.

National Energy Board. (2006). Canada's Oil Sands: Opportunities and Challenges to 2015: An Update – An Energy Market Assessment – June 2006. National Energy Board, Calgary, 71 pp.

Neville, C.J. (2001). Oned_1 Analytical Solution.

Nicholson, R.V., Cherry, J.A., and Reardon, E.J. (1983). Migration of Contaminants in Groundwater at a Landfill: A Case Study, 6. Hydrogeochemistry. Journal of Hydrology, 63: 131-176.

Niemann, W.L. and Rovey II, C.W. (2009). A systematic field-based testing program of hydraulic conductivity and dispersivity over a range in scale. Hydrogeology Journal, 17: 307-320.

Nix, P.G. and Martin, R.W. (1992). Detoxification and Reclamation of Suncor's Oil Sand Tailings Ponds. Environmental Toxicology and Air Quality, 7: 171-188.

Oiffer, A.A.L. (2006). Integrated Solid Phase and Numerical Investigation of Plume Geochemistry at an Oil Sand Mining Facility. MSc Thesis, University of Waterloo, Waterloo, Ontario, Canada.

Oldham, T.L. (1998). Use of Falling Head Permeameters to Determine Hydraulic Conductivity. Department of Earth and Environmental Sciences, University of Waterloo, Waterloo, Ontario, Canada.

Ptak, T. and Teutsch, G. (1994). Forced and natural gradient tracer tests in a highly heterogeneous porous aquifer: instrumentation and measurements. Journal of Hydrology, 159: 79-104.

Quagraine, E.K., Headley, J.V., and Peterson, H.G. (2005). Is Biodegradtion of Bitumen a Source of Recalcitrant Naphthenic Acid Mixtures in Oil Sands Tailing Pond Waters?. J. of Environ. Sci. And Health (Part A Toxic/Hazardous Substances & Environmental Engineering), A40(3): 671-684.

Quagraine, E.K., Peterson, H.G., and Headley, J.V. (2005). In Situ Bioremediation of Napthenic Acids Contaminated Tailing Pond Waters in the Athabasca Oil Sands Region—Demonstrated Field Studies and Plausible Options: A Review. J. of Environ. Sci. And Health (Part A Toxic/Hazardous Substances & Environmental Engineering), A40(3): 685-722.

Reinhard, M., Hopkins, G.D., Orwin, E., Shang, S., and Lebron, C.A. (1995). In situ demonstration of anaerobic BTEX biodegradation through controlled-release experiments. In: R.E. Hinchee, J.A. Kittel, and H.J. Reisinger (eds.). Applied Bioremediation of Petroleum Hydrocarbons. Battelle Press. Columbus, Oh. pp. 263-270.

Rügge, K., Bjerg, P.L., and Christensen, T.H. (1995). Distribution of Organic Compounds from Municipal Solid Waste in the Groundwater Downgradient of a Landfill (Grindsted, Denmark). Environmental Science and Technology, 29: 1395-1400.

Sansone, F.J., Andres, C.C., Okamoto, M.Y. (1987). Adsorption of short-chain organic acids onto nearshore marine sediments. Geochimica et Cosmochimica Acta, 51: 1889-1896.

Schramm, L.L., Smith, R.G., and Stone, J.A. (1984). The Influence of Natural Surfactant Concentration on The Hot Water Process for Recovering Bitumen from the Athabasca Oil Sands. AOSTRA Journal of Research, 1: 5-13.

Schramm, L.L., Stasiuk, E.N., and MacKinnon, M. (2000). Surfactants in Athabasca Oil Sands Slurry Conditioning, Flotation Recovery, and Tailings Processes. In: Surfactants, Fundamentals, and Applications in the Petroleum Industry. Schramm, L.L., Ed., Cambridge University Press: Cambridge, UK, 2000. 365-430.

Schulze-Makuch, D., Carlson, D.A., Cherkauer, D.S., and Malik, P. (1999). Scale Dependency of Hydraulic Conductivity in Heterogeneous Media. Ground Water, 37: 904-919.

Scott, A.C., MacKinnon, M.D., Fedorak, P.M. (2005). Naphthenic Acids in Athabasca Oil Sands Tailings Waters Are Less Biodegradable than Commercial Naphthenic Acids. Environmental Science and Technology, 39: 8388-8394.

Scott, J.D., Dusseault, M.B. and Carrier III, W.D. (1985). Behaviour of the Clay/Bitumen/Water Sludge System from Oil Sands Extraction Plants. Applied Clay Science, 1: 207-218.

Shaw, D.G., Alperin, M.J., Reeburgh, W.S. and McIntosh, D.J. (1984). Biogeochemistry of acetate in anoxic sediments of Skan Bay, Alaska. Geochimica et Cosmochimica Acta. 48: 1819-1825.
Siddique, T., Fedorak, P.M., MacKinnon, M.D., and Foght, J.M. (2007). Metabolism of BTEX and Naptha Compounds to Methane in Oil Sands Tailings. Environ. Sci. Technol, 41(7): 2350-2356.

Smith, B.E., Lewis, C.A., Belt, S.T., Whitby, C. and Rowland, S.J. (2008). Effects of Alkyl Chain Branching on the Biotransformation of Naphthenic Acids. Environmental Science and Technology, 42: 9323-9328.

St. John, W.P., Rughani, J., Green, S.A., and McGinnis, G.D. (1998). Analysis and characterization of naphthenic acids by gas chromatography-electron impact mass spectrometry of *tert*.-butyldimethylsilyl derivatives. Journal of Chromatography A, 807: 241-251.

Stumm, W., and Sulzberger, B. (1992). The cycling of iron in natural environments: Considerations based on laboratory studies of heterogeneous redox processes. Geochimica et Cosmochimica Acta, 56: 3233-3257.

Suarez, D.L., and Langmuir, D. (1976). Heavy metal relationships in a Pennsylvania soil. Geochimica et Cosmochimica Acta, 40: 589-598.

Sudicky, E.A., Cherry, J.A. and Frind, E.O. (1983). Migration of Contaminants in Groundwater at a Landfill: A Case Study, 4. A Natural-Gradient Dispersion Test. Journal of Hydrology, 63, 81-108.

Suncor Energy Inc. (2007). 2007 Report on Sustainability. http://www.suncor.com/doc.aspx?id=114.

Tang, J., Whittecar, G.R., Johannesson, K.H. and Daniels, W.L. (2004). Potential contaminants at a dredged spoil placement site, Charles City County, Virginia, as revealed by sequential extraction. Geochmical Transactions, 5(4): 49-60.

Tessier, A., Campbell, P.G.C. and Bisson, M. (1979). Sequential Extraction Procedure for the Speciation of Particulate Trace Metals. Analytical Chemistry, 51(7): 844-851.

Wang, X.C., and Lee, C. (1993). Adsorption and desorption of aliphatic amines, amino acids and acetate by clay minerals and marine sediments. Marine Chemistry, 44: 1-23.

Waterloo Hydrogeologic Inc. (2006). Visual MODFLOW v.4.2 User's Manual For Professional Applications in Three Dimensional Groundwater Flow and Contaminant Transport Modeling. Waterloo Hydrogeologic, Inc., Waterloo, ON, 632 pp.

Zachara, J.M., Fredrickson, J.K., Smith, S.C. and Gassman, P.L. (2001). Solubilization of Fe(III) oxide-bound trace metals by a dissimilatory Fe(III) reducing bacterium. Geochimica et Cosmochimica Acta, 65(1): 75-93.

Zou, L., Han, B., Yan, H., Kasperski, K.L., Xu, Y., and Hepler, L.G. (1997). Enthalpy of Adsorption and Isotherms for Adsoprtion of Napthenic Acid onto Clays. J. of Colloid and Interface Science, 190: 472-475.